

# Sheffield Hallam University

*Extrusion honing using mixtures of polyborosiloxanes and grit*

TRENGOVE, Sean Alexander

Available from the Sheffield Hallam University Research Archive (SHURA) at:

<http://shura.shu.ac.uk/3178/>

## A Sheffield Hallam University thesis

This thesis is protected by copyright which belongs to the author.

The content must not be changed in any way or sold commercially in any format or medium without the formal permission of the author.

When referring to this work, full bibliographic details including the author, title, awarding institution and date of the thesis must be given.

Please visit <http://shura.shu.ac.uk/3178/> and <http://shura.shu.ac.uk/information.html> for further details about copyright and re-use permissions.



286874

Sheffield Hallam University

**REFERENCE ONLY**

ProQuest Number: 10701098

All rights reserved

INFORMATION TO ALL USERS

The quality of this reproduction is dependent upon the quality of the copy submitted.

In the unlikely event that the author did not send a complete manuscript and there are missing pages, these will be noted. Also, if material had to be removed, a note will indicate the deletion.



ProQuest 10701098

Published by ProQuest LLC (2017). Copyright of the Dissertation is held by the Author.

All rights reserved.

This work is protected against unauthorized copying under Title 17, United States Code  
Microform Edition © ProQuest LLC.

ProQuest LLC.  
789 East Eisenhower Parkway  
P.O. Box 1346  
Ann Arbor, MI 48106 – 1346

# **Extrusion honing using mixtures of polyborosiloxanes and grit**

---

**Sean Alexander Trengove BSc (Hons)**

**A thesis submitted in partial fulfilment  
of the requirements of Sheffield Hallam University  
for the degree of Doctor of Philosophy.**

**September 1993**

**Collaborating Establishment: Extrude Hone Ltd.  
6 Centurion Court  
Brick Close  
Kiln Farm  
Milton Keynes  
MK11 3JB**

# PREFACE

---

This thesis refers to research completed during the period October 1988 to September 1991 within the Division of Materials and Process Engineering (formerly the Department of Metals and Materials Engineering), School of Engineering, Sheffield Hallam University (formerly Sheffield City Polytechnic), and the premises of Extrude Hone Ltd., Milton Keynes.

Post-graduate courses were attended during the above period in process metallurgy, mechanical metallurgy, applied thermodynamics, numerical analysis and computer programming (FORTRAN 77), economics, accountancy, surface hardening and heat treatment, metals and competitive materials, quality assurance, automatic and computer aided control, oxygen steelmaking and corrosion resistant and high temperature materials.

Within the University this work has been presented at the 1989 and 1990 Polymer group seminars as well as at two research colloquia. In addition, this work was presented by the Author at the Institute of Metals 'Metals and Materials '90' conference at the University of Liverpool. This work was also presented by the Author at the 'Surface Engineering; Current Trends and Future Prospects' conference at the University of Toronto in June 1990 (Appendix B).

I confirm that this work has not been presented for any other award.

S. A. Trengove

September 1993

# ABSTRACT

---

Extrusion honing is a technique used for the finish machining of engineering components. The process may be used to deburr, radius or polish depending on the specific application. Extrusion honing utilises a polyborosiloxane polymer, which is mixed with fine abrasive particles and forced through or around components using an extrusion honing machine to achieve the machining action.

It is evident that the machining process is very dependent upon the physical and mechanical characteristics of the polyborosiloxane. However, the process to date has largely been developed empirically, and further developments will require a greater understanding of the relationship between the characteristics of the polymer and the machining action.

The rheology of the C-11 polyborosiloxane has been investigated using a concentric cylinder, a slit-die and a capillary rheometer. The shear history of the polyborosiloxane prior to testing with the capillary rheometer was found to significantly affect the results produced.

At shear strain rates up to  $100 \text{ s}^{-1}$  and a temperature of  $30^\circ\text{C}$  the rheology of the polyborosiloxane has been approximated to a power law equation ( $K = 789 \text{ Pa}\cdot\text{s}^n$ ,  $n = 0.935$ ). At shear strain rates greater than  $100 \text{ s}^{-1}$  the pseudoplasticity of the polyborosiloxane increases significantly.

Using this power law equation the velocity, shear strain rate and the shear stress within the polyborosiloxane in an extrusion die has been modelled mathematically.

In some cases the extrusion barrel pressure and the mass flow rate through the extrusion die have both been shown to vary considerably during the constant ram velocity extrusion of polyborosiloxane in the capillary rheometer.

It is tentatively proposed that such variations in the extrusion barrel pressure during capillary flow are a result of periodic slipping and sticking of the polyborosiloxane to the extrusion die wall. This mechanism is thought to be considerably influenced by the polyborosiloxane temperature, the extrusion ram velocity and the flow passage geometry. It is proposed that the measured variations in the mass flow rate of the polyborosiloxane through the extrusion dies are a result of pressure induced density variations within the extrusion barrel. This mechanism has been mathematically modelled.

Temperature profiles within the C-11 polyborosiloxane have been measured on an extrusion honing machine and the results suggest significant heat generation towards the periphery of the restriction. These results have been used to model mathematically the heat generation and transfer within the polyborosiloxane during operation of the extrusion honing machine. It is proposed that heat generation during extrusion honing is by friction at the medium/workpiece interface and internal shear within the medium. Both of these mechanisms would cause the greatest heat generation towards the periphery of an orifice restriction.

# ACKNOWLEDGEMENTS

---

The Science and Engineering Council and Extrude Hone Limited for financial support.

Dr A J Fletcher for supervision throughout the research programme, and for help in the organisation of this thesis.

Mr. J Mackie (Extrude Hone Limited) for advice and support throughout the research programme.

Dr J B Hull (now of The University of Bradford) for supervision during the initial phase of the research.

The technical staff of the School of Engineering at the Sheffield Hallam University for their valuable help during the three years.

The staff of Extrude Hone Limited (Milton Keynes) and Extrude Hone Corporation (USA) for their advice and assistance.

My family and friends for their valuable support throughout my academic career.

# TABLE OF CONTENTS

---

	<b>Page</b>
Preface	i
Abstract	ii
Acknowledgements	iii
Nomenclature used in the thesis	x
CHAPTER 1: INTRODUCTION	1
1.1 Objectives of the research	1
CHAPTER 2: LITERATURE REVIEW	4
2.1 Introduction	4
2.2 Surface finishing	5
2.2.1 Surface finishing in modern manufacturing	5
2.2.2 Quantification of surface finish	6
2.2.3 Measurement of surface finish	7
2.3 Extrusion honing	7
2.3.1 Principles of extrusion honing	7
2.3.2 Process research and development	11
2.4 The rheological response of polymers to deformation and flow	13
2.5 The capillary rheometer	18
2.5.1 Introduction	18
2.5.2 Die entrance effects and end corrections	19
2.5.3 Barrel height effects and piston friction	21
2.5.4 Wall velocity and slip-stick phenomena	21
2.5.5 Velocity and shear profiles in capillary flow	25
2.5.6 Wall pressure and flow rate fluctuations	27
2.5.7 Extrudate distortion and melt fracture	32
2.5.8 Flow curve discontinuity	34

2.5.9	Heat generation and transfer in capillary flow	36
2.5.10	Density variations during capillary flow	40
2.5.11	Shear history prior to capillary flow	42
2.6	The rheological properties of polyborosiloxane	45
<b>CHAPTER 3: EXPERIMENTAL PROCEDURES</b>		<b>50</b>
3.1	Materials	50
3.2	Experimental	51
3.2.1	Thermal conductivity measurements	51
3.2.2	Heat capacity measurements	51
3.2.3	The measurement of the polyborosiloxane temperature in an extrusion honing machine	52
3.2.4	The capillary rheometer - procedure 1 - extrusion ram accelerating throughout extrusion	54
3.2.5	The capillary rheometer - procedure 2 - constant ram velocity throughout extrusion	56
3.2.6	The capillary rheometer - further procedure improvements	56
3.2.7	Variations in the charging procedure for the capillary rheometer	58
3.2.8	Variations in the polyborosiloxane temperature on the capillary rheometer	60
3.2.9	Manual measurement of the extrusion rate on the capillary rheometer	61
3.2.10	Capillary rheometer experiments with polystyrene	62
3.2.11	The slit die rheometer	63
3.2.12	The concentric cylinder rheometer	63
3.2.13	The measurement of the polyborosiloxane density as a function of temperature and pressure	64
3.3	Calculation methods	65
3.3.1	Wall shear strain rate calculations	65
3.3.2	Wall shear stress calculations	66
3.3.3	Shear viscosity calculations	67

3.3.4	Velocity distribution within the die	68
3.3.5	Shear strain rate distribution within the die	68
3.3.6	Shear stress distribution within the die	69
3.4	Mathematical models	69
3.4.1	Heat transfer during extrusion honing	69
3.4.1.1	Steady state heat transfer model	69
3.4.1.2	Transient heat transfer model	71
3.4.2	Mathematical model of polyborosiloxane density and flow rate variations during capillary flow	74
<b>CHAPTER 4: EXPERIMENTAL RESULTS</b>		<b>76</b>
4.1	Introduction	76
4.2	Heat capacity and thermal conductivity	78
4.3	Temperature distributions within polyborosiloxane during extrusion honing	78
4.3.1	Introduction	78
4.3.2	Steady state temperature distributions within the die and polyborosiloxane during extrusion honing	79
4.3.3	Transient temperature distributions within the die and polyborosiloxane during extrusion honing	80
4.4	Extrusion honing heat transfer models	81
4.4.1	Introduction	81
4.4.2	Heat generation (steady state model)	82
4.4.3	Surface heat transfer coefficient between polyborosiloxane and the inner cylinder wall (steady state model)	82
4.4.4	Transient heat generation model	82
4.5	Density of the polyborosiloxane	83
4.6	The capillary rheometer	83
4.6.1	Introduction	83
4.6.2	Experimental method development	84
4.6.3	Effect of ram velocity on capillary flow	87

4.6.3.1	Average barrel pressure during extrusion	87
4.6.3.2	Variation in barrel pressure during an extrusion	88
4.6.4	Effect of die geometry on capillary flow	89
4.6.4.1	Average barrel pressure during extrusion	89
4.6.4.2	Variation in barrel pressure during an extrusion	89
4.6.5	Effect of temperature on capillary flow	89
4.6.5.1	Average barrel pressure during extrusion	90
4.6.5.2	Variation in barrel pressure during an extrusion	90
4.6.6	Effect of charging procedure on capillary flow	91
4.6.6.1	Average barrel pressure during extrusion	91
4.6.6.2	Variation in barrel pressure during an extrusion	92
4.6.7	Die mass flow rate during capillary flow	92
4.7	Slit die rheometer	94
4.7.1	Introduction	94
4.7.2	Effect of ram velocity and temperature on wall pressure	94
4.8	Calculated shear stress and shear strain rate	95
4.8.1	Capillary rheometer	95
4.8.2	Slit die rheometer	96
4.8.3	Concentric cylinder rheometer	96
4.9	Shear stress/shear strain rate relationships	97
4.10	Calculated velocity profiles	98
4.11	Calculated shear stress and shear strain rate profiles	99
4.12	Results of control experiments using polystyrene	100
4.13	Mathematical model of density and mass flow rate during capillary flow	101
<b>CHAPTER 5: DISCUSSION</b>		<b>103</b>
5.1	Introduction	103
5.2	The accuracy of the experimental data	104

5.2.1	The accuracy of the measured rheometer extrusion barrel pressure	104
5.2.2	The accuracy of the measured rheometer ram velocity	105
5.2.3	The accuracy of the measured polyborosiloxane flow rate through a capillary die	105
5.2.4	The accuracy of the measurements of the temperature in the polyborosiloxane and die	108
5.3	The validity of the calculations	109
5.3.1	The validity of the shear strain rate calculations	109
5.3.2	The validity of the shear stress calculations	114
5.3.3	The validity of the heat generation calculations	117
5.4	The rheology of the C-11 polyborosiloxane	120
5.4.1	Introduction	120
5.4.2	Constitutive rheological equations of the C-11 polyborosiloxane	120
5.4.3	The flow mechanism of the C-11 polyborosiloxane	123
5.4.3.1	Introduction	123
5.4.3.2	A general flow mechanism for C-11 polyborosiloxane	123
5.4.3.3	Flow mechanisms during constant ram velocity extrusion	126
5.5	Application of the proposed flow mechanisms to the extrusion honing process	131
5.5.1	Heat generation and temperature control during extrusion honing	131
5.5.2	Flow phenomena during extrusion honing	132
CHAPTER 6: CONCLUSIONS		134
CHAPTER 7: FURTHER WORK		137
List of References		139
Tables		146
Figures		157

Appendix A	The measurement of extrusion honing media flow properties for quality assurance purposes - a technico-economic case study	A1
Appendix B	Computer modelling of the abrasive flow machining process: paper presented at the 'Surface Engineering: Current Trends and Future Prospects' conference at the University of Toronto in June 1990.	B1

# NOMENCLATURE USED IN THE THESIS

---

$a$	acceleration
$a_i$	internal surface area of a die
$a_o$	external surface area of a die
$A$	a cross sectional area
$A_{pw}$	amplitude of pressure fluctuation
$C_p$	specific heat capacity
$e$	Bagley end correction parameter
$h$	height of slit die flow path
$h_i$	surface heat transfer coefficient between a die and a polymer.
$h_o$	surface heat transfer coefficient between a die and air.
$K, K_1, K_2, K_3$	mathematical constants
$l$	length
$m$	mass
$M_d$	torque at the measuring spindle on the concentric cylinder rheometer
$n$	mathematical constant or rotor r.p.m. on the concentric cylinder rheometer
$p$	pressure
$P_d$	pressure drop down the length of a die
$P_{min}$	minimum pressure
$\Delta P$	pressure drop
$\Delta P_c$	die pressure drop corrected for entrance and exit effects
$\Delta P_l$	long die pressure drop
$\Delta P_w$	pressure drop across whole die
$\Delta P_o$	zero length (orifice die) pressure drop
$\dot{q}$	heat generation rate
$Q$	volumetric flow rate

$r$	radius
$r_a$	radius of concentric cylinder rheometer cup
$r_d$	die radius
$r_i$	radius of concentric cylinder rheometer rotor
$r_{tci}$	radial position of inner thermocouple
$r_{tco}$	radial position of outer thermocouple
$R_a$	arithmetic or centre-line average surface roughness parameter
$R_{max}$	surface roughness parameter-largest single peak to valley height in 5 adjoining sample lengths
$R_z$	surface roughness parameter-average height differences between the five highest peaks and the five lowest valleys within an assessment length
$S$	shear stress 'scale factor' on the concentric cylinder rheometer (full scale = 100)
$t$	time
$\Delta t$	time interval
$v_r$	velocity at a radius $r$
$v_s$	slip velocity
$w$	width of slit die flow path
$W_{pw}$	wavelength of pressure fluctuation
$x$	element size
$\dot{\gamma}$	shear strain rate
$\dot{\gamma}_r$	shear strain rate at a radius $r$
$\dot{\gamma}_w$	"true" wall shear strain rate
$\dot{\gamma}_{w,a}$	apparent wall shear strain rate
$\eta$	dynamic viscosity
$\eta_o$	zero shear rate viscosity
$\eta_a$	apparent dynamic viscosity
$\theta$	temperature

$\theta_a$	ambient air temperature
$\theta_p$	temperature of polymer at the die wall
$\theta_r$	temperature at a radius $r$
$\theta_{tci}$	temperature of inner thermocouple
$\theta_w$	temperature at the die wall
$\lambda_p$	thermal conductivity of the polymer
$\lambda_w$	thermal conductivity of the die wall
$\pi$	mathematical constant (3.141593)
$\rho$	density
$\tau$	shear stress
$\tau_r$	shear stress at a radius $r$
$\tau_w$	wall shear stress
$\tau_y$	yield shear stress
$\Phi$	heat flow rate

# 1. INTRODUCTION

---

Extrusion honing is a process used to finish machine edges and surfaces of engineering components by the controlled extrusion of an abrasive laden viscoelastic polymer (polyborosiloxane) across these edges and surfaces [1]. The process may be used to deburr or modify the intersections of machined surfaces, or polish machined areas, resulting in a significant improvement to the surface finish. Additional benefits of the process include surface texture modifications and the removal of surface layers which have been subject to mechanical or thermal damage [2].

Since the initial development of the process in the mid-1960's, to deburr hydraulic control blocks for Phantom jets, the process has gained widespread acceptance across the broad spectrum of modern manufacturing industry [3]. Applications now range from high technology aerospace components to high volume automotive components.

It is evident that the machining process is very dependent upon the physical and mechanical characteristics of the abrasive laden compound [4]. However, the process to date has largely been developed empirically, and further developments will require a greater understanding of the relationship between the characteristics of the polymer and the machining action.

## 1.1 Objectives of the research

The aim of the research programme was to achieve a better understanding of the thermal and fluid flow properties of polyborosiloxanes, in order to establish a basis for the control and optimisation of the extrusion honing process. The proposed approach to achieve these

objectives was to determine both thermal and rheological properties of the polyborosiloxane in order to formulate mathematical models which may be either used predictively for specific extrusion honing operations, or used more generally to explore some of the mechanisms of extrusion honing.

The rheological characteristics of the polyborosiloxane were to be determined using a capillary rheometer, a slit die rheometer and a concentric cylinder rheometer. It was intended that the capillary rheometer would be used for the majority of the rheological experimentation due to its similarity with the extrusion honing process both in terms of geometry and operating mechanism. Experiments were to be completed over a broad shear rate range at temperatures between 20-70°C, which would cover most extrusion honing applications. From this data it was intended to formulate constitutive rheological equations such that the shear stress at the die wall may be predicted from the shear rate and polyborosiloxane temperature. In addition it was intended to model the velocity, shear rate and shear stress variations within a die during extrusion honing. Such data would be useful as it may be related to the efficiency of the extrusion honing process (stock removal, surface finish etc.). The shear stress at the die wall was expected to be a function of the polyborosiloxane temperature. It would therefore be necessary to calculate the temperature distribution within the die during extrusion honing. In order to complete such calculations it was intended that the thermal properties of the polyborosiloxane would be determined. These properties would include the heat capacity, the thermal conductivity and the surface heat transfer coefficient between the polyborosiloxane and the die to be extrusion honed. The heat generation within the polyborosiloxane during extrusion honing was to be calculated from temperature measurements taken within the extrusion die. It was intended that when this heat generation term had been quantified a mathematical model would be formulated to predict temperature profiles within a die during extrusion honing. When this

temperature distribution was known the constitutive rheological equations may be used to calculate the velocity, shear rate and shear stress distributions within the extrusion die.

It was intended that the data generated from the experiments and mathematical models would be used to discuss the flow mechanism of the polyborosiloxane. The data generated and the proposed flow mechanism would be discussed with specific reference to the extrusion honing process.

## **2. LITERATURE REVIEW**

---

### **2.1 Introduction**

The literature review has been divided into five main sections. Initially, by means of an introduction, the general concept of surface finishing in modern manufacturing has been discussed (section 2.2). This has included a brief review of both the quantification and the measurement of surface finish.

Following on from this introductory section the specific surface finishing technique of extrusion honing has been reviewed (section 2.3). This section reviews the basic principles of the process, as well as relevant process research and development completed to date.

The extrusion honing process utilises the properties of a polyborosiloxane material [1] to achieve a surface finish improvement. Consequently, the properties of this polyborosiloxane material have been studied in order to gain a greater understanding of the extrusion honing process. The response of polymers to deformation and flow have been reviewed within section 2.4. Current literature on the rheological techniques utilised to study this material within the research programme have been reviewed within section 2.5. The final section of this chapter contains a review of previous work completed to characterise the rheological properties of the polyborosiloxane material (section 2.6).

## **2.2 Surface finishing**

### **2.2.1 Surface finishing in modern manufacturing**

Surface finishing of engineering components has been cited [5] as an increasingly important factor in modern manufacturing. It has been further suggested [5] that the various reasons for achieving improved surface finish may be classified into two broad categories; functional requirements or appearance requirements [5]. Typical product functional benefits obtained as a result of improved surface finish are well documented within the literature [5,6]. These may include increased wear resistance, better lubricant retention or an increase in corrosion resistance. Other benefits listed [5] include increased efficiency of gears and other power transmissions, a reduction in failures (by the removal of potential stress raisers such as burrs, nicks etc.), and reduced turbulence and increased flow rates of fluids through components.

Many engineering components require coatings, such as plating, painting or anodising. The surface quality of a component prior to processing has been cited [5] as a key factor in the determination of the final quality of such applied coatings. Further benefits of improvements to surface finish have been listed [5] as greater ease of assembly, improved performance, and in some cases increased fatigue strength.

Improving the appearance of a product for purely aesthetic reasons has also been reported [5] as an important consideration. This is because a more aesthetically pleasing product may often have increased salability over competitive products, and reflects a concern for quality by the producer.

## 2.2.2 Quantification of surface finish

Most countries with an industrial or partly industrial society have their own national roughness standards [7]. This has resulted in an extremely large variety of roughness parameters and definitions. However, international standard, ISO R468 [8], embodies three universal surface roughness definitions which are briefly outlined below.

The most universally recognised and used parameter to describe surface roughness has been identified as the arithmetic or centre-line average,  $R_a$ [7]. This is described as the arithmetic mean of the departures of the profile from the mean line, and is normally determined as the mean result over several sampling lengths. It has been stated by Thomas [7] that whilst  $R_a$  provides a useful surface roughness control parameter it can reveal neither the greatest extent nor the nature of the irregularities. Thomas [7] further explains that as  $R_a$  is a calculated average it may produce an identical value for surfaces of vastly differing characteristics. Gillespie [6] also expresses concern at the use of  $R_a$  in isolation to characterise surface finish, as even surfaces with low  $R_a$  values may contain relatively deep tool scratches. Both Gillespie [6] and Thomas [7] recommend the use of the internationally used parameter of  $R_{max}$  or  $R_z$  in addition to the  $R_a$  value described above. The parameter  $R_{max}$ , defines the maximum peak-to-valley height, and is calculated from the largest single peak-to-valley height in five adjoining sample lengths [7]. The mean peak-to-valley height  $R_z$ , is described by Thomas [7] as the average height differences between the five highest peaks and the five lowest valleys within the assessment length.

These three surface roughness parameters are all vertical descriptors, giving quantitative information relating to the peak and trough heights of the surface, without giving any indication as to the 'openness' or 'closeness' of the surface [7]. The 'openness' or 'closeness' of the structure may be described by horizontal descriptors. Thomas [7] has concluded that these horizontal descriptors, mostly reduce either to the number of peaks

per unit length of the profile (peak density) or the number of times the profile intersects its own mean line (zero-crossing density) [7].

### **2.2.3 Measurement of surface finish**

It has been reported [7] that the most commonly used instruments to measure surface roughness are those based on the use of the stylus instrument, where a sharp probe traverses a surface and transforms its minute irregularities into some other form of energy, such as an electric signal. Other surface measurement instruments described [7] include optical methods, contact methods, electrical methods (including capacitance, induction and skin resistance), and fluid methods (including scraping, sand patch, outflow meter, pneumatic, gauging, oil droplet, stagnant layer and flowing drop).

## **2.3 Extrusion honing**

### **2.3.1 Principles of extrusion honing**

Extrusion honing has been described by Rhoades [2] as a process in which a semi-solid abrasive medium is forced (or extruded) through a workpiece passage. Rhoades [2] further states that this medium will only abrade the area or areas that form the greatest restriction in its flow path, and that by controlling this abrasive flow, a range of precision machining and finishing effects can be produced, including deburring, radiusing, polishing, and thermal recast layer removal.

A number of authors [2, 9, 10] have described the extrusion honing process as consisting of three major elements ((i) the machine, (ii) the fixture (or tooling), and (iii) the abrasive medium). Each of these three major elements are reviewed in the sections below.

### ***The extrusion honing machine***

Kohut [10] has described the general configuration of an extrusion honing machine, such as the one shown in figure 1 [11], as consisting of two vertically opposed cylinders which close to hold a component (or fixture containing a component) between them. Kohut [10] further explains that by repeatedly extruding abrasive medium from one cylinder to the other, an abrasive action is produced wherever the abrasive medium enters a restrictive passage, as it travels through or across the component. Similarly, Perry [9] has described how the extrusion honing machine must perform two main functions. Firstly it must clamp and seal a component such that the abrasive mixture is contained within the system, and secondly, it must have the capability to pump a preselected quantity of abrasive medium through the component at a specified pressure.

Whilst the overall configuration of extrusion honing machines remains constant throughout the literature, some variation in the design of specific components of a machine may vary. For example Perry [9] has described a particular design where each of the vertically opposed abrasive medium cylinders are driven by two hydraulic cylinders whereas Spiotta [12] describes a design where only one hydraulic cylinder drives each abrasive medium cylinder. Similarly the mechanism for clamping components in position between the media cylinders may be hydraulic as described by Spiotta [12] or mechanical with worm screw jacks as described by Perry [9].

The two main variations in design between different extrusion honing machines reported within the literature are the physical size of the machine, and the force with which the abrasive medium is pumped. Typical applications of the different size machines available have been described by Rhoades [2]. Rhoades [13] also describes how the pressure at which the abrasive medium is pumped may be adjusted in the range 0.7 to 22 MPa

depending on the application. Perry [14] describes a particular extrusion honing design where the pressure is limited to 3.5 MPa.

One feature which is often incorporated on extrusion honing machines, is a heat exchanger to control the temperature of the abrasive medium [9, 15]. It has been reported [16] that the abrasive medium temperature is controlled in order to maintain constant abrasive medium viscosity, and therefore a constant machining action.

### ***The fixtures or tooling***

The function of tooling in extrusion honing has been described [17, 18] as a means to hold the workpiece in position and to contain and direct the flow of abrasive medium. Rhoades [17] further explains that when designing tooling, the areas where abrasion is desired are first identified. The tooling is then constructed so that the flow of media through or across these areas is restricted. Stackhouse [18] also supports this approach to tool design; explaining that in general the greatest machining action occurs at the greatest flow path restriction. For a workpiece with straight-through passages such as a tube, an internal spline, a valve plate, or an extrusion die, the tooling merely holds the parts in place between the cylinders and allows the through-passages to restrict the media flow.

To process external edges or surfaces, the part is contained within a flow passage, so that the flow is restricted between the outside of the part and the interior of the flow passage [17]. Counterbores, recessed areas, or even blind cavities can be processed using a restrictor or mandrel to fit inside the components and restrict the flow at the desired areas [17].

Rhoades [17, 19] has described how large numbers of parallel restrictions may be processed at once, and that in many cases, two (occasionally more than two) successive

restrictions in the same flow stream can be abraded, so long as the cross-sectional areas of the successive restricting passages are equal. This enables the processing of more than one component in one operation if suitable tooling is designed [19]. Stackhouse [18] has reported that the number of workpieces processed in each fixture will depend on the size of the extrusion honing machine and the viscosity of the abrasive medium used. Stackhouse [18] further describes how the number of workpieces to be processed in each fixture is often determined by reviewing the results obtained in preliminary tests using a single component tool.

It has been reported [17] that very complex parts, such as valve bodies, may require processing in two or more operations, processing some areas in one operation and others, with different flow paths in the next. Similarly very large parts can be processed in sections [17].

### ***The abrasive medium***

Rhoades [2] has described how the finishing action in the extrusion honing process is produced by the transfer of the machine extrusion force through a putty-like polymer carrier in which a mixture of abrasive grains are evenly dispersed.

The exact composition of the base polymer to which the abrasive grains are added is not well documented, possibly because it is considered industrially sensitive by companies utilising the process. However the material is generally reported [1, 20] to be a viscoelastic polyborosiloxane polymer such as that supplied by The Extrude Hone Corporation for the purposes of this research programme. Current published rheological data relevant to this material has been reviewed within section 2.6. Perry [4] describes how a wide range of extrusion honing bases are available depending on the application. It has been reported [9,21] that higher viscosity bases are more appropriate for extrusion honing large orifices

or if a large number of orifices are to be processed at once. For smaller holes, or longer passages requiring extrusion honing, lower viscosity bases are generally more appropriate [9]. It has also been reported [9] that lower viscosity base is more appropriate for generating radii at intersections within components.

The abrasive grain, which is mixed into the polyborosiloxane carrier, could be almost any material, but most common are: silicon carbide, aluminium oxide, and boron carbide [22, 23]. Diamond may be used to polish harder materials such as tungsten carbide [9]. Perry [4] has reported that the size of the predominant abrasive particles used in any particular extrusion honing medium is determined by the amount of stock removal and the surface finish desired. It has also been reported by a number of authors [2, 9, 10] that the size of the abrasive grains used must be appropriate to the dimensions of the flow path within the component or blockage may occur.

### **2.3.2 Process research and development**

Very few workers have completed detailed investigations into the mechanism of the extrusion honing process, and the relative importance of the various process variables. Williams [24] has completed the most comprehensive investigation into the extrusion honing process. However, Williams [24] has concentrated on quantifying the relationship between medium viscosity, extrusion pressure and machining time on the metal removal and surface finish produced rather than a specific investigation into the machining action.

Whilst the exact mechanism of the extrusion honing process has not been investigated in detail a number of papers have been published which have investigated various aspects of the process. Within these publications [2, 9, 12, 14, 24] it is generally accepted that the finishing action of the extrusion honing action is produced by the transfer of the machine extrusion force through the abrasive medium to the workpiece edges and surfaces.

The two factors which control the abrasion produced have been stated by Rhoades [2] to be the depth of cut and the number of cuts made by the abrasive grains. The number of cuts made was given as a function of the volume of abrasive medium passed through the restriction and of the size and concentration of abrasive in the abrasive medium [2]. The depth of cut made by the abrasive grains was given as a function of the size, relative hardness, and sharpness of the abrasive grains, and the extrusion pressure [2]. In support of the last proposals the relationship between metal removal and extrusion pressure in extrusion honing has been shown to be significant by Williams [24].

The importance of abrasive medium viscosity on the abrasive action achieved has been discussed by various authors [2, 9, 12, 14]. Rhoades [2] has cited the abrasive medium viscosity as being an important parameter in determining the quantity of hydraulic extrusion pressure transmitted to the abrasive grains at the component interface. He proposed that whenever the polymeric component of the abrasive medium was forced into a restriction its viscosity increased substantially resulting in significant abrasion of the passageways. It was suggested that when the thickened portion of abrasive medium left the restrictive passageway, its viscosity returned to a much lower value. In this case little or no abrasion was produced.

This ability of the extrusion honing process to abrade selectively in areas of restriction has also been discussed by Perry [9]. However, Perry [9] does not relate the selective nature of the process to any changes in media viscosity but simply states that the abrasion is greatest where media velocity is highest. Perry [9] describes how high viscosity polymers provide a very elastic matrix for the abrasive grain and provide the highest material removal rates per unit flow. Spiotta [12] has also discussed the affect of media viscosity on the machining process. Spiotta [12] proposes that low viscosity bases provide a more flexible matrix, more appropriate for flow through small holes and for generating edge radii.

Literature referring to the rheological properties of the polyborosiloxane material utilised in the extrusion honing process has been reviewed in greater detail within section 2.6.

## **2.4 The rheological response of polymers to deformation and flow**

Rheological equations of state express mathematically the relationship between stress, strain and time [25]. Brydson [25] has described the simplest such relationship, exhibited by Newtonian fluids, where the shear stress is linearly proportional to the shear strain, the constant of proportionality being the shear viscosity. The rheological equation of state for Newtonian fluids may be written as [25]

$$\tau = \eta \dot{\gamma} \quad (2.1)$$

However, Dealy [26] explains that most polymers are non-Newtonian, such that a single measure of viscosity is not sufficient to predict rheological behaviour for any deformation. The viscosity of such fluids is no longer constant, but is a function of the shear rate [26]

$$\eta = \eta(\dot{\gamma}) \quad (2.2)$$

If the viscosity increases as the shear rate increases then the material is known as dilatant [26]. Pseudoplastic behaviour is represented by a decrease in viscosity as the shear rate increases [26]. Pseudoplastic behaviour is the more common phenomena [26].

It is well documented within the literature [26, 27, 28] that this variation in viscosity with shear rate is due to changes in the molecular structure of the polymer. Consequently, at very low shear rates, these materials may exhibit constant viscosity, as there are few changes to the material structure due to the minimal amount of deformation [26]. This low

shear rate viscosity is given the symbol  $\eta_0$ , and is known as the zero shear rate viscosity [26].

The most commonly used non-Newtonian rheological equation is the power law or Ostwalde-de Waele [29] equation which may be written as

$$\tau = K\dot{\gamma}^n \quad (2.3)$$

The extent of the use of the power law equation has been highlighted by Tachibana et al [30] who reviewed the works of 26 authors who have studied the steady laminar flow of non-Newtonian fluids; 16 of these authors had used the power law relationship.

Many other authors [25-29] have described the power law equation as the most commonly used to describe the flow behaviour of polymer melts. Other inelastic flow models which are contained within the literature are described below.

#### **Herschel-Bulkley model [23]**

$$\tau = \tau_y + K\dot{\gamma}^n \quad (2.4)$$

This equation represents the behaviour of a plastic material to which a certain stress known as the “yield stress” can be applied without deformation occurring. However, if a stress in excess of this “yield value” is applied then the material will yield and viscous flow will commence [26]. The “yield stress” of a plastic material may be determined by measuring the resultant shear stress when the material is subjected to a range of shear deformation rates; as the shear deformation rate approaches zero, the shear stress will approach a finite limiting value, which is the “yield stress” [26].

### Vocadlo model [28]

$$\tau = (\tau_y^{1/n} + K\dot{\gamma})^n \quad (2.5)$$

This model is similar to the Herschel-Bulkley model in that a yield stress is included although the flow response described above the yield stress is modified.

### Ellis model [29]

$$\dot{\gamma} = K_1\tau + K_2\tau^n \quad (2.6)$$

This model with  $n > 1$ , shows Newtonian behaviour at low shear stresses and power law behaviour at high stresses [28].

### Ree-Eyring model [28]

$$\tau = C_1 \sinh^{-1} K_1\dot{\gamma} + C_2 \sinh^{-1} K_2\dot{\gamma} \dots \quad (2.7)$$

### Casson model [29]

$$\sqrt{\tau} = \sqrt{\tau_y} + K_1\sqrt{\dot{\gamma}} \quad (2.8)$$

### Power series models [28,29]

$$\dot{\gamma} = K_1\tau + K_2\tau^3 + K_3\tau^5 \dots \quad (2.9)$$

$$\tau = K_1\dot{\gamma} + K_2\dot{\gamma}^3 + K_3\dot{\gamma}^5 \dots \quad (2.10)$$

These series include only odd powers of the variables so that they still apply if the directions of stress and strain rate are reversed [28].

If the viscosity of the polymer is solely a function of the shear rate (being either pseudoplastic or dilatant) then the material may be categorised as a generalised Newtonian

fluid [26]. However, it is unusual for non-Newtonian fluids to be completely rheologically categorised by either pseudoplastic or dilatant viscosity expressions. This is because they usually exhibit one or more of the flow phenomena of plasticity, time dependent structures or viscoelasticity. Plasticity within polymer melts has been discussed above. The “yield stress” associated with such materials forms an intrinsic part of the Herschel-Bulkley [28], Vocadlo [28] and Casson [29] models listed above. The flow phenomena of time dependent structures and viscoelasticity are briefly reviewed in the sections below.

### ***(i) Time dependent structures.***

The structure of some polymers may take time to change as the material deforms at a certain shear rate, so that the viscosity measured will vary with time [26]. Thus the viscosity becomes a function of shear rate and time. There are two main types of time dependent structures; thixotropic and rheotropic. A thixotropic material gives a decrease in viscosity with time whereas a rheotropic material gives an increase in viscosity with time [26]. In general [28] thixotropic and rheotropic variations in viscosity with time are reversible the material being restored to its original condition by resting for a sufficient time free from stress. However, Whorlow [28] reports the occurrence of permanent reductions in viscosity. Such behaviour was termed rheomalaxis.

### ***(ii) Viscoelasticity***

A viscoelastic material is one which responds to external forces in a manner intermediate between the behaviour of an elastic solid and a viscous liquid [31]. According to Christensen [32] elastic materials are those which have a capacity to store mechanical energy whereas Newtonian viscous fluids in a non-hydrostatic stress state implies a capacity for dissipating energy. Consequently viscoelastic materials possess a capacity to both store and dissipate mechanical energy. These materials may also be characterised by their reaction to the application and cessation of applied shear stresses and strains [32].

Two such reactions exhibited by viscoelastic materials are stress relaxation and elastic recoil [26].

***(i) Stress relaxation***

Stress relaxation may be illustrated by consideration of a material subjected to steady continuous shear between two horizontal plates moved in opposite directions [26]. If the boundary plates are stopped and held in position, then for an inelastic fluid no stress is necessary to hold the plates in position once shearing has stopped. If a viscoelastic material is subjected to similar conditions then the boundary plates would require a stress to hold them in position. This stress will decay to zero over a period of time [26].

***(ii) Strain recovery (recoil)***

Strain recovery of viscoelastic materials can be illustrated in a similar way to stress relaxation. If an inelastic fluid is subjected to steady shear for a period of time and then the shear stress is removed the shear strain would be unchanged. However in the case of a viscoelastic fluid some of the shear strain will be recovered when the shear stress is removed. This is known as strain recovery or elastic recoil [26].

Whilst a material demonstrating a combination of elastic and viscous properties has been described as viscoelastic in the section above, authors such as Brydson [25] are more specific in their categorisation. Brydson [25] described materials which are predominantly viscous (with some elasticity) as viscoelastic whereas materials which are predominantly elastic (with some viscous properties) are described as elasticoviscous. However Brydson [25] states that it is not normally crucial to define the boundaries between such behaviour as the mathematical theories of viscoelasticity may be applied to viscous, viscoelastic, elasticoviscous and viscous materials.

## 2.5 The capillary rheometer

### 2.5.1 Introduction

Dealy [26] has described the capillary viscometer (or rheometer) is an instrument for measuring the flow properties of liquids. The common type of capillary rheometer for polymer melts consists of a temperature controlled barrel at the bottom of which is fitted a small die containing a capillary. There are two main types of capillary rheometer. The first is an instrument in which a plunger is forced down into the barrel (filled with polymer) at a constant rate and the pressure required is measured by a transducer or other appropriate means. Alternatively, an instrument may be used in which a load is applied to the top of the melt and the output rate for this load is measured. The load may be applied by means of weights or by the pressure of an inert gas [26].

Derivation of the shear strain rate and shear stress calculations used for capillary flow are covered in detail within many excellent texts [25, 26, 27, 28]. Dealy [26] has shown the apparent wall shear strain rate to be

$$\dot{\gamma}_{w,a} = \frac{4Q}{\pi r^3} \quad (2.11)$$

The subscript w in equation 2.11 is used to denote that the shear rate is the shear rate at the wall. The subscript a in equation 2.11 is used to denote apparent shear rate because the derivation of equation 2.11 is based on an assumption that the velocity profile perpendicular to the flow direction is parabolic which is only true for Newtonian fluids [25]. A more general expression of the shear rate at the wall, expressed as the “true shear rate” at the wall has been derived by Rabinowitsch as follows [25]

$$\dot{\gamma}_w = \frac{1}{\pi r^3} \left[ 3Q + \Delta P \frac{dQ}{d\Delta P} \right] \quad (2.12)$$

Dealy [26] has shown the apparent wall shear stress to be

$$\tau_w = \frac{\Delta P_w r}{2l} \quad (2.13)$$

Brydson [25] has reported that these equations may only be valid if the following assumptions are made.

- (i) That the flow pattern is constant along the full length of the capillary.
- (ii) That there is no slip at the capillary wall
- (iii) That the fluid is time independent
- (iv) That the flow is isothermal
- (v) That the melt is incompressible

The validity of these assumptions, as well as a number of unusual flow phenomena noted by previous workers who have studied capillary flow, are reviewed in the sections below.

## **2.5.2 Die entrance effects and end corrections**

The first of Brydson's [25] assumptions for capillary flow, listed above, is that the flow pattern is constant along the full length of the capillary. During capillary extrusion of polymer melts a pressure drop in the die entrance region has been reported by a number of authors [25, 26, 27, 28]. Similarly, a pressure drop at the die exit is also described within the literature [25, 26, 27, 28].

Dealy [26] refers to the excess pressure drop at the die entrance as the "entrance pressure drop", and the length of die required before fully developed flow commences as the "entrance length". The entrance pressure drop generally makes a substantial contribution to the measured pressure [33]. It must therefore be allowed for in the analysis of the

extrusion rheometer results [26]. Isayev and Chung [34] have found these entrance and exit pressure drops to be a particular problem when studying the flow of polymer melts in short capillaries where a significant proportion of the total pressure drop may be due to these entrance effects. Bagley [35] has studied die entrance pressure drops and described a suitable method for correcting rheometer data to allow for such pressure drops. Bagley [35] demonstrated how a plot of pressure drop against die length to internal radius ratio at a fixed wall shear rate gives a straight line relationship. The intercept of these plots were described by Bagley [35] to be equivalent to the pressure drop due to die entrance and exit effects. The Bagley [29] plot gives the value of an end correction,  $e$  [26], where  $e$  is the die length to radius ratio as read from the Bagley [35] plot between the x-axis intercept and zero die length to radius ratio. Dealy [26] has modified the wall shear stress equation to take into account this end correction parameter  $e$  as follows

$$\tau_w = \frac{\Delta P_w}{2(l/r + e)} \quad (2.14)$$

Cogswell [27] has reported that a Bagley [35] end correction calculation requires extensive experimentation using dies of several different lengths. However, Cogswell [27] has suggested that in practice two dies may be adequate to determine end correction factors. When using two dies only for end correction Cogswell [27] recommends the use of a long die of length to internal radius ratio of 32 and an orifice restriction die of nominally zero length. The entrance and exit pressure drops are calculated by subtracting the pressure drop obtained using the zero die from that obtained using the long die. The shear stress at the wall allowing for die entrance and exit pressure drops by the zero die technique has been given by Cogswell [27] as

$$\tau_w = \frac{(\Delta P_1 - \Delta P_0) r}{2l} \quad (2.15)$$

The entrance pressure drop has been studied in considerable detail by La Mantia et al [36]. They [36] were able to derive entrance corrections as functions of temperature, weight-average molecular weight and molecular weight distribution. Bagley [37] has investigated the relationship between these “end corrections” and the shear stress. For polyethylene it was found that the relationship was linear, up to a critical shear stress at which extrudate distortion began.

### **2.5.3 Barrel height effects and piston friction**

The barrel height effect is a problem encountered on rheometers which measure extrusion pressure by means of a load cell on the extrusion ram, where there may be a pressure drop between the die and the ram tip [27]. This pressure drop has been reported by Cogswell [27] to be due to frictional and reservoir flow losses. As the ram descends the effective length of the barrel decreases, thus a variable correction is required to the measured pressure to allow for flow in the reservoir and frictional forces. Cogswell [27] recommends that the measurement of pressure is made just above the die in order to eliminate these errors. More specifically, Brydson [25] suggests that a pressure transducer inserted into the side of the barrel just above the die will ensure that these errors do not prevail.

### **2.5.4 Wall velocity and slip-stick phenomena**

It is a fundamental assumption in many calculations involving polymer flow through capillary dies that the velocity of the polymer at the wall is zero [25,38,39]. However, many authors [25-28] have either demonstrated experimentally or discussed theoretically, the occurrence of non-zero wall velocities in capillary dies.

Constant wall slippage at the capillary wall has been investigated by a number of workers [25, 40, 41]. Mooney's [40] paper of 1931, contains one of the earliest calculations of wall

slip in capillary rheometer dies. Mooney's [40] original equation has been adapted by many authors including Lupton and Register [42] and Brydson [25]. The basis of the Mooney [40] equation has been presented by Brydson [25] in a general qualitative manner. Brydson explains [25] that if slip occurred at the wall a form of plug flow would superimpose on the normal flow patterns. Consequently if experiments were carried out on tubes of different dimensions, the flow curves plotted would not super-impose, because the calculated values of the shear rate would be in error [25].

Worth et al [41] have also investigated this method of calculating wall velocity, once again based on the Mooney equation adapted by Lupton and Register [42]. The Mooney equation expressed in the form used by Worth et al [41] may be written as follows

$$\frac{4Q}{\pi r^3} = 4 v_s \frac{1}{r} + \frac{1}{\pi_w^3} \int_0^{\tau_w} \tau^2 \dot{\gamma} d\tau \quad (2.16)$$

This equation is of linear form, and thus a plot of  $4Q/\pi r^3$  against  $4/r$  will give a straight line of slope equal to the slip velocity. Worth et al [41] used the Mooney equation plots to show that the wall velocity increased with increasing wall shear stress. Both of the polymer melts (low and high density polyethylenes) considered by Worth et al [41] exhibited wall slip at shear stresses above the critical shear stress for melt fracture.

Shaw [43] has also discussed the use of the Mooney [40] equation to correct capillary rheometer data for wall slip. Shaw [43] presents a compilation of experimental results of wall slip calculations from various authors.

All of the above workers have studied wall velocity in capillary flow by indirect measurements and by the use of the various forms of the Mooney [40] equation. However, a number of authors have attempted to measure wall velocity directly by a variety of

experimental techniques. One such technique for the measurement of wall velocity has been developed by Maxwell and Galt [44]. This employed a small particle tracer technique, involving random distribution of small particles throughout a molten polymer, which recorded the individual motions of the particles when stress was applied to the polymer. The movement of the individual particles was recorded by a camera focusing through a microscope onto a transparent section of an extrusion die. The camera produced dashed traces as the focal area of the camera was illuminated by a test lamp beam periodically interrupted by a rotating timing wheel. The individual particle velocities were determined from the length of the traces. All polymers tested by Maxwell and Galt [44] were low density, branched polyethylenes. Results from this experimentation showed a mixture of stationary particles, which it was concluded were stuck to the wall, and moving particles which it was concluded were slipping along the wall. Thus the particles oscillated between two distinct velocities (one of which may be zero). Such movement of the particles, and therefore the polymer, was termed slip-stick. Maxwell and Galt [44] also demonstrated that the radial extent of the boundary annulus of slip- stick behaviour at the wall could be defined by the extent of the layer of zero velocity traces from the wall. It was concluded by Maxwell and Galt [44] that the flow in the die was laminar, due to the lack of particle rotation or spin. Such movement would not be susceptible to the simple analysis of continuous slip of Mooney [40] unless an average velocity is assumed.

Additional experimental techniques for measuring wall velocity have been investigated by Rhoades [45]. Rhoades [45] was particularly interested in the flow of polyborosiloxane during extrusion honing (section 2.3). A similar technique to Maxwell and Galt [44] was employed, where high speed photography was used to record the motion of particulate matter in the polymer viewed through a transparent die. However, Rhoades [45,46] found insufficient data points could be recorded for his theoretical model, due to turbulence within the polymer. Rhoades [45] also measured the hydraulic piston displacement of his

test equipment in order to estimate polymer wall velocity. However, this method may be described as indirect and gives measurement of the average polymer velocity rather than the specific velocity of polymer at the wall. Nevertheless, evidence was found of cycling of the piston velocity at such a frequency that it was considered likely to be the result of slip-stick [45]. Rhoades [46] suggested that the technique of hot film anemometry may be very useful in further studies of wall velocity of polyborosiloxanes through extrusion dies.

The mechanism for wall slip or slip-stick has been discussed by a number of authors. Whorlow [28] stated very simply that if adhesion between the polymer and the die wall will withstand a shear stress up to some limit, local slippage will occur wherever the limit is exceeded, resulting in a non-zero wall velocity. Similarly Worth et al [41] stated that the wall slip may commence at a critical value, the value of which will depend on the particular interfacial situation, and the elastico-viscous nature of the fluid.

A number of authors [28,41] have discussed phenomena which may exaggerate wall slippage in capillary dies. Whorlow [28] states that a non-zero wall velocity will be obtained if a lubricating layer of low viscosity material occurs at the die wall, resulting in apparent slippage of the main body of the material. Worth et al [41] comment that the apparent manifestation of wall slip they recorded, in low density polyethylene, may not be true slip but a viscous heating effect caused by high shear rates near the die wall.

The mechanism proposed by Maxwell and Galt [44] extends the theories of continuous slip to slip-stick phenomena. Maxwell and Galt [44] proposed that the melt sticks to the die wall and is elastically deformed as a shear stress is applied by the bulk flow of the polymer. Once the deformation has resulted in a shear stress in excess of the adhesive force between the polymer and the die wall, the polymer slips, thus removing the elastic strain.

This process is cyclically repeated down the die resulting in an overall slip-stick effect at the wall [44].

Dealy [26] states that at flow rates above those at which slip stick occurs, a smooth extrudate may be observed. It is proposed that this results from the permanent detachment of the polymer from the die wall. Dealy [26] attached considerable importance to wall slippage as a mechanism for effects such as oscillating flow and melt fracture in capillary flow. These and other effects, considered to be closely linked with wall slippage are reviewed in the appropriate sections below.

### 2.5.5 Velocity and shear profiles in capillary flow

The velocity profile in the “fully developed flow” region of a capillary die may be considered in its simplest form if a Newtonian, isothermal, incompressible fluid is considered, where the wall velocity is zero. Whorlow [28] has presented an equation for the velocity profile of such a Newtonian fluid as follows

$$v_r = \frac{\Delta P_w}{4\eta} (r_d^2 - r^2) \quad (2.17)$$

A more complex equation to express the velocity profiles during capillary flow for time independent power law fluids has been presented by Brydson [25], as follows

$$v_r = \left( \frac{n}{n+1} \right) \left( \frac{1}{2k} \frac{dp}{dr} \right)^{1/n} r^{(n+1)/n} \left[ (r_d/r)^{(n+1)/n} - 1 \right] \quad (2.18)$$

Many authors who have studied the theoretical velocity profile of polymers in extrusion dies have assumed zero wall velocity and incompressibility. In addition, the majority of these texts have used a form of the power law equation to calculate velocity profiles. The extent of use of the power law equation has been highlighted by Tachibana et al [30] who

reviewed the works of 26 authors who have studied the steady laminar flow of non-Newtonian fluids; 17 of these authors had used the power law relationship.

Maxwell and Galt [44] have studied velocity profiles in the fully developed flow region of a capillary die. From the photographic particle tracer technique employed Maxwell and Galt [44] categorised the regions of flow within the polymer into three distinct types; the boundary annulus, the shear annulus and the “plug”. The boundary annulus was described as an annulus of polymer at the die wall, which may be subject to slip-stick behaviour as described within section 2.5.4. The shear annulus was described as an annulus of polymer between the boundary annulus and the central plug region. In this region it was stated [44] that the polymer may undergo viscous or visco-elastic shear flow. Maxwell and Galt [44] categorised the plug as a central region of the polymer where the material flows with little shear at a near uniform velocity across its section. From the result obtained Maxwell and Galt [44] found that increasing the extrusion pressure did not significantly raise the wall velocities, but did increase both the plug flow velocity and extent of the shear annulus region. The experimental values were used to calculate true shear rate data at the wall which were compared with values calculated assuming a power law relationship. It was found that the polymer was actually more non-Newtonian than that indicated by the calculated viscosity data.

Many authors have studied the velocity profile in the entrance region of capillary dies [47,48,49]. One experimental technique used extensively in this area is flow birefringance, a technique reviewed in detail in Janeschitz-Kriegl's text [49]. Alternatively, coloured discs have been used to study the flow patterns around the entrance region of capillary dies [47]. Ma et al [47] technique involved stopping the rheometer midway through an extrusion and allowing the polymer to solidify in the barrel. The polymer was then removed from the rheometer, sectioned, and the flow patterns studied. Yoganathan and

Yarlagadda [48] also studied velocity profiles in the entrance regions of capillary dies. They studied the flow patterns of viscoelastic Separan (AP-30) solutions by photographing tracer particles illuminated by laser beam.

### **2.5.6 Wall pressure and flow rate fluctuations**

Myerholtz [50] references a number of papers which report the presence of oscillating die flow rate during the capillary extrusion of polymer melts in equipment operating at constant displacement rate. Meyerholtz [50] describes how there are low and high shear rate regions where the extrusion force remains constant, but in an intermediate shear rate region, the extrusion force and actual output rate oscillate between two values. Similarly, Takaoka and Veda [51] show how for constant pressure operation of the capillary rheometer the flow rate may also vary periodically throughout extrusion.

A number of workers have investigated these oscillating flow rates and wall pressures when the rheometer is operated at either constant rate or constant extrusion pressure. Experimental work on high density polyethylene covers the majority of literature in this field and includes contributions from Bergem [52], Myerholtz [50], Bagley et. al[53], Rudin and Vlasschaert [54], Rudin and Chang [55] and Takaoka and Veda [51], which are reviewed below.

Bergem [52] found that when the rheometer ram was operated at constant velocity in a critical shear range, the response of the melt was a fluctuating flow with shear stresses oscillating between an upper and a lower value. Data was presented from extrusions at three different ram velocities within the oscillating region ( $\dot{\gamma} = 885, 1705$  and  $2525 \text{ sec}^{-1}$ ). The results of Myerholtz [50] are in general agreement with those of Bergem [52], with the shear rate for oscillating flow being in the range  $430$  to  $1100 \text{ sec}^{-1}$  with a repeatability of 3-4%. Myerholtz [50] found the average shear stress at which oscillation occurred to be

around 0.31 MPa. Meyerholtz [50] found the period of oscillation at a given plunger velocity to be a linear function of melt depth. Meyerholtz [50] proposes that the linear relationship between the period of oscillation and the melt depth suggests the system is behaving as a cavity resonator with the plunger acting as a reflection plane. The effect of melt depth has also been discussed by Rudin and Vlasschaert [54] who found that the pressure oscillation amplitude increased with decreasing polymer in the reservoir. Rudin and Vlasschaert [54] propose that the pressure fluctuations may be due to intermittent heavy loading of the mechanical train, and that variations due to melt depth occur as a result of attenuation of the pressure impulses in the melt above the pressure transducer.

Meyerholtz [50] has also shown the relationship between frequency of oscillation, plunger speed and melt depth. The frequency of oscillation for a given melt depth passes through a maximum as plunger velocity increases. The curves are essentially symmetrical, thus the same frequency can be encountered at two widely separate plunger velocities. Rudin and Vlasschaert [54] give a much simpler relationship between piston speed and waveform, simply stating that the wave period increased with increasing piston speed.

A number of other variables have been investigated with respect to their effect on wall pressure fluctuation. Meyerholtz [50] investigated the effect of both the average molecular weight (MW) and the molecular weight (MW) distribution on the shear rate required for oscillating flow for polyethylene. Meyerholtz [50] concluded that the shear rate for oscillating flow decreased with both increasing average MW and decreasing MW distribution. Meyerholtz [50] also found that increasing the test temperature resulted in an increase in the shear rate required for the onset of oscillating flow.

The effect of die geometry has been discussed by Meyerholtz [50]. The shear rate for oscillating flow was found to increase with decreasing die length to diameter ratio. Whilst

the importance of die geometry has been highlighted [50], Rudin and Chang [55] found that the oscillating flow during constant speed extrusion was independent of the die material (for steel, aluminium and brass).

Besides polyethylene, a number of other polymers have been studied with respect to oscillations in flow and pressure at constant rate extrusion. Bergem [52] found fluctuations in wall pressure during constant ram velocity extrusion of trans-1,5-polybutadiene. Rudin et al [56] found variations in the flowrate of alkathane-2-polythene when extruded in a deadweight piston rheometer although they were uncertain as to whether the cycling was a result of polymer or apparatus variations.

Rhoades and Rajagopal [45, 46] studied the constant pressure flow of polyborosiloxane by measuring the velocity of the driving piston. Although this is a somewhat indirect method of measuring flowrate through the die (as it assumes incompressibility) they did find that the piston velocity fluctuated with time during the extrusions.

The various mechanisms reported within the literature, which may be responsible for the oscillation of the pressure and die flow rate of polymers when extruded at either constant rate or pressure, are reviewed in the section below.

Myerholtz [50] stated that the results he obtained were consistent with the interpretation of oscillating flow as a series of recurring shifts between the two branches of a discontinuous flow curve. (This type of flow curve is described further in section 2.5.8.). Myerholtz [50] proposed that if the shear stress were increased from a low value then the corresponding shear rate would increase along the flow curve up to a critical shear stress. At this critical shear stress it is proposed [50] that yielding or chain disentanglement occurs, resulting in an increase in shear rate ( without increase in stress) over the flow

discontinuity “gap” (see section 2.5.8). At this point Myerholtz [50] reports that the stress decreases as the melt flows through the die at a rate greater than the piston velocity. During this decrease in shear stress it is proposed [50] that re-entanglement of molecules occurs down to a lower initial shear stress at which point the shear rate decreases rapidly (at constant shear stress) as the flow discontinuity “gap” is bridged again, but this time in the opposite direction. The shear rate then gradually increases again as the shear stress is increased and the process repeats itself [50].

Kataoka and Veda [51] also linked experimental flow-rate variations with the flow discontinuity curve. Similarly Bergem [52] refers to a critical shear stress value at which the temporary network of entangled chain molecules yields through sudden disentanglement, resulting in flow curve discontinuities. It was proposed by Bergem [52] that at these critical stresses, a thin layer of low viscosity polymer is formed at the periphery of the die entrance, and subsequently over the whole inner surface of the die. This layer is said to cause an abrupt and large increase in the rate of extrusion, which will stay high if the shear stress is kept higher than a certain critical stress.

Vinogradov et al [57] also refer to a die surface effects such as wall slip and slip-stick as being possible mechanisms for oscillating pressure fluctuations. Rudin and Chang [55] have proposed a mechanism for oscillating flow based on tensile forces within the capillary die. It was proposed [55] that the converging flow of the fluid in the reservoir must result from tensile forces exerted through an entanglement network by the polymer melt in the orifice on material in the larger upper cavity. Therefore, the polymer was not only being pushed out of the reservoir by the pressure exerted by the moving piston, it was also being pulled out by the material in the orifice and probably also outside the apparatus. Rudin and Chang [55] propose that this additional force in the extrusion direction will result in dilation of the melt when the piston is constrained to move at fixed speed, since the flowing

polymer adheres to the melt in the circulating so-called 'dead spaces' at the bottom of the reservoir and to material nearer to the piston face.

Rudin and Chang [55] proposed that this dilation would not be evident in constant pressure-extrusion because the piston can accelerate to compensate for the reduced resistance caused by the "tugging" action of polymer in the orifice. It is reported [55] that mass flow rates at given extrusion pressures are higher in this latter mode since the tensile forces urging the polymer in the reservoir into the orifice are not resisted by the limitations on the rate of advance of the piston.

Vinogradov et al [57] present a similar mechanism to that of Rudin and Chang [55]. Vinogradov et al [57] have described pressure and flow rate fluctuations in terms of 'spurt and elasticity'. They [57] state that a spurt may occur when polymers undergo an abrupt transition from the fluid to the highly elastic state. They propose that as the polymer transforms from the fluid to the elastic state it deforms reversibly causing a spurt of flow. However, the material may actually reversibly deform, degenerating the spurt effect. Vinogradov et al [57] conclude by stating that depending on the nature of the polymer system and on its state (deformation regimes) a great variety of flow irregularities and extrudate distortions (section 2.5.7) can be achieved.

A paper by Yoganathan and Yarlagadda [48] may provide one further possible mechanism for cyclic pressure oscillations observed in constant rate capillary flow. By flow visualisation techniques they found that the polymer may flow in a spiral pattern above the die in the rheometer barrel. Such a flow pattern in this region would result in a cyclic oscillation of wall pressure at a fixed point on the barrel wall which could be detected by the barrel wall pressure transducer.

### 2.5.7 Extrudate distortion and melt fracture

It is well known that when polymer melts are tested in capillary viscometers a smooth extrudate is normally obtained at sufficiently low rates of flow, in keeping with the assumption of steady laminar flow [25, 28]. However, at a critical shear-rate the onset of flow instabilities are often observed, which manifest as irregular extrudate distortions. This instability is generally termed melt fracture, and is initially observed as an extrudate waviness or spiralling which may evolve at higher extrusion rates to a grossly distorted flow [35, 55, 58].

Vinogradov et al [57] found that as the shear stresses and rates were increased during capillary flow the initial changes to be observed were small scale distortions in the extrudate shape. With an increasing pressure drop across the die the extrudate distortions became steadily more exaggerated [57]. Bagley et al [53] have described similar effects when studying the extrudate appearance of molten polyethylene. Initially the extrudate filament was smooth up to pressures of 10.7 MPa, between 10.7 MPa and 12 MPa the extrudate became wavy, and at pressures greater than 12 MPa the extrudate became extremely rough. On decreasing the pressure the filament went from rough to smooth at a pressure of 9.9 MPa.

Rudin and Chang [55] found that the constant speed extrusion of linear polyethylene produced flow oscillations corresponding to alternate periods of smooth and rough extrudate. Similar observations were made by Kataoka and Veda [51], although their extrusions were completed at constant pressure rather than constant ram velocity. Kataoka and Veda [51] found that the flow cycled between two values giving an extrudate appearance alternating between a long smooth and a short lumpy surface texture. Various mechanisms have been proposed within the literature for these extrudate distortions during capillary flow. These mechanisms are reviewed below.

Bagley et al [53] have proposed the occurrence of at least three modes of flow and corresponding extrudate appearances connected with the flow pattern in the melt reservoir above the die entry. It was stated [53] that one mode is associated with the smooth extrudate (the flow in the reservoir probably being laminar), one with the rough extrudate (probably associated with major disturbances in the flow patterns above the capillary entrance), and one corresponding to the wavy spiral filament.

Rudin and Vlasschaert [54] describe how extrudate distortion may be attributed to melt fracture resulting from periodic interruption and re-establishment of flow lines as an elastic strain is relieved and developed in the flowing melt. The role of elasticity in extrudate distortion has been described in detail by Schreiber et al [59]. They regard the flowing polymer as a sink for the absorption of applied deformation energy. They propose melt fracture as an additional means of dissipating applied energy which is actuated when the capacity of the melt for recoverably storing applied deformation energy becomes exhausted. Schreiber et al [59] describe how the flowing polymer becomes more elastically extended as the applied stress is increased and subsequently the dead zone polymer becomes more compressed. When the potential for storing deformation energy is exhausted, excess applied energy is dissipated in the flowing melt through fracture of the much less elastically deformed dead zone material into the main stream. Distortion of the extrudate is proposed to occur due to the varying elastic recovery of main stream material and dead zone material in the extrudate. From this mechanism Schreiber et al [59] concluded that less distortion should occur with increasing die length due to the increased die residence time allowing greater homogeneous mixture of elasticity. Schreiber et al [59] also proposed that more extrudate distortion occurred at greater shear stresses due to the reduced residence time in the die reducing the opportunity for smoothing of the elastic variations within the polymer. However, at very high shear stresses deformation was said to be minimal due to a smaller dead zone, and a much higher frequency of deformation.

Schreiber et al [59] also state that it is elastic heterogeneity which is the requirement for elastic deformation and not necessarily the existence of a dead zone.

Bergem [52] describes a possible mechanism responsible for sharkskin extrudate distortion. Bergem [52] proposes that these distortions are caused by tearing of the melt by die outlet fracture. The process starts at the surface of the extrudate and probably at the very moment when the melt is parting from the die. On emerging from the die the velocity distribution over the cross-section of the extrudate profoundly changes so that an acceleration of the outer layers occurs. This induces tensile stresses which may exceed the tensile strength of the melt. The melt will tear whereby the stresses are temporarily released. Further extrusion causes the process to repeat itself. Irregular repetition of the tearing process gives the surface roughness which is commonly called sharkskin.

### **2.5.8 Flow curve discontinuity**

Capillary rheometer data is often presented [25] in the form of a flow curve such that the wall pressure can be expressed as a unique single function of the flow rate for a given temperature. However, authors such as Vinogradov et al [57] have found occurrences of discontinuity of curves of flow rate against pressure (or more precisely, pressure drop across the die) and the appearance of hysteresis-like loops on them within specific pressure bands.

Brydson [25] also comments on the interesting hysteresis effect noted when making capillary flow experiments with linear polyethylene. Brydson [25] explains that if a series of die mass flow rate measurements are made at steadily increasing pressures a point is reached where there is a sudden jump in die mass flow rate. Above this pressure a more or less conventional flow curve is obtained. On reducing the pressures the point of discontinuity is at a lower pressure. Bergem [52] has described the behaviour of fluids with

double branched flow curves in greater detail with reference to Figure 2 [52]. Increasing the ram pressure from a low value gives the shear rate response A-B (Figure 2 [52]). Further increase in the extrusion pressure results in a sudden “spurt of flow” or increase in shear rate B-C, with no increase in pressure. Further increase in pressure beyond this value results in a steady increase in the shear rate along the line C-D. A reduction in ram driving pressure from point D causes the response DEFA, thus a discontinuous hysteresis loop is formed.

Vinogradov et al [57] present a similar description of the flow behaviour of material exhibiting flow curve discontinuity. They describe how when the pressure rises to a critical value a negligibly small rise in pressure causes a significant jump in the discharge rate. They refer to the stepwise increase in the discharge rate as a “spurt”.

The result of operating rheometers at constant pressure or ram velocity within the discontinuous region of flow curves has been discussed by Bergem [52] and Myerholtz [50]. Bergem [52] comments that at constant ram velocities within the flow curve discontinuity region the wall pressure was found to oscillate. Myerholtz [50] also links the oscillation of output rate to the fact that certain materials exhibit a doubly branched flow curve, rather than a single line. The oscillations in extrusion force and output rate were explained in terms of a cycling between upper and lower critical shear stresses on the two branches of the flow curve (flow rate and pressure oscillation effects have been reviewed in section 2.5.6).

The mechanism of flow curve discontinuities has been discussed by Myerholtz [50] and Tataoka and Veda [51]. Myerholtz [50] considered the disentanglement or yielding of molecules as well as slip at the capillary wall as the most likely mechanisms responsible for the initiation of oscillating flow. Tataoka and Ueda [51] also discuss the likely

contributions of finite velocity at the die wall to the existence of double values in the shear rate at a fixed shear stress. Similarly Lupton and Register [42] showed that up to 80% of the shear rate at the flow curve discontinuity can be accounted for by the postulate of slippage at the die wall.

In conclusion it is interesting to note the comments of Vinogradov et al [57] on the inappropriate nature of the terms 'non-uniqueness' and 'discontinuity of the flow curve' in the range of the function discontinuity. Vinogradov et al [57] objected to these terms because the conditions which lie at the basis of the concept of the flow function are not fulfilled. These conditions include laminar flow, steady state profile of velocity distribution along the duct and condition of polymer adhesion to the duct walls. Vinogradov et al [57] conclude from this that the concept of the flow function and viscosity under conditions of intensive manifestation of elastic turbulence are purely conventional. In this range it is suggested that consideration should be limited to the dependence of the flow rate on the pressure. This is because under conditions of intense elastic turbulence the method of constant pressure and constant plunger movement in viscometric devices do not equate to constant die shear rate or stress methods [57].

### **2.5.9 Heat generation and transfer in capillary flow**

Whenever a viscous liquid is deformed, some of the work of deformation is converted to internal energy through the mechanisms of viscous dissipation, and this results in a temperature increase [60, 61, 62]. In order to maintain the temperature at a prescribed value, this energy must be removed as heat. However, heat only flows when there is a temperature gradient. As a result it is impossible to maintain a perfectly uniform temperature in a viscous material while it is being deformed [26]. Whorlow [28] also discussed the problem of temperature non-uniformity stating that even if a viscometer

capillary was a perfect conductor and perfectly thermostated the temperature of the polymer at the centre of the capillary would differ from that at the wall.

Whorlow [28] presents a very simple calculation to estimate temperature rise due to viscous heating. Whorlow [28] proposed that the work done per second when a total pressure drop  $\Delta P$  produces a volume flow rate  $Q$  is  $\Delta PQ$ . And this energy increases the mean temperature by  $T$  where

$$\theta = \frac{\Delta PQ}{\rho Q C_p} = \frac{\Delta P}{\rho C_p} \quad (2.19)$$

However, Whorlow [28] does state that this calculation will overestimate the temperature rise for two reasons. Firstly, heat will be lost through the walls of the capillary, particularly on the long metal capillaries generally used at high pressures. Secondly, as material moves down the tube to lower pressure regions it will expand and absorb heat.

Dealy [26] has considered a uniform Newtonian fluid assuming temperature dependent viscosity where the temperature profile across a capillary die may be given as

$$\theta(r) = \theta_w + \frac{\eta \dot{\gamma}^2 r_d^2}{2K} \left[ \frac{r}{r_d} - \left( \frac{r}{r_d} \right)^2 \right] \quad (2.20)$$

This distribution gives a maximum temperature at a mid-point  $r = r_d/2$ . For non-Newtonian fluids with temperature dependent material constants, this equation is not quantitatively valid, but it does expose the role played by the various experimental variables and fluid properties [26].

In order to predict temperature profiles within polymer melts due to viscous heating it is necessary to make an assumption about what happens at the capillary wall [26]. Dealy [26] has described two limiting cases as to the heat transfer at the wall; the isothermal case

(Figure 3) where the temperature at the wall is assumed to be at uniform temperature and the adiabatic case (Figure 4) where there is no heat transfer at the wall. Dealy [26] reports that in practice temperature profiles produced within polymer melts due to viscous heating are likely to be midway between that shown in Figure 3 (isothermal) and that shown in Figure 4 (adiabatic).

A number of authors [60, 62-66] have used experimental methods to measure temperature distributions within polymer melts during capillary flow.

Gerrard et al [66] measured the temperature profiles of paraffinic bright stock oil extruded from an isothermal-wall capillary viscometer. A maximum temperature rise of  $8^{\circ}\text{C}$ - $16^{\circ}\text{C}$  (depending on the extrusion pressure) at a position 80% from the capillary centre was found to occur. At higher pressures the peak was found to increase rapidly and move closer to the wall, which may give a drop in the apparent viscosity. Crowson et al [65] also studied the effect of high shear rates and pressures on temperature non-uniformity. It was found that shear heating and compression heating caused up to a  $70^{\circ}\text{C}$  rise in melt temperature. The temperature rise was proportional to extrusion pressure for each of the materials tested.

The centre line temperature of a flowing melt has been discussed by Gerrard et al [66]. They stated that there was no heat generation in this region as the shear stress was equal to zero. Temperature variations could therefore only come about as a result of heat transfer. From this mechanism they [66] concluded that peak centre-line temperatures would be achieved at intermediate flow-rates, as at lower flow-rates heat generation would be minimal and at higher flow rates there would be insufficient residence time in the die for appreciable heat transfer to occur.

One of the main problems involved in the measurement of true temperature distributions within polymer melts is due to interaction of the measuring probe and the polymer melt, and the difficulty of insulating the probe [62]. Unless the measurements are corrected for the effects of conduction and frictional shear heating between the probe and the moving polymer melt, the measured temperature can be far removed from the actual value. In order to overcome these limitations Kim and Collins [62] developed a temperature probe system to measure radial temperature profiles of flowing polymer. Using this probe they [62] were able to develop a method to systematically correct temperature measurements for the conduction and frictional shear effects on the probe. Kim and Collins [62] found that the corrected temperature profile (true temperature) was usually a little higher than the measured profile (original uncorrected temperature) near the wall. (They [62] found that the reverse was true near the centre.)

Worth et al [41] have discussed how viscous heating may cause false conclusions to be made about the apparent manifestation of wall slip. They state that in the film of polymer adjacent to the capillary wall, where the shear rates are high, there may be significant viscous heating. Hence, the viscosity of the melt would be reduced in this region, with a corresponding increase in shear rate, which could be interpreted as wall slip (This phenomena is reviewed further within section 2.5.4).

In general, the extent of the temperature non-uniformity increases markedly as the shear rate or flow path diameter is increased [26]. It also increases with viscosity, but less sharply, and it decreases as the thermal conductivity is increased [26]. Gerrard et al [66] found that more heat was retained within melts in shorter capillaries at constant shear rate due to the reduced time for heat transfer to the capillary die. It was also found that more heat was retained within polymer melts in capillaries with large internal diameter due to the greater distance for the heat to transfer. The importance of temperature control during

flow testing has been highlighted by Gerrard et al [66] who found that having an isothermal wall compared to an adiabatic wall may allow up to a five fold increase in shear stress for the same melt temperature uniformity.

### **2.5.10 Density variations during capillary flow**

Extrusion behaviour of polymer melts is generally analysed by considering the fluid to be incompressible [25-28]. There are some qualitative reasons to expect that melt density might vary with extrusion conditions, although it is not obvious that the assumption of incompressibility can lead to serious error even if it is not strictly correct [54].

Brydson [25] has commented that at the low pressures used in most commercial viscometers (10 MPa) or less the compressibility of the polymer melt appears to be negligible. However, he stated that at higher pressures this effect can be very important. Hartado-Laguna and Aleman [67] and Rudin and Chee [68, 69] have studied the compressive bulk behaviours of polymer melts in capillary rheometers with steel plugs instead of capillaries. From their experimental results they were able to derive pressure/volume/temperature relationships.

A number of authors have investigated the variation in polymer melt density during capillary flow [54-56]. Rudin et al [56] completed low shear rate measurements using a dead-weight driven piston rheometer (i.e. constant shear stress) and found good agreement with static density test results. They found that the specific volume increased with shear rate, and that good linear relationships could be produced between specific volume and melt temperature.

Rudin and Vlasschaert [54] have studied the variations of melt density during capillary flow at constant apparent shear rate (ram velocity). Experimental work was completed on

high density polyethylene, polystyrene, polypropylene and poly (methyl-methacrylate). Density measurements were completed by cutting and weighing extrusion lengths at intervals of piston movement. At low shear rates it was found that the density results generally coincided with dilatometry or static weight volume experiments, although they did find some very minor pressure related density increases. However, at higher shear rates they found evidence of density variations during extrusions, and in particular, measurable density decreases with increasing rate of shear.

Rudin and Vlasschaert [54] also investigated the effect of die material on the density variations observed. Experiments were completed with steel, brass and aluminium dies. The mean value of the oscillating polymer densities during capillary flow were found to be comparable at similar shear rates. However, the period of density fluctuation was least for the aluminium die and greatest with the steel capillary, although it was proposed that these differences were due to slight variations in piston velocity rather than the effect of the die material.

Rudin and Chang [55] investigated the density of linear polyethylene extruded from a capillary rheometer at both constant pressure and constant rate. At constant rate the apparent density of the polyethylene was found to decrease as the shear rate approached melt fracture. The apparent density was also found to oscillate in some cases, the amplitude of which decreased with increasing piston speed. (Rudin and Chang [55] have discussed the possible mechanism for such density variations, a review of which is contained within section 2.5.6).

Rudin and Vlaschaert [54] have considered the possibility that the apparent density decreases noted at higher shear rates could be caused by back flow of the polymer melt against the advancing piston. However, this possibility was disregarded as the leakage

required to significantly affect the results would be clearly observable during experimentation, and no such leakage was observed.

### **2.5.11 Shear history prior to capillary flow**

Most descriptions of rheological properties assume an equilibrium state as the starting point, but in practical processing situations, material response at any stage of the process may be influenced by the previous thermo-mechanical history of the process and even by its history in earlier compounding operations [27]. Intense working, producing high shear, will usually lead to a reduction in viscosity and also a decrease in elastic response [27].

The effect of shear history on the flow properties of polymers has been studied by a number of authors [27, 70, 71, 72]. Cogswell [27] describes a pre-shearing technique where the melt from a capillary rheometer may also be extruded past a chamber where the material is subject to a well defined shear history. Such a method may be used for preparing melts of different shear history so that the influence of this important parameter may be evaluated.

Sholley [71] looked at the effect of regrinding and repeat processing of a styrene based polymer. It was found that the styrene showed a steady decrease in melt viscosity with each reprocessing operation. Ajji et al [71] have also studied the effect of pre-shearing on the flow data obtained from a capillary rheometer. However, they found that for linear low density polyethylene the apparent viscosity of the polymer was unaffected by its shear history in a screw extruder, although extrudate swell ratio was found to decrease with the number of passes through the extruder. Rudin and Schreiber [73] in an extensive review of a variety of materials also report that the degree of pre-shearing can effect melt elasticity without influencing melt viscosity (although melt viscosity was sometimes influenced). The effect of screw extrusion temperature on subsequent swelling behaviour was also

investigated by Ajji et al [70]. They found that the effects of pre-shearing are greater the lower the pre-shearing temperature.

If the amount of pre-shearing prior to capillary rheometer flow property evaluation may effect the apparent viscosity obtained, then it is clear that the soak duration or “relaxation time” in the rheometer barrel may have similar influence. The effect of soak or dwell time in the rheometer barrel on the “flow stability” of the melt has been investigated by Sholley [71]. Sholley [71] divided the extrusion barrel of a constant pressure capillary rheometer into four equal volume zones and timed the extrusion duration required for each zone. As each zone would be a function of dwell time in the barrel a plot of log extrusion time against dwell time was plotted to quantify the “flow stability” and “intrinsic melt viscosity”. The “flow stability” and “intrinsic melt viscosity” have been defined in ASTM standard D 3835-79 [74]. The “flow stability” or “melt viscosity stability” is the rate of change of the viscosity as a function of time at a specified temperature under the conditions of the test. The “intrinsic melt viscosity” is the viscosity on the log extrusion time against dwell time plot for zero dwell time. The “intrinsic melt viscosity” has been found to correlate well with the polymer average molecular weight [74].

A number of results are possible from such tests. If the material is heterogeneous then the data points will be spread and non-linear [74]. A straight line plot of zero slope represents a material of constant flow stability under the test conditions [71]. Both positive and negative slopes represent forms of degradation in which the physical properties of the material have changed [71]. A positive slope indicates an increasing viscosity which may result from further polymerisation or branching. A negative slope indicated decreasing viscosity which may be attributed to chemical decomposition or chain scission.

Rudin and Schreiber [73] have presented a possible mechanism to explain the effect of shear history and soak duration on the flow properties of polymers, based on an entanglement network of macromolecular chains. They [73] propose that shearing forces would cause relative movement of the chains reducing the degree of entanglement, and hence decrease the viscosity. The frequency of entanglements per unit volume of polymer and the spatial extent of the entanglement network formed can be expected to vary directly with polymer molecular weight, since larger molecules will have a statistically greater probability of participating in entanglements.

Rudin and Schreiber [73] also state that for most polymers, the effects of shearing are consistent with an explanation in which the polymer chain entanglement frequency is reduced, because disentanglement is by mechanical forces which would be expected to occur more rapidly than re-entanglement which will occur by segmental diffusion alone. This type of behaviour is consistent with the explanations of Sholley [71] that a recovery of viscosity after shearing results from further polymerisation or branching and that a decrease in viscosity after shearing is often attributed to chemical decomposition or chain scission.

In general, to minimise the effects of shear history Brydson [25] has stated that it is desirable to use samples which prior to being charged into the viscometer barrel have had similar shear and thermal histories. In the case of gas-operated viscometers in inert gas such as nitrogen is employed in instances where oxygen sensitive polymers are being tested [75]. Brydson [25] also states that where the effect of adding compound ingredients on flow properties is to be investigated, it is wise to compare the results obtained not only with those observed with the uncompounded polymer but also with the polymer to which no additional materials have been added but which has been subjected to the same mixing process as the compounded material.

Alternatively, stabilizers may be added to melts to increase their flow stability [71,74]. In the case of materials such as PVC, the material often exhibits stable flow for an initial period of time until the stabilizers become ineffective and unstable flow commences. In such cases as this, the dwell time at which unstable flow initiates can be determined and the effectiveness of the stabilizers can thus be defined [71].

Modifying the flow properties by varying the shear history of polymer melts is not always an undesirable feature. The deliberate shearing of polymer melts to reduce the manifestations of melt elasticity without significant change in molecular weight has been labelled shear refining, shear modification, or melt homogenisation [73].

Ajji et al [70] describe how, in some cases, modifying polymer properties by melt shearing may be a more practical technique than solution modification although the range of entanglement densities that can be achieved may be less. Nevertheless, they [70] discuss how measurable changes in melt elasticity can be achieved by relatively mild melt shearing, without changing the molecular weight distribution of the polymer.

## **2.6 The rheological properties of polyborosiloxane**

The extrusion honing process utilises the viscoelastic polymer polyborosiloxane [1], an investigation into the physical properties of which, forms the main bulk of this research programme. Literature documenting previous work on the rheological properties of polyborosiloxane has been reviewed below.

The first public disclosure of polyborosiloxane or “bouncing putty” as it is often referred to as, was made by the General Electric Company in 1944 [76]. A patent submitted by Wright [77] in 1944 describes processes for making the putty-like, elastic, plastic

polyborosiloxane compositions. Wright [77] described the manufacture of polyborosiloxane as being essentially of two major steps; polymerisation, and compounding the polymer with the appropriate plasticizers, fillers, and pigments to give the product its desired properties and colour.

A number of Authors have described the properties of polyborosiloxanes in a general qualitative manner. Beers [78] described the rheological properties of polyborosiloxane as soft, readily mouldable, and easily drawn into threads. He further stated that the material demonstrates a coefficient of restitution of up to 80%. Beers [78] also observed that when the material was subjected to large shear strain rate increases, such as when struck suddenly with a hammer, it shattered plastically into many small pieces. Similarly, Wright [77] described the polyborosiloxane's combination of properties as including both a high degree of elasticity under suddenly applied stresses and a high degree of plasticity when the stress is applied more slowly. Wright [77] also stated that the essential ingredients of the polyborosiloxane may be varied to obtain the desired degrees of elasticity and plasticity. Perry [14] has also described how a wide range of extrusion honing bases may be produced by varying the base chemical compositions.

Very little quantitative data referring to polyborosiloxane rheology could be found within the literature. Indeed, Benbow et al [79] and Plochocki and Maciejewski [80] are among the few workers to date who have undertaken any quantitative rheological evaluation of the polyborosiloxane material.

Benbow et al [79], were concerned with the dynamic response of a variety of viscoelastic fluids, although they also studied the steady flow behaviour of polyborosiloxane. Under steady flow conditions (Cone and plate and capillary) they stated that the viscosity appeared to be independent of the strain rate at shear rates up to  $20 \text{ s}^{-1}$ , at which strain rate

the extrudate becomes distorted. They quoted a viscosity over this range of approximately 0.1 MPas.

Plochocki and Maciejewski [80] investigated the rheology of polyborosiloxane in order to obtain data for rheological modelling of thermoplastics. Experiments were completed on a capillary rheometer with dies of various dimensions. They reported general power law pseudoplastic behaviour, with viscosities of the order of 10 KPas.

More recent work on the flow mechanisms of polyborosiloxane has been completed by Rhoades and Rajagopal [45]. Rhoades and Rajagopal [45] were particularly interested in “slip- stick” phenomena, initially proposed by Maxwell and Galt [44], which they thought occurred during the extrusion honing process.

Rhoades and Rajagopal’s [45] initial experimental approach was to flow multiple colour coded layers of polyborosiloxane (without abrasive) through transparent restrictive passage, and study the subsequent distortion of these layers after flow. However, they reported that sectioning the layers provided insufficient numbers of data points for their intended computer model. Subsequently, plastic beads were added to the polyborosiloxane and the flow lines studied with high speed photography. However, it was reported that the observed beads would not remain at the boundary wall throughout the duration of the observation, thus preventing the collection of a complete set of data points.

In addition to these initial trials Rhoades and Rajagopal [45] measured the force transferred through polyborosiloxane from a hydraulic cylinder to a cantilever beam. These recordings were all of a regular nature, showing no apparent sudden fluctuations, although they did report some indications of “slip-stick”.

Rhoades and Rajagopal [45] subsequently modified their equipment to subject the polyborosiloxane to much higher shear rates. The piston displacement was measured at constant hydraulic pressure through an orifice of approximately 1mm. The results showed significant piston velocity variations. Indeed, while extruding the medium viscosity polyborosiloxane the piston velocity actually fell to zero for a significant length of time. Rhoades and Rajagopal [45] concluded that it was highly likely that these velocity variations were a result of “slip-stick” at the cylinder wall.

Hull [1, 16] has published two recent papers (in conjunction with the author) which document work completed to investigate the rheological properties of extrusion honing polyborosiloxanes. The work of Hull [1] has concentrated on two specific grades of extrusion honing media; one of low viscosity (Extrude Hone Corporation C-21 grade) and one of high viscosity (Extrude Hone Corporation C-7 grade). (Extrude Hone Corporation C-11 grade extrusion honing compound has been used for this work). Hull [1] concluded that the medium was compressible and exhibited slip-stick during capillary flow. He also reported evidence of shear history and time dependent behaviour. In further work Hull [16] also discussed how the rheotropic properties of the polyborosiloxane were greatly affected by temperature.

Perry [14] has also studied the rheological properties of extrusion honing medium, both with and without abrasive. Perry [14] studied the properties of the extrusion honing medium by pumping the medium under hydraulic pressure through an orifice restriction. Perry [14] plotted the hydraulic extrusion pressure against the velocity of the polymer through an orifice restriction. Perry [14] maintained constant temperature (30°C) for each of his experiments and used a variety of orifice cross-sections.

Perry [14] initially tested a high viscosity extrusion honing medium which he concluded was highly pseudoplastic. When testing lower viscosity extrusion honing medium, Perry [14] observed changes in slope in his extrusion pressure/viscosity curves at certain extrusion pressures. Perry [14] proposed that these slope changes may represent transition between laminar and turbulent flow and refers to these points as “pseudoyield values”.

The effect of abrasive addition on the rheological properties of the extrusion honing medium has also been discussed by Perry [14]. Perry [14] found that increasing the hydraulic pressure significantly increased the flow speed of the abrasive mixture (pseudoplastically) and dramatically increased the cutting efficiency. However, Perry [14] suggests that high pressure may cause excessive heat generation problems due to the insulating properties of extrusion honing medium.

Extrusion honing is the main industrial use of the polyborosiloxane material. However, polyborosiloxane has also been used in the centre of golf balls to increase their resiliency [81], in automatic levelling devices, in novelty items, in athletic mouthpieces for the purpose of absorbing sudden shocks to the teeth, for reducing corona around electrical connections, in damping devices, and therapeutically for the exercise of injured arm muscles, a ball of it being worked in the hand [78]. More recently, initial trials using the polyborosiloxane in die-less wire drawing have been highly successful [82].

## 3. EXPERIMENTAL PROCEDURES

---

### 3.1 Materials

The extrusion honing process utilises the viscoelastic polymer polyborosiloxane [1], an investigation into the physical properties of which forms the basis of this research programme. Three grades of extrusion honing medium were selected from the Extrude Hone Corporation range of proprietary polymers. These three grades of polymer may be classified by their Extrude Hone references as C-7 (high viscosity), C-11 (medium viscosity) and C-21 (low viscosity).

Due to time limitations and the highly complex flow behaviour of the polyborosiloxane it was decided to concentrate on the C-11 medium viscosity polyborosiloxane (Extrude Hone Corporation batch number B-8213) for the majority of the experimental programme; particularly the capillary rheometer work. Polymer and abrasive mixtures were used for some of the temperature measurements described in section 3.2.3. These polymer abrasive mixtures consisted of medium viscosity C-11 polyborosiloxane mixed with silicon carbide abrasive in the ratio of 2:1 by mass. Two sizes of silicon carbide abrasive were used; 1.035mm and 32  $\mu\text{m}$ . These polymer and abrasive mixtures represented typical materials used in the extrusion honing process.

## **3.2 Experimental**

### **3.2.1 Thermal conductivity measurements**

A Lees disc [83] apparatus was used to determine the thermal conductivity of the C-11 polyborosiloxane material. The thermal conductivity was required as a parameter in the thermal models discussed in section 3.4.1. Operation of the Lees disc apparatus (Figure 5) was as described below.

A disc of polyborosiloxane, contained by a perspex ring, was placed between the brass steam jacket and the bottom brass disc. Steam was passed through the steam jacket until the brass disc reached a constant temperature  $\theta_1$ . At this point the rate of heat loss from the bottom disc was assumed to be just equal to the heat gained through the polyborosiloxane and containment ring. The rate of heat loss from the sides of the containment ring was considered negligible because its surface area was small.

To determine the heat flow through the polyborosiloxane and containment ring it was necessary to calculate the heat lost from the brass disc. This was calculated using the calibration methods described by Nelkon [83]. The thermal conductivity was calculated from the heat flow through the polyborosiloxane, the thickness of the polyborosiloxane and the temperature difference across the thickness.

### **3.2.2 Heat capacity measurements**

The heat capacity of the C-11 polyborosiloxane was determined using a differential scanning calorimeter (DSC). The main features of this instrument can be seen in Figure 6. The insulated enclosure contains two platinum pans, one for the sample and one for the reference. Each pan has a thermocouple and a heating element built into its base. Small

aluminium capsules with lids were used to hold the sample and aluminium reference material (aluminium is a suitable reference material for polymers because its thermal properties are known, and change little in comparison with the corresponding changes in polymers, in the temperature range from about  $-100^{\circ}\text{C}$  to  $+300^{\circ}\text{C}$ ). The Differential Scanning Calorimeter was programmed to produce a constant linear temperature rise from  $-50^{\circ}\text{C}$  to  $80^{\circ}\text{C}$  at a predefined rate of 10 K/min. Initially, liquid nitrogen was introduced to cool both the sample and the reference material. Once this has been achieved the programmed temperature rise commenced. During this period the difference in temperature between the sample and the reference holder was monitored and any difference compensated for by increasing or decreasing the independent heating to either the sample or the reference. The heat capacity was calculated from the heat input required to achieve the programmed temperature rise and the mass of the sample.

### **3.2.3 The measurement of the polyborosiloxane temperature in an extrusion honing machine**

The objective of this section of the experimental programme was to measure temperature profiles within the polyborosiloxane during extrusion honing. This experimental work was carried out on a 77 Series Extrude Hone machine (Figure 1) into which a test cylinder manufactured for the trials was clamped. The test cylinder contained two thermocouples, one 1mm from the inside surface of the cylinder and one on the outside surface of the cylinder (Figure 7). Polyborosiloxane was cycled through the test cylinder until no further increase in temperature (as recorded by the two thermocouples) with time was observed. When no further increase in temperature was observed two further sets of temperature readings were recorded as described below.

- (i) The first of these additional sets of data was a vertical temperature profile down the centre axis of the polyborosiloxane. The test cylinder was removed from the extrusion honing machine leaving the majority of the polyborosiloxane in the lower machine cylinder. A thermometer was then used to measure the temperature of the polyborosiloxane in the centre of the exposed surface. A 'slug' of polymer was then removed from the bottom machine cylinder by advancing the bottom hydraulic ram and removing the polymer extruded, thus exposing a fresh surface. A second temperature was then taken in the centre of the exposed surface. Successive 'slugs' of polymer were removed and the temperatures recorded in order to produce a vertical temperature profile down the centre of the polyborosiloxane.
  
- (ii) A horizontal temperature profile was obtained within the test cylinder. The test cylinder was removed from the extrusion honing machine and a thermocouple inserted through the centre of the polyborosiloxane to a point equidistant from the two ends of the test cylinder. Two further readings were taken in the same way, but at 2mm and 13mm from the wall of the test cylinder. The three readings together were used to produce a horizontal temperature profile of the test cylinder from 'wall-to- wall'.

Five experimental runs were completed as part of this programme; two with C-11 polyborosiloxane, one with C-21 polyborosiloxane, one with C-11 polyborosiloxane mixed with 32  $\mu\text{m}$  silicon carbide abrasive and one with C-11 polyborosiloxane mixed with 1.035mm silicon carbide abrasive. The extrusion honing machine operating parameters used for each of these trials can be seen in Table 1.

A second set of temperature measurements were completed, again using an Extrude Hone 77 series extrusion honing machine. A mild steel test cylinder (Figure 7) was clamped into

the machine into which a known mass of polyborosiloxane had been placed. Polyborosiloxane was cycled through the test cylinder by the extrusion honing machine and two thermocouples were used to measure a) the surface temperature of the test cylinder, and b) the temperature of the cylinder 1mm from its inside surface. At intervals during the experiment the test cylinder was removed from the machine and three thermocouples (held in position on a frame) were inserted into the polyborosiloxane in the test cylinder and the temperature profile obtained recorded. The thermocouples were removed, the test cylinder clamped back into position, and the extrusion honing machine restarted. A number of further profiles were obtained at regular time intervals.

### **3.2.4 The capillary rheometer - procedure 1 - extrusion ram accelerating throughout extrusion**

The rheology of the C-11 polyborosiloxane material was investigated using a Davenport capillary rheometer, shown schematically in Figure 8. The capillary rheometer consists of an extrusion barrel into which a ram can be driven by a variable speed motor and gearbox. The polyborosiloxane was extruded from the barrel through an extrusion die positioned in the bottom of the barrel. The extrusion barrel was maintained at the desired temperature by means of a thermocirculator which circulates water through the body of the extrusion barrel.

The extrusion operation was controlled by a BBC micro-computer via the rheometer control panel. As well as controlling the extrusion, the computer also recorded the ram velocity (to calculate the apparent shear rate), and the pressure drop across the die (to calculate the apparent shear stress). The pressure drop across the die was determined from a pressure transducer positioned in the sidewall of the extrusion barrel just above the top surface of the die.

Two pressure transducers were used for this series of experiments.

1. Dynisco 20.7 MPa mercury diaphragm transducer.
2. Dynisco 69 MPa mercury diaphragm transducer.

Both transducers were calibrated using a bourdon gauge test unit which had been previously calibrated.

The thermocirculator was set to the desired temperature for extrusion and sufficient time elapsed to bring the barrel to thermal equilibrium. An extrusion die was placed in the bottom of the extrusion barrel and the rheometer filled with the C-11 polyborosiloxane. At least six minutes were allowed for the polyborosiloxane to reach the required barrel temperature (shown to be satisfactory by thermocouple measurements within the polyborosiloxane). The extrusion ram was then lowered until it touched the surface of the polyborosiloxane at which point it was slowed to its lowest extrusion rate. When a constant pressure has been detected via the pressure transducer the ram velocity was increased to produce the next highest shear rate increment. The ram speed was incremented in the same way until full ram travel was complete, by which time wall pressures associated with a range of incremental ram speeds (shear rates) had been recorded. This procedure was repeated using C-11 polyborosiloxane at three different temperatures; 23°C, 30°C and 40°C. A die 20mm long with a 1mm internal radius was used, as well as a die of nominal zero length and the same internal radius to allow correction for die entrance and exit pressure drops (section 2.5.2). In addition to the zero die end correction method, attempts were made to determine Bagley [53] end correction factors by using dies with various length to radius ratios. For these trials C-11 polyborosiloxane was used at a temperature of 30°C. All dies used were of 2mm internal diameter with a length selected from 20, 25, 30, 35 and 40mm.

Following these initial experiments a number of modifications to the equipment and procedure were introduced as described in the sections below.

### **3.2.5 The capillary rheometer - procedure 2 - constant ram velocity throughout extrusion**

Following analysis of the results obtained from the experimental procedure described in section 3.2.4, it was decided to modify the experimental procedure as follows.

The extrusion ram on the laboratory capillary rheometer was to be operated at constant velocity throughout extrusion rather than at a variety of velocities as previously. In order to control the rheometer at constant ram velocity throughout extrusion it was necessary to disconnect the micro-computer previously controlling the rheometer, as the resident software would not accept constant ram velocity operation. Disconnection of the micro-computer required that a chart recorder be used to record the wall pressure from the pressure transducer during extrusion. These initial constant ram velocity trials were completed with C- 11 polyborosiloxane at 30°C. A set of five extrusion dies were used of internal diameter 2mm and lengths of 20, 25, 30, 35 and 40mm. For each of the five dies constant ram velocity extrusions were completed at both 2.5cm/min and 12.5cm/min.

### **3.2.6 The capillary rheometer - further procedure improvements**

The capillary rheometer was subject to a number of modifications following the experimental work described in section 3.2.5. Each modification is described in the sections below, and the complete modified rheometer is shown schematically in Figure 9.

#### **(i) *Ram displacement measurement***

Ram velocity was indicated on a dial gauge on the capillary rheometer. However, in order to check that pressure fluctuations obtained during constant ram velocity trials were not

due to velocity fluctuations or stalling of the drive motor the ram displacement was measured independently during extrusion, using a specially constructed device, shown in Figure 9. The device consists of a ten turn linear potentiometer ( $\pm 1\%$ ) driven by a pulley system connected by chart recorder wire to the extrusion ram. Thus, as the ram descended the potentiometer was driven by the pulley system and the resultant potentiometer output voltage would give a direct indication of ram displacement. The potentiometer output voltage was recorded on a data logger.

Trials were completed to compare ram velocities from this potentiometer device with the set point ram velocity as indicated on the rheometer dial gauge.

**(ii) *Electronic measurement of the cumulative mass of polymer extruded***

In order to investigate flow and density variations during constant ram velocity extrusions the cumulative mass of polyborosiloxane extruded was measured continuously on a piezo-electric force transducer, and the resultant signal from the charge amplifier recorded on a data logger.

**(iii) *Recording of data on the data logger***

A Solatron sixty channel data logger was used to record the analogue signals from the charge amplifier (cumulative mass extruded), the potentiometer (ram displacement) and the pressure transducer (wall pressure). The data from each experimental run was recorded by the data logger printer for subsequent analysis.

Rheological measurements were completed using C-11 polyborosiloxane at  $30^{\circ}\text{C}$  on the capillary rheometer. Each experimental run was completed at constant ram speed and the barrel charging procedure was as described in section 3.2.4.

The ram displacement and cumulative mass of polyborosiloxane extruded were measured as described above. The analogue outputs for ram displacement, cumulative mass extruded and wall pressure were recorded on a data logger. For each of four dies of internal diameter 2mm and respective lengths of nominal zero, 20, 30 and 40mm the rheometer was operated at ram velocities of 5, 10, 15 and 20 cm/min giving a total of 16 sets of results.

The original ram tip fitted to the capillary rheometer was deformed along one side, possibly allowing some leakage of polyborosiloxane between the rheometer ram and barrel. In order to eliminate this possibility a new ram tip was fitted to the extrusion ram.

The mass of polyborosiloxane leakage between the extrusion barrel and ram at a range of shear rates with both the old and the new ram tip was investigated.

After the new ram tip had been fitted rheological measurements were completed using C-11 polyborosiloxane at 30°C using two dies, of internal diameter 2mm, and respective lengths of nominal zero, and 40mm. For each of these dies the rheometer was operated at ram velocities of 1.58, 4.65, 7.68, 10.86 and 15.67cm/min.

### **3.2.7 Variations in the charging procedure for the capillary rheometer**

All experiments described in the previous sections utilised the capillary rheometer charging procedure described in section 3.2.4. In this procedure, whilst a minimum time of six minutes was always used to produce the required temperature, the exact charging procedure was subject to some variation, and in some cases the six minute time period prior to extrusion was extended by various amounts. In order to investigate the effect of such changes to the charging procedure on the extrusion barrel pressures obtained during extrusion, experiments were completed with the time between charging to the barrel and extrusion varying in each case. For these experiments C-11 polyborosiloxane was used at

30°C. Extrusion was at a constant ram velocity of 15 cm/min, and an extrusion die of 2mm internal diameter and 40mm length was used.

The extrusions were completed using the general charging procedure described below, with the duration of the second barrel stand period being the only variable (4, 14 and 24 minutes).

For the remaining experiments completed on the laboratory capillary rheometer the following barrel charging procedure was adopted.

- 1 Fresh un-tested C-11 polyborosiloxane was placed into the barrel charging piston, and allowed to stand for 15 minutes.
- 2 The rheometer barrel was charged with polyborosiloxane at a ram velocity of 2.5 cm/min from the barrel charging cylinder until polymer appeared at the exit of the extrusion die.
- 3 The polyborosiloxane was left to stand in the barrel for 2 minutes.
- 4 The ram was lowered into the barrel at 2.5 cm/min until a pressure was detected from the extrusion barrel pressure transducer.
- 5 The ram was raised and a further 4 minutes stand time allowed.
- 6 The polyborosiloxane height was adjusted to 20mm below the top surface of the extrusion barrel.

7 The ram was lowered until level with the top surface of the polyborosiloxane.

8 The rheological test was then completed.

### **3.2.8 Variations in the polyborosiloxane extrusion temperature on the capillary rheometer**

In order to investigate the effect of temperature on the wall pressure recorded for C-11 polyborosiloxane during extrusion on the capillary rheometer, the experimental programme described below was completed.

For each experiment the laboratory capillary rheometer was charged according to the procedure described in the later part of section 3.2.7. Each experiment was completed using C-11 grade polyborosiloxane. Two different extrusion barrels were used for this series of experiments; (i) a thermocirculator temperature controlled 'cold barrel' and, (ii) an electrically temperature controlled 'hot barrel'.

Using the thermocirculator temperature controlled barrel described in section 3.2.4 experiments were completed at three different temperatures: 30°C, 39°C and 45°C. At each of these temperatures five extrusions were completed at ram velocities of 1.25, 2.5, 5, 10 and 15 cm/min respectively.

In order to complete experiments at higher temperatures the 'cold' barrel was removed from the capillary rheometer and an electrically heated 'hot' barrel fitted. This 'hot' barrel was set to a temperature of 70°C and extrusions completed at 1.25, 5 and 15 cm/min.

In order to test the repeatability of the results obtained from the capillary rheometer, one of the runs was picked at random and repeated a further 3 times. This repeatability test was

completed on C-11 polyborosiloxane at 30°C using a die of 2mm internal diameter and 40mm long at a ram velocity of 5 cm/min.

### **3.2.9 Manual measurement of the extrusion rate on the capillary rheometer**

In order to investigate polyborosiloxane density variations which may occur within the capillary rheometer during constant ram velocity extrusions a manual technique for measuring flowrate through the die during extrusion was devised as described below.

A stopwatch was attached to the thermocirculator cooling pipes, such that it was visible when viewing the bottom of the extrusion die. This arrangement allowed the extruded polymer produced during each 15 second period to be collected into separate sample containers. The quantity of extrudate so produced was weighed and the mass flow rates during each extrusion calculated from this data.

Each experiment was completed on the capillary rheometer with C-11 polyborosiloxane charged according to the modified charging procedure described in section 3.2.7.

A preliminary experiment was completed with a barrel temperature of 30°C and a ram velocity of 1.25 cm/min in order to assess the feasibility of the method. Following the success of the initial trial, four experimental runs were completed; one at 30°C and 1.25 cm/min ram velocity, one at 39°C and 2.5 cm/min ram velocity, one at 45°C and 2.5 cm/min ram velocity and one at 45°C and 15 cm/min ram velocity.

As well as the manual flow rate measurements the wall pressure and ram displacement were recorded on the data logger as previously described (section 3.2.6).

### **3.2.10 Capillary rheometer experiments with polystyrene**

To provide a comparison with a second polymer, rheological measurements were undertaken with polystyrene using the equipment developed for C-11 polyborosiloxane rheological determination. The purpose of this was to establish that the unusual rheological results observed (section 4.6) were indeed a property of the C-11 polyborosiloxane material and not an intrinsic function of the experimental equipment or procedure. Polystyrene was selected for this purpose since its rheological characteristics have been extensively studied and the characteristics of interest have not been reported.

In each case the electrically heated hot barrel was used at a set point temperature of 230°C. For the first series of experiments the polystyrene granules were loosely charged into the barrel via a funnel and allowed to soak for 6 minutes prior to extrusion. This first series of experiments consisted of 5 runs at ram velocities of 2.5, 5, 10, 15 and 20 cm/min.

To conclude this section of work a series of extrusions were completed where a controlled packing procedure was adopted as described below.

The polystyrene granules were poured into the rheometer barrel via a funnel and tightly packed with a plunger. After a 2 minute soak the rheometer ram was lowered at 2.5 cm/min, until a pressure was detected by the wall pressure transducer, after which a further 7 minute soak was allowed prior to extrusion.

Ten extrusions were completed using the constant charging procedure described above using two dies, both of 2mm internal diameter, one of nominal zero length and one 40mm long at ram velocities of 1.25, 2.5, 5, 10 and 15 cm/min.

### **3.2.11 The slit die rheometer**

The capillary die fitted to the capillary rheometer described in section 3.2.4 was removed for this series of experiments and replaced with a slit die of the dimensions shown in Figure 10. The slit die contains four pressure transducers placed at equal distances down the longest side of the internal wall of the slit.

The temperature of the slit die was controlled by circulating water from a thermostatically controlled water bath through a water jacket around the slit die. A thermocouple within the body of the slit die confirmed that the set point temperature had been achieved and was being maintained.

The four slit die pressure transducer signals were recorded on a data logger via the pressure transducer display panel. In addition, the solatron data logger was also used to record the ram displacement and barrel wall pressure. A schematic of the laboratory rheometer, slit die, temperature control systems, and associated instrumentation can be seen in Figure 11.

In each experiment the constant barrel charging procedure described in section 3.2.7 was adopted. C-11 polyborosiloxane was used for all of these slit die experiments. The slit die was operated at two temperatures; 30°C and 43°C. For each of these temperatures the rheometer was operated at 3 ram velocities; 1.25, 2.5 and 5 cm/min.

### **3.2.12 The concentric cylinder rheometer**

In addition to the capillary rheometer measurements, the rheology of the C-11 polyborosiloxane has also been studied on a Haake Rotovisco RV3 concentric cylinder rheometer.

A schematic of the Haake concentric cylinder rheometer can be seen in Figure 12. The rheometer consists of a rotating cylinder (called the rotor) and a fixed cylinder (called the cup or beaker). The RV3 rheometer was fitted with a MK500 torque measuring head and a MVIII viscosity sensor system.

The temperature of the system was maintained at 30°C by the use of a thermocirculator, which circulated water through the fixed cylinder body. C-11 polyborosiloxane was placed in the annular space between the rotor and the cup, the rotor turned at a defined rate, and the resulting torque measured. The rotor speed, and therefore the shear rate was controlled by a programmable controller. Initial trials involved recording the torque and rotor velocity whilst the rotor was accelerated from zero up to a maximum. Six experiments were completed at acceleration rates of 1, 5, 10, 20, 30 and 40 r.p.m.<sup>2</sup>. Subsequently, the rheometer was operated at a fixed rate of rotation at intervals in the range of 0.1 to 2 r.p.m., and the resultant variation in torque with time was recorded.

Further experimentation was completed where the rotor was rotated until a constant torque value was reached, the drive was disconnected, and the reduction in rotor torque monitored with time. Such tests were completed at a variety of rotor speeds between 0.1 and 2 r.p.m.

Measurements of rotor torque above 2 r.p.m. (at constant rotor speed) were not possible due to limitations in the range of the MK 500 torque measuring head, although rotor speeds of 1000 r.p.m. are within the capabilities of the equipment.

### **3.2.13 The measurement of the polyborosiloxane density as a function of pressure and temperature**

The density of the C-11 polyborosiloxane has been investigated as a function of both pressure and temperature.

The capillary rheometer was used to measure the density of C-11 polyborosiloxane with varying pressure by placing a 'blank' die in the bottom of the rheometer barrel. Thus the pressure could be measured from the barrel pressure transducer, and the density calculated from the mass of polymer in the barrel and the volume of the rheometer barrel (from barrel geometry and ram position).

In order to investigate the variation in C-11 polyborosiloxane density with temperature, polymer was placed in graduated glassware within a water bath. The mass of polyborosiloxane was known, and the volume could be noted from the glassware graduations across a range of temperatures. Thus the density of the C-11 polyborosiloxane could be expressed as a function of temperature.

### 3.3 Calculation methods

#### 3.3.1 Wall shear strain rate calculations

##### a) *Capillary rheometer*

The apparent wall shear rate has been calculated from equation 3.1 [25-28], viz

$$\dot{\gamma}_{w,a} = -\frac{4Q}{\pi r^3} \quad (3.1)$$

In addition to the apparent shear rate the 'true' wall shear rate has been calculated by the use of the Rabinowitsch equation [25], as follows

$$-\dot{\gamma}_w = \frac{1}{r^3} \left[ 3Q + \Delta P \frac{dQ}{d(\Delta P)} \right] \quad (3.2)$$

**b) Slit die rheometer**

The apparent wall shear rate has been calculated from equation 3.3 given by Brydson [25];

$$\dot{\gamma}_{w,a} = \frac{6Q}{h^2} w \quad (3.3)$$

In addition to the apparent shear rate, the ‘true’ wall shear rate has been calculated by the use of equation 3.4 [25], which is analogous to the Rabinowitsch equation for capillary flow.

$$-\dot{\gamma}_w = \frac{2}{wh^2} \left[ 2Q + \Delta P \frac{dQ}{d\Delta P} \right] \quad (3.4)$$

**c) Concentric cylinder rheometer**

The apparent wall shear rate has been calculated from equation 3.5 [84]

$$\dot{\gamma}_{w,a} = \frac{\Pi}{15} \frac{ra^2}{(ra^2 - ri^2)} n \quad (3.5)$$

### 3.3.2 Wall shear stress calculations

**a) Capillary rheometer**

The wall shear stress,  $\tau_w$  during constant ram velocity operation of the capillary rheometer has been calculated from equation 3.6 [25]

$$\tau_w = \frac{r\Delta P}{2l} \quad (3.6)$$

Pressure drops across the extrusion die due to entrance and exit effects have been compensated for in the calculations by use of the zero die end correction method as described in section 2.5.2. This gives the pressure drop across the die as

$$\Delta P_c = \Delta P_l - \Delta P_o \quad (3.7)$$

**b) Slit die rheometer**

The wall shear stress during constant ram velocity operation on the capillary rheometer has been calculated from equation 3.8 [25]

$$\tau_w = \frac{h\Delta P}{2l} \quad (3.8)$$

The pressure drop down the slit die has been calculated by completing a linear regression on the average of each of the four die pressure measurements during a constant ram velocity extrusion.

**c) Concentric cylinder rheometer**

The wall shear stress for the concentric cylinder rheometer has been calculated from equation 3.9 [84]

$$\tau_w = \frac{M_d}{S} \frac{981}{2\pi h r_i^2} \quad (3.9)$$

**3.3.3 Shear viscosity calculations**

In all the rheological experiments (slit die, capillary die and concentric cylinder) the apparent shear viscosity has been calculated using equation 3.10 [25], below

$$\eta_a = \frac{\tau_w}{\dot{\gamma}_w} \quad (3.10)$$

Data for the C-11 polyborosiloxane has been fitted to a power law equation of the form

$$\tau_w = K \dot{\gamma}_w^n \quad (3.11)$$

Where K and n are constants which can be determined by plotting  $\log \dot{\gamma}_w$  against  $\log \tau_w$ . A straight line plot gives a gradient n and an intercept  $\log K$ .

### 3.3.4 Velocity distribution within the die

For the power law fluid approximation the velocity at a point within a cross-section of polyborosiloxane has been calculated from equation 3.12, below

$$V_r = \left[ \frac{n}{n+1} \right] \left[ \frac{P}{2Kl} \right]^{1/n} r_d^{((n+1)/n)} \left[ 1 - \frac{r}{r_d} \right]^{((n+1)/n)} \quad (3.12)$$

(Assuming zero wall velocity)

The constants n and K were determined by the graphical methods described in section 3.3.3.

### 3.3.5 Shear strain rate distribution within the die

A shear rate profile across the capillary die for polyborosiloxane if a power law fluid is assumed, is obtained by differentiation of the velocity profile given in section 3.3.4. viz

$$\dot{\gamma}_r = \frac{dv_r}{dr} = - \left[ \frac{P}{2Kl} \right]^{1/n} r^{1/n} \quad (3.13)$$

### 3.3.6 Shear stress distribution within the die

The shear stress profile across the capillary die for a power law fluid has been assumed to be linear, such that the stress is a maximum at the wall and a minimum at the centreline (zero) [25]

$$\tau_r = \tau_w \frac{r}{r_d} \quad (3.14)$$

## 3.4 Mathematical models

### 3.4.1 Heat transfer during extrusion honing

#### 3.4.1.1 *Steady state heat transfer model*

In order to calculate surface heat transfer coefficients between mild steel tooling and polyborosiloxanes, a steady state thermal mathematical model of the extrusion honing process has been developed.

For the purposes of this model it has been assumed that all the extrusion honing medium is at a uniform temperature. It is also assumed that all heat transfer is from the polymer through the die wall to the surrounding air (i.e. no heat loss to the extrusion honing machine).

The temperature of the polymer at the polymer/test die interface is required for calculation of the surface heat transfer coefficient within the steady state model. This temperature, as well as the temperature within the test cylinder walls were measured according to the procedure described in section 3.2.3.

The heat transferred through the test die wall was calculated from equation 3.15, shown below. A shape factor has been used to remove the variable cross sectional area from the equation. It has been assumed for the purposes of this calculation that the temperatures recorded by the two thermocouples represents the temperature at their respective radii along the entire length of the die (parallel to the flow direction).

$$\Phi = \frac{2\pi\lambda_w l(r_{tci} - r_{tco})}{\ln(r_{tco}/r_{tci})} \quad (3.15)$$

Thus equation 3.15 was used to estimate the total heat transfer through the die wall. thermal steady state was assumed such that this heat flux could be equated to the total heat generation within the extrusion honing medium in the die (axial heat transfer parallel to the flow direction was assumed to be negligible).

As well as the heat generation, the model was also used to calculate the surface heat transfer coefficient at both the inner and outer die walls. In order to calculate the surface heat transfer coefficient at the inner die wall it was necessary to determine the inner wall temperature of the die. This temperature was obtained by assuming a linear temperature profile through the die wall and re-arranging a form of equation 3.15 to give

$$\theta_w = \frac{\Phi \ln\left[\frac{r_{tco}}{r_{tci}}\right]}{2\pi\lambda_w l} + \theta_{tci} \quad (3.16)$$

Using this calculated die inner wall temperature the surface heat transfer coefficient at the die inner wall was calculated from

$$h_i = \frac{\Phi}{a_i(\theta_p - \theta_w)} \quad (3.17)$$

Similarly the surface heat transfer coefficient at the outer die wall was calculated from

$$h_o = \frac{\Phi}{a_o(\theta_{tco} - \theta_a)} \quad (3.18)$$

The steady state mathematical thermal model utilises computer spreadsheet software. All constants (dimensions, die properties etc.) were contained within the spreadsheet, as well as the equations described above. For each experiment completed the two thermocouple temperatures, the temperature of the polymer at the inner die wall and the ambient air temperature were entered, and the heat generation and surface heat transfer coefficients calculated. The steady state model was used to calculate the heat generation and the surface heat transfer coefficient from the steady state temperatures obtained with C-21 polyborosiloxane, C-11 polyborosiloxane mixed with 32  $\mu\text{m}$  silicon carbide abrasive and C-11 polyborosiloxane mixed with 1.035mm silicon carbide abrasive. The thermal model was also used to produce a graphical representation of the temperature distribution assumed for the purposes of the calculations, within the polymer, die and surrounding air.

#### **3.4.1.2 Transient heat transfer model**

The objective of the development of an extrusion honing transient heat generation model was to predict temperature distribution within the polyborosiloxane during extrusion honing. Such calculated temperature distributions may be used to develop flow equations which incorporate temperature dependence. In addition such thermal modelling may enable a greater understanding of the heat generation mechanisms during extrusion honing.

The model was initially used to calculate heat generation within the polyborosiloxane during extrusion honing from experimentally measured temperature profiles (Figure 22). It was intended that when the heat generation term had been quantified for a range of

operating conditions it may be incorporated into the model, and the model used for temperature prediction.

On completion of this research programme the transient thermal model was in development, and further refinement was still required. In particular shape factors require incorporation into the heat balance equations, which at present assume constant cross-section with increasing radius.

Despite this shape factor error and the further developments required, for completeness of the thesis, the transient model development to date is briefly described below. (Possible further developments of this model are briefly discussed in section 6).

The extrusion honing transient thermal model was based on the finite difference calculation method and was coded in FORTRAN 77 computer language. The modelling system was divided into 5 elements from the centre axis of the polyborosiloxane to the outside wall of the die; 3 elements in the polyborosiloxane and 2 in the die wall. A heat balance was completed on each element and the following equations formulated.

Zone 1 - Inner polyborosiloxane annulus

$$\rho x A C_p (\theta_1^{m+1} - \theta_1^m) = \dot{q}_1 + \frac{\lambda_p A (\theta_2^m - \theta_1^m) \Delta t}{x} \quad (3.19)$$

Zone 2 - Middle polyborosiloxane annulus

$$\rho x A C_p (\theta_2^{m+1} - \theta_2^m) = \dot{q}_2 + \frac{\lambda_p A (\theta_3^m - \theta_2^m) \Delta t}{x} - \frac{\lambda_p A (\theta_2^m - \theta_1^m) \Delta t}{x} \quad (3.20)$$

Zone 3 - Outer polyborosiloxane annulus

$$\rho x A C_p (\theta_3^{m+1} - \theta_3^m) = \dot{q}_3 - \frac{\lambda_p A (\theta_3^m - \theta_2^m) \Delta t}{x} - h_i A (\theta_3^m - \theta_4^m) \Delta t \quad (3.21)$$

Zone 4 - Inner die wall

$$\rho x A C_p (\theta_4^{m+1} - \theta_4^m) = h_i A (\theta_3^m - \theta_4^m) \Delta t - \frac{\lambda_w A (\theta_4^m - \theta_5^m) \Delta t}{x} \quad (3.22)$$

Zone 5 - Outer die wall

$$\rho x A C_p (\theta_5^{m+1} - \theta_5^m) = -h_o A (\theta_5^m - \theta_A) \Delta t + \frac{\lambda_w A (\theta_4^m - \theta_5^m) \Delta t}{x} \quad (3.23)$$

The measured temperature distribution within the polymer and die wall with time (section 3.2.3) was entered into the model. Thus the model contained five equations and five unknowns and could subsequently be solved. The five unknowns were the heat generation within each of the 3 polymer elements and the surface heat transfer coefficient at both the inner and outer die wall.

The following assumptions were made in the formulation of the model.

- (i) All heat transfer was assumed to be radial with no heat transfer to the extrusion honing machine in the vertical axis, parallel to the flow direction.
- (ii) Uniform temperature distribution in the vertical axis parallel to the flow direction was assumed along the length of the die.

The model was used to calculate heat generation within the three polymer zones from the measured temperature distributions described in section 4.3.3. (Figure 22).

### 3.4.2 Mathematical model of polyborosiloxane density and flow rate variations during capillary flow

Following the unusual cycling of both the extrusion barrel pressure and the die mass flow rate during capillary flow at constant ram velocity (section 4.6) a mathematical model was formulated in order to support the proposed mechanisms discussed in section 5.4.3. The objective of the mathematical model was to calculate the die mass flow rate on the capillary rheometer at constant ram velocity from the extrusion barrel pressure assuming pressure dependent density. The calculation sequence of this model was as described below;

- (i) The measured extrusion barrel pressure was approximated to an equation of the form

$$P = \left( \sin \left( \frac{t}{W_{pw}} - \text{Int} \left( \frac{t}{W_{pw}} \right) \right) \times \Pi \times A_{pw} \right) + P_{\min} \quad (3.24)$$

- (ii) At regular time intervals (duration of ram travel) the volume of polyborosiloxane in the extrusion barrel was calculated from the initial volume in the barrel, the barrel cross-section, the ram velocity and the extrusion duration.
- (iii) The density of the polyborosiloxane in the extrusion barrel was calculated from the pressure given in (i) and the polyborosiloxane pressure/density relationship previously determined (Figure 28).
- (iv) The mass of polyborosiloxane in the extrusion barrel was calculated from the volume (ii) and density (iii) of polyborosiloxane in the extrusion barrel.

- (v) The die mass flow rate was calculated from the change in mass of polyborosiloxane in the extrusion barrel for the given time interval.

The model was used to calculate die mass flow rates from extrusion barrel pressures measured during extrusion of C-11 polyborosiloxane at a ram velocity of  $1.25 \text{ cm min}^{-1}$  and a temperature of  $30^\circ\text{C}$ , at a ram velocity of  $2.5 \text{ cm min}^{-1}$  and a temperature of  $39^\circ\text{C}$ , at a ram velocity of  $2.5 \text{ cm min}^{-1}$  and a temperature of  $45^\circ\text{C}$  and at a ram velocity of  $15 \text{ cm min}^{-1}$  and a temperature of  $45^\circ\text{C}$  (Data from Figures 85-89).

## 4. EXPERIMENTAL RESULTS

---

### 4.1 Introduction

It is intended that the experimental results presented in this thesis will provide a greater understanding of the flow properties of the C-11 polyborosiloxane extrusion honing medium. Such information may be useful in the further optimisation and development of the extrusion honing process, as well as providing additional knowledge as to the exact mechanism of the machining action. It was intended that a predictive model should be developed as part of the research programme in order to model the flow properties of the C-11 polyborosiloxane during extrusion honing.

The relationship between shear stress, shear strain rate, duration of shear, and temperature for C-11 polyborosiloxane has been investigated by use of the concentric-cylinder, the slit-die and the capillary rheometer. The capillary rheometer was initially selected due to its close analogy with an extrusion honing machine, both in terms of geometry and operating mechanism. The slit-die and concentric cylinder rheometers were used to provide data across a wider range of shear strain rates in order to give a more complete rheological characterisation. In addition, the concentric cylinder and slit die rheometers were used to quantify the effects of flow geometry (die surface area etc.) on the flow properties of the C-11 polyborosiloxane.

It was intended that the rheological characterisation of the polyborosiloxane would enable the shear stress to be calculated at a specified shear strain rate, duration of shear, and temperature. This is important because the wall shear stress may be directly related to the extrusion honing action produced [24]. The shear strain rate and the duration of shear may be specified from the piston velocity and the flowpath geometry. However, the prediction

of the temperature within the C-11 polyborosiloxane during extrusion honing required the quantification of the heat generation within the polymer (due to internal shear and friction at the polymer/workpiece interface), and the determination of the heat transfer properties of the system (heat capacity, thermal conductivity and surface heat transfer coefficients). From these parameters it was intended that thermal calculations would be completed to predict temperature within the polyborosiloxane. These temperatures coupled with the shear rate and duration of shear would enable the prediction of wall shear stresses.

The initial parameters required for the thermal calculations have been determined. These include, heat capacity (DSC), thermal conductivity (Lees disc), surface heat transfer coefficient (steady state model) and density (blank die and graduated glassware). The steady state thermal model (section 3.4.1.1) was used to calculate the heat generation within the polyborosiloxane during extrusion honing. This is in addition to the determination of the surface heat transfer coefficients.

A first attempt at the development of a transient heat generation model to predict the variation in temperature throughout the polyborosiloxane during extrusion honing was completed in the later stages of this research project (section 4.4.4). It is intended that in future work these predicted temperatures may be incorporated into the calculation of wall shear stresses from the flow equations derived in section 4.9. In order to predict the occurrence of, and explore the mechanism of, the variations in flow rate which occurred during constant ram velocity capillary extrusion (Figures 77-81) a mathematical model was developed to calculate the die mass flow rate from the extrusion barrel pressure (section 4.13).

It was originally intended to present experimental results on polyborosiloxane/ abrasive mixtures. Whilst some of the thermal work described within this chapter has been

completed on such mixtures, only pure C-11 polyborosiloxane has been used for rheological experimentation. The exclusion of abrasive mixtures from the rheological work was due to two main reasons. Firstly, a long development period was required to establish experimental procedures for the pure polymer (constant charging procedure, single ram velocity operation, flow rate measurement etc.). This left no additional experimental time for work with abrasives. Secondly, rheological experimentation with polymer/abrasive mixtures would be highly destructive to the test apparatus (dies, transducers etc.), and would therefore require considerable modification to the rheological equipment

## **4.2 Heat capacity and thermal conductivity**

The specific heat capacity and thermal conductivity of the C-11 polyborosiloxane were required for use in the extrusion honing heat transfer models described in section 4.4.

The thermal conductivity for C-11 polyborosiloxane has been determined by Lees disc to be  $0.17 \text{ Wm}^{-1}\text{K}^{-1}$ . Specific heat capacities of C-11 polyborosiloxane have been tabulated at  $10^\circ\text{C}$  intervals between  $20^\circ\text{C}$  and  $80^\circ\text{C}$  in Table 2. The heat capacity generally decreases from  $1.64 \text{ J g}^{-1}\text{K}^{-1}$  at  $20^\circ\text{C}$  to  $1.39 \text{ J g}^{-1}\text{K}^{-1}$  at  $80^\circ\text{C}$ .

## **4.3 Temperature distributions within polyborosiloxane during extrusion honing**

### **4.3.1 Introduction**

Temperature profiles within the C-11 polyborosiloxane and the containing die during extrusion honing have been determined experimentally in order to calculate both heat

generation within the polyborosiloxane, and surface heat transfer coefficients between the polyborosiloxane and the die. These parameters were calculated by use of the thermal models described in section 3.4.1. These models were intended to predict the temperature profiles within polyborosiloxane during extrusion honing, to enable calculation of wall shear stresses from the flow equations derived in section 4.9. This is important because the wall shear stress may be directly related to the extrusion honing action produced [24].

#### **4.3.2 Steady state temperature distributions within the die and polyborosiloxane during extrusion honing**

When the 77 Series Extrude Hone machine was operated according to the procedure described in section 3.2.3 with a charge of polyborosiloxane, or polyborosiloxane/abrasive mixtures the temperature of the die increased with time up to a steady state value with the inner die thermocouple hotter than the outer (Figures 13, 14, 15 and 16).

The duration of the machine operating time required to produce steady state temperatures varied with the mode of machine operation (automatic or manual) , viscosity of polyborosiloxane used and size of abrasive particle (Table 1). Steady state temperatures were achieved in shorter time periods when in automatic than in manual mode, and the addition of abrasive grit increased the temperatures recorded.

A greater maximum temperature under steady state conditions was achieved with the use of the coarse (1.035 mm) Silicon carbide grit (77°C) than the finer (32 µm) silicon carbide grit (66°C). By contrast the C-11 polyborosiloxane without abrasive produced a maximum temperature of 57°C while the C-21 polyborosiloxane on its own gave rise to a maximum temperature of 39°C. The lower viscosity C-21 polyborosiloxane reached thermal steady state in a shorter machine operating time than was the case with the medium viscosity C-11 polyborosiloxane.

The media temperature distribution across the die from wall to wall after the extrusion honing machine was stopped were generally constant with the exception of the C-11 polyborosiloxane, which was approximately 10°C cooler at the wall than in the centre (Figure 17).

The temperature distributions in an axial direction down the media parallel to the die walls after the extrusion honing machine had stopped all showed higher temperatures in the centre section of polymer with cooler material in the upper and lower portion of the polymer (Figures 18-21). This effect is less prominent for the C-21 grade polyborosiloxane (Figure 19).

#### **4.3.3 Transient temperature distributions within the die and polyborosiloxane during extrusion honing**

The results described within this section were obtained by the procedure described within section 3.2.3. The initial temperature of the C-11 polyborosiloxane and the die was between 21-22°C prior to operation of the extrusion honing machine (Figure 22). Operation of the extrusion honing machine produced an increase in the C-11 polyborosiloxane temperature up to a maximum of 54°C (after 43 minutes). During operation of the extrusion honing machine a temperature gradient developed within the C-11 polyborosiloxane with a maximum at the die wall, and a minimum at the polyborosiloxane centreline. This temperature gradient became more pronounced with the duration of extrusion honing machine operation (Figure 22). Similarly, temperatures increased within the die wall as the trial progressed, with a temperature gradient developing between the inner (44°C) and outer (39°C) die walls.

During cooling of the die after the extrusion honing operation the temperature of the C-11 polyborosiloxane in the centre of the die increases slightly by 3°C, before cooling down

to 42°C (Figure 23). Polyborosiloxane at the die wall cooled very quickly down to a temperature of 38°C at the end of the trial. Temperatures generally decreased within the cylinder wall, with a gradual decrease in the slope of the temperature gradients previously established (Figure 23).

## **4.4 Extrusion honing heat transfer models**

### **4.4.1 Introduction**

Prediction of wall shear stresses in order to provide a greater understanding of the extrusion honing process requires a knowledge of the temperature distribution of the polyborosiloxane. These temperatures may be calculated by the use of thermal models of the extrusion honing process. Such models must consider the heat generation within the polymer (due to internal shear and friction at the polymer/workpiece interface), as well as the heat transfer properties of the system (heat capacity, thermal conductivity and surface heat transfer coefficients).

The steady state thermal model quantifies the heat generation within the polyborosiloxane during extrusion honing in addition to the calculation of the surface heat transfer coefficients.

The initial phase of a transient heat generation model to predict the variation in temperature throughout the polyborosiloxane during extrusion honing has been completed in the final stages of the research project.

#### **4.4.2 Heat generation (steady state model)**

Steady state heat transfer model results (Figures 24, 25, and 26) have shown much greater heat generation in the polyborosiloxane/ grit mixtures than in the C-21 and C-11 polyborosiloxane without abrasive. Heat generation within the die in the C-21 polyborosiloxane was 147W. Of the two polyborosiloxane/ abrasive mixtures the coarser (1.035 mm) silicon carbide gave the greater heat generation (975W) than the fine (320  $\mu\text{m}$ ) silicon carbide (487W).

#### **4.4.3 Surface heat transfer coefficient between polyborosiloxane and the inner cylinder wall (steady state model)**

The surface heat transfer coefficient between the polyborosiloxane and inner die wall in the case of the C-21 polyborosiloxane could not be calculated as the polyborosiloxane and die wall temperatures were too close. Of the two polyborosiloxane/abrasive mixtures the coarser (1.035 mm) silicon carbide gave a greater transfer coefficient (5503  $\text{J}/\text{m}^2\text{K}$ ) than the finer (32  $\mu\text{m}$ ) silicon carbide (3171  $\text{J}/\text{m}^2\text{K}$ ).

#### **4.4.4 Transient heat generation model**

The transient heat generation model was intended to predict heat generation and temperature profiles within polyborosiloxane during extrusion honing. Prediction of polyborosiloxane temperatures during extrusion honing may allow the calculation of the workpiece wall shear stress from the shear rate and the duration of shear. This is important because the workpiece wall shear stress has been shown to be a function of the machining action achieved [24]. The heat transfer model calculation was completed using the experimental temperature profiles generated previously (Figure 22). The internal heat generation terms calculated by the model show that during operation of the extrusion honing machine heat generation in polyborosiloxane at the die wall is much greater than

in the polyborosiloxane in the centre of the die (Figure 27). For a period of 43 minutes heat generation at the die wall was  $210 \text{ GJ/m}^3$  compared with 75 and  $61.4 \text{ GJ/m}^3$  in the centre of the die (Figure 27).

## **4.5 Density of the polyborosiloxane**

The density of the C-11 polyborosiloxane increased linearly from  $0.965 \text{ g/cm}^3$  to  $0.985 \text{ g/cm}^3$  when the pressure was increased from atmospheric to 16 MPa, at an initial pre-compression temperature of  $30^\circ\text{C}$  (Figure 28).

An increase in the temperature of the C-11 polyborosiloxane from 15 to  $70^\circ\text{C}$  decreased the density from 0.96 to  $0.92 \text{ g/cm}^3$  at atmospheric pressure (Figure 29). The density of the C-11 polyborosiloxane decreased steadily as the temperature increased from  $15^\circ\text{C}$  to  $50^\circ\text{C}$ . At  $50^\circ\text{C}$  the density increased to a maximum of  $0.93 \text{ g cm}^{-3}$  at  $58^\circ\text{C}$  before decreasing as the temperature approaches  $70^\circ\text{C}$ .

## **4.6 The capillary rheometer**

### **4.6.1 Introduction**

The relationship between shear stress, shear strain rate, duration of shear, and temperature for C-11 polyborosiloxane has been explored by the use of suitable rheometers. These include the concentric-cylinder rheometer, the slit-die rheometer, and the capillary rheometer. The capillary rheometer was selected due to its close analogy to the extrusion honing machine, both in terms of geometry, and operating mechanism. (The slit-die and concentric cylinder rheometers were used to provide data across a wide range of shear

strain rates in order to give a more complete rheological characterisation of the extrusion honing media. In addition, the concentric cylinder and slit die rheometers were used to quantify the effects of flow geometry (die surface area etc.) on the flow properties of the C-11 polyborosiloxane.)

It was originally intended to examine polyborosiloxane/abrasive mixtures in the capillary rheometer. However, only pure C-11 polyborosiloxane has been used in this experimental programme. The exclusion of abrasive mixtures from the rheological work was due to the unexpectedly long development period required to establish a satisfactory procedure with the polymer alone (section 4.6.2.). In addition, the use of polymer/abrasive mixtures on the capillary rheometer would be highly destructive to the test apparatus (dies, transducers etc.), and would therefore require considerable modification to the rheometer.

#### **4.6.2 Experimental method development**

The capillary rheometer was selected to study the flow properties of the C-11 polyborosiloxane on account of the similarity of the process in this instrument with that in the extrusion honing machine, both in terms of geometry, and in terms of operating mechanism.

As previously described within section 3.2.4 the capillary rheometer was initially operated with the ram velocity increasing in a step like manner throughout extrusion with the extrusion barrel pressure recorded at each ram velocity. In these initial experiments (Figures 30, 31 and 23) the extrusion barrel pressure generally increased during extrusion as the ram velocity increases at temperatures of 23, 30 and 40°C. At a barrel temperature of 30°C considerable scatter in the data occurred. Similar scatter in the results was observed (Figure 33) when experiments were completed using dies of various lengths (between 20-40 mm), although a general increase in barrel pressure with piston velocity

could be observed. (These experiments were completed to determine Bagley [35] end correction parameters in order to correct the recorded pressure data for errors due to the die entrance and exit pressure drops. The scatter of the data was such that Bagley end correction factors could not be determined.

At this stage of the experimental programme it was decided to operate the rheometer at constant ram velocity throughout extrusion (section 3.2.5) in order to try and reduce the amount of scatter on the curves showing the relationship between extrusion barrel pressure and piston velocity. The rheometer was operated at a constant velocity of 2.5 cm/min and 12.5 cm/min with dies of various lengths between 20 and 40 mm. At constant ram velocity the wall pressure was found to vary considerably during extrusion. At both 2.5 cm/min (Figure 34) and 12.5 cm/min (Figure 35) the wall pressure generally increased throughout the extrusion process. The 2.5 cm/min results show a notable peak wall velocity after approximately 100 seconds of ram movement.

Following these trials a device was developed to measure independently from the rheometer instrumentation the ram velocity during the course of the experiment (section 3.2.6). Additionally, instrumentation was developed to measure simultaneously the wall pressure and cumulative mass of polyborosiloxane extruded (section 3.2.6). Such modifications and additions to the rheometer instrumentation were completed in order to investigate further the wall pressure variability during constant ram velocity operation of the capillary rheometer.

Sixteen experiments were completed in this part of the work using C-11 polyborosiloxane at a temperature of 30°C, with dies of zero, 20, 30 and 40mm length, and ram velocities of 5, 10, 15, and 20 cm/min (Figures 36-47). At a ram velocity of 5 cm/min considerable variation in the extrusion barrel pressure occurred during ram travel within the dies of 20,

30 and 40mm length (Figures 36, 37 and 38). The wall pressure for zero length dies were constant throughout ram travel for ram velocities of 5, 10, 15 and 20 cm/min (Figures 36, 39, 42, and 45). Much less variation in barrel pressure was noted with the use of constant ram velocity at higher ram velocities (10, 15, and 20 cm/min) (Figures 39- 47). In all these trials the additional ram displacement instrumentation showed the ram velocity to be constant throughout ram travel (Figure 48).

Prior to the commencement of the remaining rheological experimental work, a new extrusion ram was fitted to the capillary rheometer. Replacement of the extrusion ram on the rheometer reduced the leakage of C-11 polyborosiloxane occurring between the ram tip and the rheometer barrel. Figure 49 shows how for 100 seconds of extrusion the new ram reduced leakage from 1g to 0.5g.

A range of experiments were completed on the rheometer with the new ram using C-11 polyborosiloxane at a temperature of 30°C. A die of 40mm length and 2mm internal diameter and ram velocities of 1.58, 4.65, 7.68, 10.86 and 15.67 cm/min were used (Figures 50-54). At a ram velocity of 1.58 the barrel pressure cycled between 1 and 17.5 MPa throughout the extrusion at a frequency of about 0.008 s<sup>-1</sup> (Figure 50). At a higher ram velocity (4.65 cm/min) cycling of the wall pressure still occurred throughout the extrusion process, but superimposed onto this was a steady increase in wall pressure throughout the passage of the polyborosiloxane through the die (Figure 51). At higher ram velocities the wall pressure generally increased throughout extrusion (Figure 52, 53, and 54).

No correlation between the average extrusion barrel pressure during extrusion and the extrusion ram velocity could be determined at this stage of the experimental method development (Figure 55). It was thought that variations in the rheometer charging

procedure may be responsible for the poor correlation between the average extrusion barrel pressure and the ram velocity. Therefore the effect of rheometer charging procedure on the wall pressure recorded at constant ram velocity was investigated. The average wall pressure for C-11 polyborosiloxane at 30°C at constant ram velocity (15 cm/min) increased with increasing second barrel soak duration, when charged to the rheometer according to the modified charging procedure described in section 3.2.7 (Figure 56). For an increase in the time between charging the polyborosiloxane to the extrusion barrel and commencing extrusion of 20 minutes (4-24 minutes) the average wall pressure increased by 30% (4.4-5.75 MPa).

Once the importance of the time between charging the polyborosiloxane to the extrusion barrel and commencing extrusion on the subsequent barrel pressure during extrusion had been established, a strict rheometer charging procedure (section 3.2.7) was adopted for the remainder of the capillary rheometer trials.

The effect of temperature and ram velocity on the flow properties of the C-11 polyborosiloxane was investigated on the capillary rheometer using the procedures and instrumentation established during the period of experimental method development described above (Figures 57-77). The results of this section of the rheological investigation, as well as results from the earlier method development period are described in the sections below.

### **4.6.3 Effect of ram velocity on capillary flow**

#### ***4.6.3.1 Average barrel pressure during extrusion***

Prior to the adoption of the constant charging procedure (section 3.2.7) no correlation between the average barrel pressure and rheometer piston velocity using C-11 polyborosiloxane in the capillary rheometer at 30°C could be observed (Figure 55).

However experiments completed with the modified charging method (section 3.2.7) show a general decrease in average extrusion barrel pressure with increasing piston velocity (Figure 78). At temperatures above 30°C there is a good correlation between piston velocity and average extrusion barrel pressure using the modified charging method at all experimental temperatures (Figure 79). The average wall pressure increases with piston velocity at temperatures above 30°C. The rate of increase in average wall pressure with piston velocity is greater at higher polyborosiloxane temperature.

#### ***4.6.3.2 Variation in barrel pressure during an extrusion***

In general, low ram velocity tends to generate one of two types of extrusion barrel pressure variation during capillary flow; either a cycling of the wall pressure between a minimum and maximum value throughout extrusion (Figure 57); or a constant wall pressure throughout extrusion with very little variation (Figure 65).

At higher ram velocities a third type of extrusion barrel pressure variation may be observed during capillary flow; a steady increase in wall pressure throughout extrusion (Figure 69).

The effect of ram velocity on extrusion barrel pressure variation during capillary flow can be seen from the relevant values of the standard deviation of the extrusion barrel pressure (Figure 80). At lower temperatures the standard deviation of the wall pressure was at a maximum at low ram velocity and decreased steadily to a minimum as the ram velocity increased. However, at higher temperatures (greater than 30°C) the standard deviation of the extrusion barrel pressure increased with increasing ram velocity. For polyborosiloxane temperature above 30°C the standard deviation of the extrusion barrel pressure generally increased as the polyborosiloxane temperature decreased.

#### **4.6.4 Effect of die geometry on capillary flow**

##### ***4.6.4.1 Average barrel pressure during extrusion***

At constant internal die diameter, an increase in die length resulted in a proportional increase in the average extrusion barrel pressure during extrusion (Figure 81). At a ram velocity of 5 cm/min the average wall pressure increased linearly from 3 MPa with a zero length die (2mm internal diameter) up to 10 MPa with a 40mm die (2mm internal diameter). Similar increases in average wall pressure with increasing die length were recorded with ram velocities of 10, 15 and 20 cm/min (Figure 81).

##### ***4.6.4.2 Variation in barrel pressure during an extrusion***

The variation in extrusion barrel pressure during capillary flow generally increased with increasing die length (Figure 82). This was particularly so at the lower ram velocities. At 5 cm/min the standard deviation varied from 0.05 MPa for the zero length die up to 4.7 MPa for the 40mm long die. At a ram velocity of 20 cm/min the standard deviation of the extrusion barrel pressure varied by 0.75 MPa between the zero die and the 40mm long die.

For all experiments completed with orifice dies, the variation in the extrusion barrel pressure throughout extrusion was low at all ram velocities (Figure 82).

#### **4.6.5 Effect of temperature on capillary flow**

All capillary flow results described within this section were completed using a die of 40mm length and 2mm internal diameter. Polyborosiloxane was charged to the rheometer barrel using the procedure described in section 3.2.7.

#### **4.6.5.1 Average barrel pressure during extrusion**

The effect of temperature on the average extrusion barrel pressure during extrusion of C-11 polyborosiloxane is highly dependent on the ram velocity (Figures 79, and 83). At a low ram velocity (1.25 cm/min) the average extrusion barrel pressure remains constant at 10 MPa over the temperature range 30-70°C. However, at higher piston velocities the average wall pressure generally increases with increasing temperature. This effect is greatest at a piston velocity of 15 cm/min where the average wall pressure increased from 3 to 50 MPa for a corresponding temperature increase of 40°C (30-70°C).

The largest increase in average extrusion barrel pressure occurred in the lower temperature range between 30°C and 45°C, whereas the average extrusion barrel pressure increases were proportionally smaller in the 45°C to 70°C range.

Beyond 70°C the second order polynomials fitted to the data in Figure 83 would indicate that the average wall pressures may decrease with further increases in temperature. A maximum average wall pressure is given by the fitted equations at approximately 60°C irrespective of ram velocity.

#### **4.6.5.2 Variation in barrel pressure during an extrusion**

At low ram velocities (1.25 to 2.5 cm/min) an increase in the polyborosiloxane temperature changed the form of the extrusion barrel pressure variation during capillary flow from a mixture of constant pressure and cycling between minimum and maximum values (Figures 57, 58 and 66 ) to one of steady constant pressure throughout extrusion (Figures 65, 70 and 71).

At higher ram velocities (5 to 15 cm/min) an increase in the polyborosiloxane temperature from 30°C to 39°C resulted in the transition from generally constant extrusion barrel

pressure during capillary flow (Figures 59-64) to a general increase in the extrusion barrel pressure throughout extrusion (Figures 67-69). Continued increase in the polyborosiloxane temperature from 39°C to 70°C, at these higher ram velocities resulted in a transition from the general increase in extrusion barrel pressure during extrusion (Figures 68 and 69) to constant extrusion barrel pressures throughout extrusion (Figure 77).

At very low ram velocity (1.25 cm/min) it was difficult to discern any definite effect of polyborosiloxane temperature on the standard deviation of the extrusion barrel pressure during capillary flow (Figure 80). However, at higher ram velocities there are some clear trends to be noted (Figure 80); an increase in the temperature from 30°C to 39°C results in an increase in the variation of the extrusion barrel pressures recorded during capillary flow; whilst a further increase in temperature from 39°C to 70°C resulted in a decrease in the recorded extrusion barrel pressure variation. Thus, maximum variation in the recorded extrusion barrel pressure occurred at a temperature of 39°C in the polyborosiloxane.

#### **4.6.6 Effect of charging procedure on capillary flow**

##### ***4.6.6.1 Average barrel pressure during extrusion***

The average extrusion barrel pressure during constant ram velocity extrusion at 15 cm/min and 30°C was found to increase as the time between charging the polyborosiloxane to the extrusion barrel and commencing extrusion was increased (Figure 56). For an increase of 20 minutes in the time between charging the polyborosiloxane to the extrusion barrel and commencing extrusion the average extrusion barrel pressure increased by 30%, from 4.4 to 5.75 MPa.

#### **4.6.6.2 Variation in barrel pressure during an extrusion**

An increase in the time between charging the polyborosiloxane to the extrusion barrel and commencing extrusion had little effect of the variability of the extrusion barrel pressure during capillary flow; the extrusion barrel pressure variation during extrusion being low in each case (Figure 84).

#### **4.6.7 Die mass flow rate during capillary flow**

The mass flow rate during capillary flow through the die has been calculated at a variety of ram velocities. (This calculation assumed constant flow throughout the extrusion process and was obtained by dividing the mass extruded by the duration of extrusion). By this method the mass flow rate at 1.25 cm/min ram velocity was 57.5 mg/sec. At 2.5 cm/min and 15 cm/min the flow rate was determined as 111.3 mg/sec and 681 mg/sec respectively (Table 5).

Actual mass flow rates through the die have been determined experimentally by the method described in section 3.2.9 (Figures 85-89). The average values of these experimentally determined mass flow rates are in good agreement with the calculated values described above (Table 5). However, there was a wide range in the variation of the mass flow rate during capillary flow, the extent of which depended on the ram velocity and the polyborosiloxane temperature. The degree of variation of the mass flow rate during capillary flow is a close function of the variability of the extrusion barrel pressure (Figures 85-89).

During capillary flow of C-11 polyborosiloxane at 30°C and a ram velocity of 1.25 cm/min both the extrusion barrel pressure and the mass flow rate through the die varied in a cyclic manner throughout extrusion (Figure 85 and 86). The frequency of the variation in both the extrusion barrel pressure and the die mass flow rate variations was 0.02 s<sup>-1</sup>. However,

the two were out of phase, with the peaks of the mass flow rate, generally occurring at the troughs of the extrusion barrel pressure fluctuations. At 30°C and a ram velocity of 1.25 cm/min the amplitude of the mass flow rate variation during capillary flow suffered attenuation during the course of the extrusion (Figure 86). However, the amplitude of the corresponding wall pressure fluctuation remained constant throughout the extrusion process.

At a higher ram velocity (2.5 cm/min) and a higher polyborosiloxane temperature (39°C) a similar relationship can be noted between the extrusion barrel pressure and the die mass flow rate fluctuations during capillary flow (Figure 87), with the mass flow rate through the die out of phase of the extrusion barrel pressure. However, the frequency of oscillation of the extrusion barrel pressure and mass flow rate through the die was more variable than at the lower ram velocity ranging from about 0.017 s<sup>-1</sup> to 0.025s<sup>-1</sup>. As with the oscillations at the lower rate (1.25 cm/min) the amplitude of the die mass flow rate suffered attenuation during the period of extrusion, whilst the amplitude of the corresponding wall pressure fluctuation remained constant.

At higher temperatures (45°C) much more constant mass flow rates are obtained during capillary flow through the die. At a ram velocity of 2.5 cm/min this flow rate remains constant throughout extrusion at 109.1 mg/sec whilst the wall pressure also remained constant at 18 MPa (Figure 88). At higher temperature (45°C) and ram velocity (15 cm/min) the mass flow rate remains relatively constant throughout extrusion with only a slight increase in flow rate in the centre portion of the extrusion (Figure 89). The corresponding wall pressure generally increased throughout the extrusion process.

## **4.7 Slit die rheometer**

### **4.7.1 Introduction**

The quantitative relationships between shear stress, shear strain rate, duration of shear, and temperature for C-11 polyborosiloxane have been explored in order to provide a greater understanding of the extrusion honing process . Three rheometers have been used to determine the flow properties of the C-11 polyborosiloxane; the concentric cylinder rheometer, the slit die rheometer, and the capillary rheometer.

The slit die rheometer has been used to provide C-11 polyborosiloxane flow property data across a broader shear strain rate range than would be possible from capillary rheometer data alone. In addition, comparison of slit die and capillary die wall shear stresses at similar shear strain rates may allow the effect of restriction geometry on the flow properties of the C-11 polyborosiloxane to be evaluated.

### **4.7.2 Effect of ram velocity and temperature on wall pressure**

The total average pressure drop down the length of the slit die was linearly related to the die flow rate (calculated from ram velocity, assuming incompressibility, Figure 90). At both 30°C and 43°C the average pressure drop down the length of the slit die increased linearly with die flow rate.

At die flow rates below 11.5 cm<sup>3</sup>/min higher average die pressure drops were produced at 43°C than at 30°C for the same flow rate. However, at higher flow rates the reverse was obtained (Figure 90). At both temperatures and all ram velocities (1.25, 2.5 and 5 cm/min) linear pressure drops along the length of the die restriction were achieved (Figure 91). The slope of the pressure/distance along the die wall curve generally increased as either the ram velocity or temperature increased.

The average values described above were calculated from the individual wall pressure values (Figures 92-97) during extrusion in the slit die. These recorded wall pressures varied little throughout extrusion, with no excessive cycling, or increase in the pressure, as had been noted in the capillary die experiments. One exception to the generally constant wall pressures obtained in the slit die was the experiment conducted with the 5 cm/min ram velocity, and 43°C barrel temperature. In this case the wall pressure increased during the first 60 seconds of ram travel. This period of wall pressure increase was followed by a drop in the wall pressure of approximately 3 MPa over a period of 20 seconds, after which constant wall pressure values were maintained for the remainder of the extrusion (Figure 97).

## **4.8 Calculated shear stress and shear strain rate**

### **4.8.1 Capillary rheometer**

At test temperatures of (30, 39 and 45°C) C-11 polyborosiloxane has been shown to be highly pseudoplastic in the capillary rheometer (Figure 98). The greatest pseudoplasticity was exhibited at the lower polyborosiloxane temperature. Comparison of apparent viscosity data (Figure 98) with Rabinowitch [25] corrected data (Figure 99) showed the same general pseudoplastic trends at 30°C. However the Rabinowitch [25] viscosity was independent of the shear strain rate at 39°C and 45°C (Figure 99).

The apparent shear viscosity at low shear strain rate ( $75 \text{ s}^{-1}$ ) was constant at about 1.6 KPa·s at all test temperatures. When the strain rate increased to  $600 \text{ s}^{-1}$  at 30°C the shear viscosity was reduced to 0.02 KPa·s. At higher temperatures (39 and 45°C) a similar increase in strain rate resulted in a reduction in the shear viscosity to 0.2 and 0.7 KPa·s respectively.

#### 4.8.2 Slit die rheometer

The apparent rheological properties of the C-11 polyborosiloxane as measured by the slit die rheometer have been shown to vary greatly at different test temperatures (Figure 100). At 43°C the C-11 polyborosiloxane behaved as a pseudoplastic material with the viscosity dropping from 1.024 to 0.797 KPas, for a corresponding increase in apparent shear strain rate from 23.8 s<sup>-1</sup> to 95.0 s<sup>-1</sup>. However, at 30°C the same grade of polymer exhibited dilatent behaviour, with the apparent shear viscosity increasing from 0.4 to 0.89 KPas for a corresponding increase in shear strain rate from 23.8 to 95.0 s<sup>-1</sup>.

#### 4.8.3 Concentric cylinder rheometer

Concentric cylinder rheology at 30°C has shown that the shear stress of the C-11 polyborosiloxane is a function of the rotor acceleration during the test as well as the instantaneous shear rate. At a shear rate of 1 s<sup>-1</sup> a shear stress of 200 Pa was recorded with a rotor acceleration of 40 r.p.m.<sup>2</sup>, whereas the corresponding shear stress was 400 Pa at a rotor acceleration of 20 r.p.m.<sup>2</sup>. In general, for a given shear rate, the greater the rotor acceleration the lower the shear stress (Figure 101).

The variation in shear stress during the application of shear at a variety of constant rotor speeds can be seen in Figure 102. In each case the shear stress increased to a maximum plateau level within about 15 seconds. The higher the rotor speed (shear rate), the higher the shear stress obtained. The disconnection of the rheometer drive, after the shear stress plateau described above had been obtained resulted in a steady decrease in the recorded shear stress to zero (Figure 103). Individual shear stress values have been taken from Figure 94 and have been tabulated together with shear rate in Table 9. The shear stress increased from 66 to 550 Pa for a corresponding increase in shear rate of 0.046 to 0.869s<sup>-1</sup>. Results from the concentric cylinder rheometer show the C-11 polyborosiloxane to be pseudoplastic at 30°C over the measured range (0.046 - 0.869 s<sup>-1</sup>) (Figure 104).

## 4.9 Shear stress/shear strain rate relationships

At 30°C there is a linear relationship between log shear stress and log apparent shear strain rate for C-11 polyborosiloxane subjected to a strain rate of up to 100 s<sup>-1</sup> (Figure 105). This linear relationship is based on data obtained with the use of the concentric-cylinder and the slit die rheometer. A power law equation has been fitted to this data to describe the rheological behaviour of the C-11 polyborosiloxane at a temperature of 30°C and shear rates between 0 and 100 s<sup>-1</sup>.

$$\tau = 0.989 (\dot{\gamma})^{0.938}$$

At the top limit of the valid range of the power law approximation the shear stress data obtained from the slit die (84 KPa at 95 s<sup>-1</sup>) is in reasonable agreement with the data obtained from the capillary die (120 KPa at 76 s<sup>-1</sup>). At shear rates greater than 100 s<sup>-1</sup> the pseudoplastic nature of the polyborosiloxane increases rapidly and the shear stress decreases with increasing strain rate (Figure 105). (It should be noted that data presented at shear rates greater than 100 s<sup>-1</sup> are based on average extrusion barrel pressures during capillary flow. In some cases the extrusion barrel pressure varied significantly throughout extrusion. This is discussed further within section 5).

The pseudoplastic nature of the polyborosiloxane decreases as the temperature is increased at shear strain rates greater than 50 s<sup>-1</sup> (Figure 106). (However, as above, it should be noted that this data is based on average extrusion barrel pressures which in some cases varied significantly throughout extrusion).

At 30°C the shear viscosity of the polyborosiloxane may be approximated to 1 KPa·s at shear strain rates less than 100 s<sup>-1</sup> (Figure 107). At shear strain rates greater than 100 s<sup>-1</sup> and temperatures of 30°C the polyborosiloxane has been shown to be highly pseudoplastic

(Figure 107). At temperature greater than 30°C the pseudoplastic nature of the polyborosiloxane decreases significantly at shear strain rates greater than 100 s<sup>-1</sup> (Based on average capillary rheometer data).

#### **4.10 Calculated velocity profiles**

The power law shear viscosity equation described in section 4.9 and the velocity profile equation given in section 3.3.5 may be used to calculate the variation of velocity of the C-11 polyborosiloxane in the die under a range of operating conditions. The results of such calculations are described below.

With fixed die dimensions (1mm internal radius and 40mm length) the polymer velocity variation across the die during capillary flow increased from almost uniform values across the section with 5 MPa pressure drop to a parabolic variation at a 50 MPa pressure drop (Figure 108). Whilst the wall velocity was zero in both cases, the centreline velocity increased from 0.04 m/s to 0.70 m/s as the die pressure drop increased by the same amount (Figure 108).

At a pressure drop of 25 MPa a reduction in the die length from 40mm to 20mm significantly increased the magnitude of the variation in the polyborosiloxane velocity over the die cross section (Figures 108 and 109). Such a reduction in die length also resulted in an increase in centreline velocity from 0.33 m/s to 0.7 m/s. Conversely, an increase in the die length from 40mm to 100mm resulted in a significant reduction of the velocity variation over the cross-section (Figure 109). Such an increase in die length resulted in a decrease in centreline velocity from 0.33 m/s to 0.13 m/s.

The velocity variation across the die cross-section was found to increase in magnitude when the internal radius of the die was increased from 1mm to 1.5mm whilst maintaining a die length of 40mm and a die pressure drop of 25 MPa. Such an increase in die width resulted in an increase in centreline velocity from 0.33 m/s to 0.75 m/s (Figure 109). In all the calculations the die wall velocity was assumed to be zero.

#### **4.11 Calculated shear stress and shear strain rate profiles**

For the purposes of these calculations the shear stress and shear strain rate during capillary flow have been assumed to be zero at the die centreline with all die pressure drops in the range 5 MPa to 50 MPa for a die of 1mm internal radius and 40mm length (Figures 110 and 111).

At low pressure drops (5 MPa) very small variations in shear stress and shear strain rate are produced across the die cross-section, and the magnitudes of the wall shear stresses and wall strain rates are low (Figures 110 and 111). However, an increase in the die pressure drop, at fixed die dimensions (1mm internal radius, 40mm long) resulted in significant increase to both the wall shear stress and the wall strain rates (Figures 110 and 111). Such changes in the die pressure drop resulted in the shear stress and strain rate variation across the section of the die to become progressively more parabolic as opposed to the flatter profiles obtained at lower die pressure drops. Increases in the die pressure drop from 5 MPa to 50 MPa resulted in an increase in die wall shear stress from 50 KPa to 600 KPa (Figure 110) and an increase in wall shear rate from  $100 \text{ s}^{-1}$  to  $1500 \text{ s}^{-1}$  (Figure 111). For a fixed die pressure drop (25 KPa) and fixed die internal radius (1mm) an increase in the die length resulted in a significant reduction in the variation of both the shear stress and the shear strain rate across the die section (Figures 112 and 113). Increases in the die length from 40mm to 100mm resulted in a reduction of wall shear stress from

300 KPa to 100 KPa (Figure 112) and a reduction in wall shear strain rate from  $700 \text{ s}^{-1}$  to  $200 \text{ s}^{-1}$  (Figure 113). Conversely, a reduction in the die length resulted in an increase in the variation in both the shear stress and the shear strain rate across the section. Shortening the die length from 40mm to 20mm resulted in an increase in wall shear stress from 300 KPa to 600 KPa and an increase in wall shear strain rate from  $200 \text{ s}^{-1}$  to  $1500 \text{ s}^{-1}$  (Figures 112 and 113).

The use of wider dies also increased the wall shear stress and strain rate and increased the parabolic nature of both distributions across the section (at fixed die length (40mm) and fixed die pressure drop (25 MPa)). An increase in the die internal radius from 1.0mm to 1.5mm resulted in an increase in wall shear stress from 300 KPa to 500 KPa (Figure 112) and an increase in wall shear strain rate from  $200 \text{ s}^{-1}$  to  $1300 \text{ s}^{-1}$  (Figure 113).

#### **4.12 Results of control experiments using polystyrene**

It has been shown in the previous sections that the extrusion barrel pressure during the extrusion of C-11 polyborosiloxane at constant ram velocity in the capillary rheometer may vary considerably throughout this process. In order to ensure that these extrusion barrel pressure variations were genuine material properties of the C-11 polyborosiloxane, and not an intrinsic feature of the experimental equipment, a sample of polystyrene was tested on the capillary rheometer, as described in section 3.2.10.

The polystyrene tested on the capillary rheometer as a control experiment has been shown to demonstrate power law pseudoplastic behaviour at  $230^{\circ}\text{C}$  (Figure 126). The extrusion barrel pressure recorded during capillary flow at all ram velocities (1.25, 2.5, 5, 10 and 15 cm/min) was constant throughout extrusion. No cycling of the pressure, or pressure increases, of the form exhibited by the C-11 polyborosiloxane were noted during the

extrusion of the polystyrene (Figures 114-123). Changes in the packing tightness of the polystyrene granules prior to soak had very little effect on the average wall pressures obtained during capillary flow (Figure 124).

The calculated shear stress increased pseudoplastically with shear strain rate (Figure 125), and the rheology of the polystyrene may be approximated to a pseudoplastic power law model as demonstrated by the linear form of the log shear stress against log shear rate graph (Figure 126).

#### **4.13 Mathematical model of density and mass flow rate during capillary flow**

The experimental results shown in Figures 86-89 were used as the data source for the mathematical model calculations of the density and die mass flow rate during capillary flow. The extrusion barrel pressure during capillary flow was approximated to a function from the maximum pressure, the minimum pressure and the pressure wavelength using the calculation method described in section 3.4.2. The approximated extrusion barrel pressure variations used in the mathematical model (Figures 127-130) are in good agreement with the experimental values (Figures 86-89). The die mass flow rate during extrusion was calculated from the approximated extrusion barrel pressures by the calculation methods described in section 3.4.2

For a temperature of 30°C and a ram velocity of 1.25 cm min<sup>-1</sup> the calculated die mass flow rate oscillates initially between 30 and 90 mg s<sup>-1</sup> (Figure 127). The variation in the calculated die mass flow rate attenuates linearly throughout extrusion to between 55 and 65 mg s<sup>-1</sup> when the extrusion is near completion. This variation in the die mass flow rate

calculated from the extrusion barrel pressure (Figure 127) is in excellent agreement with the experimentally measured value (Figure 86).

Similarly the calculated die mass flow rate of C-11 polyborosiloxane extruded at 2.5 cm min<sup>-1</sup> and 39°C (Figure 128) is in excellent agreement with the experimentally measured value (Figure 87) both in terms of fluctuation and of attenuation in the fluctuation throughout extrusion.

At an extrusion rate of 2.5 cm min<sup>-1</sup> at 45°C the experimental extrusion barrel pressure and the die mass flow rate were constant throughout extrusion (Figure 88). The mathematically modelled die mass flow rate showed similar consistency (Figure 129). At higher ram velocities (15 cm/min) at 45°C the experimental extrusion barrel pressure increases considerably and the die mass flow rate increases slightly throughout extrusion (Figure 89). A similar slight increase in die mass flow rate was calculated from the extrusion barrel pressure using the mathematical model (Figure 130).

In conclusion it has been found that the mathematical model accurately predicts the die mass flow rate from the extrusion barrel pressure under a variety of experimental conditions (oscillating pressure, constant pressure and increasing pressure) as compared with experimentally measured die mass flow rates.

## 5. DISCUSSION

---

### 5.1 Introduction

The primary objective of this research programme was to achieve a greater understanding of the thermal and rheological characteristics of the C-11 grade polyborosiloxane extrusion honing medium, in order to provide information which may enable greater control and optimisation of the extrusion honing process to be exercised.

In order to complete this objective a number of thermal and rheological experiments have been completed, data from which has been used to calculate the thermal and rheological properties of the C-11 polyborosiloxane. These experiments and calculations have been used as the basis for the proposed flow mechanisms (section 5.4) of the C-11 polyborosiloxane. These mechanisms, in turn, have been discussed with respect to the extrusion honing process (section 5.5).

Prior to discussion of the calculated thermal and rheological properties of the C-11 polyborosiloxane, the quality of the basic experimental data on which these calculations are based has been discussed (section 5.2). The basic experimental data has been critically discussed with respect to any possible experimental errors which may have occurred. Assumptions, possible errors, and the validity of the thermal and rheological calculations have also been critically discussed (within section 5.3). The final sections of the chapter include a discussion of the possible flow mechanisms and thermal behaviour of the C-11 polyborosiloxane as well as discussion of possible implications of these mechanisms to the extrusion honing process.

## **5.2 The accuracy of the experimental data**

### **5.2.1 The accuracy of the measured rheometer extrusion barrel pressure**

The accuracy and calibration of the Dynisco, mercury diaphragm pressure transducers, used on both the capillary and slit die rheometers, have been established by testing the transducers on a pressure chamber against a calibrated Bourdon test gauge. All pressure transducers tested by this method were found to be in excellent calibration (Figure 131). It may also be noted that calibrations were completed using the data logger recording system described in section 3.2.6, and so, it was in fact the entire transducer and associated instrumentation (data logger etc.) which was shown to be in calibration, rather than the transducer alone.

In addition to these calibrations the capillary rheometer was operated with polystyrene as a test material. The purpose of these tests was to establish that the extrusion barrel pressure variations, such as those illustrated in Figure 86, which occurred during constant ram velocity extrusion of C-11 polyborosiloxane, were functions of the polyborosiloxane material properties alone and not an intrinsic function of the test equipment (electrical interference etc.). Extrusion barrel pressures recorded during extrusion of polystyrene through the capillary rheometer at various constant ram velocities remained constant throughout the period of ram travel, as can be seen in Figures 114-123. These polystyrene results further substantiate the proposal that the variations in extrusion barrel pressure which may occur during constant ram velocity extrusion of C-11 polyborosiloxane are a function of the properties of the polymer and independent of the test equipment and instrumentation.

The response time of the pressure recording system including the transducers and associated equipment has also been considered. During the calibration programme the

response of the data logger output to applied pressure on the transducer was found to be less than 0.5 seconds in all cases. The minimum interval of data collection in this experimental programme was 2 seconds. Therefore, the resolution of the experimental equipment was always a minimum of 4 times the resolution of the data collection frequency.

### **5.2.2 The accuracy of the measured rheometer ram velocity**

The majority of the capillary and slit die rheometer experiments have been completed with the rheometer set to extrude at constant ram velocity. The assumption of constant ram velocity is fundamental in the discussion of the flow mechanism of the polyborosiloxane. Consequently, it is important to establish that the actual ram velocity corresponds to the set point ram velocity, and that ram velocity is constant throughout extrusion.

During operation of the capillary and slit die rheometers, no stalling or speed variation of the rheometer ram could be observed by visual inspection with the naked eye. The assumption of constant ram velocity was tested more quantitatively by the use of the additional ram displacement measuring device described in section 3.2.6. The ram displacement was recorded on the data logger for all experimental runs and showed the ram to be moving at constant ram velocity in each case. However, the actual ram velocity was found to be slightly lower than the set point velocity (Figure 48). Consequently, an appropriate correction was applied to the calculations.

### **5.2.3 The accuracy of the measured polyborosiloxane flow rate through a capillary die**

An accurate measurement of the volumetric flow rates through the capillary and slit dies is critical to the accurate determination of the apparent wall shear rate within the dies.

Calculation of the theoretical volumetric flow-rate through the capillary and slit dies can be completed from a knowledge of the ram velocity, the extrusion barrel dimensions, and the die internal dimensions. However, such a calculation is only valid if constant density of the C-11 polyborosiloxane is assumed and no leakage occurs between the rheometer barrel and ram. Both of these assumptions are thought to be in some doubt in this case. Firstly, leakage of C-11 polyborosiloxane between the rheometer ram and the extrusion barrel has been shown to occur, although this was significantly reduced after the replacement of the extrusion ram tip (Figure 49). Leakage of C-11 polyborosiloxane in this manner, is not considered significant enough to affect seriously the rheological properties determined from the slit-die or the capillary rheometer. This statement can be quantitatively supported by consideration of a typical capillary rheometer extrusion. For a ram velocity extrusion of 5 cm/min (240 seconds of shear) the total leakage of C-11 polyborosiloxane between the extrusion barrel and the ram would be 0.75 g (Figure 49). Such an extrusion would take about 240 seconds which would give an average leakage rate of 3.125 mg/second. The corresponding calculated die extrusion rate would be 230 mg/second. Leakage would therefore only account for 1.39% of the total die extrusion rate, and have minimal effect on subsequent calculations.

The theoretical die volumetric flow rate, obtained by calculation has been checked by experimental measurements. Traditional methods of measuring die mass flow rate usually involve cutting lengths of extrudate at intervals and weighing them [54,55]. It was initially thought that this technique would be impractical with the C-11 polyborosiloxane as it is fluid at room temperature and its adhesive properties make it difficult to divide into separate samples. Consequently, as an alternative, a piezo- electric force transducer was placed under the extrusion barrel in order to measure the cumulative mass of polyborosiloxane extruded. However, the device probably dampened any short term variations in mass flow rate due to the delay between the exit of the C-11 polyborosiloxane

from the extrusion die and its arrival on the balance pan. A more satisfactory method of measuring the die exit mass flow rates was produced, which involved the taking of samples manually at the die exit at 15 second intervals (the edge of the sample container was 'smeared' against the bottom of the die in order to separate the polyborosiloxane into individual samples). It was estimated that the maximum error in the interval between the taking of each sample was  $\pm 0.5$  seconds which gives a maximum error of  $\pm 3.3\%$ . As the die exit mass flow rate has been shown to vary by as much as  $\pm 38\%$  ( Figure 86 - ram velocity 1.25 cm/min), the sample time interval error of 3.3% is so low that it may be considered to have minimal effect on the recorded mass flow rates. It is interesting to note that both Rudin and Vlasschaert [54] and Rudin and Chang [55], who determined die mass flow by cutting and weighing lengths of extrudate, do not discuss the variation associated with such manual techniques. It may be concluded from this, that they also consider the variation involved with such techniques to be minimal, when compared to the magnitude of density and pressure variations being studied. Despite the large variations in mass flow rate which have been measured during capillary flow (Figure 86) the average mass flow rates agree closely with those calculated from the ram velocity, and the dimensions of the die and rheometer barrel (Table 5). This correlation clearly indicates that the observed variations in mass flow rate are a genuine effect associated with the rheological characteristics of the material and not an effect due to the experimental technique.

One factor which could cause variations in the die mass flow rate during constant ram velocity capillary flow is leakage between the extrusion ram and barrel. However it is thought unlikely that such variations in die mass flow rate are due entirely to C-11 polyborosiloxane leakage between the extrusion ram and the barrel. This is because the mass flow rate may vary by as much as 50 mg/sec (Figure 86) at a ram velocity of 1.25 cm/min, whereas, average leakage during such an extrusion is only 3.9 mg/sec (Figure 49). Leakage can therefore only account for a maximum of 7.8% of the total mass flow rate

variation occurring. Rudin and Vlasschaert's [54] study of the density of polymer melts during extrusion similarly concluded that backflow of the polymer melt against the advancing piston was unlikely to cause the density variations they observed within the rheometer barrel. They calculated that the volume of polymer which would need to "backflow" to maintain constant density would have been clearly visible to the naked eye. They observed no such leakage.

#### **5.2.4 The accuracy of the measurements of the temperature in the polyborosiloxane and die**

In order that discussion of possible heat generation mechanisms during extrusion honing be valid, the accuracy of temperature measurements in the C-11 polyborosiloxane and dies during the experimental programme, must be considered.

The temperatures of the C-11 polyborosiloxane and dies were measured with thermocouples previously calibrated at 0°C using ice and water. However, the determination of the C-11 polyborosiloxane temperature at an instant in time during operation of the extrusion honing machine may be subject to an error due to heat transfer occurring in the period between stopping and unclamping the machine and the insertion of the thermocouples. However, changes in polyborosiloxane temperature due to this delay are likely to be minimal due to the low thermal conductivity ( $0.17 \text{ W m}^{-1}\text{K}^{-1}$ ) of the C-11 polyborosiloxane (section 4.2).

The low thermal conductivity of the C-11 polyborosiloxane is further emphasised in Figure 23, where it can be seen that the change in temperature in static polyborosiloxane over a short period of time is minimal. Comparison of profiles at 0 and 20 seconds show that the temperature only varies by approximately 1°C over this 20 second period and that the overall shape of the profile remains the same.

## **5.3 The validity of the calculations**

### **5.3.1 The validity of the shear strain rate calculations**

The shear strain rate of the C-11 polyborosiloxane has been calculated from experimental data from the capillary die, the slit die and the concentric cylinder rheometers in order to complete subsequent viscosity calculations and enable definition of the rheological characteristics of the material. For the concentric cylinder rheometer the shear strain rate was calculated from the rheometer dimensions and the rotor velocity. The shear strain rate for the capillary and slit die rheometer has been calculated from the die volumetric flow rate and the die dimensions.

When calculating the apparent wall shear strain rate from capillary rheometer and slit die rheometer data it has been assumed that the C-11 polyborosiloxane is incompressible, so that the volumetric die flow rate, may be calculated directly from the ram velocity, and the barrel internal dimensions. In this ideal situation the apparent wall shear strain rate within the die would increase instantaneously from zero to a finite value as soon as ram movement commenced. This assumption is incorrect, as the C-11 polyborosiloxane has been shown to be compressible (Figure 28).

Reference to the typical extrusion barrel pressure variations during constant ram velocity extrusion (Figures 57-77) shows that the extrusion barrel pressure increases rapidly during the first few seconds of ram travel. This period of increasing extrusion barrel pressure is thought to correspond with a period of compression of the C-11 polyborosiloxane in the barrel. If compression of C-11 polyborosiloxane in the barrel is assumed, then on initial ram movement, minimal flow through the extrusion die will occur, as the displacement of the ram will be partially compensated for by C-11 polyborosiloxane compression. However, as the ram advances further, the rate of compression of the C-11

polyborosiloxane in the barrel may decrease resulting in an increase in die volumetric flow rate. When C-11 polyborosiloxane compression has reached a maximum the die volumetric flow rate may become stable and equal to the ram displacement. Such a mechanism is well illustrated by the results for C-11 polyborosiloxane extruded from the capillary rheometer at a temperature of 45°C and a ram velocity of 2.5 cm/min (Figure 88). The ram descends for approximately 40 seconds before both the die mass flow rate and the wall pressure maintain constant stable values. During this initial 40 second period of ram travel the die mass flow rate and the wall pressure steadily increase whilst the ram advances at constant velocity. As the rate of change of the internal volume of the system is constant this must result in density variations within the rheometer. Similarly a period of approximately 10 seconds after the ram stops at the end of the extrusion is required before the wall pressure and the die mass flow rates fall to zero. It is suggested that during this period the C-11 polyborosiloxane in the barrel is decompressed, resulting in a decrease in density due to the reduced pressure within the barrel. Thus it may be concluded that during constant ram velocity extrusion the die shear strain rate on initial ram movement will be zero, but will increase rapidly as the rate of compression of the C-11 polyborosiloxane decreases with respect to the ram displacement. Similarly the die shear strain rate will steadily decrease as the C-11 polyborosiloxane in the barrel is decompressed when the ram reaches the end of its travel. This observation is true for all constant ram velocity capillary and slit die results presented within this thesis.

In some cases, particularly at higher temperatures (Figure 88 and 89), the die mass flow rate of C-11 polyborosiloxane from a capillary die has been shown to be relatively consistent throughout ram travel (excluding the initial and final ram movement discussed above). It may be concluded from these results that, provided large density variations do not occur, the die flow rate and therefore the apparent wall shear strain rate within the die remain constant throughout constant velocity ram travel. However, the mass flow rate of

C-11 polyborosiloxane from the capillary die during constant ram velocity extrusion at lower temperatures and ram velocities has been shown to vary throughout the experiment. Such variations are clearly illustrated in Figures 85-87. Rudin and Vlasschaert [54] observed similar variations in the die mass flow rate during extrusion at constant ram velocity. However, they [54] concluded that this cycling of the mass flow rate was due to variations in ram velocity originating in the rheometer mechanical train. This is clearly not the case within this experimental programme as has been demonstrated in section 5.2.2. However, whilst variations in mass flow rate during constant ram velocity have been demonstrated, it is not necessarily the case that the apparent wall shear rate also varies. This is because the apparent wall shear rate is a function of the volumetric flow rate and not the mass flow rate. A knowledge of the dynamic C-11 polyborosiloxane density in the rheometer barrel during the constant ram velocity trials is therefore necessary in order to interpret the effect of the die mass flow rate variations on the apparent wall shear rate.

If the wall shear strain rate in the die is constant throughout extrusion, then the volumetric die flow-rate throughout extrusion must also be constant. The possibility that the volumetric flow rate is constant throughout extrusion whilst the measured wall pressure and the mass flow rate fluctuate (e.g. Figure 86) has been explored by means of the following calculation. The calculated die mass flow rate at a ram velocity of 1.25 cm/min is 57.5 mg/s when incompressibility is assumed (Table 5). This compares very closely with the experimentally measured average values of 55.2 and 56.9 mg/s (Table 5). If incompressibility is assumed then the calculated die volumetric flow rate at a ram velocity of 1.25 cm/min would be 3.563 cm<sup>3</sup>/min. From these calculated die mass and volumetric flow rates the C-11 polyborosiloxane density in the die is 0.969 g cm<sup>-3</sup>. Reference to Figure 28 shows that this density corresponds to an applied pressure of 3 MPa. (This compares favourably with the experimentally measured average wall pressure for the extrusion at a mid-point in the die of 3.24 MPa (assuming a linear pressure drop down the die)).

However, the mass flow rate has been shown experimentally not to be constant at 57 mg/s but to vary between 40 and 90 mg/s (Figure 86). In order that the volumetric die flow rate, and therefore the wall shear strain rate, remain constant, the corresponding C-11 polyborosiloxane density within the die would have to vary between  $0.674 \text{ g cm}^{-3}$  and  $1.516 \text{ g cm}^{-3}$ . The C-11 polyborosiloxane density has been shown to vary between 0.965 and  $0.990 \text{ g cm}^{-3}$  across the range of static pressure capable of being generated in the capillary rheometer (Figure 28). It is therefore most unlikely that the C-11 polyborosiloxane density in the die varies across the range  $0.674 \text{ g cm}^{-3}$  to  $1.516 \text{ g cm}^{-3}$ , in order for the volumetric die flow rate (and therefore the shear strain rate) to remain constant, when the die mass flow rate varies between 40 and 90 mg/s.

Another important factor to consider when calculating the die wall shear strain rate from the ram velocity, the barrel dimensions and the die internal dimensions, is the amount of C-11 polyborosiloxane leakage between the rheometer barrel and extrusion ram. If this leakage is excessive then the actual wall shear strain rate will be lower than that calculated from the ram velocity and the internal dimensions under conditions of incompressibility. However, as has been discussed previously in section 5.2, for a ram velocity of 5 cm/min, leakage only accounted for 1.39 % of the total mass flow rate. This may be interpreted as a maximum of 1.39% variation in the wall shear strain rate if constant density is assumed. The calculated shear strain rate does not therefore require significant correction due to C-11 polyborosiloxane leakage between the rheometer barrel and the extrusion ram.

The apparent shear strain rate calculation for capillary flow assumes a zero die wall velocity and a Newtonian parabolic velocity profile across the die perpendicular to the flow direction [25]. Rabinowitsch [25] has formulated an equation (2.12) for calculating the true shear strain rate taking into account the presence of non-parabolic velocity profiles. Whilst the Rabinowitsh [25] correction has been applied to the data, the validity

of such calculations is considered limited in this case due to the large variations in extrusion barrel pressure and die mass flow rate which have been shown to occur during constant ram velocity extrusion. Consequently apparent shear strain rate data has been presented throughout the majority of the thesis. (Vinogradov et al [57] have presented a more extreme argument that only the dependence of the flow rate on the pressure should be presented under such conditions.)

In conclusion, from the experimental results produced, particularly those relating to the mass flow rate measurements in the die (Figures 85-89), it is improbable that the shear strain rate remains unchanged during operation of the capillary rheometer at constant ram velocity, particularly at low temperatures and ram velocities. The C-11 polyborosiloxane has been shown to be compressible under static test conditions. Such compression may result in a rapid increase in the die shear strain rate in the early stages of ram travel during capillary or slit die extrusion. This is due to a steady reduction in the rate of compression of the polymer. In some cases, particularly at low ram velocity, the wall shear strain rate may vary throughout extrusion due to dilation and compression of the C-11 polyborosiloxane in the extrusion barrel. The amplitude of such variations in the die mass flow rate (and if limited density variation is assumed die strain rate) have been shown to decrease throughout extrusion (as can be seen in Figures 85 and 86). This may be a consequence of the reducing volume of C-11 polyborosiloxane in the extrusion barrel. The mechanism for such compression and dilation of the C-11 polyborosiloxane in the extrusion barrel is discussed further within section 5.4.3. Considering the large variations in die mass flow rate which may occur during capillary flow it is considered appropriate to present apparent shear strain rate data rather than calculated Rabinowitsh [25] strain rate data. Leakage of polyborosiloxane between the extrusion ram and barrel has minimal effect on the calculated shear strain rate.

### 5.3.2 The validity of the shear stress calculations

The shear stress of the C-11 polyborosiloxane has been calculated from experimental data from the capillary die, the slit die and the concentric cylinder rheometers in order to complete subsequent viscosity calculations and enable definition of the rheological characteristics of the material.

For the concentric cylinder rheometer the shear stress is calculated from the rheometer dimensions and the rotor torque. The shear stress for the capillary and slit die rheometers has been calculated from the die dimensions and the extrusion barrel pressure.

The calculation of the wall shear stress from the pressure transducer output and the internal dimensions of the die for both the capillary die and the slit die were based on a force balance between the ram driving pressure and the 'shear force' resisting flow in the polymer [26]. Such a balance can be made because it is assumed that the C-11 polyborosiloxane flows at constant velocity. For such an equation to be valid it must also be assumed that flow is parallel to the die axis and that the fluid is incompressible.

However, for capillary flow a number of these assumptions, particularly the absence of acceleration components within the polyborosiloxane, have been shown to be in some doubt (Figures 85 and 86). In some cases, particularly at low ram velocity, acceleration components are clearly present in the capillary die even at constant ram velocity as has been discussed within section 5.3.1. The presence of acceleration components within the polyborosiloxane during constant ram velocity capillary extrusions may result in an error in the calculation of the wall shear stress. The importance of this acceleration component to the calculation of wall shear stress has been explored in the following section. If no acceleration is present within the die then the ram driving force will be exactly balanced by the shear force within the die. This may be expressed as

Ram driving force = shear force

$$\rho\pi r^2 = \tau 2\pi r l \quad (5.1)$$

Which can be rearranged to give the shear stress,  $\tau$ , as

$$\tau = \frac{\rho r}{2l} \quad (5.2)$$

If however, an acceleration component is present then the following equality will hold,

acceleration force = ram force - shear force

$$ma = \rho\pi r^2 l - \tau 2\pi r l \quad (5.3)$$

$$\rho\pi r^2 l a = \rho\pi r^2 l - \tau 2\pi r l \quad (5.4)$$

Which can be rearranged to give the shear stress,  $\tau$ , as

$$\tau = \frac{\rho\pi r^2 l - \rho\pi r^2 l a}{2\pi r l} \quad (5.5)$$

Collecting terms, this will give,

$$\tau = \frac{r}{2} \left[ \frac{\rho}{l} - \rho a \right] \quad (5.6)$$

The effect of this acceleration component on the calculated shear stress can now be examined. The mass flowrate for a constant ram velocity extrusion of 1.25 cm/min (Figure 86) has been shown to vary between 40 mg/s and 90 mg/s over an approximate timespan of 15 seconds. Assuming constant density this would give an acceleration of polymer in the extrusion die of  $0.001 \text{ m/s}^2$ . Such acceleration would have minimal effect on the calculated shear stress.

Although the acceleration component has been shown to have minimal effect on the derived shear stress equation, the extrusion barrel pressure has been shown in some cases (Figure 86) to vary considerably during constant ram velocity capillary rheometer tests. For the example used for the acceleration calculation above (Figure 86) the extrusion barrel pressure has been shown to vary between 2 and 10 MPa .This would result in a significant variation in the wall shear stress (between 50 KPa and 250 KPa). Such variations in wall shear stress during constant ram velocity flow must be noted when average wall shear stresses during extrusion are used to rheologically characterise the C-11 polyborosiloxane (section 5.4.2).

As well as the presence of acceleration components and variations in the extrusion barrel pressure during extrusion the effect of turbulence within the die on the calculated wall shear stress must also be considered. Deviation from parallel laminar flow within the die by the occurrence of turbulence may result in errors in the calculated wall shear stress. Any turbulence or non-laminar flow will alter the calculated shear plane area ( $\pi r^2 l$ ) and in addition the shear force will need to be resolved from a number of components which will not be parallel to the die axis.

The errors discussed above are those which may occur due to the unusual rheological properties of the polyborosiloxane. A more frequently applied correction to the calculated wall shear stress is that associated with entrance and exit turbulence in the die giving rise to non-linear pressure drops at either end of the die. These pressure drops at the entrance and the exit to the extrusion die must be quantified before wall shear stresses can be calculated. The Bagley [35] end correction method, previously described (section 2.5.2) proved unsatisfactory in experiments completed with the C-11 polyborosiloxane. This was because straight line relationships between pressure drop and die length to radius ratio could not be produced, due to the considerable variation in wall pressure which occurred

during extrusion. This was true of both increasing ram velocity capillary rheometer experiments (Figure 33) and constant ram velocity capillary rheometer experiments (Figures 34 and 35). However, the failure to produce Bagley plots with these early results may be linked to the variations in the method used to load the polymer in the rheometer. This parameter was not thought significant initially, but subsequent work showed that the length of time between charging the C-11 polyborosiloxane to the rheometer barrel and commencing extrusion, to be particularly critical (Figure 56). Following the adoption of a standard charging method, improved Bagley plots could be produced (Figure 81).

An alternative method of correcting for entrance and exit effects, using dies of nominally zero length, was found to give consistent and repeatable pressure reductions when using C-11 polyborosiloxane (Table 4). It was therefore decided that it was appropriate to use the zero die end correction method for this series of capillary extrusions.

In conclusion it is suggested that the shear stresses calculated from the capillary rheometer data are not significantly affected by the occurrence of acceleration components. However, it has not been possible to quantify the degree of turbulence occurring within the die and the effect such turbulence may have on the wall shear stress. For the purposes of subsequent calculations and discussions the flow within the extrusion die has been considered to be laminar. In some cases the calculated wall shear stress during capillary flow has been shown to be constant throughout ram travel (Figure 88). However in other cases the shear stress varies considerably during ram travel (Figure 86). The mechanisms for such variations in the wall shear stress are discussed further within section 5.4.3.

### **5.3.3 The validity of the heat generation calculations**

It has been reported [4] that during extrusion honing, the temperature of the C-11 polyborosiloxane and abrasive mixture increases. In some cases the increase in C-11

polyborosiloxane temperature may be so great that effective machining becomes negligible and the whole process must be stopped and either allowed to cool, or fresh cold polymer used. An understanding of heat generation in C-11 polyborosiloxane during extrusion may enable greater control and optimisation of the extrusion honing process. In addition, a predictive model capable of calculating temperature distribution from heat generation rates and the thermal properties of the system may be used in conjunction with the rheological models to predict temperature induced viscosity variations within the system.

If these thermal models are to be used in viscosity calculations as well as in the discussion of the heat generation mechanisms during extrusion honing then it is important to review critically the assumptions made within the respective models. Two thermal models have been developed during this research programme. The first of these models is a simple steady state model described within section 3.4.1.1. The first assumption that has been made within this model is that the system is at steady state with temperatures stable throughout the polyborosiloxane and the test cylinder. If the system were not at steady state at the time of data collection then heat generation within the polyborosiloxane may have been underestimated. However, temperature curves illustrated in Figures 13 to 16 show that in the systems studied the temperatures at all points have become virtually independent of time. Therefore, the steady state assumption is considered a reasonable one. The steady state heat generation model is based on unidirectional heat transfer in a radial direction (perpendicular to the C-11 polyborosiloxane flow direction) through the walls of the cylindrical die. No axial heat transfer has been considered. From the axial temperature profiles measured, which show an increase in polyborosiloxane temperature towards the mid point of the cylinder (e.g Figure 21), it may be assumed that heat transfer occurs axially, away from the central plug of polyborosiloxane. If this is the case, then even at steady state, the heat generation calculated from cylinder wall temperatures may be less

than that actually produced within the polyborosiloxane. For the purposes of the steady state model the system has been considered to be static with no movement of polyborosiloxane within the cylinder. Provided that the moving section of polyborosiloxane and the test cylinder have uniform temperatures in a axial direction then the model will not be affected greatly by this. If however the central (hottest) section of polymer is presented to cooler material outside the test cylinder in the extrusion honing machine cylinders then some errors may occur. Any turbulence or mixing of the polymer as it cycles through the cylinder will also compound errors within the model. Despite these possible errors it is proposed that the thermal model presented provides a good starting point for predicting heat generation within polyborosiloxane and surface heat transfer during the repeat passage of this material up and down a cylindrical cavity in a metal die.

The second thermal model developed within this research programme is based on a finite difference calculation and has the advantage of considering transient state conduction as well as the division of the polyborosiloxane mass into several elements. The transient model provides heat generation data within various zones in the polyborosiloxane at time intervals during the increase in temperature (non-steady state). Whilst this model is a considerable development on the steady state model it is based on the same assumption that the heat transfer is unidirectional. Further, movement of polymer is ignored and no turbulence or mixing is assumed to occur.

In addition the model requires the incorporation of a shape factor to take into account the cylindrical shape of the system. Despite these reservations initial results from the model indicate that heat generation is greatest at the die wall and less in the centre of the die (Figure 27), which is consistent with the assumption of high shear and friction at the wall. Heat generation within the polyborosiloxane has been discussed with respect to these calculations, the work of previous authors and the extrusion honing process within section 5.2.1.

Modifications to the models to take into account three dimensions, movement of the polymer, turbulence and mixing would be extremely complex, and time has not permitted significant development of these models within this programme. However, this may be a suitable area for further work (section 7).

## **5.4 The rheology of the C-11 polyborosiloxane**

### **5.4.1 Introduction**

The flow properties and mechanisms of the C-11 polyborosiloxane are discussed within the following section with respect to the experimental results and calculations, and to the literature review, presented within this thesis.

Initially, the general flow curve of the C-11 polyborosiloxane has been considered (Figure 105) and appropriate constitutive rheological equations discussed. The validity and limitations of the equations considered have been discussed. Following this characterisation of the general flow properties of the C-11 polyborosiloxane, possible mechanisms to explain the unusual flow properties demonstrated have been explored. The flow mechanism of the C-11 polyborosiloxane has been considered with respect to both the general flow properties (Figure 105) and to the more specific types of flow phenomena which have been observed during capillary flow with constant ram velocity.

### **5.4.2 Constitutive rheological equations of the C-11 polyborosiloxane**

The shear strain rate/shear stress relationship for C-11 polyborosiloxane at 30°C is shown in Figure 105. Shear stress and shear strain rate data for this flow curve has been obtained from concentric cylinder, capillary and slit die rheological measurements. Good

correlation to a power law relationship of the form  $\tau = 0.989 \dot{\gamma}^{0.936}$  (derived in section 4.9) can be seen at apparent shear strain rates of up to  $100\text{s}^{-1}$ . The viscosity of the C-11 polyborosiloxane at  $30^{\circ}\text{C}$  has been shown to be close to  $10^3$  Pas up to shear strain rates of  $100\text{ s}^{-1}$  (Table 10). Plochocki and Maciejewski [80] also reported general power law pseudoplastic behaviour for polyborosiloxane, although they used a polymer of higher viscosity than that used in the present work ( $\eta$ ) $10^5$ Pas). Variations in published polyborosiloxane viscosities (Fletcher [85]  $10^3$ Pas, Benbow [79]  $10^4$ Pas, and Plochocki[80]  $10^5$ Pas) may be due to variations in the proportions of plasticisers and fillers blended with the base polymer [17]. Indeed, C-11 polyborosiloxane is only one of a range of polyborosiloxane blends of various viscosities used for extrusion honing; the viscosity selected depends on the specific application.

The power law equation serves as a reasonable starting point in a description of the rheology of the C-11 polyborosiloxane. It allows prediction of wall shear stresses from apparent shear rate, as well as the prediction of shear stress, shear strain rate and velocity distributions through the C-11 polyborosiloxane (Figures 108-113).

At temperatures of  $30^{\circ}\text{C}$  and shear rates greater than  $100\text{s}^{-1}$  the viscosity of the C-11 polyborosiloxane decreases significantly and the power law equation described above is no longer valid (Figure 105). Despite this limit in the range within which the power law equation is valid, the power law equation is useful in the generation of data applicable to the extrusion honing process. This is because many extrusion honing operations are carried out at shear rates of less than  $100\text{s}^{-1}$ , where the power law equation is valid. This allows the prediction of shear strain rate, stress and velocity profiles within the polyborosiloxane.

Whilst the power law equation is a good general rheological description of the C-11 polyborosiloxane at shear strain rates up to  $100\text{ s}^{-1}$ , a number of assumptions have been

made in the generation of these equations and each must be carefully considered in turn. All capillary rheometer data points illustrated in the general flow curve (Figure 105) are based on average die wall shear stresses during constant ram velocity extrusion. Even when wall shear stresses have been shown to vary substantially (e.g. Figure 85) an average wall shear stress has been used in order to try and provide some characterisation of the complex properties exhibited. Additionally, it should be noted that the shear strain rates used are calculated from the extrusion ram velocity by a method that assumes constant density of the C-11 polyborosiloxane. This property has been shown to vary with pressure (Figure 28), and it is therefore probable that the shear rate also varies, as has been discussed in section 5.3.1. The mechanism for wall shear stress and wall shear strain rate variations during constant ram velocity capillary flow are discussed further in section 5.4.3.

These equations have assumed time independent viscosity; in other words the shear stress has been expressed purely as a function of shear strain rate at 30°C and not as a function of the duration of shear. Such time independence is considered valid for applications to extrusion honing because the polyborosiloxane is subject to a relatively short duration of shear when extruded through a component, such that time dependent properties should not be significant. However, this assumes no previous shear of the polymer prior to extrusion, either in the rheometer barrel or in the extrusion honing machine. The validity of time independent viscosity also depends on an absence of more long term shear history effects from previous deformation, such as that arising from the loading of the C-11 polyborosiloxane into the extrusion barrel. Such long term shear history effects have been demonstrated in the results obtained (Figure 56). However, insufficient data is available to allow constitutive rheological equation development incorporating time dependence/shear history affects. Possible mechanisms responsible for such affects are discussed within section 5.4.3.

### **5.4.3 The flow mechanism of the C-11 polyborosiloxane**

#### **5.4.3.1 Introduction**

The general rheological behaviour of the C-11 polyborosiloxane has been discussed in the previous section. Possible mechanisms responsible for such rheological behaviour are discussed within the following two sections. Section 5.4.3.2 presents a general flow mechanism for the C-11 polyborosiloxane with respect to the flow curve shown in Figure 105. These general flow mechanism discussions are developed further within section 5.4.3.3, which explores the flow mechanisms which may be responsible for the various unusual flow properties exhibited by the C-11 polyborosiloxane during constant ram velocity capillary extrusion.

#### **5.4.3.2 A general flow mechanism for C-11 polyborosiloxane**

The general pseudoplastic behaviour of the C-11 polyborosiloxane has been discussed previously (5.4.2). The pseudoplastic nature of the C-11 polyborosiloxane has been shown to increase rapidly at shear rates greater than  $100 \text{ s}^{-1}$ , and to be affected significantly by shear history and temperature.

The exact molecular structure and composition of the C-11 polyborosiloxane is not available to this research programme due to the industrially sensitive proprietary nature of such information. Consequently, it is not possible to discuss quantitatively the specific molecular mechanisms which may be responsible for the rheological behaviour of the C-11 polyborosiloxane. However, general molecular mechanisms such as those presented by Dealy [26] and Cogswell [25] can be discussed briefly in a qualitative manner, with respect to the rheological properties exhibited by the C-11 polyborosiloxane.

Dealy [26] states that if a polymer is allowed to stand for some time, then the molecules will assume an equilibrium distribution of shapes and a random distribution of

orientations. He further elaborated that if the polymer is subsequently subjected to some form of deformation (for example, if it is sheared or stretched at a significant rate), then the polymer molecules will have forces applied to them that will change the shapes of the molecules away from the equilibrium distribution. An additional affect of this shear may be an alignment of the polymer molecules to some preferred flow axis. Figure 56, shows how an increase in the time between charging the C-11 polyborosiloxane to the rheometer barrel and the commencement of extrusion may result in an increase in the recorded average extrusion barrel pressure (all other experimental conditions being constant). If the C-11 polyborosiloxane is considered to contain an entanglement network of long chain molecules, of the type described by Dealy [26], then this network will be broken down during the considerable shear of the polyborosiloxane on loading into the rheometer barrel via the charging piston. Thus molecules immediately after charging to the rheometer may be considerably aligned in the flow direction resulting in decreased viscosity on subsequent flow. However, the longer the material is left in the barrel between charging to the barrel and extrusion the greater will be the extent of the re-establishment of the entanglement network of molecules such that greater resistance to flow (higher viscosity) will occur during extrusion (Figure 56). Considerable variations in the absolute value of average extrusion barrel pressures were obtained at the same ram velocity and temperature prior to the adoption of the constant barrel charging method described in section 3.2.7 (Figure 55). It is considered that these variations may be due to slight variations in charging methods used resulting in a slightly different shear history of the materials prior to extrusion. Initially the charging method and the length of time between charging the C-11 polyborosiloxane into the rheometer and the commencement of extrusion was variable (although this time was always sufficient to allow the C-11 polyborosiloxane to reach the desired temperature for the experiment). However, the capillary rheometer results presented in Figure 105, illustrating the general flow properties of the C-11 polyborosiloxane, were produced using the same predefined charging procedure as

described in section 3.2.7. This charging procedure has been shown to produce repeatable results where clear trends can be observed (Figure 105).

This general molecular theory which has been applied to the effect of shear history on the C-11 polyborosiloxane may also be extended to the more general flow properties of the polymer. As well as the shape and orientation of the molecules the interaction between the molecules must also be considered. There is considerable indirect evidence (Ferry [86] ) that rheological behaviour is governed by very strong interactions between molecules. This interaction of molecules is sometimes termed an entanglement network [26]. The decrease in the viscosity with shear rate of the C-11 polyborosiloxane may be interpreted in terms of an entanglement network, where the shearing process may increase the rate of loss of existing entanglements, but not the rate of generation of new ones. Thus the number of entanglements in a given volume of material (the entanglement density ) has lower equilibrium values at progressively larger shear rates, resulting in a general decrease in the viscosity.

The effect of temperature on the flow curve of the C-11 polyborosiloxane can be seen in Figure 107. From the capillary rheometer results presented an increase in C-11 polyborosiloxane temperature results in an increase in the apparent shear viscosity of the material. This is contrary to the established theory [86] that as heat is supplied to a polymer, the molecules vibrate more rapidly with a subsequent increase in mobility (decrease in viscosity). Indeed, the increase in temperature, and subsequent decrease in polyborosiloxane viscosity is a commonly cited problem during extrusion honing [87].

It is proposed that this apparent increase in polyborosiloxane viscosity with increasing temperature is not a real effect, but an apparent effect caused by backpressure within the rheometer barrel as a result of polyborosiloxane adhesion within the capillary die. This

increased tendency to adhere to metallic surfaces at elevated temperatures has been previously observed in the industrial application of the polyborosiloxane to extrusion honing [87]. Further evidence of this phenomenon, by which C-11 polyborosiloxane adheres to the die wall, causing a restriction to flow and consequent compression and increased pressure in the extrusion barrel, may be obtained by consideration of the temperature/extrusion barrel pressure relationships illustrated in Figure 83. At low ram velocity the rheometer barrel pressure can be seen to be constant despite the increase in polyborosiloxane temperature. This may be because the C-11 polyborosiloxane adheres to the die wall but ram advancement is sufficiently slow to prevent the build up of backpressure on account of the flow of low viscosity fluid through the centre of the die cavity. However, as the ram velocity is increased the flowrate generated by the advancing ram increases to a value greater than the flow through the die (restricted by polymer adhering to the wall) and backpressure occurs, resulting in an increase in extrusion barrel pressure and an apparent increase in media viscosity. This mechanism has been discussed further with specific reference to some of the unusual flow properties measured during constant ram velocity capillary die and slit die flow in the following section.

#### ***5.4.3.3 Flow mechanisms during constant ram velocity extrusion***

The extrusion barrel pressure and die mass flow rate have been shown to follow one of three main patterns during constant ram velocity flow of C-11 polyborosiloxane. These include (i) constant barrel pressure throughout extrusion (e.g. Figure 88), (ii) a steady increase in barrel pressure throughout extrusion (e.g. Figure 89), or (iii) a cycling in barrel pressure between a minimum and maximum value throughout extrusion (e.g. Figure 86). The following section contains a proposed flow mechanism to describe these flow phenomena exhibited by the C-11 polyborosiloxane during flow through both a capillary and a slit die.

The most unusual flow behaviour exhibited by the C-11 polyborosiloxane is the cycling in the barrel wall pressure between a minimum and maximum value during constant ram velocity extrusion (e.g. Figure 86). It is proposed that such flow behaviour may be caused by a combination of cyclic polymer adhesion and slip at the die wall (commonly known as slip-stick [44]), and cyclic density variations within the rheometer barrel. The degree of slip-stick and density variations, and therefore cyclic flow behaviour is thought to be considerably influenced by the C-11 polyborosiloxane temperature, the extrusion ram velocity and the flow passage geometry.

This mechanism may be explored further by consideration of the results presented in Figures 57-77. At lower temperatures and ram velocity large amplitudes in the cycling of the recorded wall pressure (and die mass flow rate) may occur. This may correspond to cyclic adhesion and slip of polyborosiloxane at the die wall. This slip-stick mechanism was originally proposed by Maxwell and Galt [44]. If adhesion at the die wall occurs then the C-11 polyborosiloxane at the die wall will be stationary whilst the polymer still flows down the centre of the die. Such a situation may result in an elastic deformation of the C-11 polyborosiloxane and a restriction to flow with consequent build up of barrel pressure as the ram advances. This compression within the rheometer barrel will continue to increase as the die mass flow rate is restricted and the ram continues to advance (N.B. the compressibility of the C-11 polyborosiloxane is demonstrated in Figure 28). The barrel pressure will continue to increase until the shear stress within the material exceeds the adhesive force of the C-11 polyborosiloxane to the die wall. At this point slip of the C-11 polyborosiloxane at the die wall will occur, which releases the elastic stress within the C-11 polyborosiloxane, and the pressure in the rheometer barrel. This slip and subsequent barrel decompression would be expected to result in a surge in the die mass flow rate, which has been demonstrated experimentally to be the case (Figure 86). This process may be repeated continually throughout extrusion resulting in oscillating slip-stick and corresponding

oscillations in barrel pressure and die mass flow at the die wall. Whilst slip-stick, backpressure and C-11 polyborosiloxane density variations are thought to be the primary mechanisms for oscillating flow, the oscillations are thought to be enhanced by molecular mechanisms such as those described by Rudin and Chang [55]. It was proposed that the polymer is not only pushed out of the reservoir by the pressure exerted on the moving piston, but that it is also pulled out by material in the orifice and probably also outside the apparatus. They associated this with a tensile force acting axially through an entanglement network between the polymer melt in the die and material in the larger rheometer barrel. Rudin and Chang [55] further proposed that this additional force in the extrusion direction would result in dilation of the melt when the piston is constrained to move at constant speed, since the flowing polymer would adhere to the melt in the so called 'dead zone' at the bottom of the reservoir and to material near to the 'dead zone'.

At 30°C oscillation of the extrusion barrel pressure and polymer mass flow rate under conditions of constant ram velocity has been shown to diminish as the ram velocity is increased (Figures 57-64). At ram velocities greater than 5cm/min the extrusion barrel pressure remains constant throughout ram travel. It may be that at these higher ram velocities the shear rate at the die wall is such that the wall shear stress exceeds the adhesive forces between the C-11 polyborosiloxane and the die wall. This results in a continual slip condition at the die wall, throughout the period that the ram travels in the cylinder. This slip condition will result in less resistance to flow, as well as minimal backpressure or compression within the extrusion barrel. This produces a lower and more consistent extrusion barrel pressure. At temperatures above 30°C it is tentatively proposed that the adhesive properties of the C- 11 polyborosiloxane increase significantly and that this has an influence on the flow properties of the polymer. At 39°C oscillating extrusion barrel pressure (and polymer mass flow rate in the die) occurs at intermediate ram velocities (2.5 and 5 cm/min). The mechanism for these oscillations is considered to be

essentially the same as that obtained at 30°C (see above). However, at higher and lower ram velocities than those referred to, two different variations in extrusion barrel pressure occur. Firstly at low ram velocity (1.25 cm/min), the extrusion barrel pressure is constant throughout extrusion. It is proposed that at 39°C the C-11 polyborosiloxane adheres to the die wall but due to the slow ram velocity (1.25 cm/min) and the decreased viscosity, insufficient flow restriction is present to cause backpressure in the extrusion barrel and resultant slip at the die wall. This may be further supported by comparison of the variation in wall pressure during constant ram velocity at 1.25 cm/min at 30°C and 39°C. The constant pressure at 39°C of 12 MPa corresponds to the oscillation maximum at 30°C. The minimum value of the wall pressure of 4 MPa at 30°C corresponds to slippage of the polymer at the die wall associated with the reduced adhesive properties of the C-11 polyborosiloxane at the lower temperature.

At higher ram velocities (10 cm/min and 15 cm/min) at 39°C the extrusion barrel pressure can be seen to increase throughout extrusion (Figures 68 and 69). This is considered to be the result of sticking in the extrusion die which causes a flow restriction. As the ram velocity is high the volume displacement of the advancing ram exceeds the flow rate through the restricted extrusion die, which results in compression in the extrusion die and an increase in barrel pressure throughout extrusion. Oscillation of the extrusion barrel pressure at these high ram velocities may not occur because the mass flow rate of the polymer through the die is too high for the oscillation mechanisms proposed by Rudin and Chang [55] to occur.

At 45°C no oscillation of the extrusion barrel pressure during constant ram velocity extrusion of C-11 polyborosiloxane has been found to occur ( Figures 70-74). This has been attributed to the high adhesive force associated with the high temperature of the polymer, which prevents any slip at the wall, together with reduced viscosity of the polymer.

The above section describes a flow mechanism for the C-11 polyborosiloxane during constant ram velocity extrusion through a die. The mechanism has been described with respect to barrel temperature and ram velocity. The third parameter which is thought to influence significantly the flow properties exhibited by the C-11 polyborosiloxane due to the particular flow mechanism is the flow passage geometry.

If surface adhesion at the die wall is a primary component of the flow mechanism of the C-11 polyborosiloxane, then as extrusion dies of progressively larger cross sectional area are used then the influence of surface adhesion mechanisms (e.g. wall pressure cycling etc.) would be expected to have a less pronounced effect on the flow characteristics. This statement is supported by consideration of wall pressures during slit die extrusion. The slit die, which is considerably larger in cross-sectional area than the capillary die produced no fluctuations in the wall pressure during constant ram velocity extrusion (Figures 92-97). In addition surface adhesion would be expected to influence flow properties when longer dies were utilised, which would contain large internal surface areas for adhesion. This is indeed the case as can be seen in Figures 24 and 25. When using orifice dies during constant ram velocity extrusion, constant wall pressures occurred at all ram velocities. As the orifice dies present minimal internal area for C-11 polyborosiloxane adhesion this data is consistent with a flow mechanism which is highly influenced by adhesion of polymer to the die wall.

## **5.5 Application of the proposed flow mechanisms to the extrusion honing process**

### **5.5.1 Heat generation and temperature control during extrusion honing**

Heat generation and temperature control present problems during certain extrusion honing operations. Increases in the temperature of the polyborosiloxane/abrasive mixtures has been reported [81] to increase the flow velocity during extrusion honing in the case of constant hydraulic pressure. This would suggest a general decrease in the viscosity of the polyborosiloxane/abrasive mixture as the temperature increased. The temperature at which the reduced efficiency of the extrusion honing process associated with increased polymer fluidity occurs is not well documented. However, the maximum temperature of the polyborosiloxane/abrasive mixture that can be achieved during extrusion honing is known to be in excess of 85°C.

It is proposed that heat generation during extrusion honing involves two main mechanisms (i) friction or abrasion at the media/workpiece interface and (ii) heat generation within the bulk medium due to internal shear. Both of these mechanisms would cause the greatest heat generation towards the periphery of an orifice restriction. This is the region in which both friction and shear will be at a maximum. Temperature profiles measured within the medium in an extrusion honing machine support these proposed mechanisms, with higher temperatures generated towards the cylinder walls (Figure 22). The transient heat generation model based on these temperatures also supports this suggestion, showing that heat generation is significantly greater towards the cylinder walls than in the central section of media (Figure 27).

The addition of abrasive grit increases the thermal conductivity of the polyborosiloxane, so an increased abrasive content would assist in the heat transfer process. However, the

increased percentage of abrasive may cause increased heat generation as it will increase the friction and internal shear heat generation. (Further thermal modelling would be required to optimise this balance).

### **5.5.2 Flow phenomena during extrusion honing**

The flow mechanisms proposed in section 5.4 are briefly discussed with respect to the extrusion honing process in the following section. However it should be noted that whilst all rheological data was completed with pure polyborosiloxane the extrusion honing process utilises a mixture of polyborosiloxane and abrasive grit. Rheological work with abrasive grit mixtures has not been completed during the present work due to the destructive effect such mixtures would have on the rheometers (wear of dies/transducer heads etc.). Despite this consideration a number of interesting results observed within the experimental programme are relevant to the industrial extrusion honing process and as such are briefly discussed.

It has been reported within the literature [2] that whenever the polyborosiloxane was forced into a restriction its viscosity increased substantially resulting in significant abrasion of the restriction.

It is tentatively proposed that this reported viscosity increase is due to an increase in the shear stress and shear strain rate in the restriction entrance region resulting in the polyborosiloxane assuming a rubber, solid like physical state.

The shear history and charging method effects previously discussed probably have a significant affect on the extrusion honing process. The recorded wall shear stresses were found to be significantly increased by increases in length of time between successive deformations. Thus it may be proposed that the longer the medium is left in a machine

prior to use the higher will be both the initial resultant shear stresses and machining rates. Evidence that this effect occurs during extrusion has been reported [89]. The first component of a batch processed after a machine has been inoperative for some time has been shown to take longer to process than subsequent components when a constant hydraulic extrusion pressure is maintained [89]. This effect is not thought to be caused by temperature variations as the reduction in media viscosity occurs very quickly after machine startup and is not sustained. Media viscosity variations due to temperature increases (heat generation) are generally more gradual processes [89]. Breakdown of the polyborosiloxane viscosity after a set period of deformation may also be coupled with the work of Rhoades [7] who showed that the majority of machining action occurred during the first cycle of the extrusion honing process and that successive cycles were significantly less effective.

Any polymer adhesion at the workpiece surface may inhibit the machining action as no abrasive movement and therefore no work will occur under such conditions. However, on slipping the particle movement may be greater than that which occurs during constant wall velocity flow. Thus it may be that the overall workrate at a component surface would be expected to be similar whether slip-stick or constant wall slip occurs. If continuous sticking of a surface layer of polyborosiloxane occurs then the work done may be severely reduced due to this protective surface layer, which prevents contact between the grit and the machined surface.

The addition of abrasive to polyborosiloxane is expected to significantly reduce any effects involving change in the density of the medium which may be responsible for the mechanism by which the polyborosiloxane flows. This would be because any pressure induced density variation of the polyborosiloxane/ abrasive mixture would be significantly less than the pure polyborosiloxane due to the minimal pressure dependency of the density of the abrasive grit.

## 6. CONCLUSIONS

---

1. The shear history of the polyborosiloxane prior to rheological evaluation was found to affect the results produced. When the time interval between the charging of the polyborosiloxane into the capillary rheometer and the start of the extrusion process was increased the measured extrusion pressure was likewise increased (Figure 56). It is tentatively suggested that this is due to the reforming of the molecular network within the polymer which had been broken down previously during the charging of the polyborosiloxane to the rheometer barrel.
2. In some cases the extrusion barrel pressure and the mass flow rate through the extrusion die have both been shown to vary during the constant ram velocity extrusion of polyborosiloxane in the capillary rheometer (Figure 86). Such variations generally occurred at low ram velocities.
3. It is tentatively proposed that the variations in the extrusion barrel pressure which have been reported during capillary flow are a result of periodic sticking and slipping of the polyborosiloxane to the extrusion die wall. This mechanism is thought to be considerably influenced by the C-11 polyborosiloxane temperature, the extrusion ram velocity and the flow passage geometry.
4. It is proposed that the measured variations in the mass flow rate of the polyborosiloxane through the extrusion dies during capillary flow (figures 85-88) are a result of pressure induced density variations within the extrusion barrel. This proposed mechanism can be mathematically modelled for a range of mass flow rate variations (Figures 127-130).

5. The rheological behaviour of the C-11 polyborosiloxane at 30°C may be approximated to pseudoplastic power law relationship at shear strain rates up to 100s<sup>-1</sup> (Figure 105). The power law approximation is of the form

$$\tau = 0.989 \dot{\gamma}^{0.938}$$

At shear strain rates less than 100s<sup>-1</sup> the pseudoplasticity of the polyborosiloxane is low and the shear viscosity may be approximated to 10 Pas.

6. Using the power law approximation shown above the velocity, shear strain rate and shear stress distribution within the polyborosiloxane in an extrusion die may be calculated. From the mathematical modelling (Figures 108 and 109) the variation in velocity across the die was found to increase with increasing extrusion pressure, increasing die internal diameter and decreasing die length. Also from the modelling it has been concluded that both the wall shear strain rate and the wall shear stress increase with increasing extrusion pressure and die diameter and decrease with increasing die length (Figures 110-113).
7. The pseudoplastic nature of the polyborosiloxane increases significantly at shear rates greater than 100 s<sup>-1</sup> and the power law equation stated above is no longer valid (Figure 106).
8. The generally reported concept within the literature [2] that whenever the polyborosiloxane is forced into a restriction its viscosity increases substantially. It is tentatively proposed that this reported viscosity increase is due to an increase in the shear stress and shear strain rate in the restriction entrance region resulting in the polyborosiloxane assuming a rubber, solid like physical state.

9. It is proposed that the apparent increase in polyborosiloxane viscosity with increasing temperature from the capillary rheometer results (Figure 98) is not a real effect, but an apparent effect caused by backpressure within the rheometer barrel as a result of polyborosiloxane adhesion within the capillary die.
10. It is proposed that heat generation during extrusion honing involves two main mechanisms (i) friction or abrasion at the medium/workpiece interface and (ii) heat generation within the bulk medium due to internal shear. Both of these mechanisms would cause the greatest heat generation towards the periphery of an orifice restriction. This is the region in which both the friction and shear will be at a maximum (Figure 27).
11. The addition of abrasive grit increases the thermal conductivity of the polyborosiloxane, so an increased abrasive content would assist in the heat transfer process. However, the increased percentage of abrasive may increase the friction and internal shear heat generation.

## 7. FURTHER WORK

---

1. An investigation into the adhesive properties of the C- 11 polyborosiloxane to metallic surfaces over a temperature range of 20-100°C. This would enable validation of the tentative proposal that the adhesive properties of the C-11 polyborosiloxane affect the rheological measurements on the capillary rheometer (Section 6).
2. The completion of capillary rheometer experiments with C-11 polyborosiloxane using dies of varying length (1- 100mm) and internal diameter (1-10mm) in order to investigate fully the effect of flow path geometry on the measured rheological properties.
3. To investigate the thermal and rheological properties of C-7 (high viscosity) and C-21 (low viscosity) polyborosiloxane extrusion honing media.
4. To modify the capillary rheometer such that rheological experimentation with polyborosiloxane/abrasive mixtures can be determined. This would enable the quantification of the effect of abrasive grit addition on the polyborosiloxane rheology.
5. Extrusion honing trials may be completed on dies under controlled conditions and the machining action generated (stock removal, surface finish) quantified. This data may be used to investigate which rheological characteristics of the polyborosiloxane are important to the extrusion honing process (a PhD research programme in this field is being undertaken by Peter Davies at Sheffield Hallam University at the time of publication of this thesis).

6. Further development of the extrusion honing heat generation model (section 3.4.1.2) requires the incorporation of shape factors into the formulated equations. The model may be modified to calculate heat transfer axially as well as radially and to incorporate polyborosiloxane movement through the die. A detailed understanding of the heat generation mechanisms during extrusion honing may assist in the design of industrial cooling systems for the process.

## REFERENCES

---

1. Hull, J.B., et al, Rheology of Carrier Media used in Abrasive Flow Machining, IMF7 Conference, Limerick, Ireland, September 1991.
2. Rhoades, L.J., Abrasive flow machining and its uses, Nontraditional Machining; Cincinnati, Ohio, U.S.A., 2-3 Dec. 1985.
3. Rhoades, L.J., Pittsburgh High Technology, Nov-Dec., pp 8-16,1988.
4. Perry, W.B., Abrasive Engineering Society Magazine, Sept-Oct, pp 12-15, 1982.
5. Tool and Manufacturing Engineers Handbook, Volume 3, Materials, Finishing and Coatings, Section 15-1.
6. Gillespie, L.K., Machine and Tool bluebook, pp 100-103, Feb. 1976.
7. Thomas, T.R., Rough Surfaces, Longman.
8. ISO R468, International Standard on Surface Roughness Parameters.
9. Perry, W.B., Abrasive flow machining; principles and practices, Nontraditional machining; Cincinnati, Ohio, U.S.A., 2-3 Dec. 1985.
10. Kohut, T., Surface finishing with abrasive flow machining, Vol. 2 of the Proc. of the Fourth International Aluminium Extrusion Technology Seminar, Washington DC, The Aluminium Association, 1988.
11. Extrude Hone Corporation, 'Innovation in the pursuit of Excellence' sales document.
12. Spiotta, R.H., Machine and tool blue book, Feb., pp 80-87, 1976.
13. Rhoades, L.J., Manufacturing Engineering, pp 75-78, Nov. 1988.
14. Perry, W.B., Society of Manufacturing Engineers paper MR75-831, 1975.
15. Cost Guide for Automatic Finishing Processes, Edited by Lawrence J Rhoades, Society of Manufacturing Engineers.

16. Hull, J.B., et al, The effects of temperature rise on the rheology of carrier media used on abrasive flow machining, Third International Conference; Advances in Coatings and Surface Engineering for corrosion and wear resistance, Newcastle-upon-Tyne, UK, 11-12 May, 1992.
17. Rhoades, L.J., Modern machine shop, Dec., 55, (7); pp 60-71, 1982.
18. Stackhouse, J., Society of Manufacturing Engineers, Technical paper MR76-690, 1976.
19. Rhoades, L.J., Metal Finishing, July 1987.
20. Anon., Metalworking Magazine, pp 240-243, April 1992.
21. Anon., Dynaflo Media system, Technical Bulletin 500, Dynetics Corporation.
22. Atkey, M., Lacey, K., Machine and Production Engineering, 138 (3546), pp 50-54, 21 Jan 1981.
23. Dvorak, J., Machine Design, pp 131-134, Dec. 10, 1987.
24. Williams, R., MS thesis, University of Nebraska, 1989.
25. Brydson, J.A., Flow properties of polymer melts, George Godwin Ltd.
26. Dealy, J.M., Rheometers for Moulten Plastics, Van Nostrand Reinhold.
27. Cogswell, F.N., Polymer melt rheology, A guide for industrial practice, George Godwin Ltd.
28. Whorlow, R.W., Rheological Techniques, Ellis Horwood.
29. Harris, J., Rheology and Non-Newtonian Flow, Longman.
30. Tachibana, M., et al., Journal of Rheology, 30,3, pp 518-538, 1986.

31. Aklonis, J., et al, Introduction to Polymer Viscoelasticity, Wiley-Interscience .
32. Christensen, R.M., Theory of Viscoelasticity, Academic Press.
33. Walters, K., Rheometry, Chapman and Hall.
34. Isayev, A.I., and Chung, B., Flow of polymeric melts in short tubes, Society of Manufacturing Engineers, pp 433-438, 1984.
35. Bagley, E.B., J. Appl. Phys., 28:624, 1957.
36. La Mantia, F.P., et al, Rheol. Acta. 22, pp 299-307, 1983.
37. Bagley, E.B., J. Appl. Phys., 31:1126, 1960.
38. Winter, H., Polymer Engineering and Science, 15, 2, pp 84-89, 1975.
39. Bernhardt, E.C., Processing of Thermoplastic Materials, Robert E. Krieger.
40. Mooney, M., Journal of Rheology, 2, pp 210-222, 1931.
41. Worth, R., et al, Polymer Engineering and Science, 17, 4, pp 257-265, 1977.
42. Lupton, J.M., and Register, J.W., Polymer Engineering and Science, 5 235, 1965.
43. Shaw, M., An alternative analysis of capillary rheometer data, SPE Annual Technical Conference, 32, pp 707-710, 1986.
44. Galt, J., Maxwell, B., plastics engineering, Dec. 1964.
45. Rhoades, L.J., Rajagopal, K.R., Modelling of the flow behaviour of industrial polyborosiloxane, NSF-SBIR Phase I final report, August 1985.
46. Rhoades, L.J., and Rajagopal, K.R., Modelling of the flow behaviour of industrial polyborosiloxane - a proposal, 1985.

47. Ma, C-Y., et al, Die flow characteristics of compounds of low density polyethylene with small particulates, Proceedings of the 43<sup>rd</sup> Annual Technical Conference - antec 85, Washington DC, April 29-May 2, 1985.
48. Yoganathan, A.P., and Yarlagadda, P., Flow of viscoelastic fluids in a sudden tubular contraction, SPE annual technical conference, 30, pp 429-432, 1984.
49. Janeschitz-Kriegl, H., Polymer Melt Rheology and Flow Birefringence, Springer-Verlag.
50. Myerholtz, R.W., Journal of Applied Polymer Science, 11, pp 687-698, 1967.
51. Kataoka, T., and Ueda, S., Rheological Acta, 10, 446-447, 1971.
52. Bergem, N., Visualisation studies of polymer melt flow anomalies in extrusion, Proceedings - 7<sup>th</sup> Int. Congress on Rheology, pp 50-54, 1976.
53. Bagley, J.B., et al, Journal of Applied Physics, 29, 1, pp 109-110, 1958.
54. Rudin, A., and Vlasschaert, A.G., Trans. Soc. Rheol., 15:3, pp 551-582, 1971.
55. Rudin, A., and Chang, R-J., Journal of Applied Polymer Science, Vol. 22, pp 781-799, 1978.
56. Rudin, A., et al, Journal of Polymer Science; Part C, 30, pp 415-427, 1970.
57. Vinogradov, G.V., et al, Polymer Engineering and Science, 12, 5, pp 323-334, 1972.
58. Everage, A.E., and Ballman, R.L., Journal of Applied Polymer Science, 18, pp 933-937, 1973.
59. Schreiber, H.P., et al, Journal of Applied Polymer Science, 4, 12, pp 362-363, 1960.
60. Bird, R.B., Society of Plastics Engineers Journal, 11, 7, pp 35-40, 1951.

61. Martin, B., *Int. J. Non-linear Mech*, 2, pp 285-301, 1967.
62. Kakouris, A.K., et al, *Polym. Eng. and Sci.*, Mid-Oct, Vol 27, No. 18, 1987.
63. Kamal, H., and Nyun, H., *Polymer Engineering and Science*, 20, 21, pp 110-119, 1980.
64. Stevenson, J., et al, An experimental study and simulation of disk filling by injection molding, *SPE Annual Technical Conference*, 22, pp 282-288, 1976.
65. Crowson, R.J., et al, *Polymer Engineering and Science*, 21, 12, pp 748-754, 1981.
66. Gerrard, J.E., et al, *Industrial and Engineering Chemical Fundamentals*, 5, 2, pp 260-263, 1966.
67. Hurtado-Laguna, F., and Aleman, J.V., *Journal of Polymer Science; Part A*, 26, pp 2631-2649, 1988.
68. Chee, K.K., and Rudin, A., *J. Macromol. Sci-Phys*, B7(3), pp 503-523, 1973.
69. Chee, K.K., and Rudin, A., *I and EC Fundamentals*, 9, 1, pp 177-179, 1970.
70. Aji, A., et al., Solution and shear history effects in polyethylene, *SPE Annual Technical Conference*, 30, pp 426-428, 1984.
71. Sholley, C.K., Use of the automatic capillary rheometer in quality control, *Proceedings of Quality Assurance of Polymeric Materials and Products*, Nashville, USA, 1981.
72. Smith, F.P., and Tong, P.P., *Polym. Eng. and Sci.*, Mid-Apr. 1982, Vol. 22, No. 5., pp 280-286.
73. Rudin, A., and Schreiber, H.P., *Polymer Engineering and Science*, 23, 8, pp 422-430, 1983.
74. Standard test method for rheological properties of thermoplastics, *ASTM standard D 3835-79*, 1983.

75. Wissbrun, K.F., and Zahorchak, A.C., *J. Polm. Sci., A-1*, 9:2093, 1971.
76. Anon., *New Yorker*, 20, 18-19, Nov. 25, 1944.
77. Wright, J.G.E., (to General Electric Co.), U.S. Pat. 2, 541, 85, 1951.
78. Beers, M.D., *Handbook of Materials*.
79. Benbow, J.J., et al, *Rheological Acta.*, Vol. 15, No. 5, 1976.
80. Plochocki, A., and Maciejewski, J., *Polimery (Warsaw)*, Vol. 26, No. 11/12, pp 426-30, 1981.
81. Martin, F.S., (to US Rubber Co.), U.S. Pat. 2, 609, 201, 1951.
82. Symmons, R., Sheffield Hallam University, Private Communication, 1990.
83. Nelkon, M., *Heat*, Blackie.
84. *Instruction Manual, Model Rotovisco RV3, Haake Viscometers*.
85. Fletcher, A.J., et al, *Computer modelling of the abrasive flow machining process, Surface Engineering Conference, University of Toronto, Canada, 1990*.
86. Ferry, J.D., *Viscoelastic properties of polymer*, Wiley.
87. Powell, C.J., Extrude Hone Limited, Private Communication, 1992.
88. *Nuffield data book, Nuffield Science Publications*.
89. Morter, J., Extrude Hone Limited, Private Communication, 1992.

# TABLES

---

**Table 1.**  
**Results and experimental conditions for the temperature measurements**  
**completed on the extrusion honing machine**  
**(section 3.2.3).**

EXPERIMENT NUMBER	1	2	3	4	5
POLY-BOROSILOXANE GRADE	C-11	C-11	C-21	C-11	C-11
ABRASIVE	-	-	-	SiC 32 $\mu$ m	SiC 1035mm
MACHINE OPERATION MODE	AUTO	MANUAL	MANUAL	AUTO	AUTO
HYDRAULIC PRESSURE (MPa)	2.1	2.1	2.1	4.8	4.8
MACHINE STROKES PER MIN.	3.8	7.8	10.44	15.6	17.76
TIME TO REACH CONST. TEMP. (S)	-	2260	1170	900	804
MAX. DIE TEMP. INSIDE T/C (°C)	40	57	39	67	77
MAX. DIE TEMP. OUTER T/C (°C)	35	-	37	60	65
MAX. POLY-BOROSILOXANE TEMP. (°C)	-	50	33	73	85
MAX. POLY-BOROSILOXANE TEMP. AT THE DIE WALL (°C)	-	40	33	65	76

**Table 2.**

**The specific heat capacity of C-11 polyborosiloxane as determined by differential scanning calorimetry (section 3.2.2).**

<b>SAMPLE TEMPERATURE °C</b>	<b>SPECIFIC HEAT CAPACITY J g<sup>-1</sup> K<sup>-1</sup></b>
20	1.64
30	1.64
43	1.60
50	1.52
60	1.48
70	1.43
80	1.39

**Table 3.**

The average and the standard deviation of the extrusion barrel pressure measured during constant ram velocity capillary rheometer experiments. All experiments were completed prior to the constant barrel charging procedure described in section 3.2.7.

EXPERIMENT NO.	TEMPERATURE °c	DIE LENGTH mm	RAM VELOCITY cm min <sup>-1</sup>	AVERAGE EXTRUSION BARREL PRESSURE KPa	STANDARD DEVIATION OF EXTRUSION BARREL PRESSURE KPa
1	30	20	2.5	6937	2639
2	30	25	2.5	5587	1951
3	30	30	2.5	6485	2726
4	30	35	2.5	8439	4414
5	30	40	2.5	8640	4808
6	30	20	12.5	5895	1615
7	30	25	12.5	6929	1757
8	30	30	12.5	11250	4966
9	30	35	12.5	13939	5365
10	30	40	12.5	14008	6412
11	30	ZERO	5	2741	49
12	30	20	5	9034	3350
13	30	30	5	7444	4193
14	30	40	5	13562	4683
15	30	ZERO	10	3897	207
16	30	20	10	6954	1615
17	30	30	10	6736	1303
18	30	40	10	7361	1787
19	30	ZERO	15	4220	215
20	30	20	15	5972	475
21	30	30	15	6546	574
22	30	40	15	8190	1516
23	30	ZERO	20	4609	262
24	30	20	20	6784	511
25	30	30	20	7995	673
26	30	40	20	9726	1027
27	30	40	1.58	11495	6337
28	30	40	4.65	9570	5460
29	30	40	7.68	7357	2346
30	30	40	10.86	12103	4853
31	30	40	15.67	10139	3357
32	30	ZERO	1.58	1338	37
33	30	ZERO	4.65	2680	59
34	30	ZERO	7.68	3658	253
35	30	ZERO	10.86	3741	226
36	30	ZERO	15.67	4069	102

**Table 4.**

The average and the standard deviation of the extrusion barrel pressure measured during constant ram velocity capillary rheometer experiments. All experiments were completed using the constant barrel charging procedure described in section 3.2.7.

EXPERIMENT NO.	TEMPERATURE °c	DIE LENGTH mm	RAM VELOCITY cm min <sup>-1</sup>	AVERAGE EXTRUSION BARREL PRESSURE KPa	STANDARD DEVIATION OF EXTRUSION BARREL PRESSURE KPa
1	30	40	1.25	10830	2941
2	30	40	2.5	4464	1152
3	30	40	5	5808	1547
4	30	40	10	4924	228
5	30	40	15	2444	631
6	30	ZERO	1.25	627	187
7	30	ZERO	2.5	1442	114
8	30	ZERO	5	2274	109
9	30	ZERO	10	3599	360
10	30	ZERO	15	4067	266
11	39	40	1.25	10794	1123
12	39	40	2.5	10678	5517
13	39	40	5	14252	7846
14	39	40	10	13053	11348
15	39	40	15	17463	9741
16	39	ZERO	1.25	277	64
17	39	ZERO	2.5	868	79
18	39	ZERO	5	2060	120
19	39	ZERO	10	3164	460
20	39	ZERO	15	3868	486
21	45	40	1.25	10349	159
22	45	40	2.5	19029	135
23	45	40	5	22968	5670
24	45	40	10	36456	8160
25	45	40	15	43099	10253
26	45	ZERO	1.25	184	59
27	45	ZERO	2.5	766	170
28	45	ZERO	5	1194	79
29	45	ZERO	10	2388	111
30	45	ZERO	15	3907	262
31	30	40	1.25	7745	3953
32	30	40	1.25	6478	4136
33	39	40	2.5	9877	5187
34	45	40	2.5	18483	1081
35	45	40	15	33516	13522
36	30	40	5	5412	3630
37	30	40	5	5230	2162
38	30	40	5	5683	3563
39	70	40	1.25	8606	746
40	70	40	5	25252	1605
41	70	40	15	45421	3248

**Table 5.**

The calculated (from the ram velocity, barrel dimensions and initial mass) and measured (by collecting and weighing extrusion samples) die mass flow rates for experiments completed with C-11 polyborosiloxane on the capillary rheometer.

TEMPERATURE °c	RAM VELOCITY cm min <sup>-1</sup>	AVERAGE DIE MASS FLOW RATE	
		MEASURED mg sec <sup>-1</sup>	CALCULATED mg sec <sup>-1</sup>
30	1.25	55.168	57.508
30	1.25	56.914	57.508
39	2.5	110.46	111.328
45	2.5	109.072	111.328
45	15	670.32	680.989

**Table 6.**

**Shear viscosity data for C-11 polyborosiloxane at 30°C, 39°C and 45°C calculated from constant ram velocity experiments on the capillary rheometer. (All experiments were completed using the standard charging procedure described in section 3.2.7).**

TEMPERATURE °C	RAM VELOCITY cm min <sup>-1</sup>	LONG DIE PRESSURE DROP KPa	ZERO DIE PRESSURE DROP KPa	CORRECTED PRESSURE DROP KPa	VOLUME FLOW RATE cm <sup>3</sup> min <sup>-1</sup>	APPARENT SHEAR RATE s <sup>-1</sup>	APPARENT SHEAR STRESS KPa	RABINOWITZ SHEAR RATE s <sup>-1</sup>	APPARENT VISCOSITY KPa·s	TRUE VISCOSITY KPa·s
30	1.25	10830	627	10203	3.56	75.6	127.5	26.4	1.687	4.83
30	2.5	4464	1442	3022	7.13	151.3	37.8	65.4	0.250	0.58
30	5	5808	2274	3534	14.26	302.6	44.2	109.2	0.146	0.41
30	10	4924	3599	1325	28.51	605.0	16.6	375.9	0.027	0.04
30	15	2444	4067	-	42.76	907.4	-	680.6	-	-
39	1.25	10794	277	10517	3.56	75.6	131.5	492.7	1.739	0.267
39	2.5	10678	868	9810	7.13	151.3	122.6	515.3	0.810	0.239
39	5	14252	2060	12192	14.26	302.6	152.4	715.6	0.504	0.13
39	10	13053	3164	12739	28.51	605	159.2	876.3	0.263	0.182
39	15	17463	3868	13595	42.76	907.4	170.0	1232.1	0.187	0.138
45	1.25	10349	184	10165	3.56	75.6	127.1	176	1.681	0.722
45	2.5	19029	766	18263	7.13	151.3	228.3	286	1.509	0.798
45	5	22968	1194	21774	14.26	302.6	272.2	366.2	0.899	0.743
45	10	36456	2388	34068	28.51	605	425.9	589.1	0.704	0.723
45	15	43099	3907	39192	42.76	907.4	489.9	758.8	0.540	0.645

**Table 7.**

The average and standard deviation the extrusion barrel and slit die pressure readings for C-11 polyborosiloxane extruded at 30°C and 43°C on the slit die rheometer.

TEMPERATURE °c	RAM VELOCITY cm min <sup>-1</sup>	AVERAGE OR SD	PRESSURE BARREL KPa	TRANSDUCER NUMBER			
				1 KPa	2 KPa	3 KPa	4 KPa
30	1.25	average sd	1586 170	2551 124	2155 130	1313 67	385 22
30	2.5	average sd	8533 1366	8041 1005	6925 888	- -	927 113
30	5	average sd	27366 1762	20488 1180	16907 1134	8134 693	1623 226
43	1.25	average sd	8265 207	6165 163	5105 134	- -	682 22
43	2.5	average sd	13335 424	10643 557	8944 487	- -	1107 56
43	5	average sd	25981 1149	18925 1040	15940 881	- -	1933 95

**Table 8.**

Shear viscosity data for C-11 polyborosiloxane at 30°C and 43°C calculated from constant ram velocity experiments on the slit-die rheometer. (All experiments were completed using the standard charging procedure described in section 3.2.7).

TEMP-ERATURE °C	RAM VELOCITY cm min <sup>-1</sup>	PRESSURE DROP KPa	VOLUM- ETRIC FLOW RATE cm <sup>3</sup> min <sup>-1</sup>	WALL SHEAR STRESS KPa	APPARENT SHEAR RATE s <sup>-1</sup>	TRUE SHEAR RATE s <sup>-1</sup>	APPARENT VISCOSITY KPa s	TRUE VISCOSITY KPa s
30	1.25	3028	3.563	9.46	23.8	18.8	0.397	0.503
30	2.5	10183	7.127	31.82	47.5	41.7	0.669	0.763
30	5	26986	14.255	84.33	95.0	89.9	0.888	0.938
43	1.25	7788	3.563	24.34	23.8	27.1	1.023	0.898
43	2.5	13588	7.127	42.46	47.5	51.4	0.894	0.826
43	5	24223	14.255	75.70	95.0	98.5	0.797	0.769

**Table 9.**  
**Shear viscosity data for C-11 polyborosiloxane calculated from concentric cylinder rheometer experimental results at 30 C.**

<b>SHEAR STRAIN RATE s<sup>-1</sup></b>	<b>SHEAR STRESS Pa</b>	<b>SHEAR VISCOSITY KPa·s</b>
0.046	66	1.435
0.082	121	1.475
0.172	209	1.215
0.350	350	1.000
0.440	428	0.973
0.869	550	0.633

**Table 10.**

**Summary table of all the calculated apparent rheological data for C-11 polyborosiloxane determined within the experimental programme. (Data generated during the experimental method development not included).**

TEMPERATURE °C	RHEOMETER	APPARENT STRAIN RATE s <sup>-1</sup>	APPARENT STRESS KPa	APPARENT VISCOSITY KPa·s
30	cylinder	0.046	0.066	1.435
		0.082	0.121	1.475
		0.172	0.209	1.215
		0.350	0.350	1.000
		0.440	0.428	0.973
		0.869	0.550	0.633
30	capillary	75.6	119.6	1.58
		151.3	38.5	0.25
		302.5	44.2	0.15
		605.0	16.6	0.027
30	slit-die	23.8	9.46	0.40
		47.5	31.82	0.67
		95	84.33	0.89
39	capillary	75.6	133.7	1.768
		151.3	123.2	0.815
		302.5	149.9	0.495
		605.0	129.6	0.214
		907.5	169.1	0.186
43	slit-die	23.8	24.34	1.024
		47.5	42.46	0.894
		95	75.70	0.797
45	capillary	75.6	126.9	1.68
		151.3	228	1.51
		302.5	272	0.90
		605	426	0.70
		907.5	500	0.56

# FIGURES

---

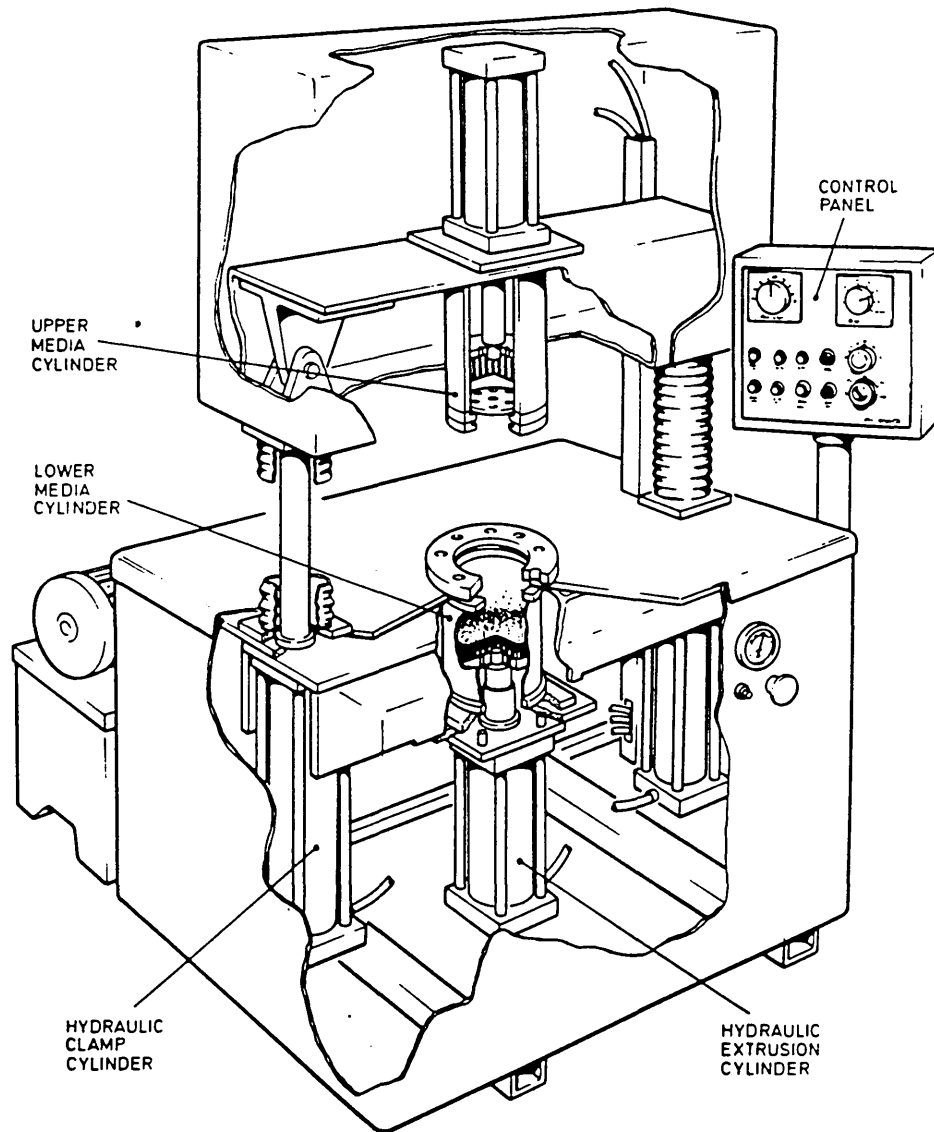


Figure 1. A typical industrial extrusion honing machine (courtesy of The Extrude Hone Corporation [11]).

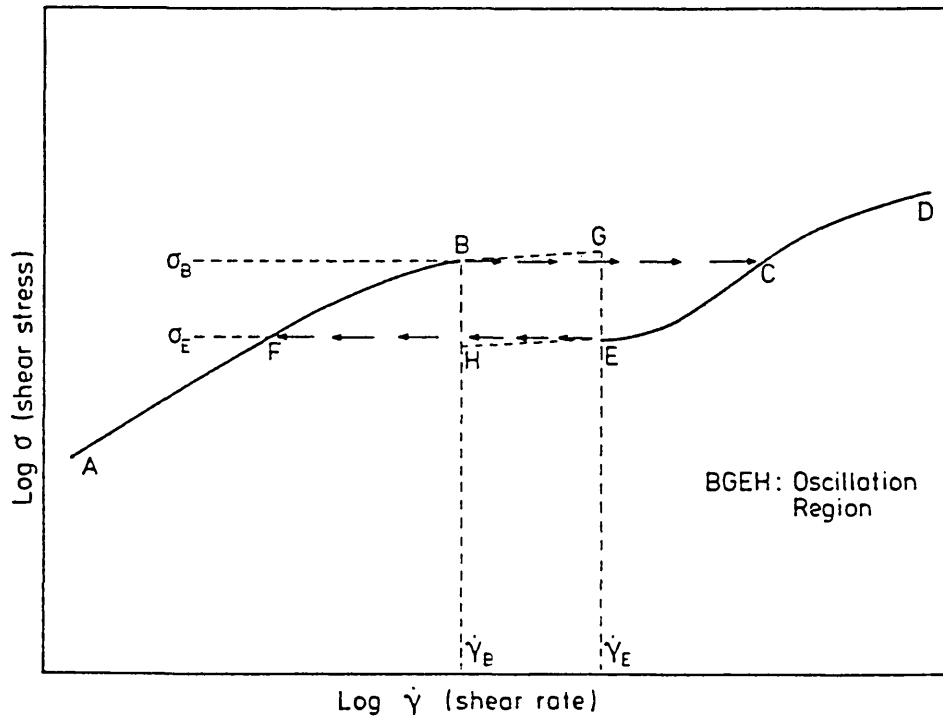


Figure 2. Schematic illustration of the double-branched form of a flow curve for polymer melts (after Bergem [52] - section 2.5.8)

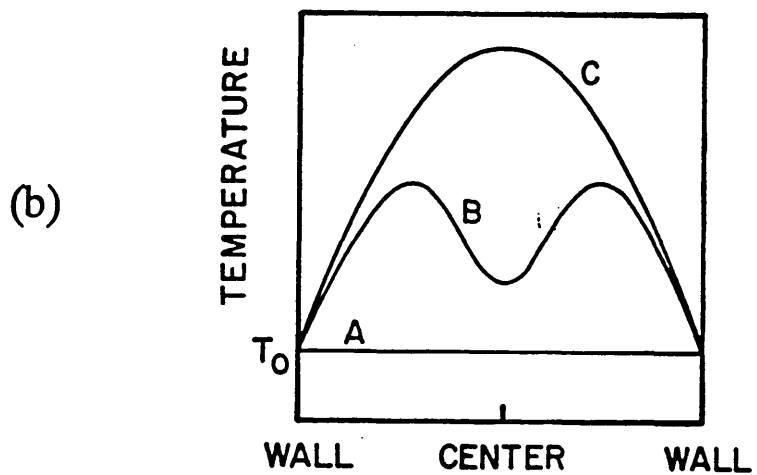
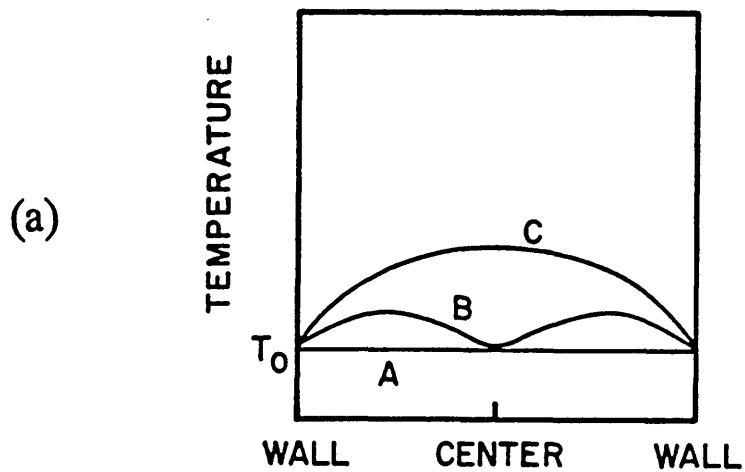


Figure 3. Temperature distributions for capillary flow with isothermal wall: curve A, at the entrance; curve B, some distance from the entrance; curve C, far from the entrance. (a) low flow rate (b) high flow rate (After Dealy [26] - section 2.5.9)

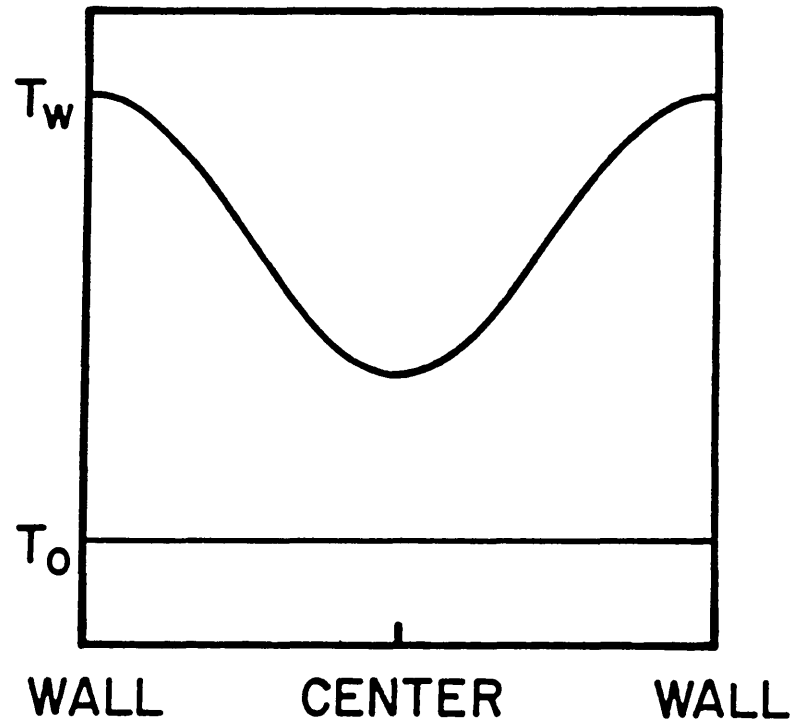


Figure 4. Temperature distribution for adiabatic flow in a capillary.  $T_0$  is the entrance temperature and  $T_w$  is the wall temperature some distance downstream (after Dealy [26] - section 2.5.9

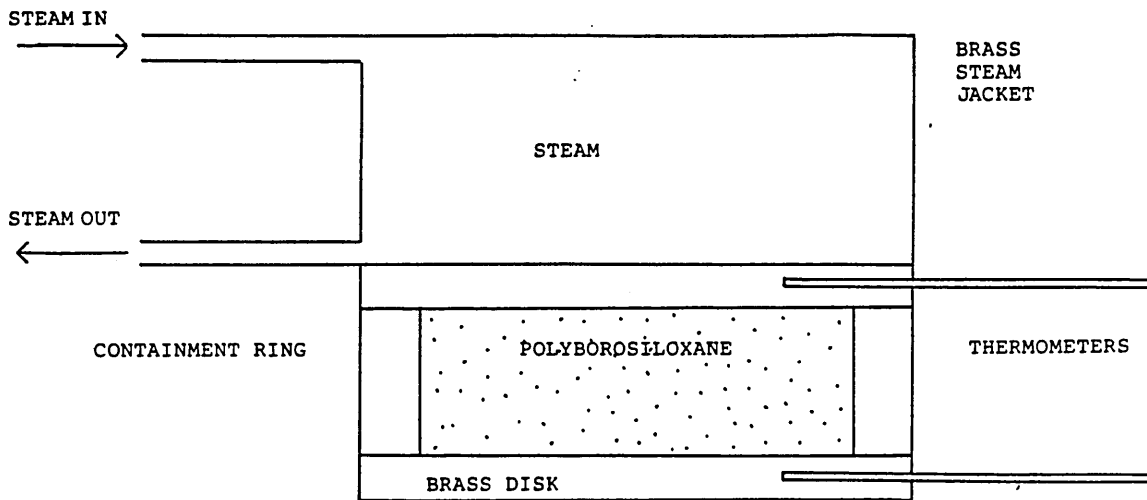


Figure 5. The main components of the Lees Disk equipment used for the determination of thermal conductivity (section 3.2.1).

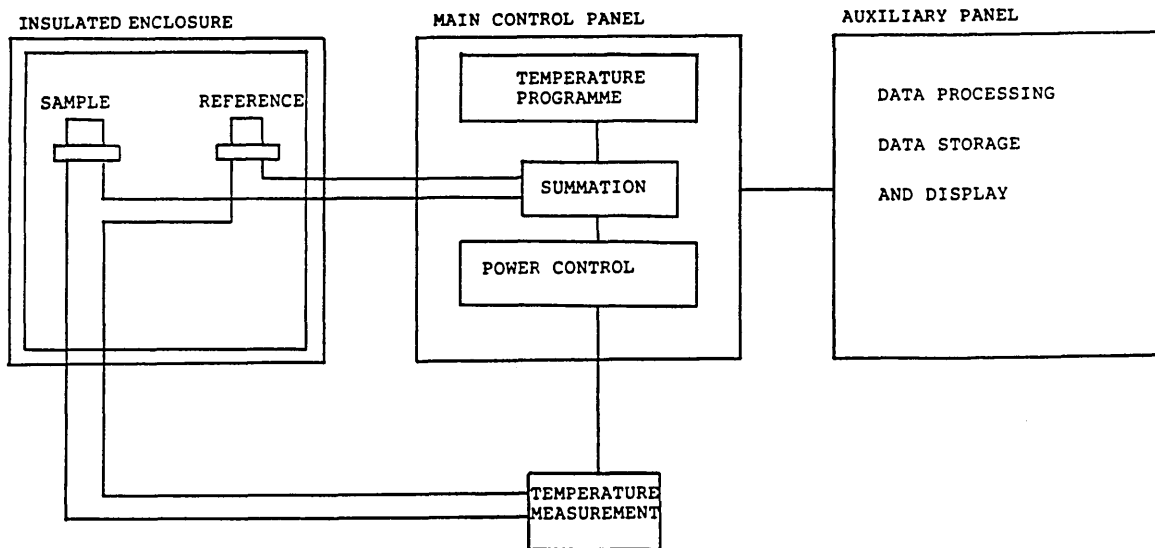


Figure 6. The main components of the Differential Scanning Calorimeter used for the determination of Specific Heat Capacity (section 3.2.2).

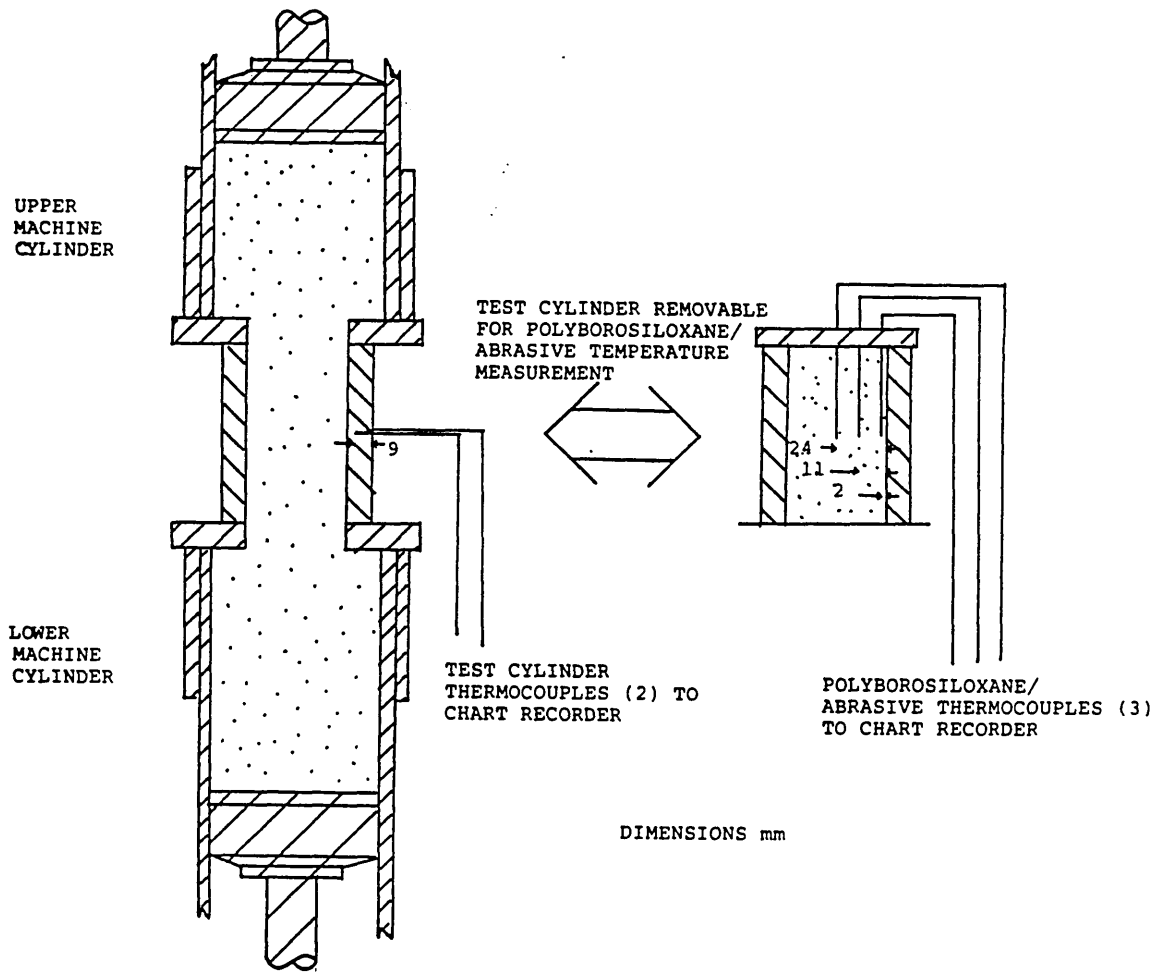


Figure 7. The position of the thermocouples used to measure the temperature distribution within the polyborosiloxane and die on the extrusion honing machine (section 3.2.3).

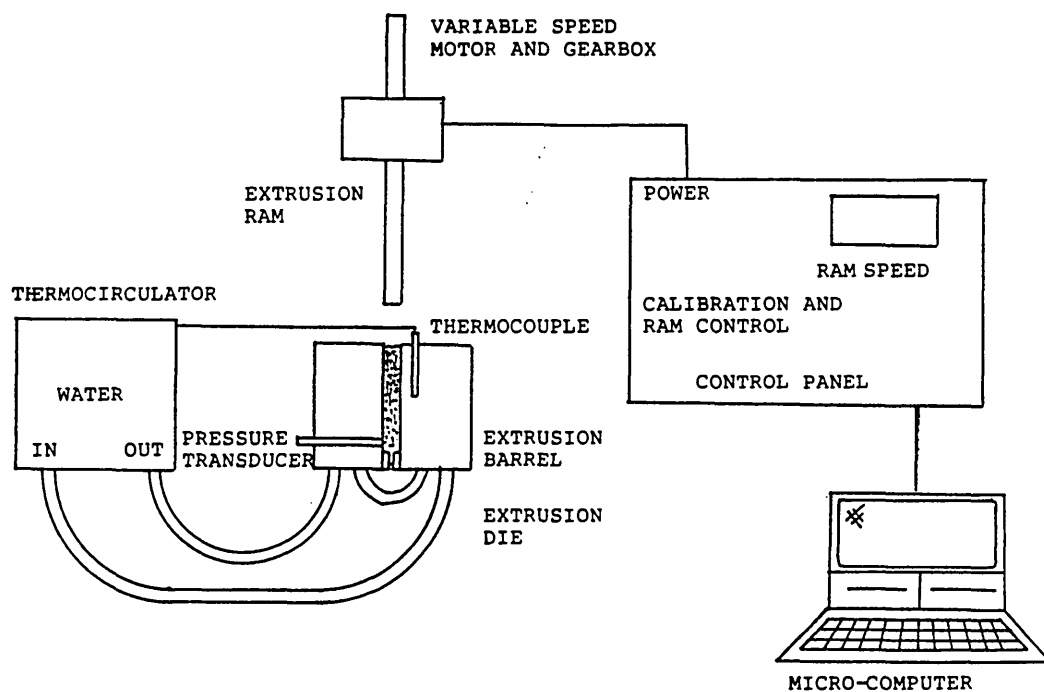


Figure 8. The main components of the capillary rheometer used to determine the rheological properties of the C-11 polyborosiloxane (section 3.2.4.).

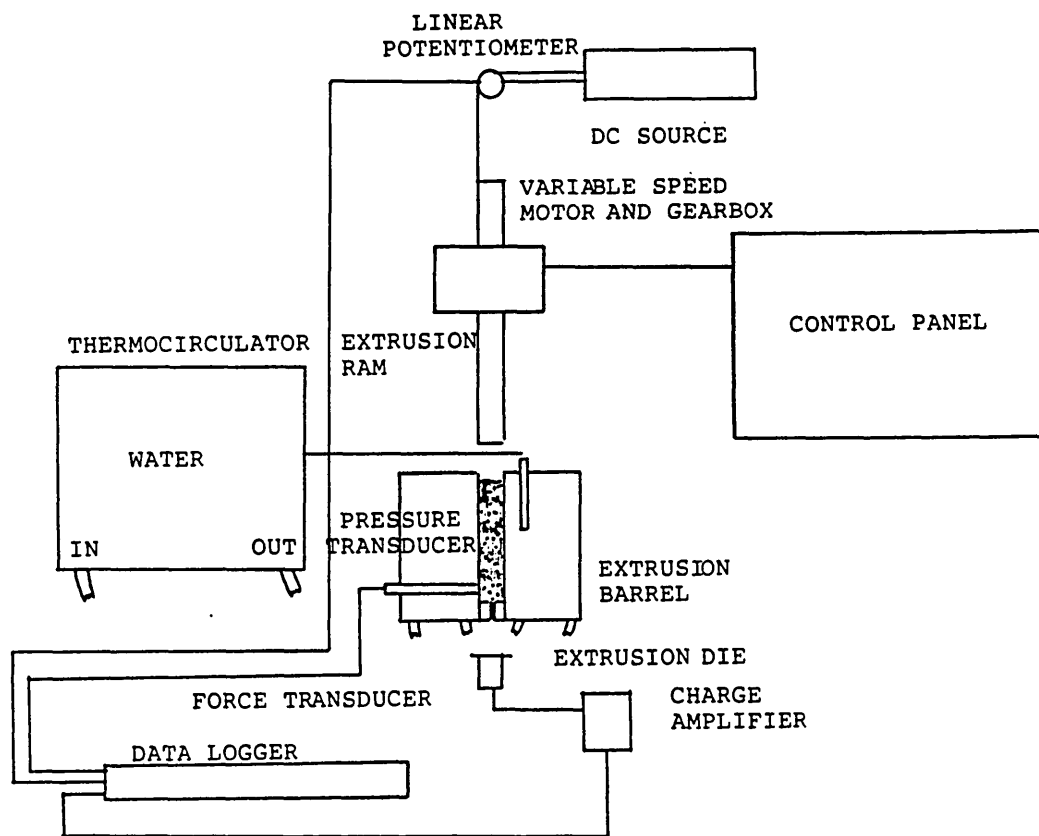


Figure 9. The additional instrumentation added to the capillary rheometer used to determine the rheological properties of the C-11 polyborosiloxane (section 3.2.6).

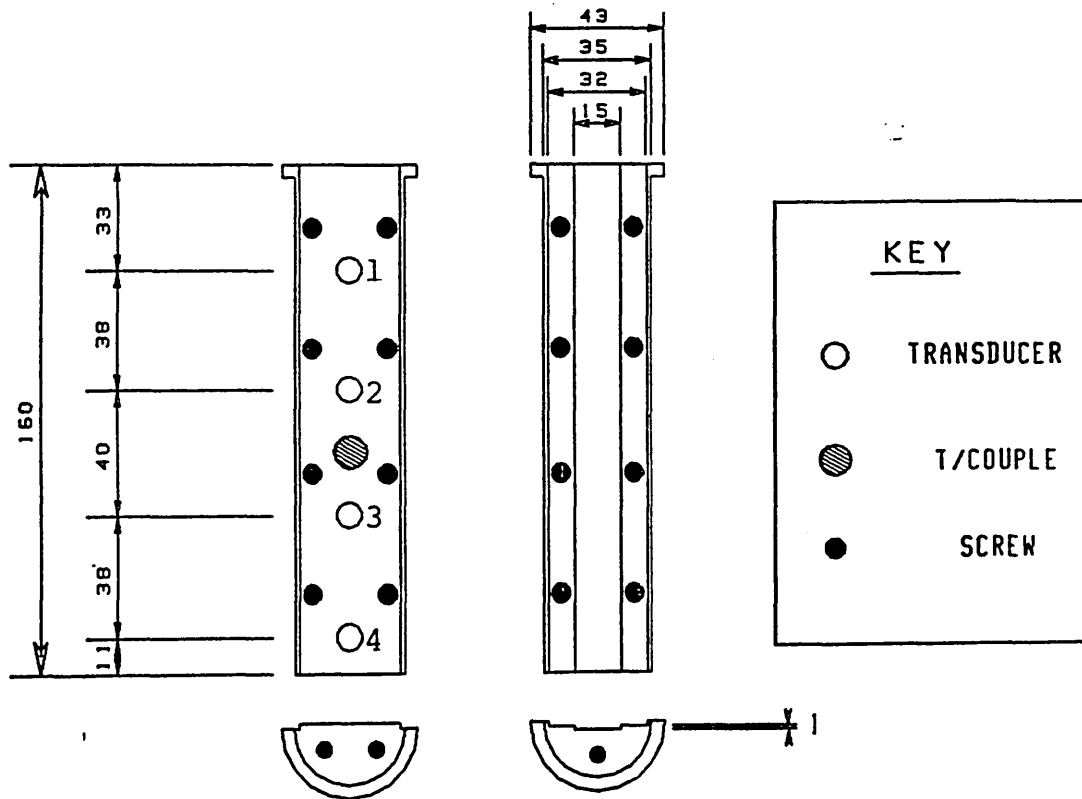


Figure 10. The dimensions (mm) of the slit-die used on the Davenport rheometer, showing the location of the thermocouple and pressure transducers (section 3.2.11).

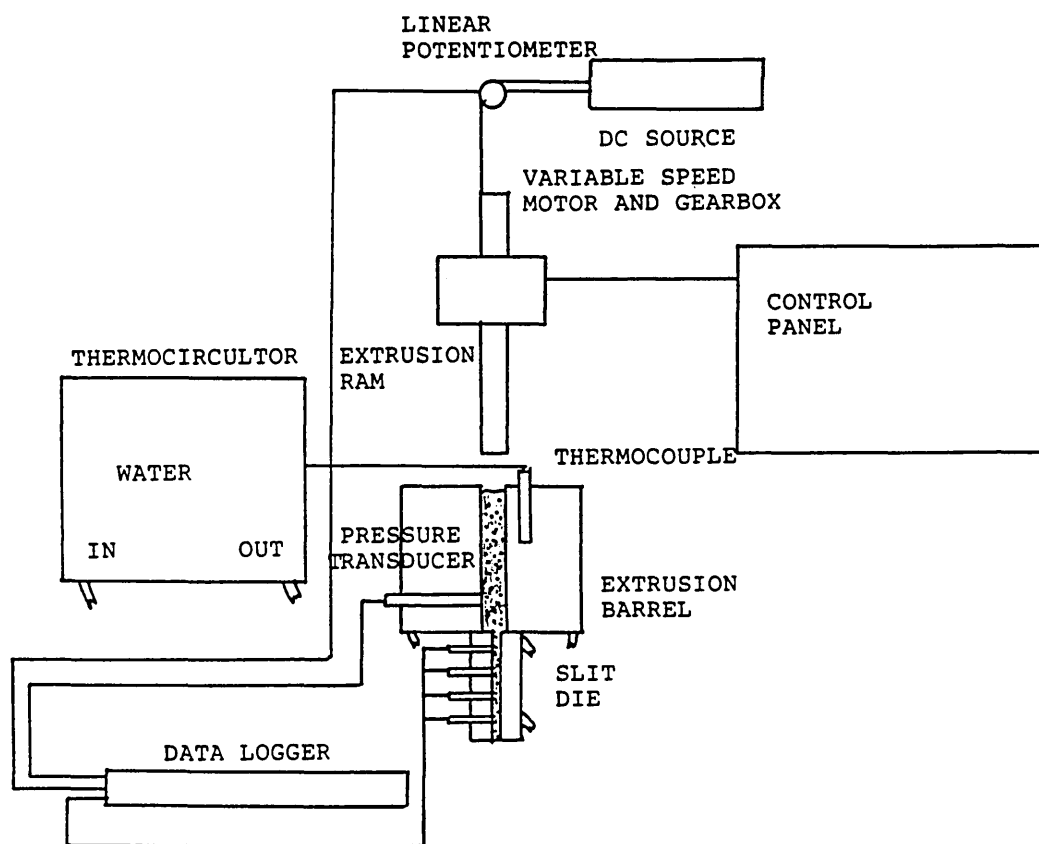


Figure 11. The main components of the slit-die rheometer, showing the temperature control and associated instrumentation (section 3.2.11).

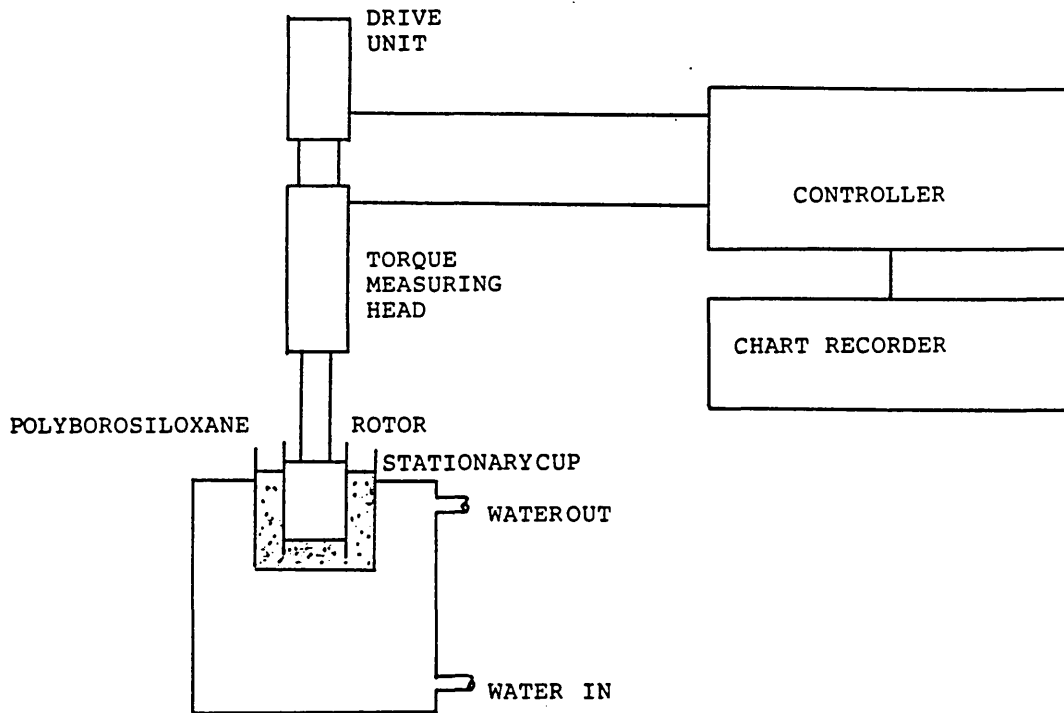


Figure 12. The main components of the Haake concentric cylinder rheometer (section 3.2.12).

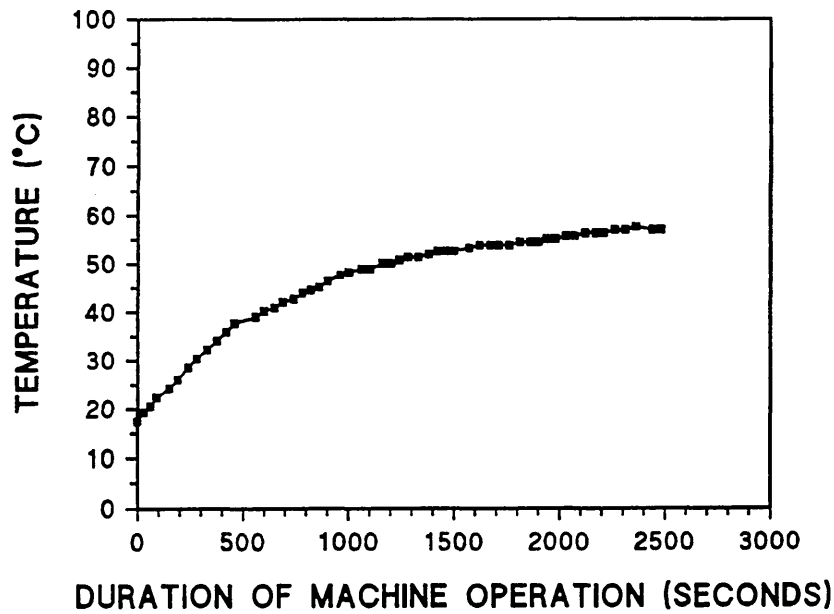


Figure 13. The increase in die wall temperature with time during operation of the extrusion honing machine charged with C-11 polyborosiloxane without abrasive (section 4.3.2.).

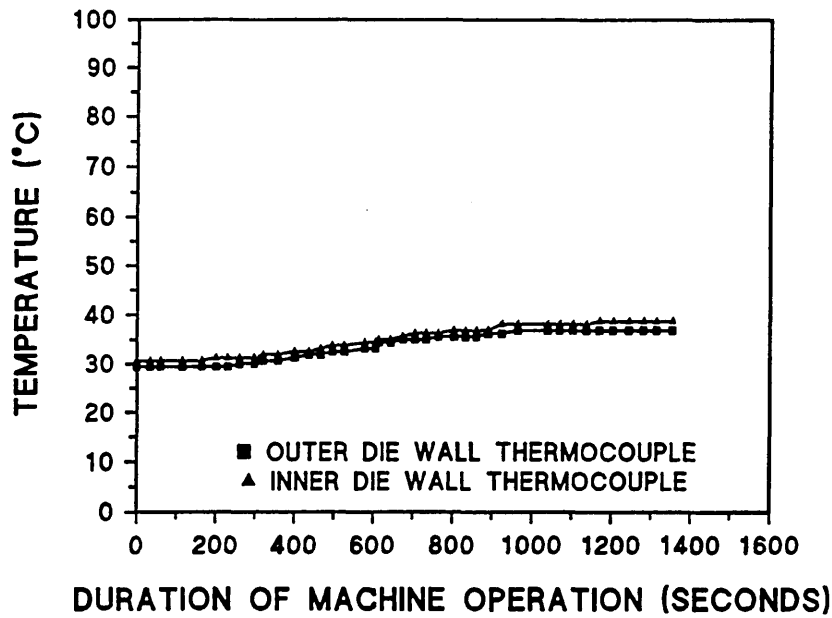


Figure 14. The increase in die wall temperature with time during operation of the extrusion honing machine charged with C-21 polyborosiloxane without abrasive (section 4.3.2.).

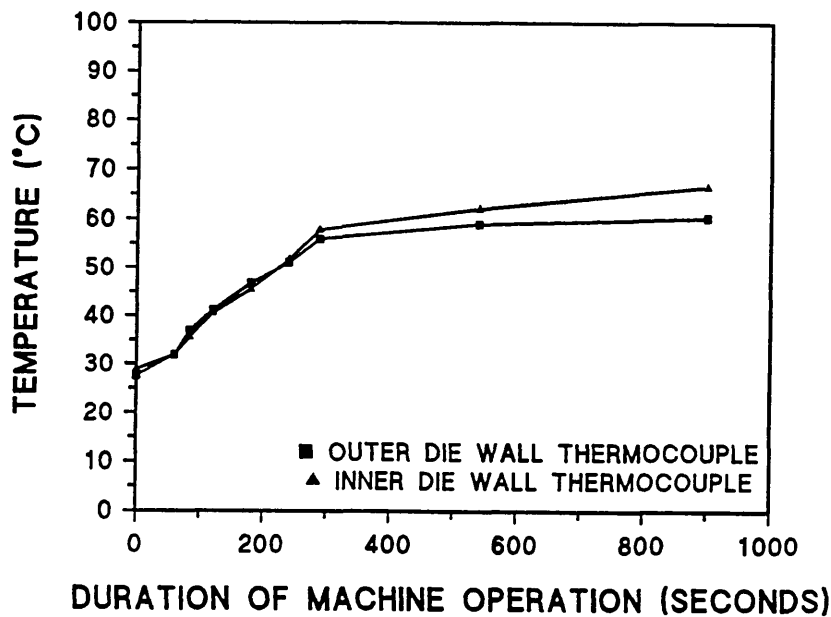


Figure 15. The increase in die wall temperature with time during operation of the extrusion honing machine charged with C-11 polyborosiloxane mixed with 32 μm abrasive (silicon carbide) grit (section 4.3.2.).

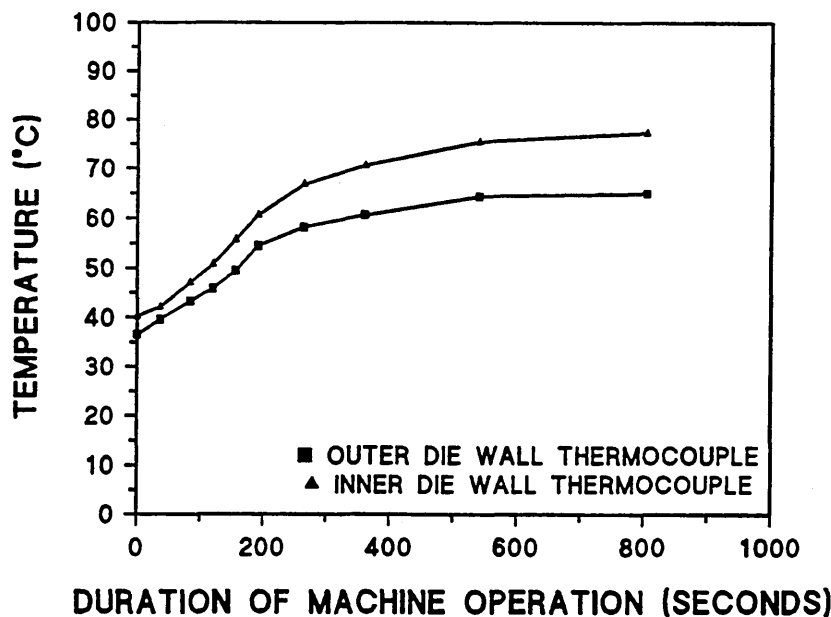


Figure 16. The increase in die wall temperature with time during operation of the extrusion honing machine charged with C-11 polyborosiloxane mixed with 1.035 mm abrasive (silicon carbide) grit (section 4.3.2.).

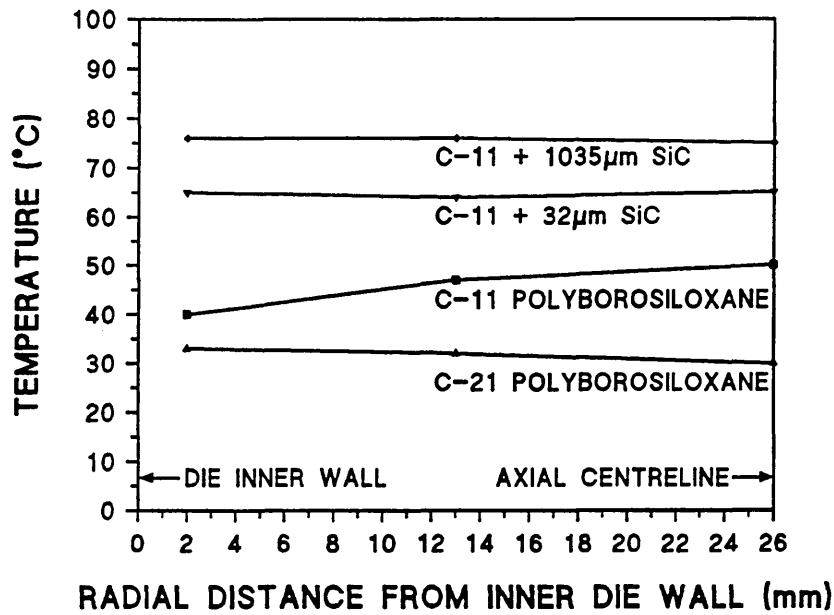


Figure 17. The temperature distribution through polyborosiloxane both with and without abrasive addition from wall to wall of a die following operation of an extrusion honing machine until thermal steady state had been achieved (section 4.3.2.).

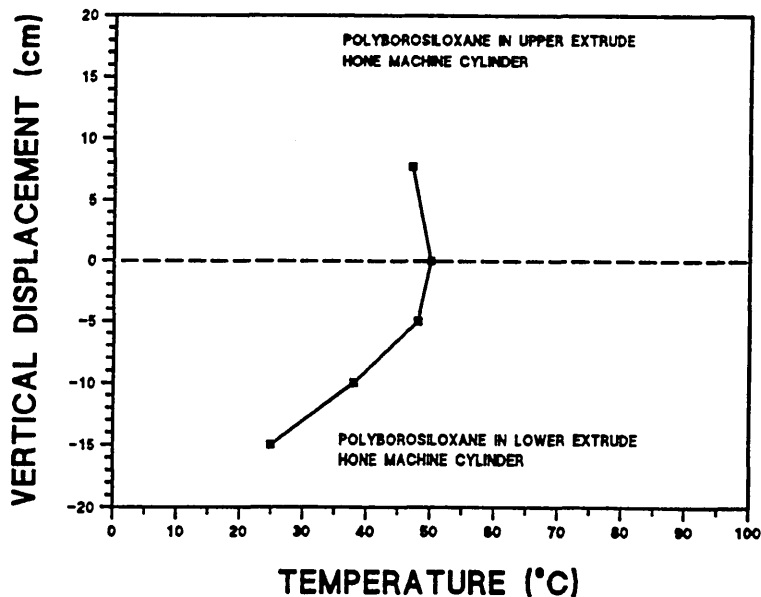


Figure 18. The temperature distribution axially down through C-11 polyborosiloxane within a die following operation of an extrusion honing machine until thermal steady state had been achieved (section 4.3.2.).

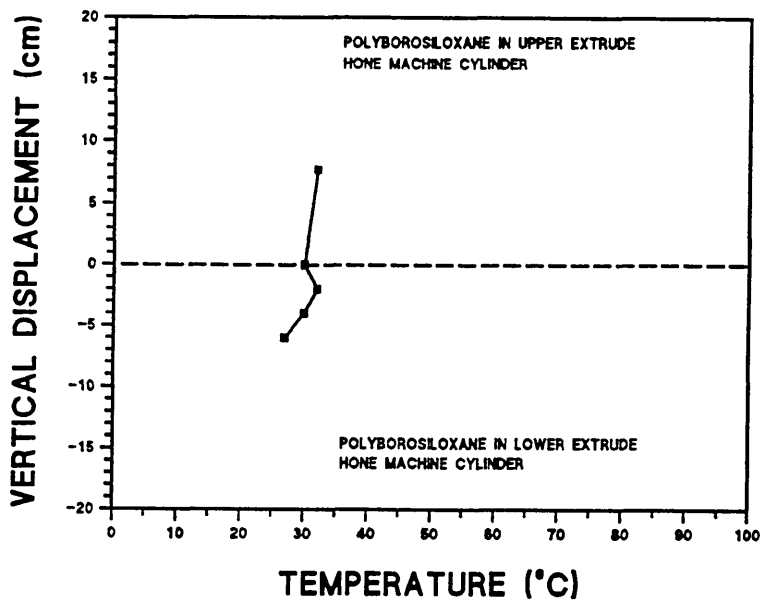


Figure 19. The temperature distribution axially down through C-21 polyborosiloxane within a die following operation of an extrusion honing machine until thermal steady state had been achieved (section 4.3.2.).

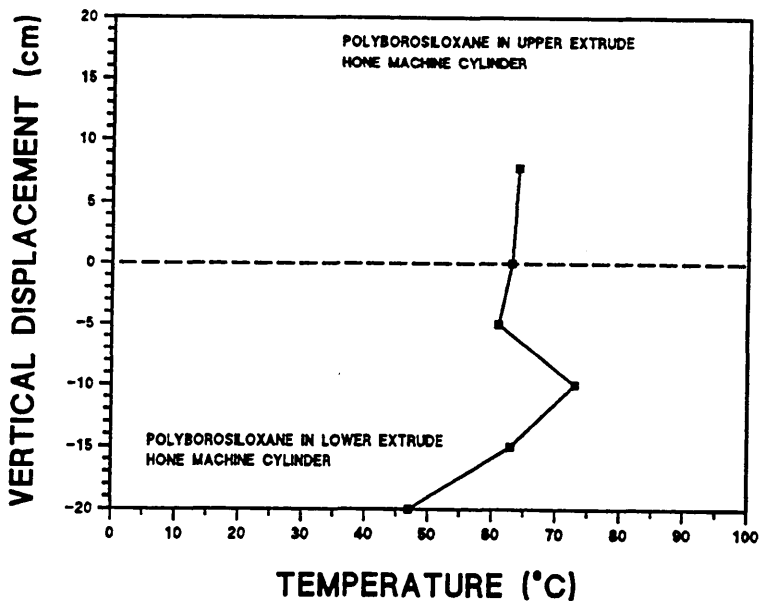


Figure 20. The temperature distribution axially down through C-11 polyborosiloxane mixed with 32 μm silicon carbide abrasive grit within a die following operation of an extrusion honing machine until thermal steady state had been achieved (section 4.3.2.).

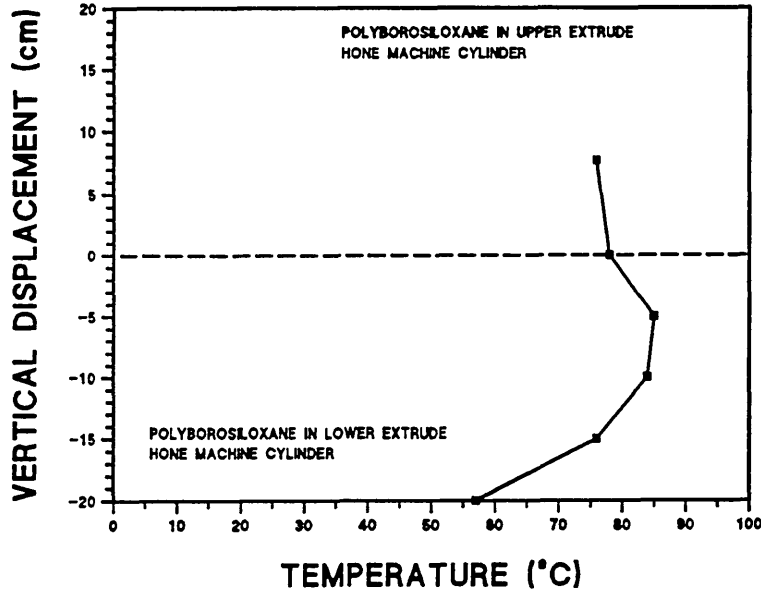


Figure 21. The temperature distribution axially down through C-11 polyborosiloxane mixed with 1.035 mm silicon carbide abrasive grit within a die following operation of an extrusion honing machine until thermal steady state had been achieved (section 4.3.2.).

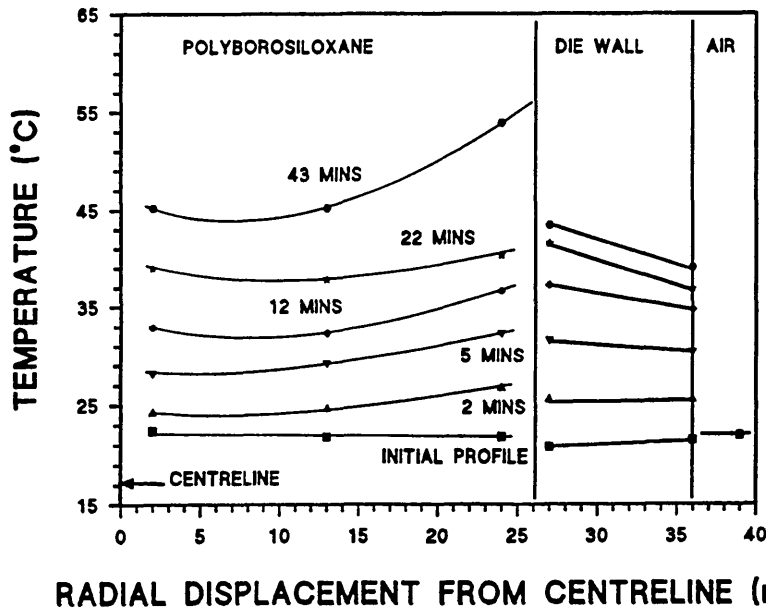


Figure 22. The temperature distribution through C-11 polyborosiloxane, from the centreline radially out to the die wall, and through the die wall, at time intervals during the operation of the extrusion honing machine (section 4.3.3.).

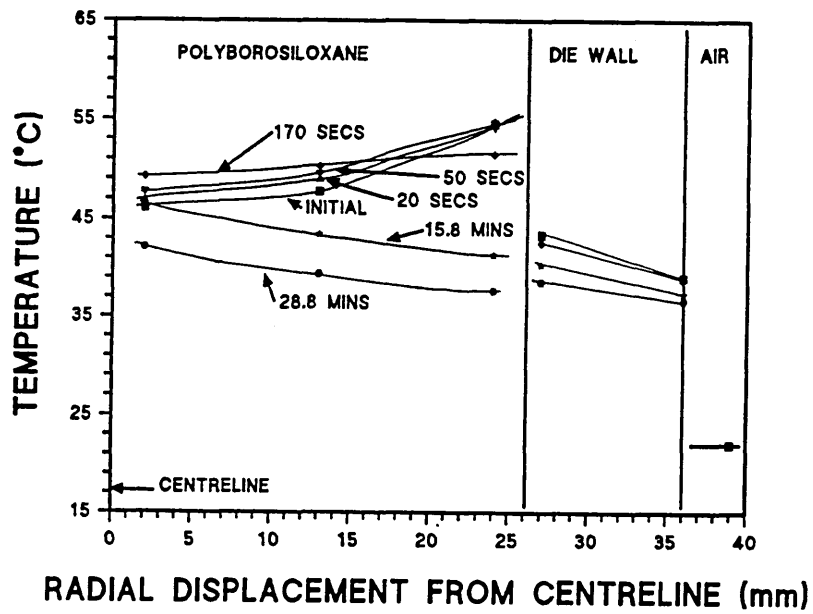


Figure 23. The temperature distribution through C-11 polyborosiloxane, from the centreline radially out to the die wall, and through the die wall, at time intervals during cooling after a period of extrusion honing machine operation (section 4.3.3.).

**EXTRUSION HONING THERMAL MODEL**

DATE: April 1989  
 POLYMER: C-21  
 ABRASIVE: None  
 EXPT. NO.: 3

**CONSTANTS**

Thermal conductivity of mild steel ( $W\ m^{-2}\ K^{-1}$ ) 25  
 Length of test die(m) 0.154  
 Inside radius of test die(m) 0.026  
 Radius to inner thermocouple(m) 0.0265  
 Radius to outer thermocouple(m) 0.036

**INPUT DATA**

Inner thermocouple temperature ( $^{\circ}C$ ) 38.7  
 Outer thermocouple temperature ( $^{\circ}C$ ) 36.8  
 Polymer at the wall temperature ( $^{\circ}C$ ) 38.8  
 Ambient air temperature ( $^{\circ}C$ ) 22

**STEADY STATE THERMAL MODEL CALCULATIONS**

Heat transfer between thermocouples (W) 146.9  
 Temperature of inside die wall ( $^{\circ}C$ ) 38.8  
 Surface heat transfer coefficient  
 (Die/Polymer- $J\ m^{-2}\ K^{-1}$ )  
 Surface heat transfer coefficient  
 (Die/Air- $J\ m^{-2}\ K^{-1}$ ) 284.1

**TEMPERATURE PROFILE**

Radius(m)	Description	Temperature ( $^{\circ}C$ )
0	Centre of polymer	38.81
0.02599	Polymer at the die wall	38.81
0.026	Inside die wall	38.81
0.036	Outer die wall	36.84
0.03601	Ambient air	22
0.05	Ambient air	22

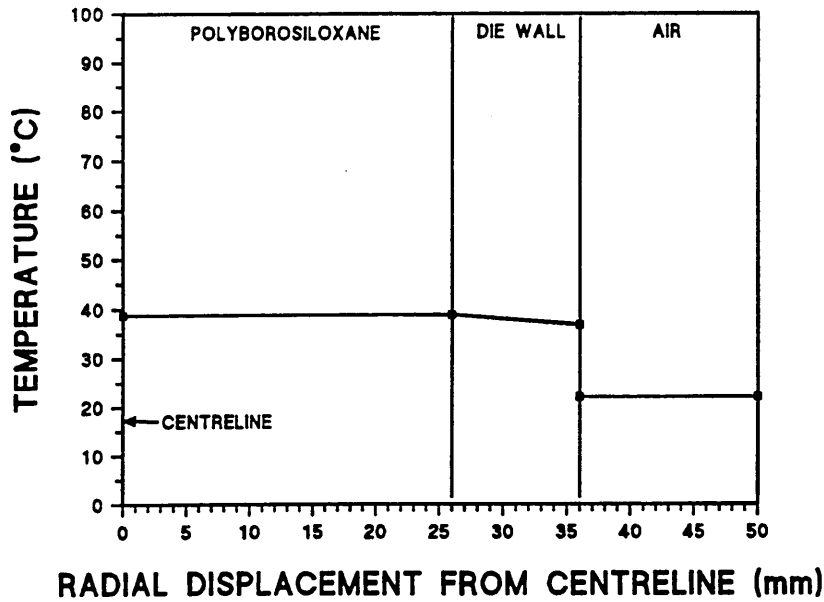


Figure 24. The results of the steady state thermal model for C-21 polyborosiloxane without abrasive subject to extrusion honing through a die (section 4.4.2.).

**EXTRUSION HONING THERMAL MODEL**

DATE: April 1989  
 POLYMER: C-11  
 ABRASIVE: SiC 32um 2:1 by mass  
 EXPT. NO.: 4

**CONSTANTS**

Thermal conductivity of mild steel ( $W m^{-2} K^{-1}$ ) 25  
 Length of test die(m) 0.154  
 Inside radius of test die(m) 0.026  
 Radius to inner thermocouple(m) 0.0265  
 Radius to outer thermocouple(m) 0.036

**INPUT DATA**

Inner thermocouple temperature ( $^{\circ}C$ ) 66.5  
 Outer thermocouple temperature ( $^{\circ}C$ ) 60.32  
 Polymer at the wall temperature ( $^{\circ}C$ ) 73  
 Ambient air temperature ( $^{\circ}C$ ) 22

**STEADY STATE THERMAL MODEL CALCULATIONS**

Heat transfer between thermocouples (W) 487.9  
 Temperature of inside die wall ( $^{\circ}C$ ) 66.9  
 Surface heat transfer coefficient  
 (Die/Polymer- $J m^{-2} K^{-1}$ ) 3171.4  
 Surface heat transfer coefficient  
 (Die/Air- $J m^{-2} K^{-1}$ ) 365.6

**TEMPERATURE PROFILE**

Radius(m)	Description	Temperature ( $^{\circ}C$ )
0	Centre of polymer	73
0.02599	Polymer at the die wall	73
0.026	Inside die wall	66.88
0.036	Outer die wall	60.32
0.03601	Ambient air	22
0.05	Ambient air	22

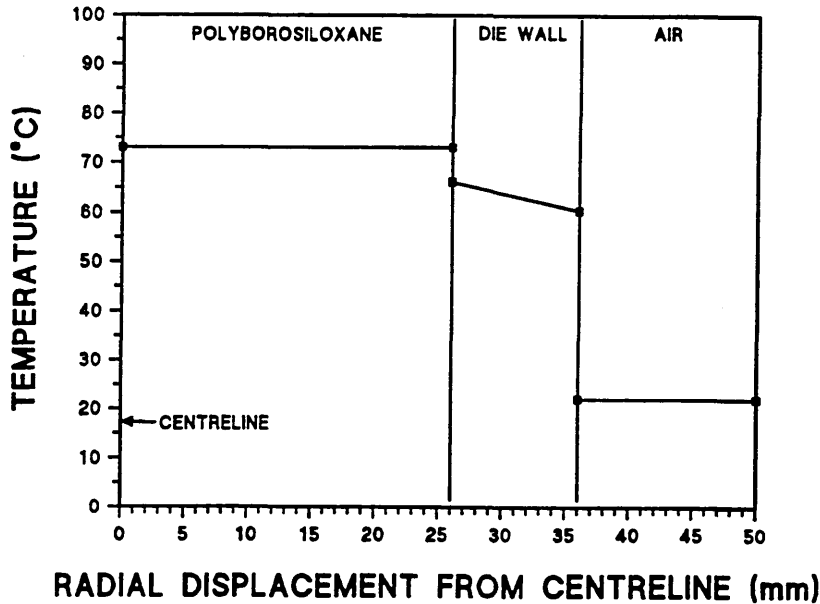


Figure 25. The results of the steady state thermal model for C-11 polyborosiloxane mixed with 32  $\mu m$  silicon carbide abrasive grit subject to extrusion honing through a die (section 4.4.2.).

**EXTRUSION HONING THERMAL MODEL**

DATE: April 1989  
 POLYMER: C-11  
 ABRASIVE: SiC 1.035mm 2:1 by mass  
 EXPT. NO.: 5

**CONSTANTS**

Thermal conductivity of mild steel ( $W m^{-2} K^{-1}$ ) 25  
 Length of test die(m) 0.154  
 Inside radius of test die(m) 0.026  
 Radius to inner thermocouple(m) 0.0265  
 Radius to outer thermocouple(m) 0.036

**INPUT DATA**

Inner thermocouple temperature ( $^{\circ}C$ ) 77.29  
 Outer thermocouple temperature ( $^{\circ}C$ ) 64.94  
 Polymer at the wall temperature ( $^{\circ}C$ ) 85  
 Ambient air temperature ( $^{\circ}C$ ) 22

**STEADY STATE THERMAL MODEL CALCULATIONS**

Heat transfer between thermocouples (W) 975.1139  
 Temperature of inside die wall ( $^{\circ}C$ ) 78.06  
 Surface heat transfer coefficient (Die/Polymer- $J m^{-2} K^{-1}$ ) 5503.2  
 Surface heat transfer coefficient (Die/Air- $J m^{-2} K^{-1}$ ) 651.9

**TEMPERATURE PROFILE**

Radius(m)	Description	Temperature ( $^{\circ}C$ )
0	Centre of polymer	85
0.02599	Polymer at the die wall	85
0.026	Inside die wall	78.06
0.036	Outer die wall	64.94
0.03601	Ambient air	22
0.05	Ambient air	22

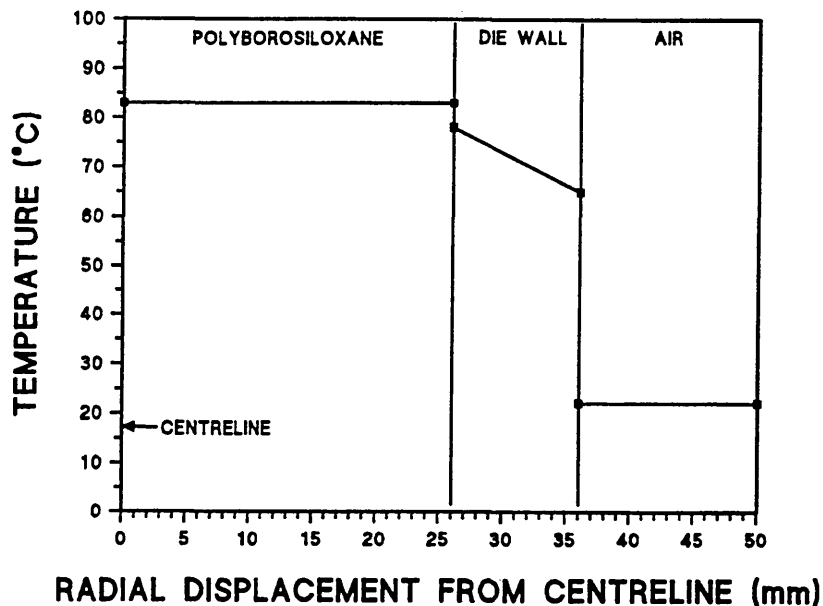


Figure 26. The results of the steady state thermal model from C-11 polyborosiloxane mixed with 1.035 mm silicon carbide abrasive grit subject to extrusion honing through a die (section 4.4.2.).

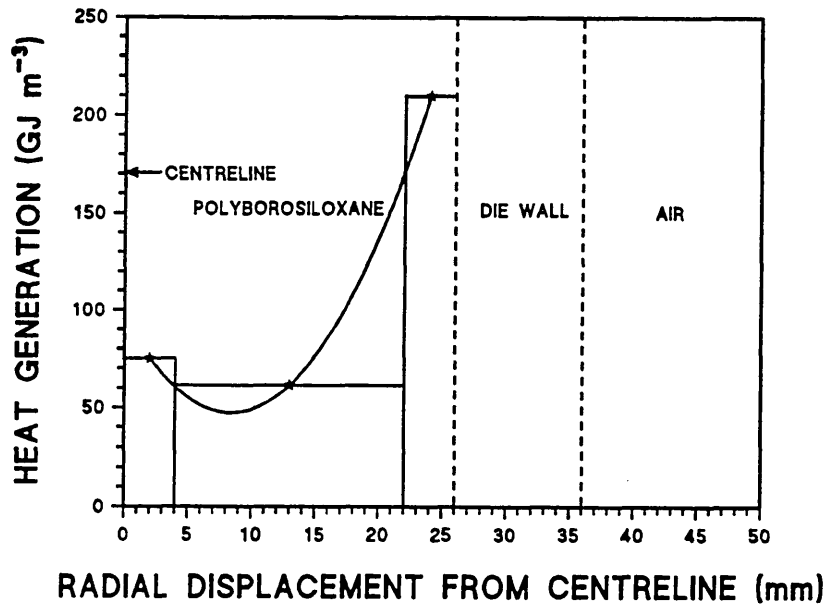


Figure 27. The calculated total heat generation within the polyborosiloxane within an extrusion die during extrusion honing machine operation over a period of 43 minutes (section 4.4.4)

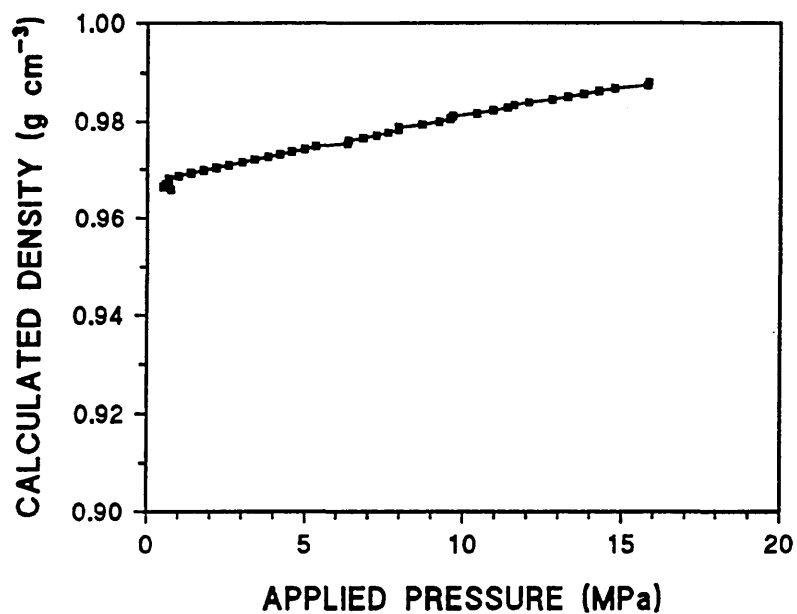


Figure 28. The variation in C-11 polyborosiloxane density with pressure at 30°C (section 4.5).

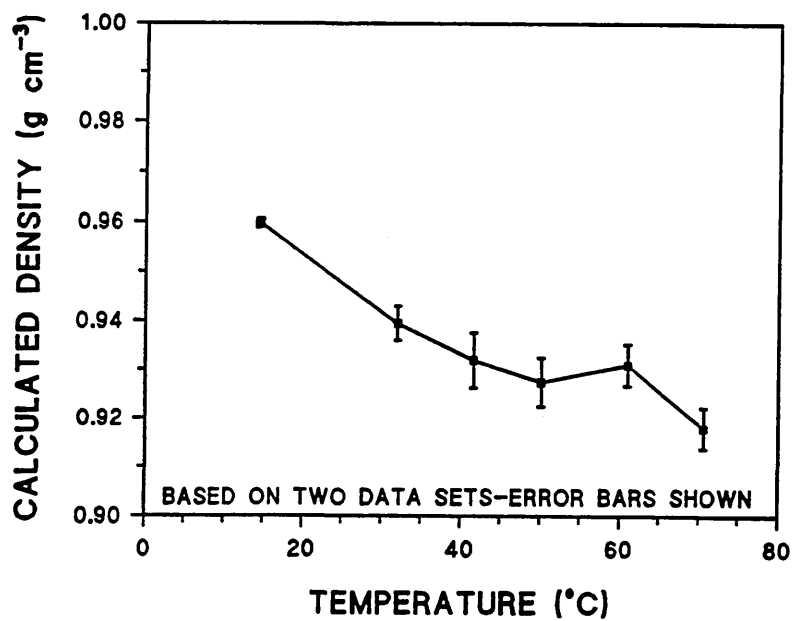


Figure 29. The variation in C-11 polyborosiloxane density with temperature at atmospheric pressure (section 4.5).

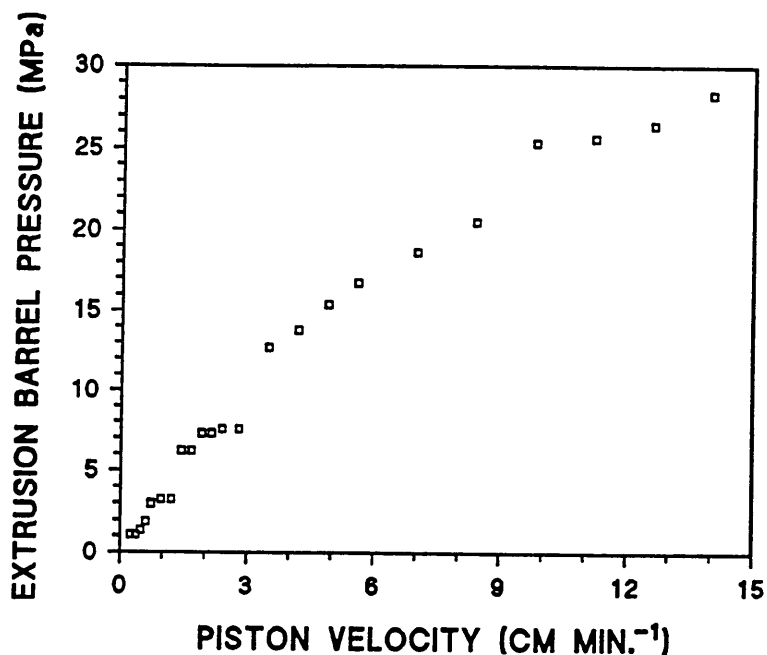


Figure 30. The variation in extrusion barrel pressure with ram velocity during the extrusion of C-11 polyborosiloxane on the capillary rheometer at 23°C using a die of 2mm internal diameter and 20mm long (rheometer operated with the ram velocity increasing throughout extrusion) (section 4.6.2).

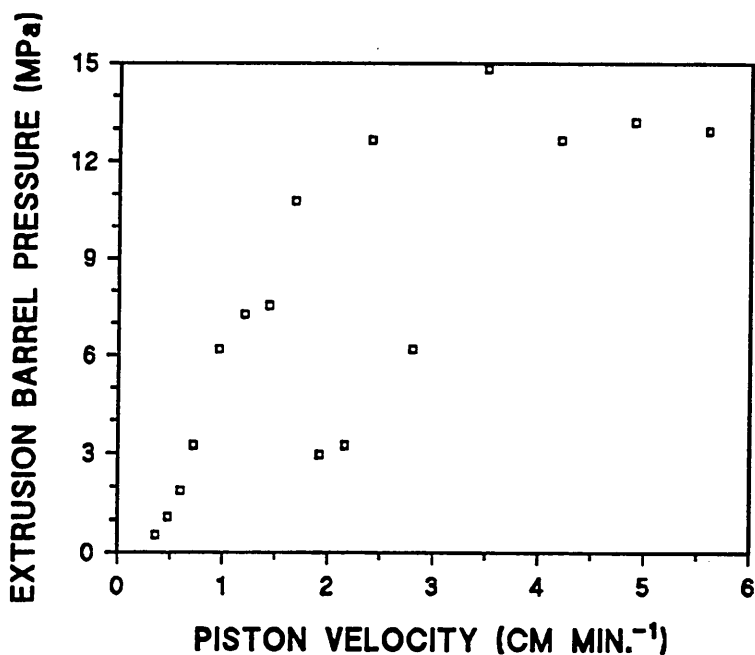


Figure 31. The variation in extrusion barrel pressure with ram velocity during the extrusion of C-11 polyborosiloxane on the capillary rheometer at 30°C using a die of 2mm internal diameter and 20mm long (rheometer operated with the ram velocity increasing throughout extrusion) (section 4.6.2).

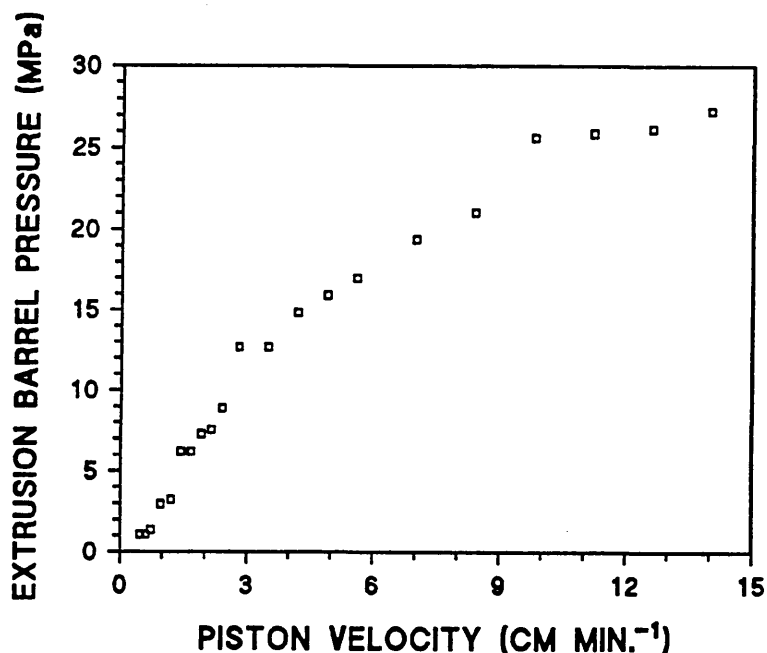


Figure 32. The variation in extrusion barrel pressure with ram velocity during the extrusion of C-11 polyborosiloxane on the capillary rheometer at 40°C using a die of 2mm internal diameter and 20mm long (rheometer operated with the ram velocity increasing throughout extrusion) (section 4.6.2).

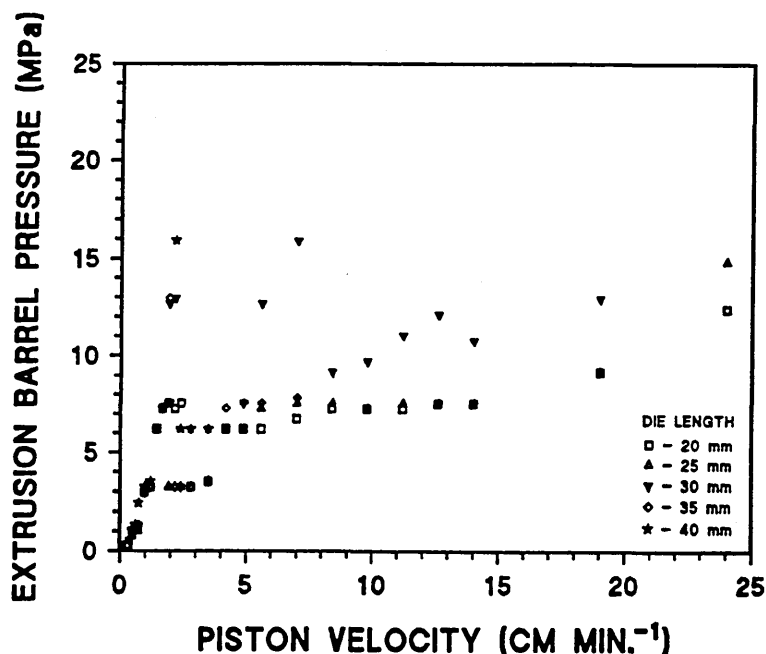


Figure 33. The variation in extrusion barrel pressure with ram velocity during the extrusion of C-11 polyborosiloxane on the capillary rheometer at 30°C using dies of 2mm internal diameter and 20, 25, 30, 35 and 40mm long (rheometer operated with the ram velocity increasing throughout extrusion) (section 4.6.2).

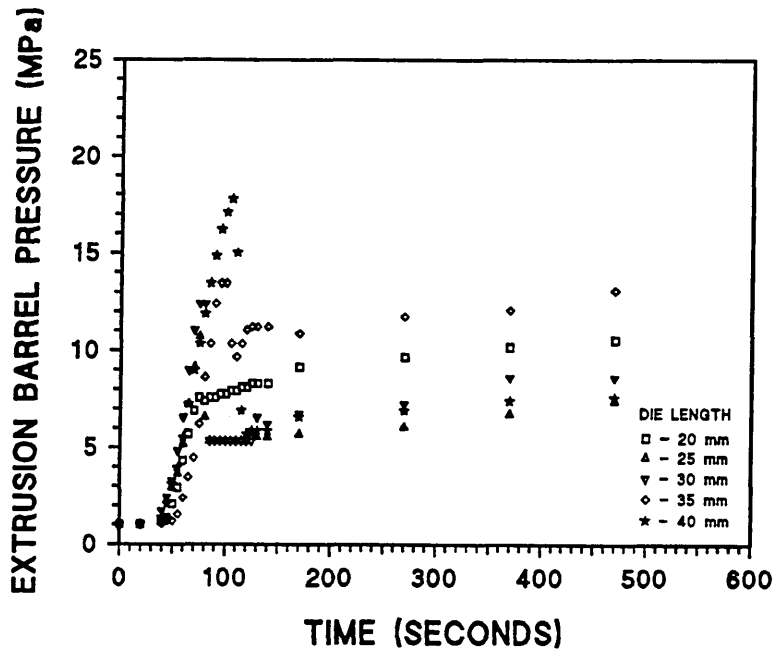


Figure 34. The variation in extrusion barrel pressure during extrusion of C-11 polyborosiloxane on the capillary rheometer at a constant ram velocity of 2.5 cm/min at 30°C using dies of 2mm internal diameter and 20, 25, 30, 35 and 40mm long (section 4.6.2).

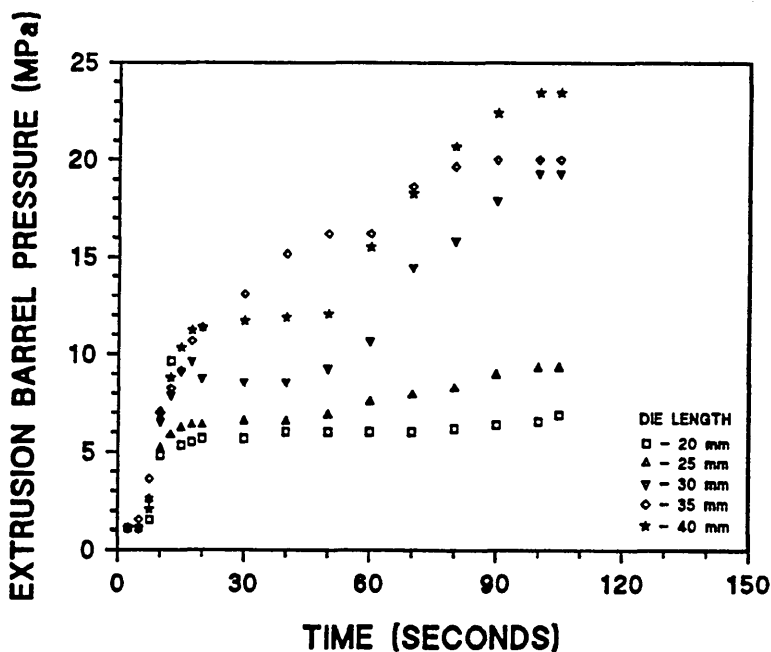


Figure 35. The variation in extrusion barrel pressure during extrusion of C-11 polyborosiloxane on the capillary rheometer at a constant ram velocity of 12.5 cm/min at 30°C using dies of 2mm internal diameter and 20, 25, 30, 35 and 40mm long (section 4.6.2).

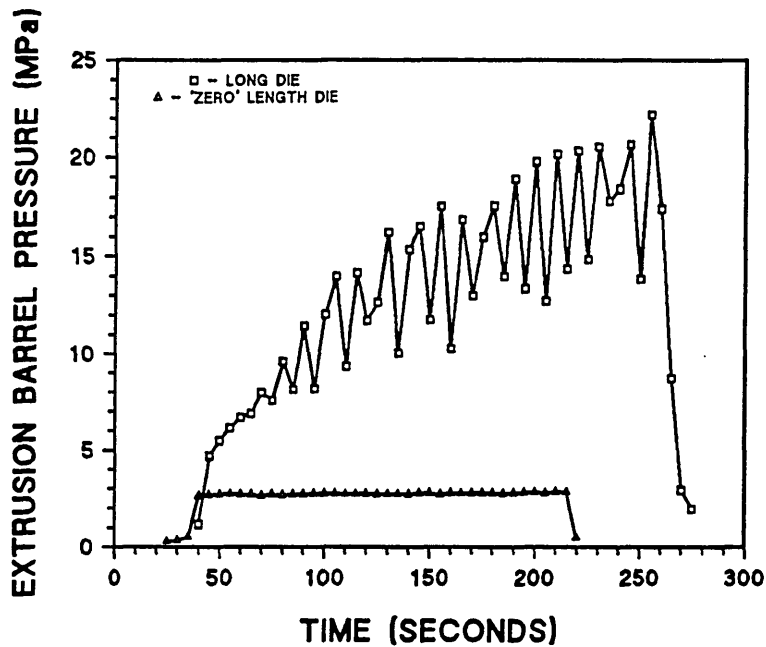


Figure 36. The variation in extrusion barrel pressure during extrusion of C-11 polyborosiloxane on the capillary rheometer at a constant ram velocity of 5 cm/min at 30°C using dies of 2mm internal diameter and both nominally zero (orifice die) and 40mm long (section 4.6.2).

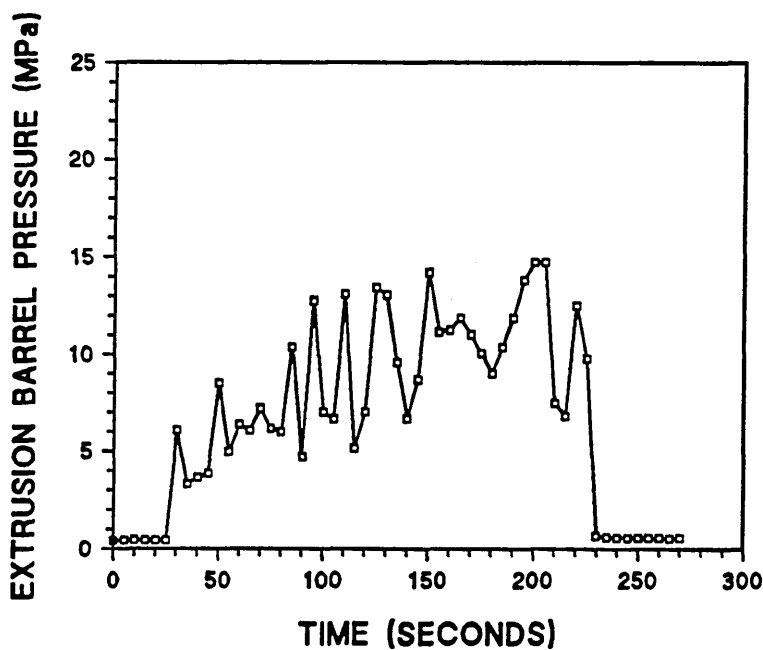


Figure 37. The variation in extrusion barrel pressure during extrusion of C-11 polyborosiloxane on the capillary rheometer at a constant ram velocity of 5 cm/min at 30°C using a die of 2mm internal diameter and 20mm long (section 4.6.2).

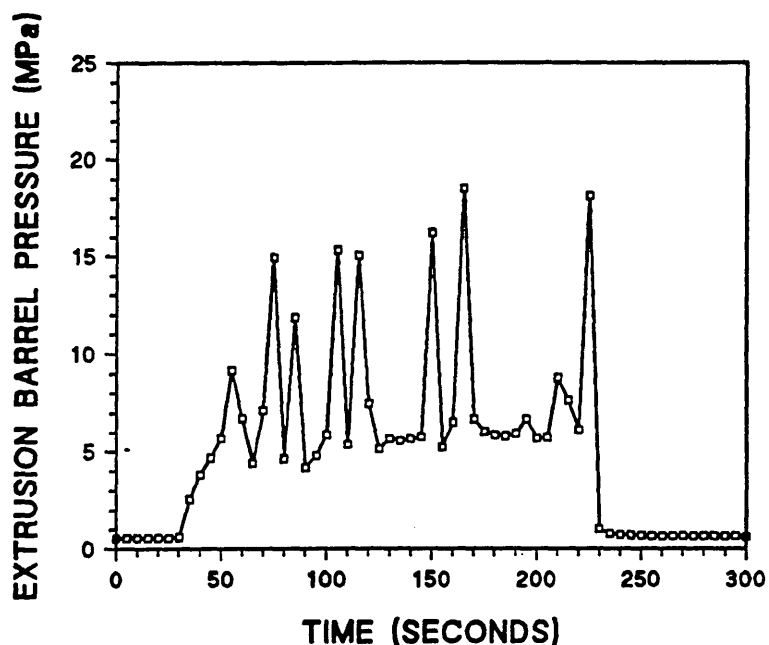


Figure 38. The variation in extrusion barrel pressure during extrusion of C-11 polyborosiloxane on the capillary rheometer at a constant ram velocity of 5 cm/min at 30°C using a die of 2mm internal diameter and 30mm long (section 4.6.2).

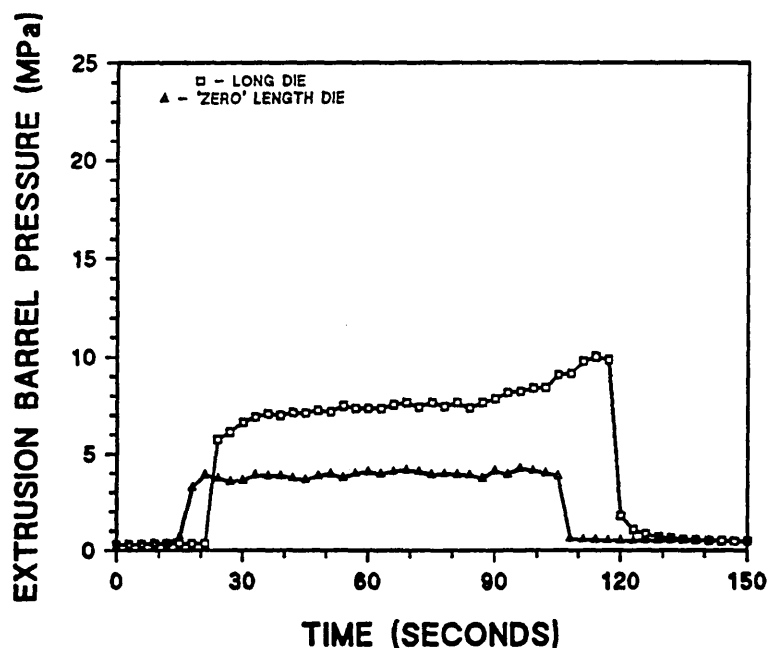


Figure 39. The variation in extrusion barrel pressure during extrusion of C-11 polyborosiloxane on the capillary rheometer at a constant ram velocity of 10 cm/min at 30°C using dies of 2mm internal diameter and both nominally zero (orifice die) and 40mm long (section 4.6.2).

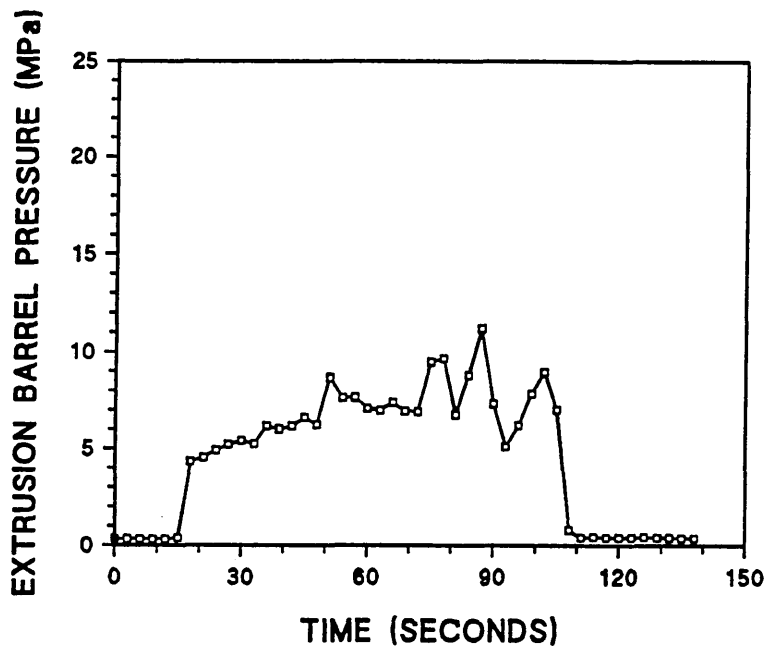


Figure 40. The variation in extrusion barrel pressure during extrusion of C-11 polyborosiloxane on the capillary rheometer at a constant ram velocity of 10 cm/min at 30°C using a die of 2mm internal diameter and 20mm long (section 4.6.2).

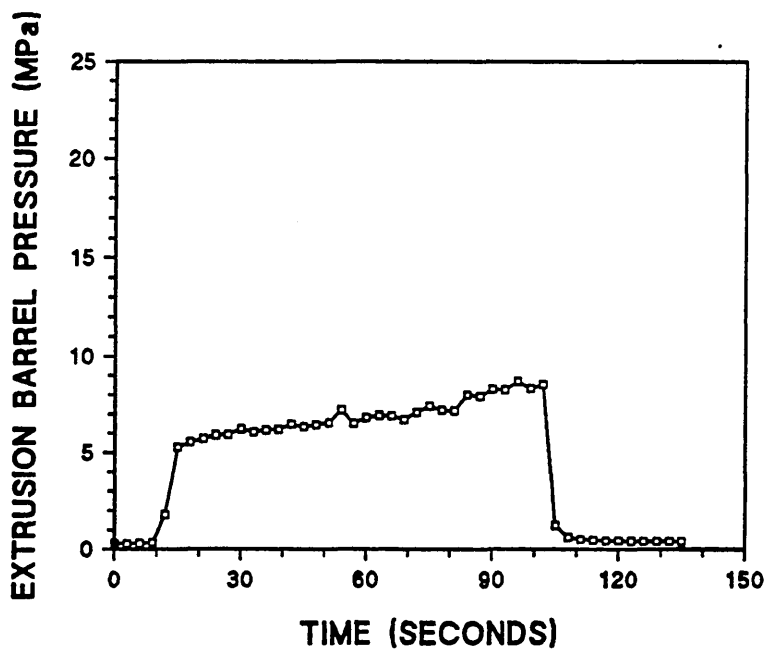


Figure 41. The variation in extrusion barrel pressure during extrusion of C-11 polyborosiloxane on the capillary rheometer at a constant ram velocity of 10 cm/min at 30°C using a die of 2mm internal diameter and 30mm long (section 4.6.2).

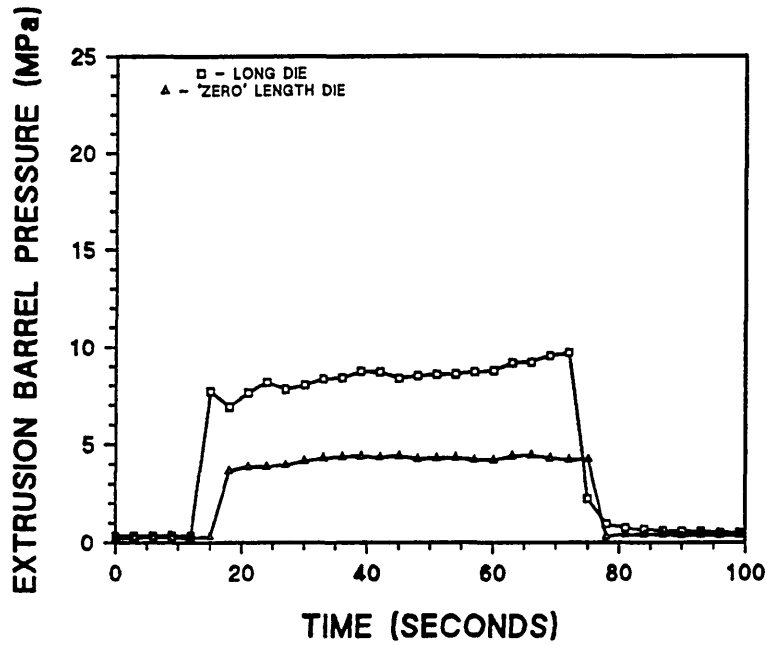


Figure 42. The variation in extrusion barrel pressure during extrusion of C-11 polyborosiloxane on the capillary rheometer at a constant ram velocity of 15 cm/min at 30°C using dies of 2mm internal diameter and both nominally zero (orifice die) and 40mm long (section 4.6.2).

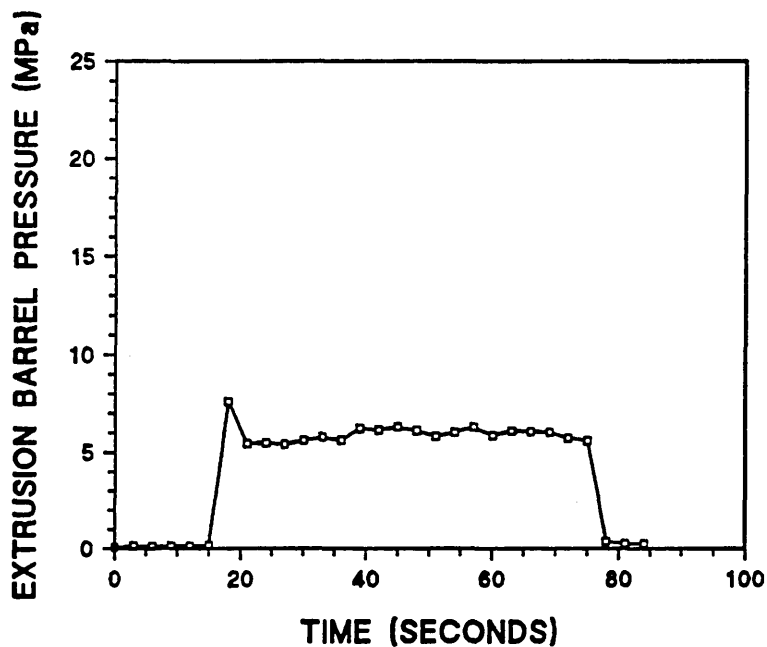


Figure 43. The variation in extrusion barrel pressure during extrusion of C-11 polyborosiloxane on the capillary rheometer at a constant ram velocity of 15 cm/min at 30°C using a die of 2mm internal diameter and 20mm long (section 4.6.2).

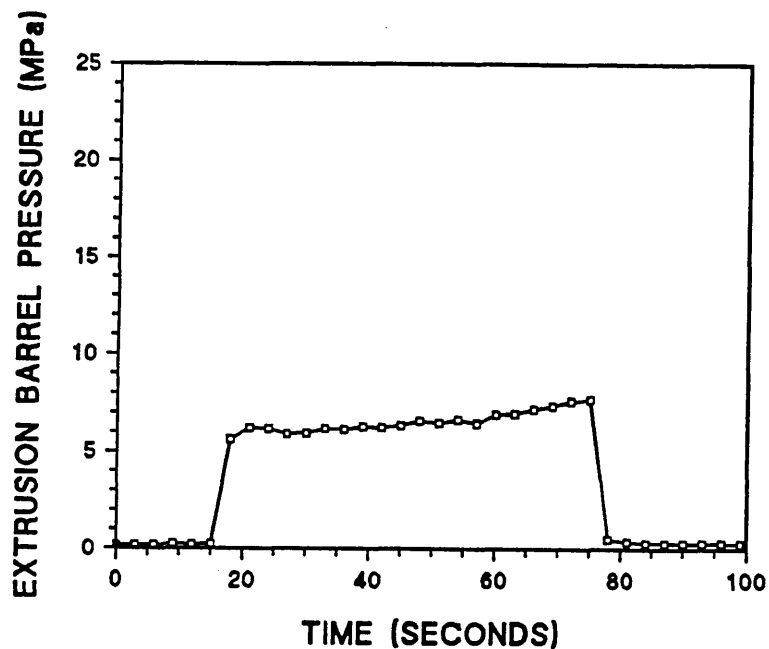


Figure 44. The variation in extrusion barrel pressure during extrusion of C-11 polyborosiloxane on the capillary rheometer at a constant ram velocity of 15 cm/min at 30°C using a die of 2mm internal diameter and 30mm long (section 4.6.2).

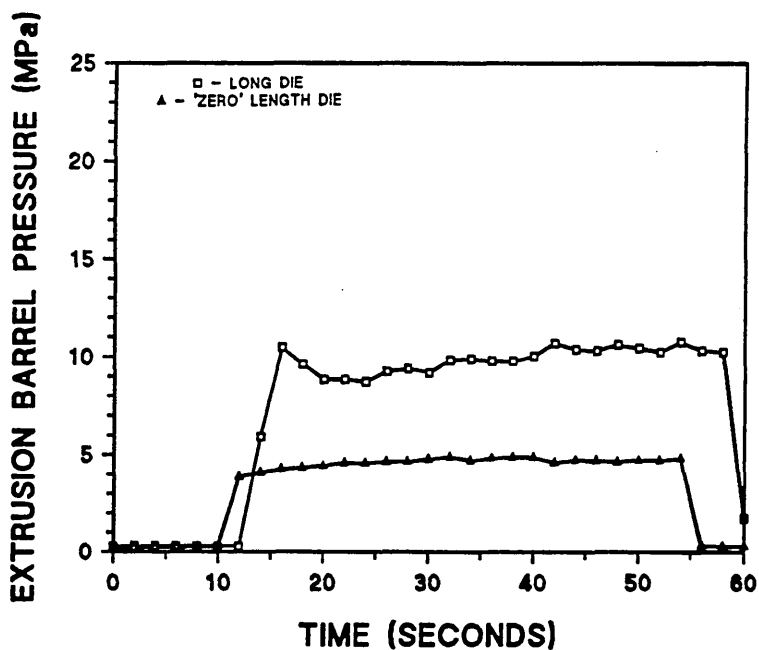


Figure 45. The variation in extrusion barrel pressure during extrusion of C-11 polyborosiloxane on the capillary rheometer at a constant ram velocity of 20 cm/min at 30°C using dies of 2mm internal diameter and both nominally zero (orifice die) and 40mm long (section 4.6.2).

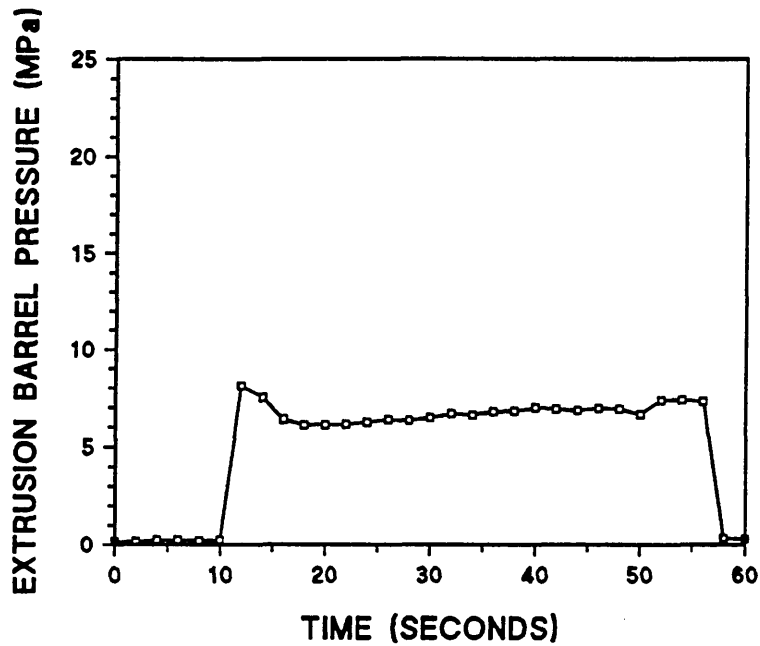


Figure 46. The variation in extrusion barrel pressure during extrusion of C-11 polyborosiloxane on the capillary rheometer at a constant ram velocity of 20 cm/min at 30°C using a die of 2mm internal diameter and 20mm long (section 4.6.2).

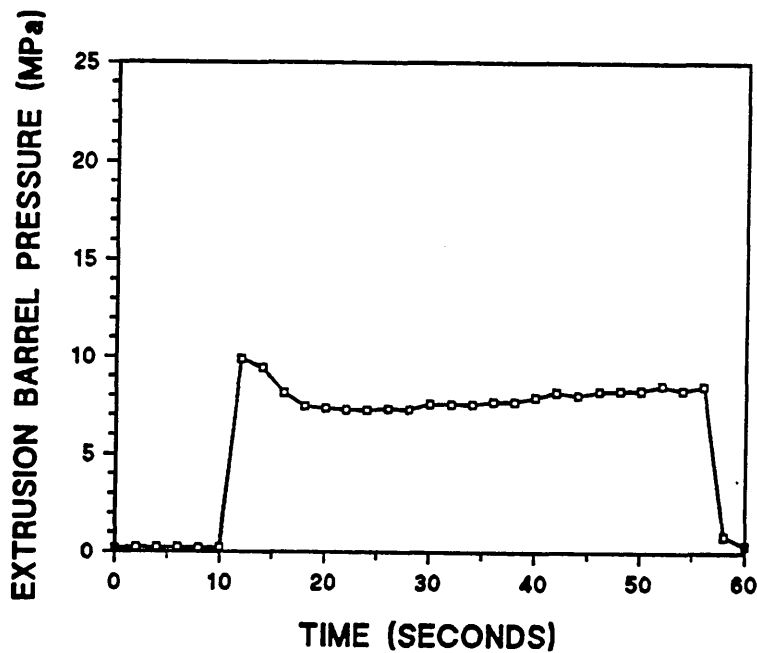


Figure 47. The variation in extrusion barrel pressure during extrusion of C-11 polyborosiloxane on the capillary rheometer at a constant ram velocity of 20 cm/min at 30°C using a die of 2mm internal diameter and 30mm long (section 4.6.2).

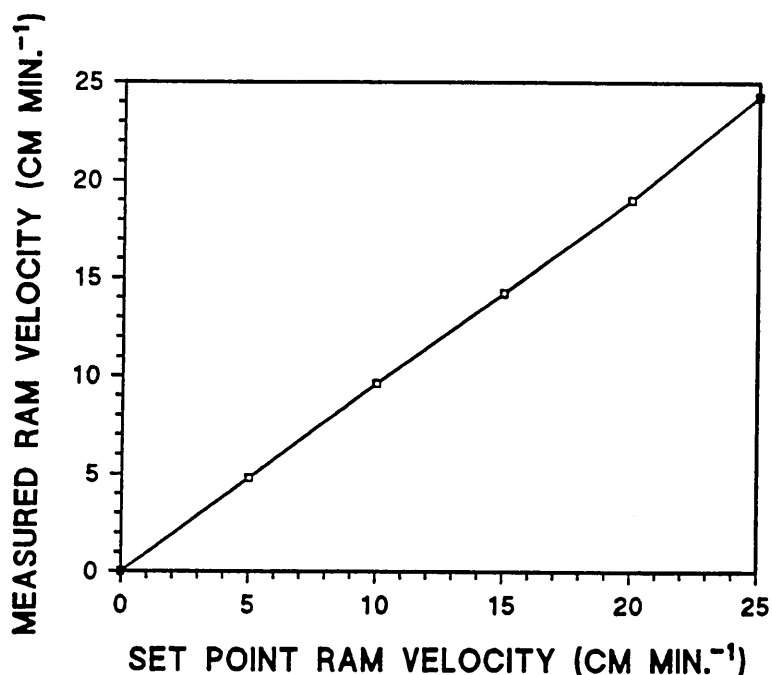


Figure 48. The extrusion ram velocity on the capillary rheometer as measured by the additional instrumentation described in section 3.2.6 against that indicated on the dial gauge on the rheometer control panel (set point).

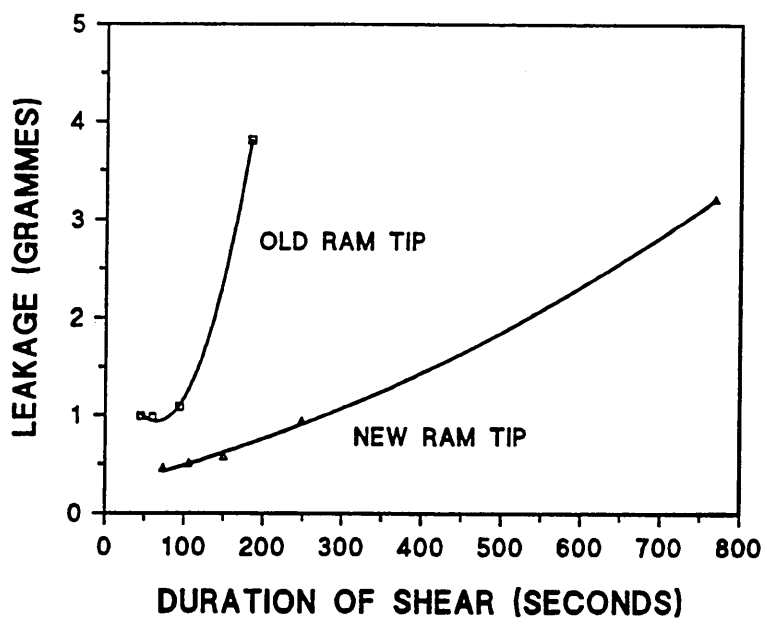


Figure 49. The relationship between the quantity (mass) of C-11 polyborosiloxane leakage between the capillary rheometer ram and extrusion barrel with the duration of extrusion for the original extrusion ram and the new extrusion ram fitted during the course of the research programme (section 3.2.4).

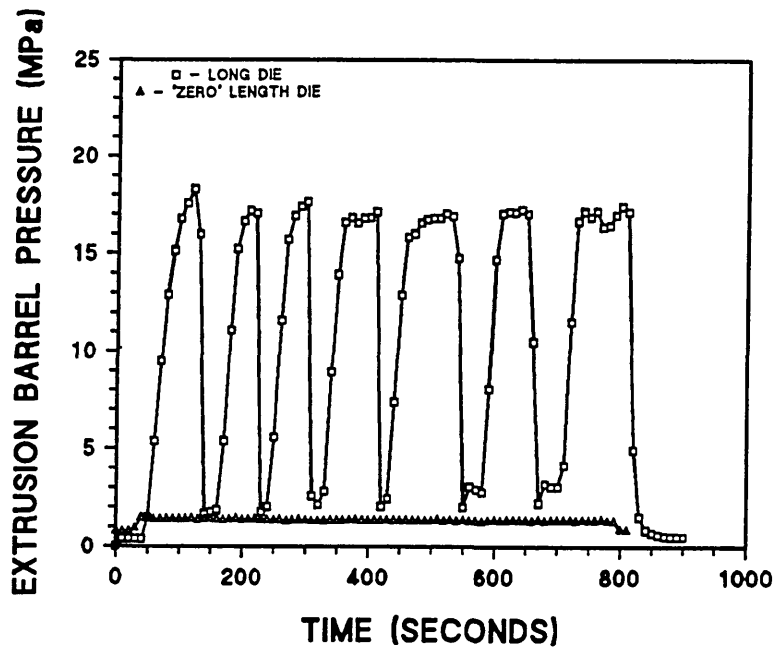


Figure 50. The variation in extrusion barrel pressure during extrusion of C-11 polyborosiloxane on the capillary rheometer at a constant ram velocity of 1.58 cm/min at 30°C using dies of 2mm internal diameter and both nominally zero (orifice die) and 40mm long (section 4.6.2).

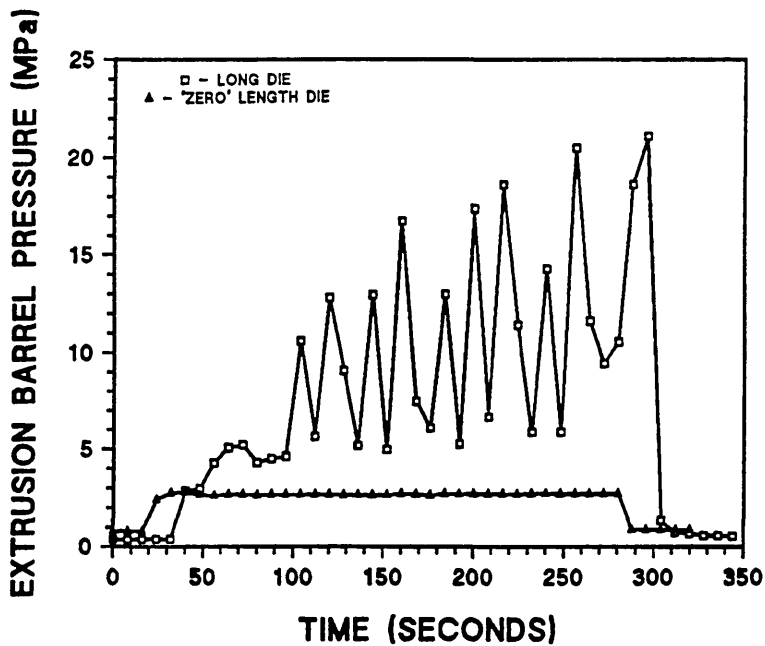


Figure 51. The variation in extrusion barrel pressure during extrusion of C-11 polyborosiloxane on the capillary rheometer at a constant ram velocity of 4.65 cm/min at 30°C using dies of 2mm internal diameter and both nominally zero (orifice die) and 40mm long (section 4.6.2).

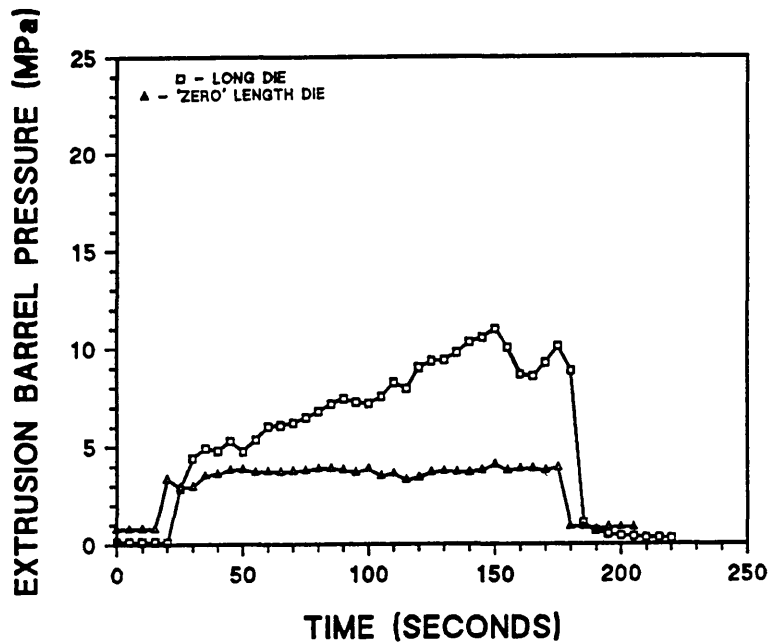


Figure 52. The variation in extrusion barrel pressure during extrusion of C-11 polyborosiloxane on the capillary rheometer at a constant ram velocity of 7.68 cm/min at 30°C using dies of 2mm internal diameter and both nominally zero (orifice die) and 40mm long (section 4.6.2).

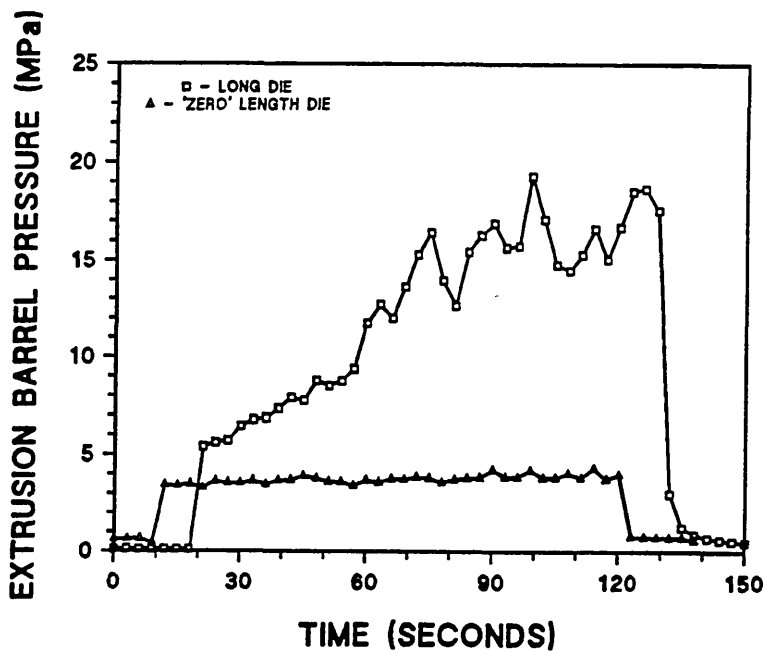


Figure 53. The variation in extrusion barrel pressure during extrusion of C-11 polyborosiloxane on the capillary rheometer at a constant ram velocity of 10.86 cm/min at 30°C using dies of 2mm internal diameter and both nominally zero (orifice die) and 40mm long (section 4.6.2).

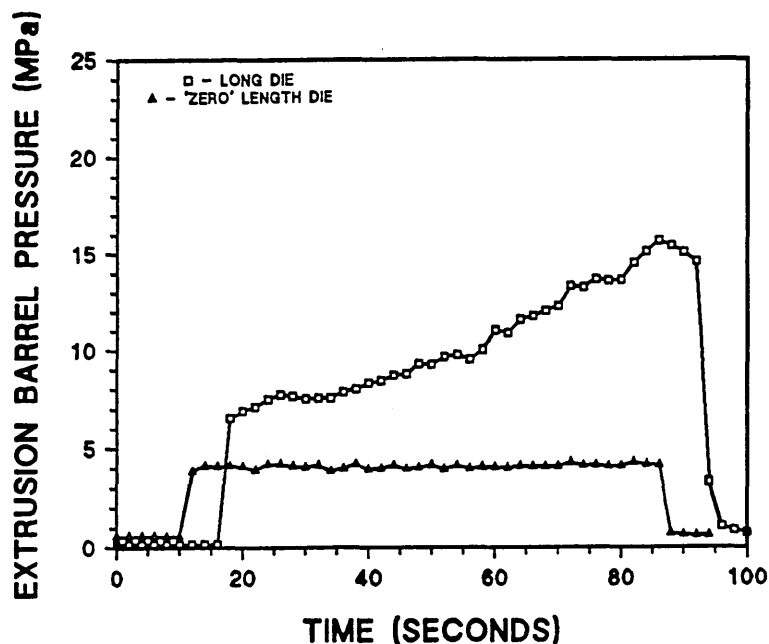


Figure 54. The variation in extrusion barrel pressure during extrusion of C-11 polyborosiloxane on the capillary rheometer at a constant ram velocity of 15.67 cm/min at 30°C using dies of 2mm internal diameter and both nominally zero (orifice die) and 40mm long (section 4.6.2).

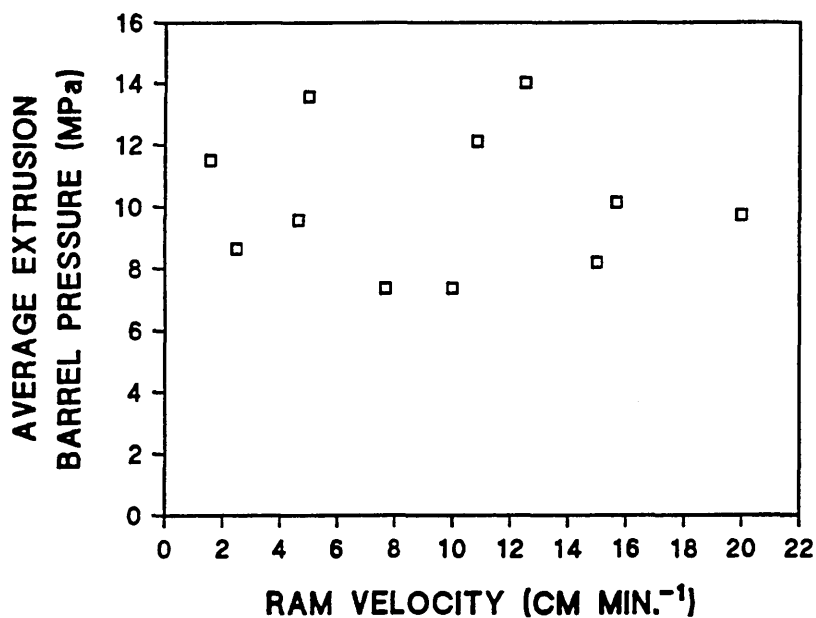


Figure 55. Average extrusion barrel pressure against ram velocity for C-11 polyborosiloxane extruded at constant ram velocity at 30°C on the capillary rheometer through a die 40 mm long with a 2mm internal diameter. All results prior to the introduction of the constant charging procedure described in section 3.2.7.

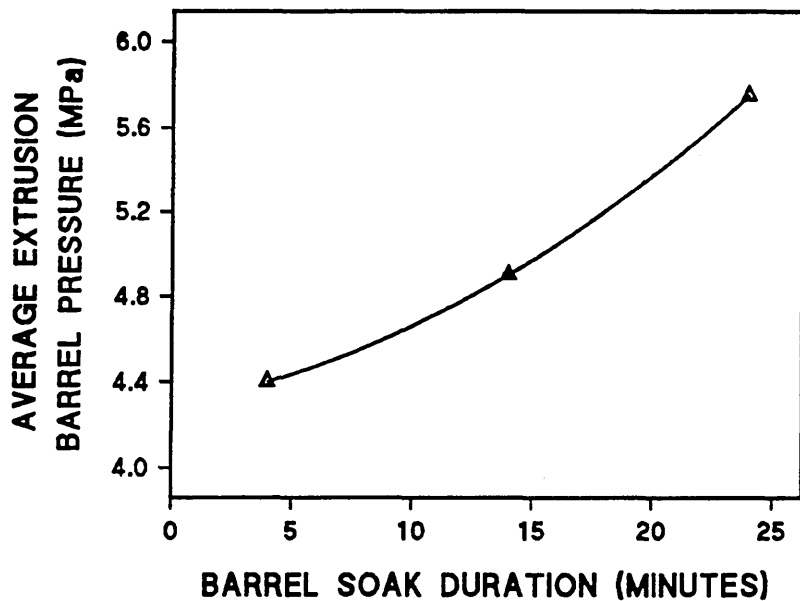


Figure 56. The relationship between the average barrel pressure during extrusion on the capillary rheometer and the time between charging the C-11 polyborosiloxane to the rheometer barrel and commencing extrusion (section 4.6.2.).

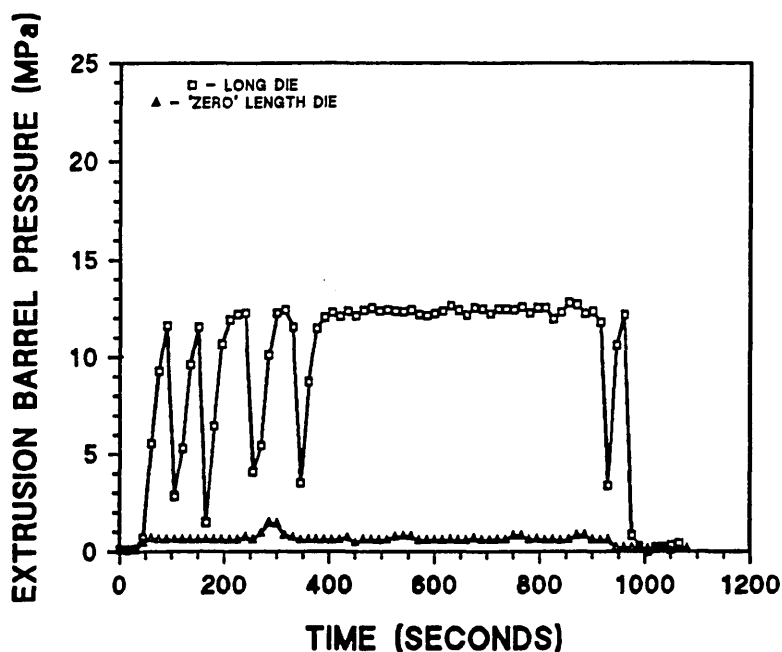


Figure 57. The variation in extrusion barrel pressure during extrusion of C-11 polyborosiloxane on the capillary rheometer at a constant ram velocity of 1.25 cm/min at 30°C using dies of 2mm internal diameter and both nominally zero (orifice die) and 40mm long (section 4.6.2).

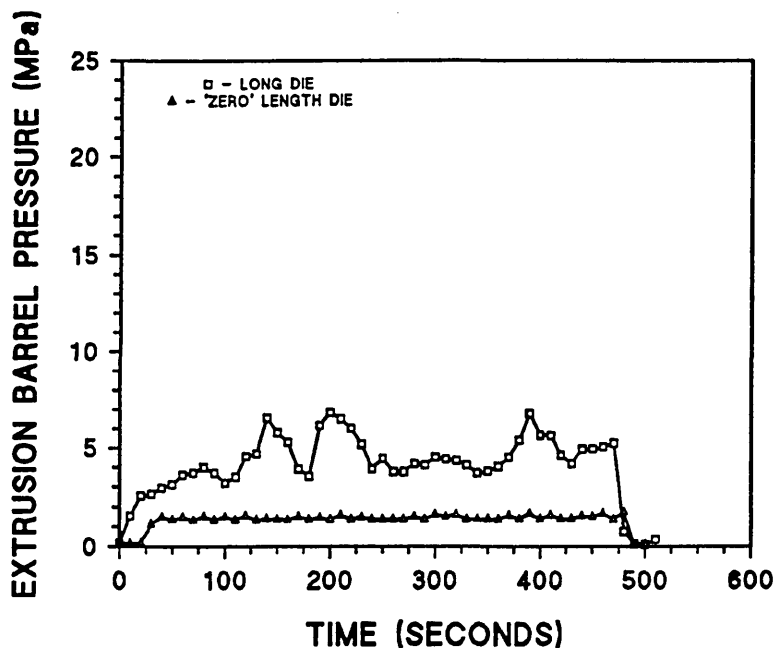


Figure 58. The variation in extrusion barrel pressure during extrusion of C-11 polyborosiloxane on the capillary rheometer at a constant ram velocity of 2.5 cm/min at 30°C using dies of 2mm internal diameter and both nominally zero (orifice die) and 40mm long (section 4.6.2).

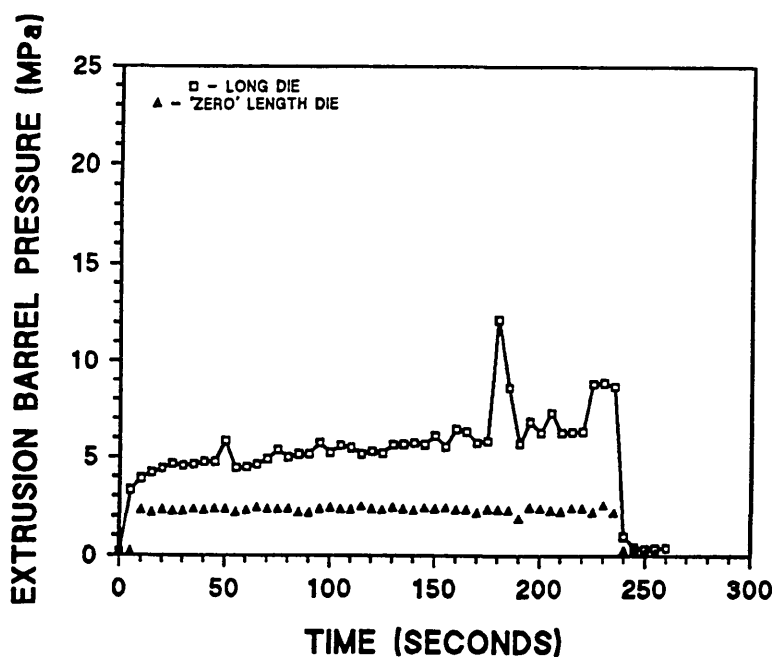


Figure 59. The variation in extrusion barrel pressure during extrusion of C-11 polyborosiloxane on the capillary rheometer at a constant ram velocity of 5 cm/min at 30°C using dies of 2mm internal diameter and both nominally zero (orifice die) and 40mm long (section 4.6.2).

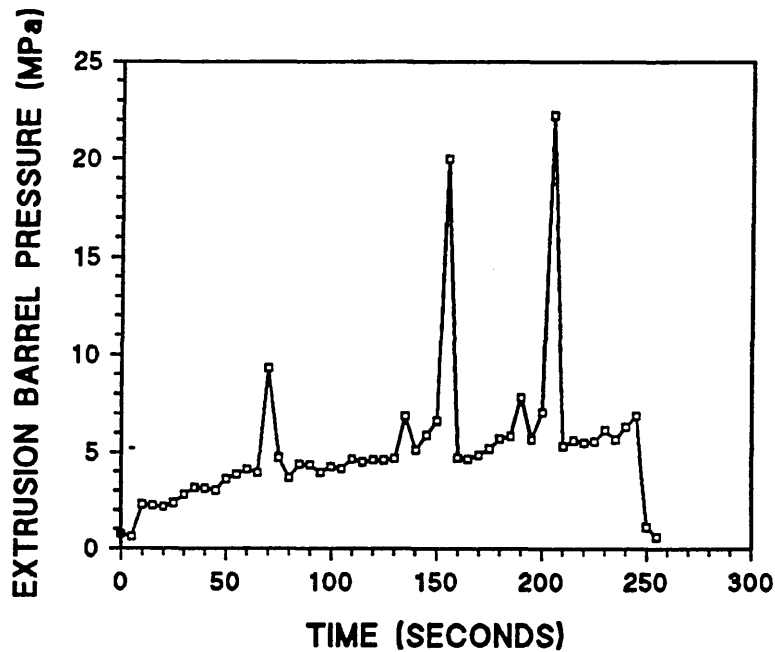


Figure 60. The variation in extrusion barrel pressure during extrusion of C-11 polyborosiloxane on the capillary rheometer at a constant ram velocity of 5 cm/min at 30°C using dies of 2mm internal diameter and both nominally zero (orifice die) and 40mm long (section 4.6.2).

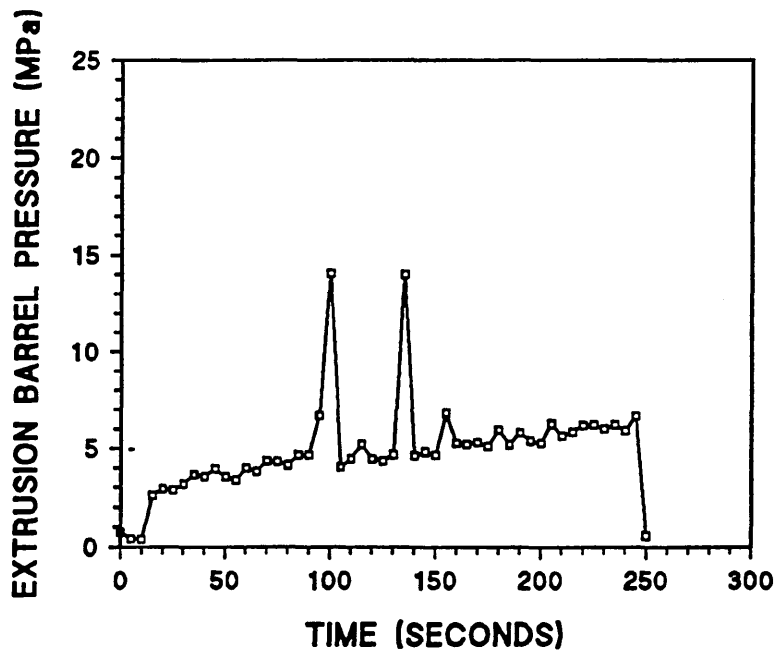


Figure 61. The variation in extrusion barrel pressure during extrusion of C-11 polyborosiloxane on the capillary rheometer at a constant ram velocity of 5 cm/min at 30°C using dies of 2mm internal diameter and both nominally zero (orifice die) and 40mm long (section 4.6.2).

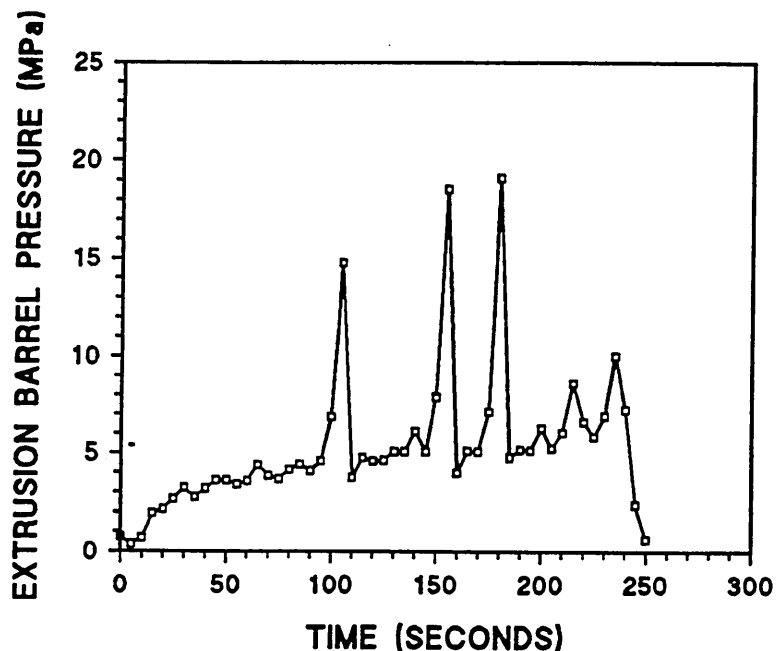


Figure 62. The variation in extrusion barrel pressure during extrusion of C-11 polyborosiloxane on the capillary rheometer at a constant ram velocity of 5 cm/min at 30°C using dies of 2mm internal diameter and both nominally zero (orifice die) and 40mm long (section 4.6.2).

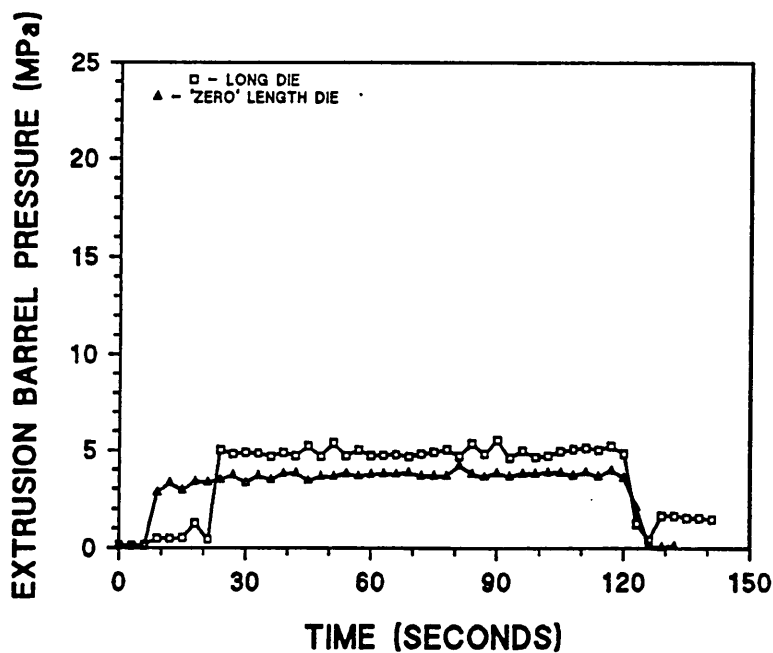


Figure 63. The variation in extrusion barrel pressure during extrusion of C-11 polyborosiloxane on the capillary rheometer at a constant ram velocity of 10 cm/min at 30°C using dies of 2mm internal diameter and both nominally zero (orifice die) and 40mm long (section 4.6.2).

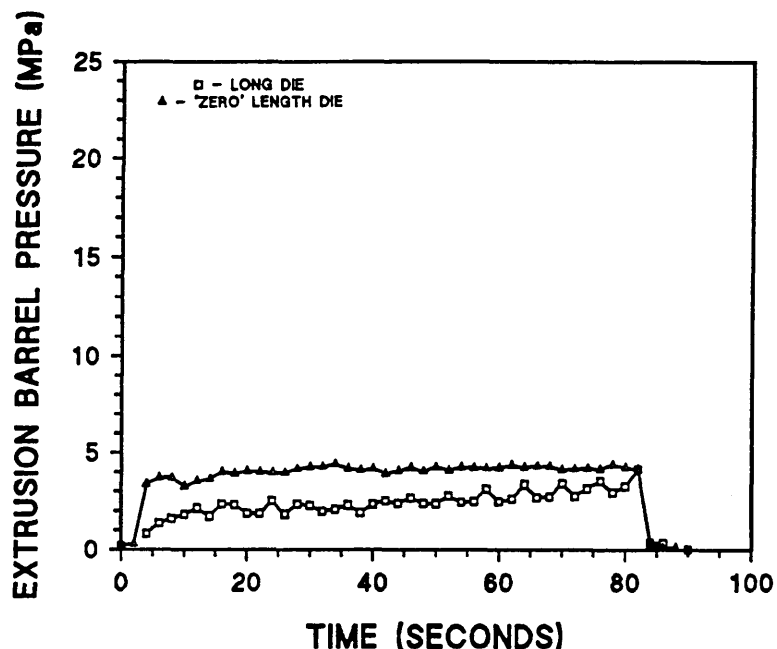


Figure 64. The variation in extrusion barrel pressure during extrusion of C-11 polyborosiloxane on the capillary rheometer at a constant ram velocity of 15 cm/min at 30°C using dies of 2mm internal diameter and both nominally zero (orifice die) and 40mm long (section 4.6.2).

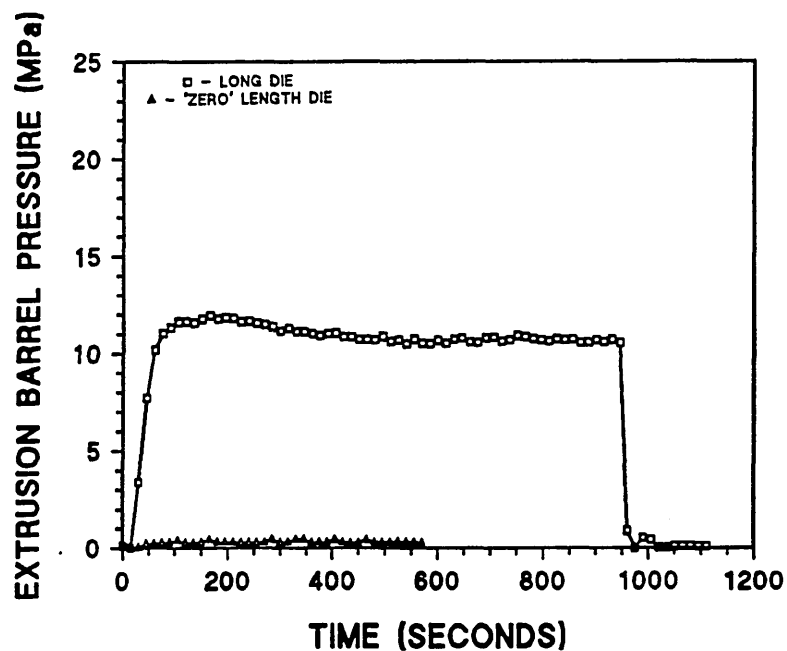


Figure 65. The variation in extrusion barrel pressure during extrusion of C-11 polyborosiloxane on the capillary rheometer at a constant ram velocity of 1.25 cm/min at 39°C using dies of 2mm internal diameter and both nominally zero (orifice die) and 40mm long (section 4.6.2).

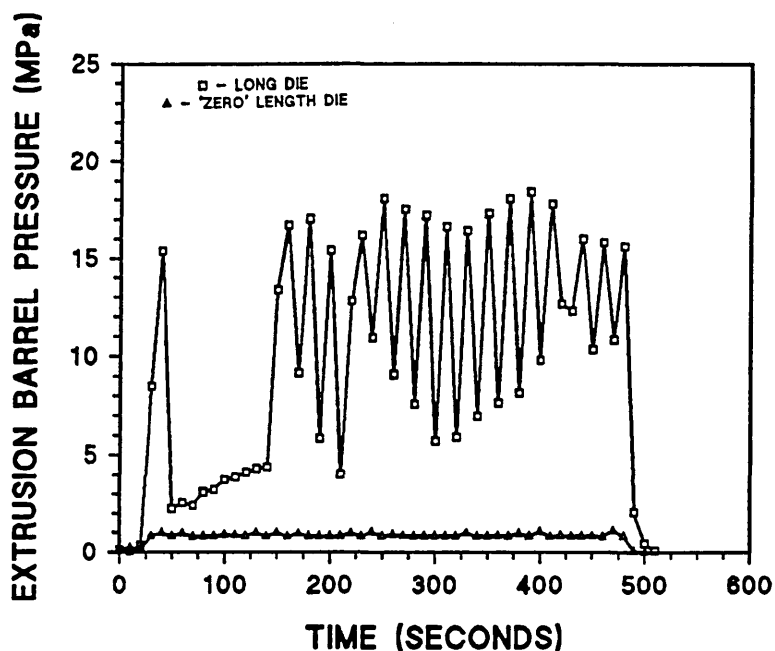


Figure 66. The variation in extrusion barrel pressure during extrusion of C-11 polyborosiloxane on the capillary rheometer at a constant ram velocity of 2.5 cm/min at 39°C using dies of 2mm internal diameter and both nominally zero (orifice die) and 40mm long (section 4.6.2).

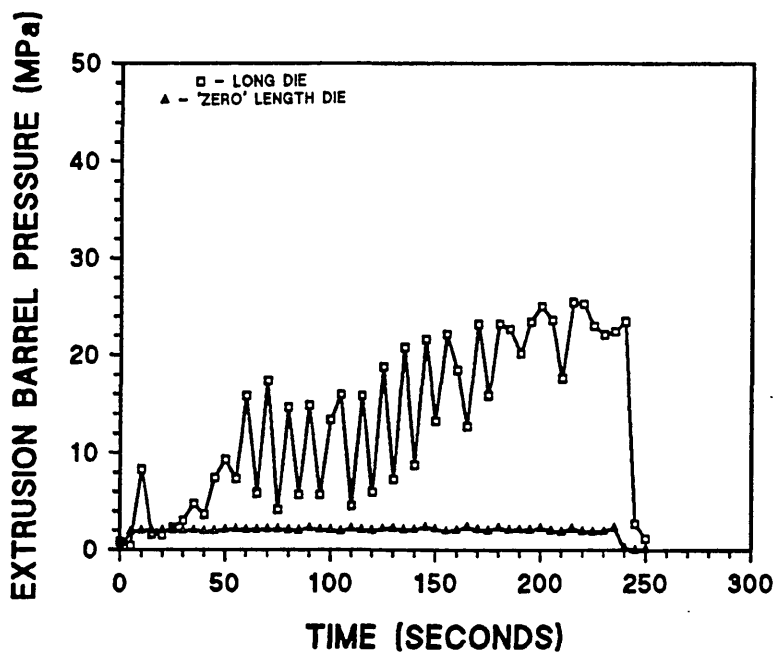


Figure 67. The variation in extrusion barrel pressure during extrusion of C-11 polyborosiloxane on the capillary rheometer at a constant ram velocity of 5 cm/min at 39°C using dies of 2mm internal diameter and both nominally zero (orifice die) and 40mm long (section 4.6.2).

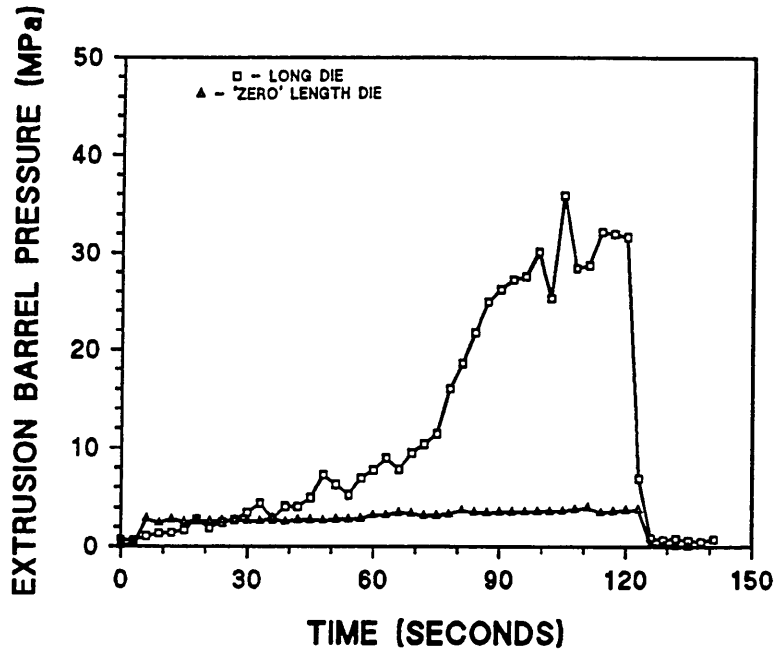


Figure 68. The variation in extrusion barrel pressure during extrusion of C-11 polyborosiloxane on the capillary rheometer at a constant ram velocity of 10 cm/min at 39°C using dies of 2mm internal diameter and both nominally zero (orifice die) and 40mm long (section 4.6.2).

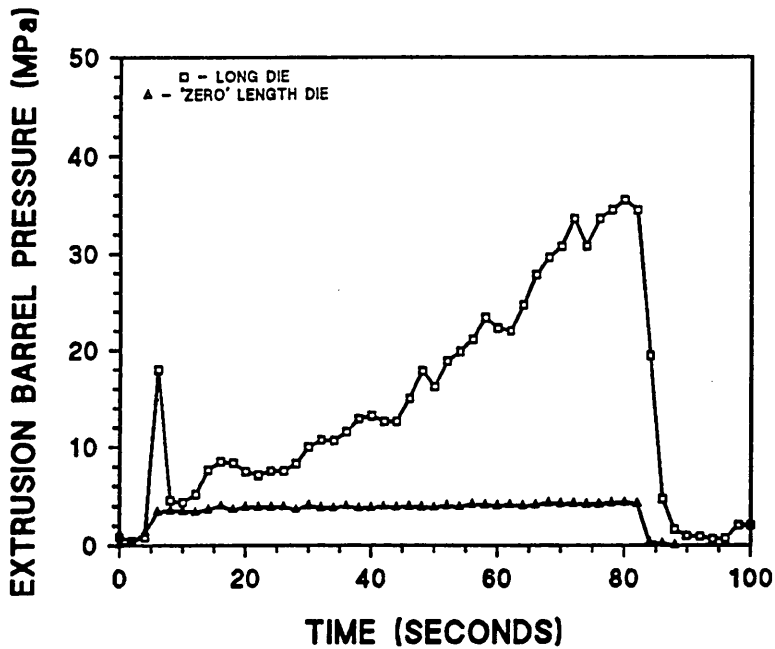


Figure 69. The variation in extrusion barrel pressure during extrusion of C-11 polyborosiloxane on the capillary rheometer at a constant ram velocity of 15 cm/min at 39°C using dies of 2mm internal diameter and both nominally zero (orifice die) and 40mm long (section 4.6.2).

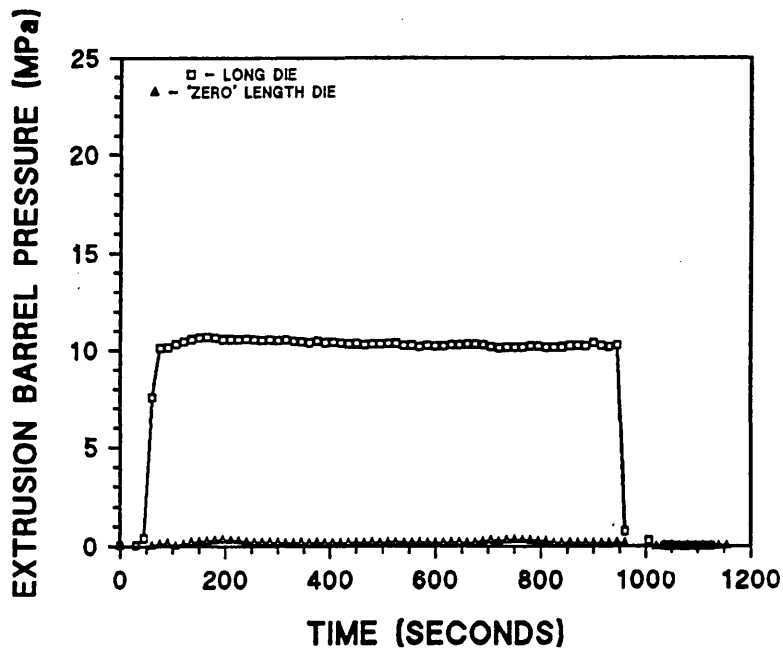


Figure 70. The variation in extrusion barrel pressure during extrusion of C-11 polyborosiloxane on the capillary rheometer at a constant ram velocity of 1.25 cm/min at 45°C using dies of 2mm internal diameter and both nominally zero (orifice die) and 40mm long (section 4.6.2).

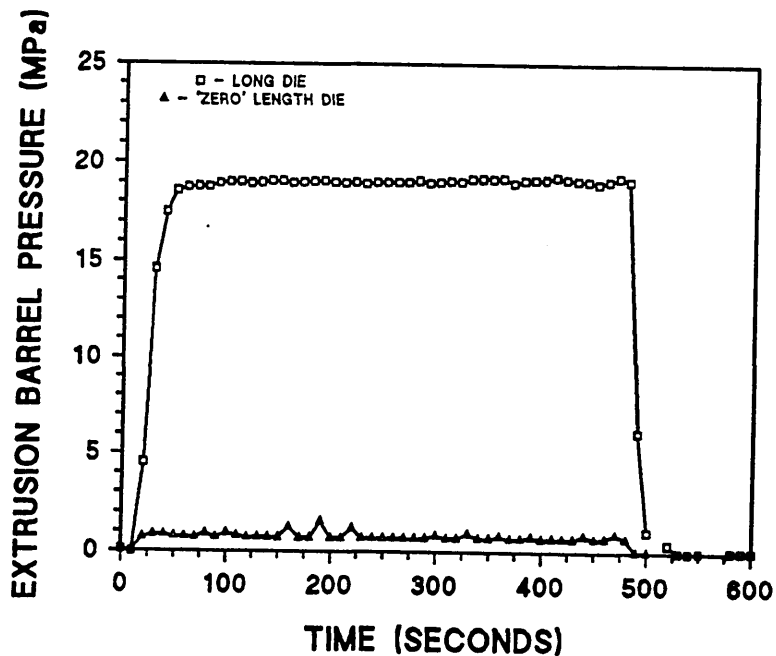


Figure 71. The variation in extrusion barrel pressure during extrusion of C-11 polyborosiloxane on the capillary rheometer at a constant ram velocity of 2.5 cm/min at 45°C using dies of 2mm internal diameter and both nominally zero (orifice die) and 40mm long (section 4.6.2).

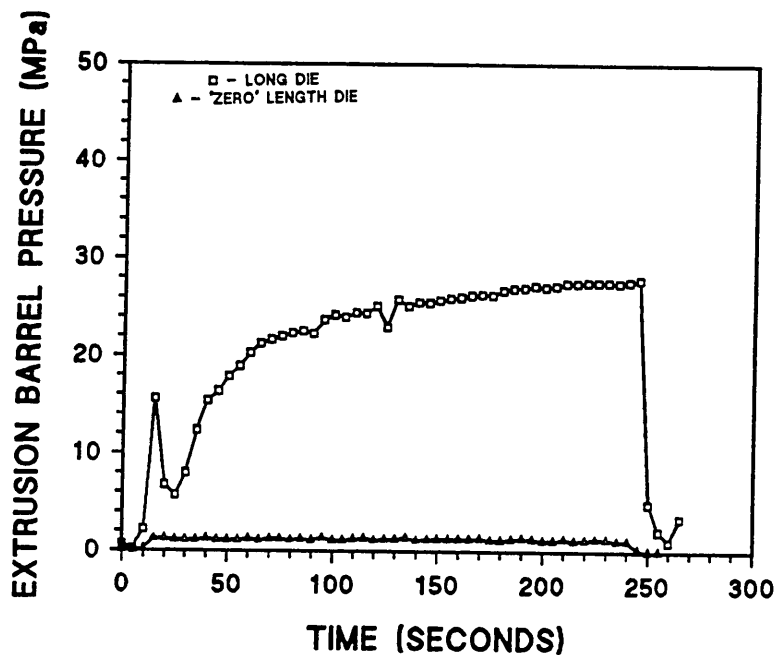


Figure 72. The variation in extrusion barrel pressure during extrusion of C-11 polyborosiloxane on the capillary rheometer at a constant ram velocity of 5 cm/min at 45°C using dies of 2mm internal diameter and both nominally zero (orifice die) and 40mm long (section 4.6.2).

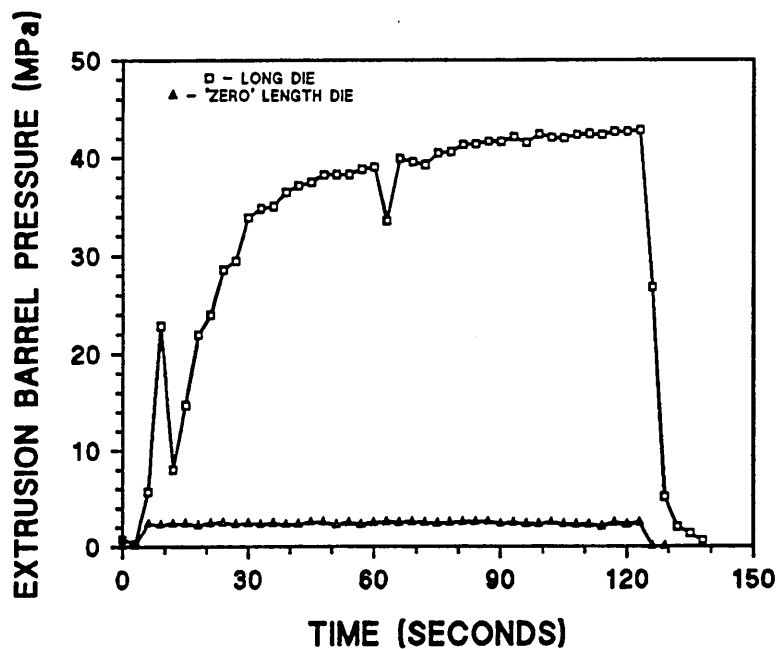


Figure 73. The variation in extrusion barrel pressure during extrusion of C-11 polyborosiloxane on the capillary rheometer at a constant ram velocity of 10 cm/min at 45°C using dies of 2mm internal diameter and both nominally zero (orifice die) and 40mm long (section 4.6.2).

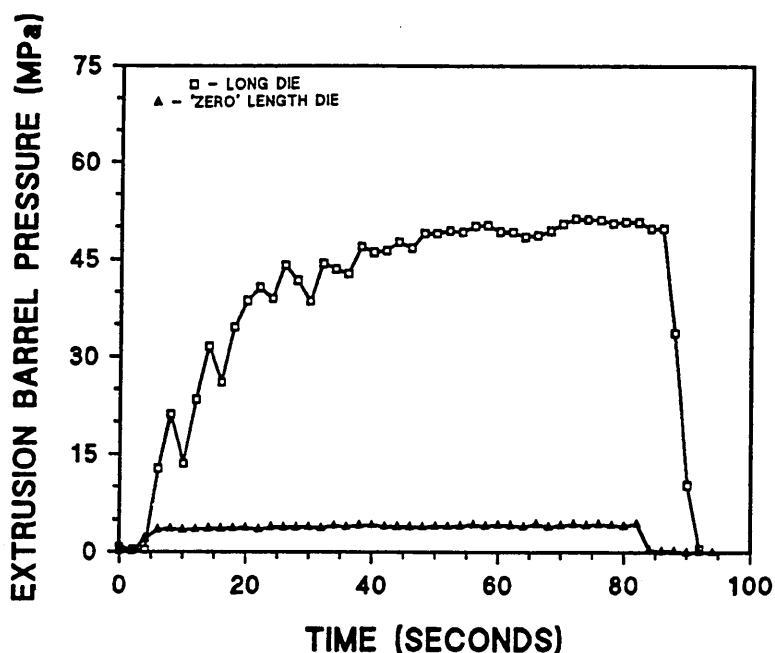


Figure 74. The variation in extrusion barrel pressure during extrusion of C-11 polyborosiloxane on the capillary rheometer at a constant ram velocity of 15 cm/min at 45°C using dies of 2mm internal diameter and both nominally zero (orifice die) and 40mm long (section 4.6.2).

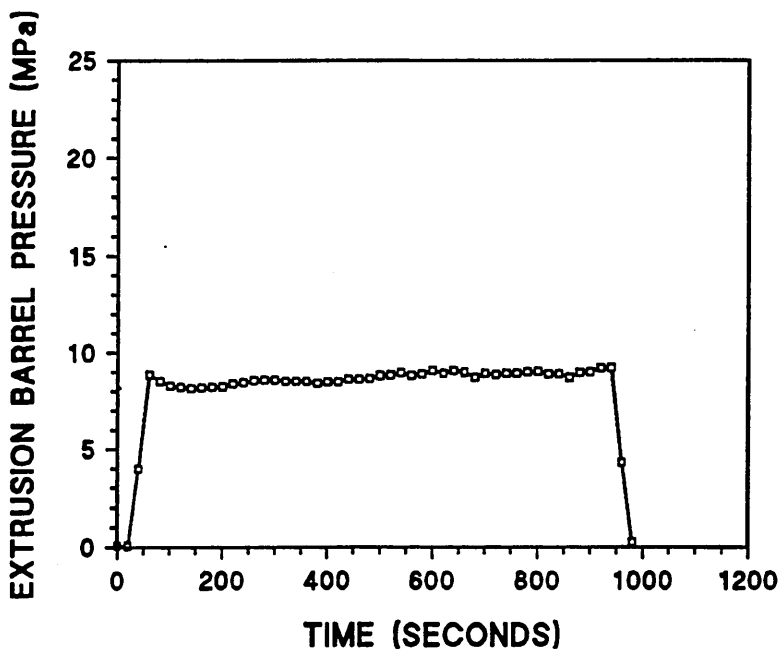


Figure 75. The variation in extrusion barrel pressure during extrusion of C-11 polyborosiloxane on the capillary rheometer at a constant ram velocity of 1.25 cm/min at 70°C using dies of 2mm internal diameter and both nominally zero (orifice die) and 40mm long (section 4.6.2).

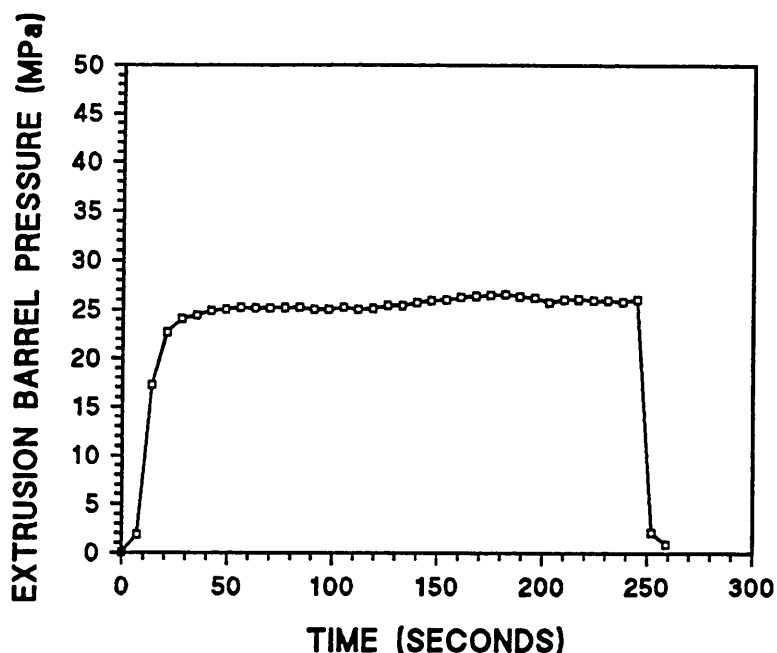


Figure 76. The variation in extrusion barrel pressure during extrusion of C-11 polyborosiloxane on the capillary rheometer at a constant ram velocity of 5 cm/min at 70°C using dies of 2mm internal diameter and both nominally zero (orifice die) and 40mm long (section 4.6.2).

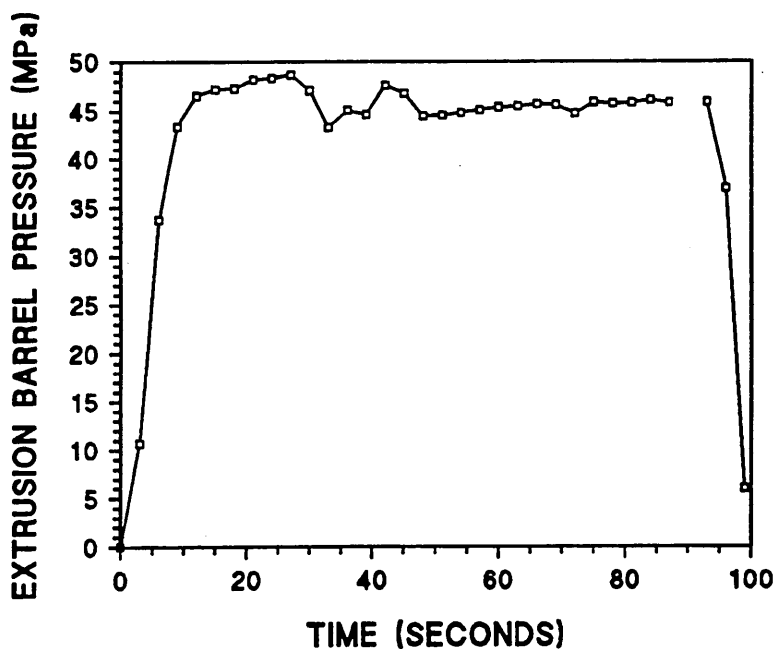


Figure 77. The variation in extrusion barrel pressure during extrusion of C-11 polyborosiloxane on the capillary rheometer at a constant ram velocity of 15 cm/min at 70°C using dies of 2mm internal diameter and both nominally zero (orifice die) and 40mm long (section 4.6.2).

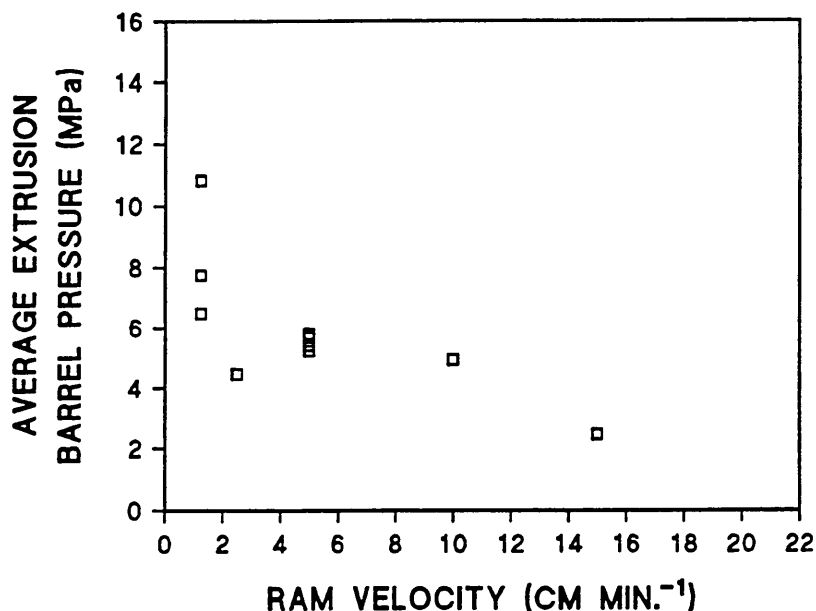


Figure 78. The average extrusion barrel pressure against the ram velocity for C-11 polyborosiloxane extruded at constant ram velocity at 30°C on the capillary rheometer through a die 40 mm long with a 2 mm internal diameter. All results are after the introduction of the constant charging procedure described in section 3.2.7.

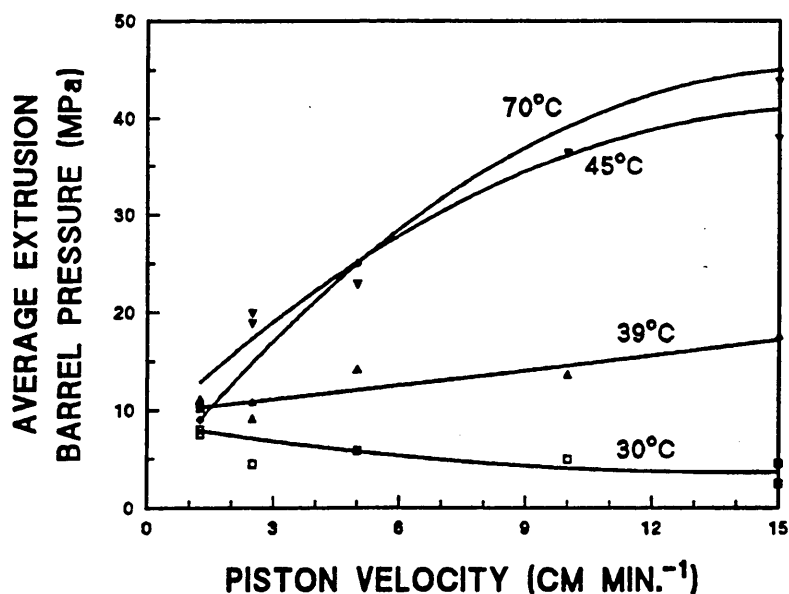


Figure 79. The relationship between average barrel pressure and the piston velocity during extrusion of C-11 polyborosiloxane on the capillary rheometer at 30°C, 39°C, 45°C and 70°C (section 4.6.3.). All results completed after the introduction of the constant charging procedure described in section 3.2.7.

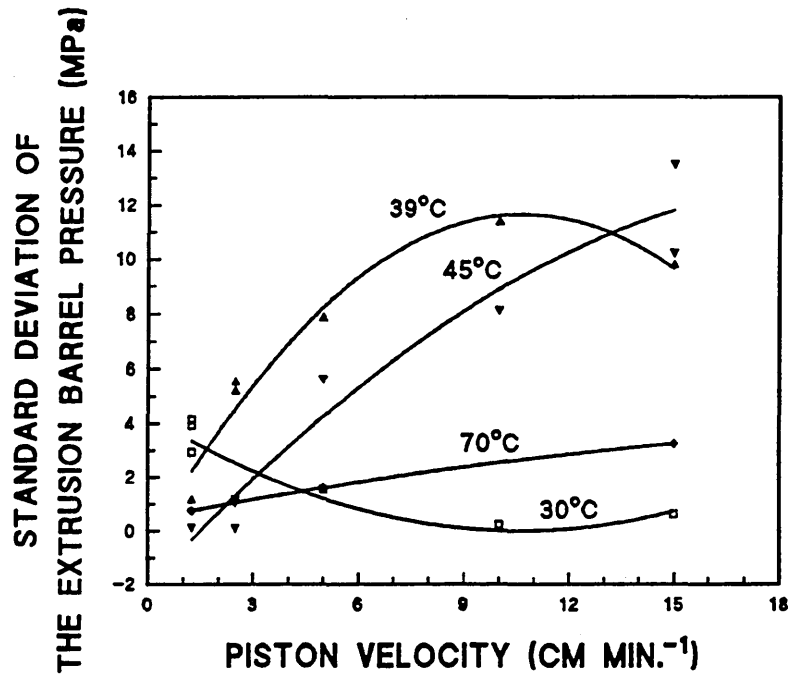


Figure 80. The relationship between the standard deviation of the barrel pressure during extrusion of C-11 polyborosiloxane on the capillary rheometer and the piston velocity at 30°C, 39°C, 45°C and 70°C (section 4.6.3.).

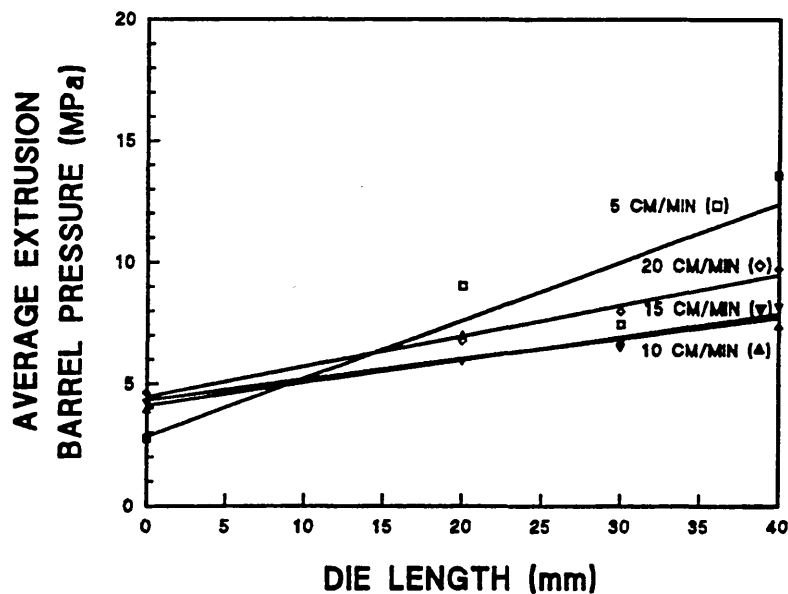


Figure 81. The relationship between average barrel pressure during extrusion of C-11 polyborosiloxane on the capillary rheometer and the extrusion die length (extrusion die diameter fixed at 2mm ) at 30°C (section 4.6.4.).

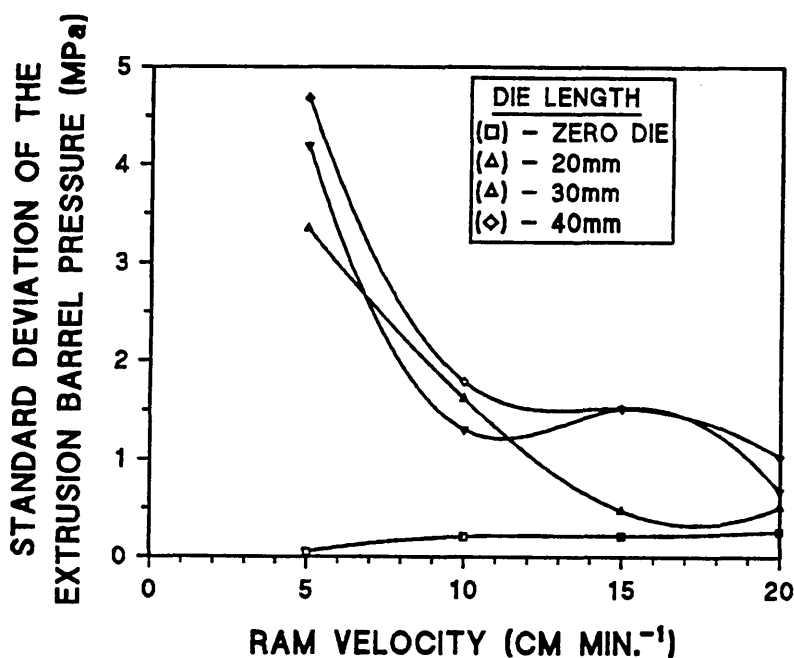


Figure 82. The relationship between the standard deviation of the barrel pressure during extrusion of C-11 polyborosiloxane on the capillary rheometer and the extrusion die length (extrusion die diameter fixed at 2mm ) at 30°C (section 4.6.4.).

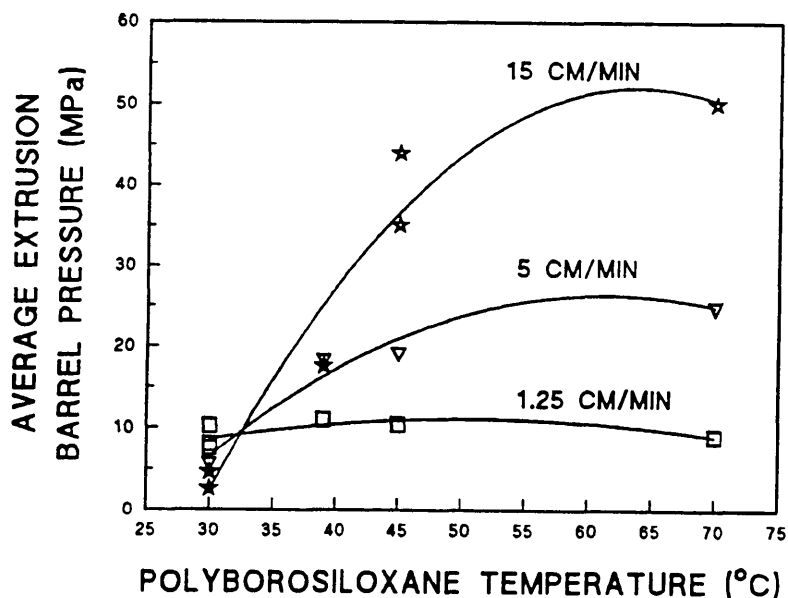


Figure 83. The relationship between average barrel pressure during extrusion of C-11 polyborosiloxane on the capillary rheometer and the barrel temperature at extrusion ram velocities of 1.25, 5 and 15 cm/min (section 4.6.5.).

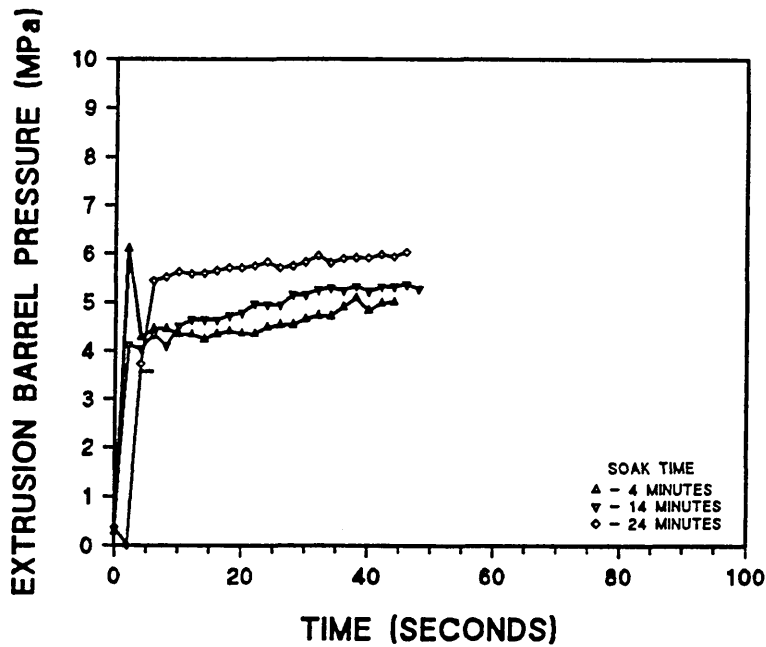


Figure 84. The variation in barrel pressure during extrusion of C-11 polyborosiloxane in the capillary rheometer at a ram velocity of 15 cm/min and a temperature of 30°C for duration of time between charging to the rheometer barrel and extrusion of 4 minutes, 14 minutes and 24 minutes (section 4.6.6.2.).

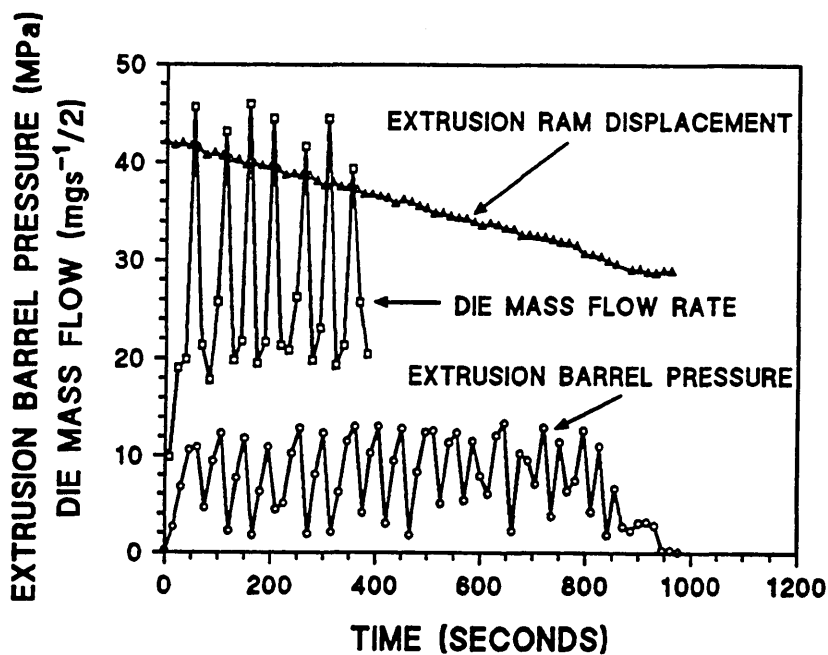


Figure 85. The variation in the extrusion barrel pressure, the ram position and the die mass flow rate during extrusion at a ram velocity of 1.25 cm/min and a temperature of 30°C on the capillary rheometer (section 4.6.7.).

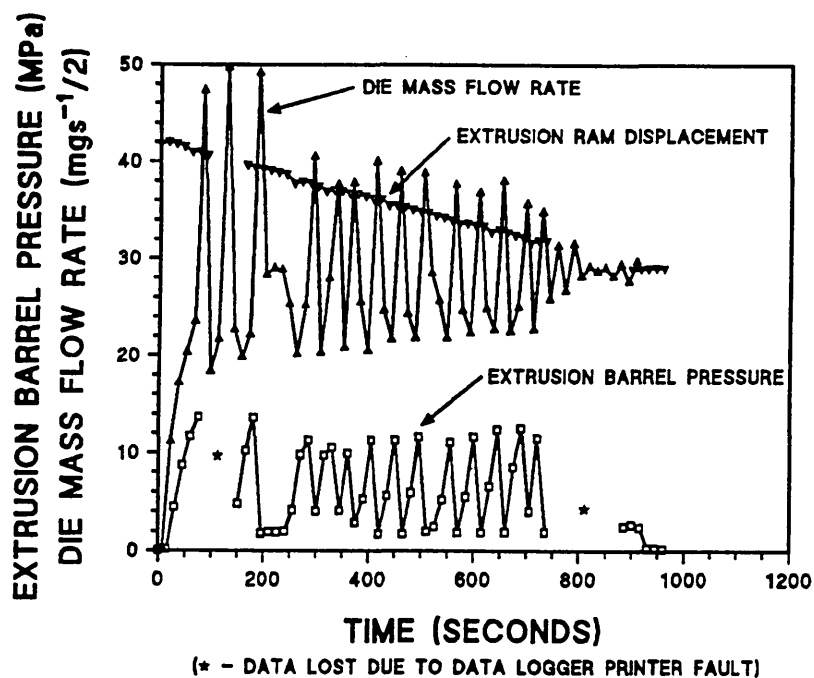


Figure 86. The variation in the extrusion barrel pressure, the ram position and the die mass flow rate during extrusion at a ram velocity of 1.25 cm/min and a temperature of 30°C on the capillary rheometer (section 4.6.7.).

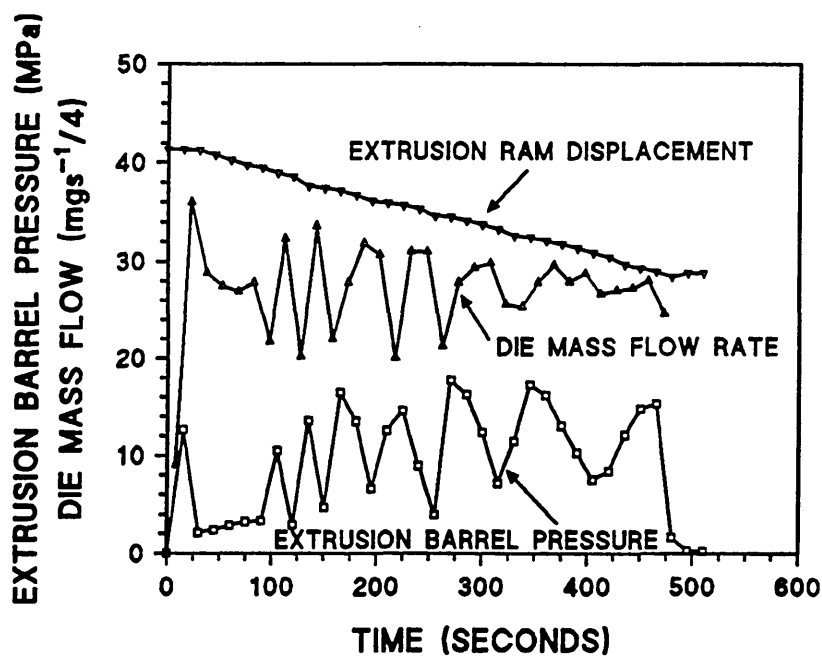


Figure 87. The variation in the extrusion barrel pressure, the ram position and the die mass flow rate during extrusion at a ram velocity of 2.5 cm/min and a temperature of 39°C on the capillary rheometer (section 4.6.7.).

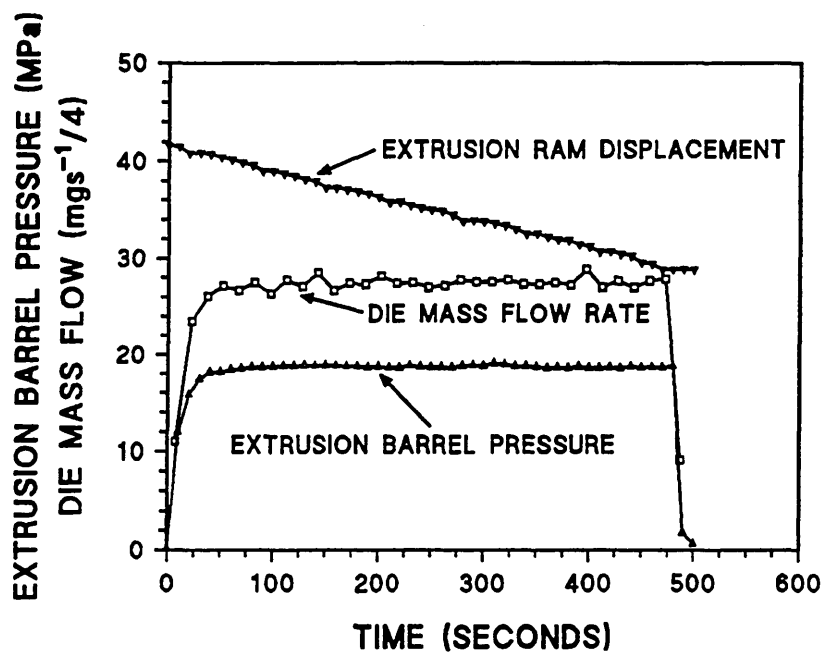


Figure 88. The variation in the extrusion barrel pressure, the ram position and the die mass flow rate during extrusion at a ram velocity of 2.5 cm/min and a temperature of 45°C on the capillary rheometer (section 4.6.7.).

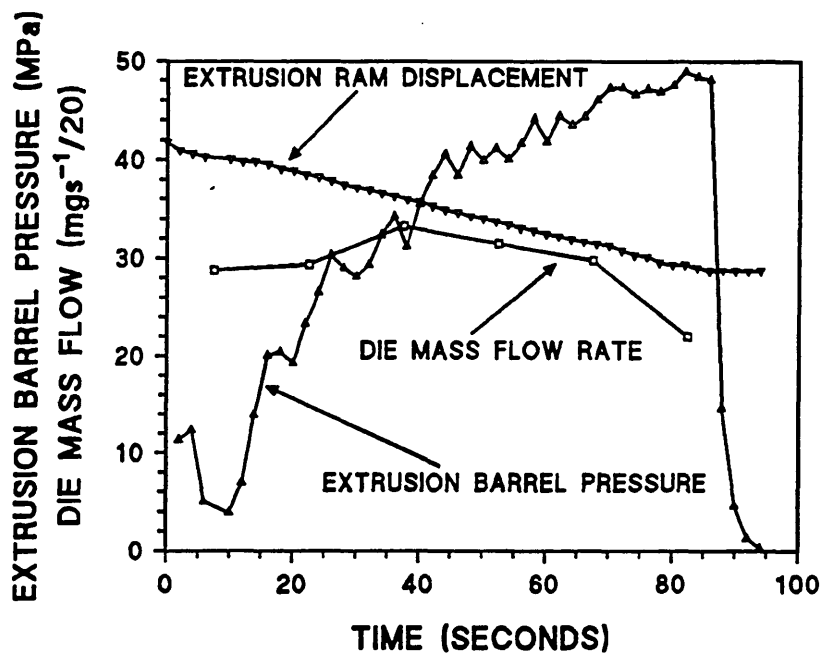


Figure 89. The variation in the extrusion barrel pressure, the ram position and the die mass flow rate during extrusion at a ram velocity of 15 cm/min and a temperature of 45°C on the capillary rheometer (section 4.6.7.).

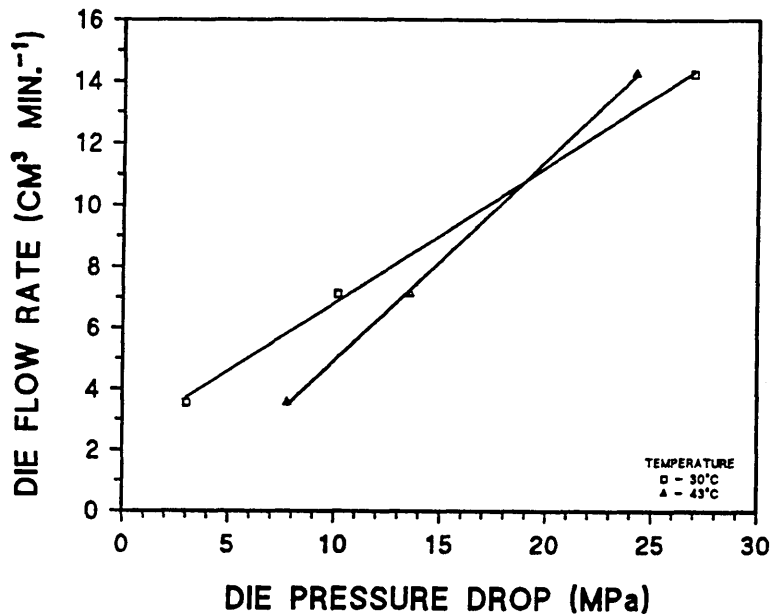


Figure 90. The variation in pressure drop down the slit die with slit die flow rate for C-11 polyborosiloxane on the slit die rheometer at 30°C and 43°C (section 4.7.2).

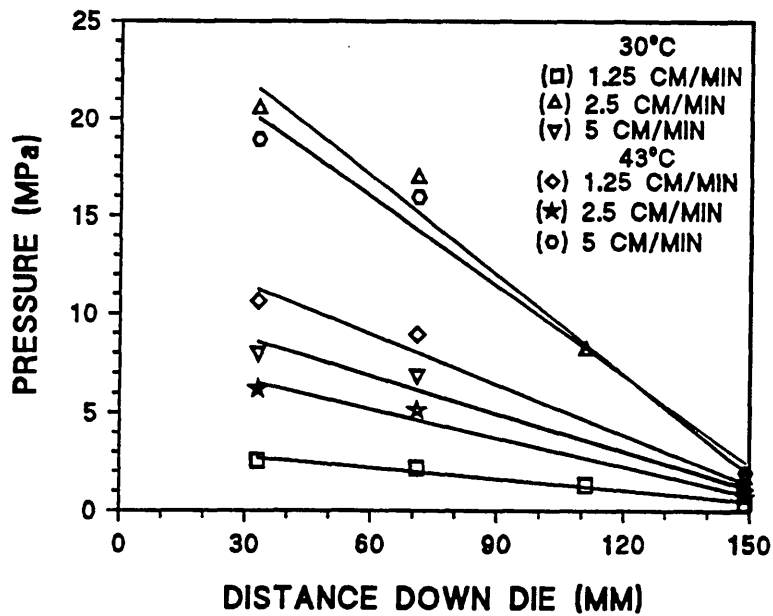


Figure 91. The variation in the average measured wall pressure down the length of the slit die during the slit die extrusion of C-11 polyborosiloxane at temperatures of 30°C and 43°C and ram velocities of 1.25, 2.5 and 5 cm/min (section 4.7.2).

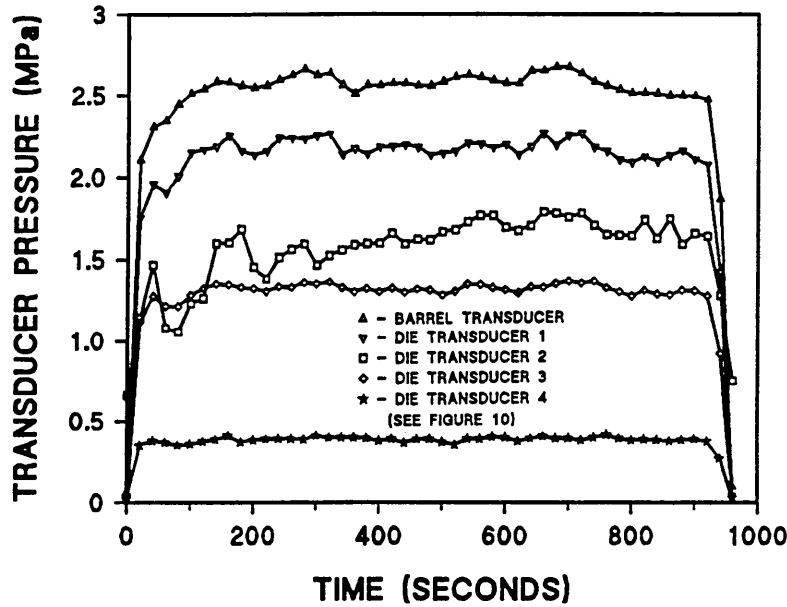


Figure 92. The variation in measured wall pressure down the length of the slit die during the extrusion of C-11 polyborosiloxane through the slit die at a temperature of 30°C and a ram velocity of 1.25 cm/min (section 4.7.2).

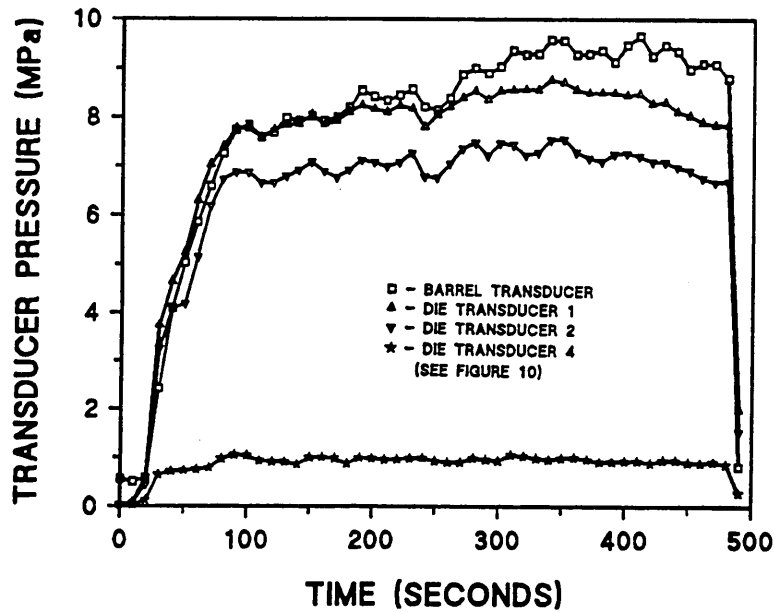


Figure 93. The variation in measured wall pressure down the length of the slit die during the extrusion of C-11 polyborosiloxane through the slit die at a temperature of 30°C and a ram velocity of 2.5 cm/min (section 4.7.2).

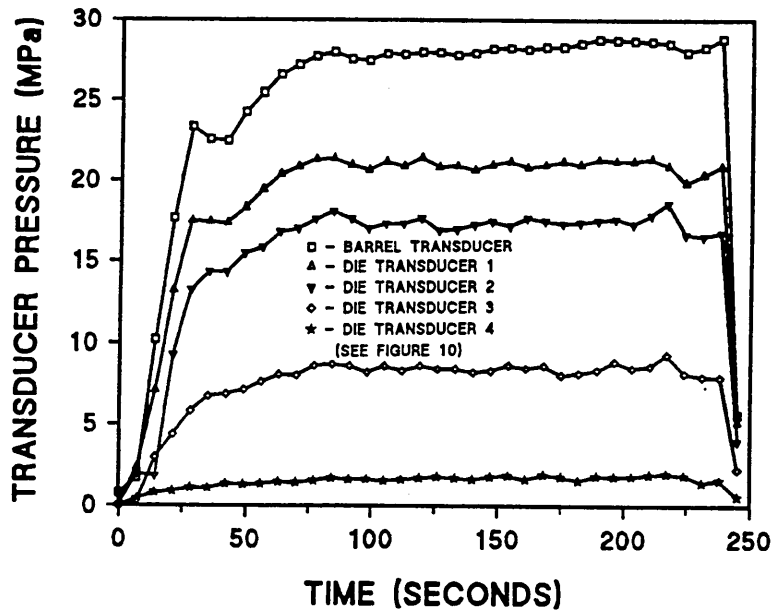


Figure 94. The variation in measured wall pressure down the length of the slit die during the extrusion of C-11 polyborosiloxane through the slit die at a temperature of 30°C and a ram velocity of 5 cm/min (section 4.7.2).

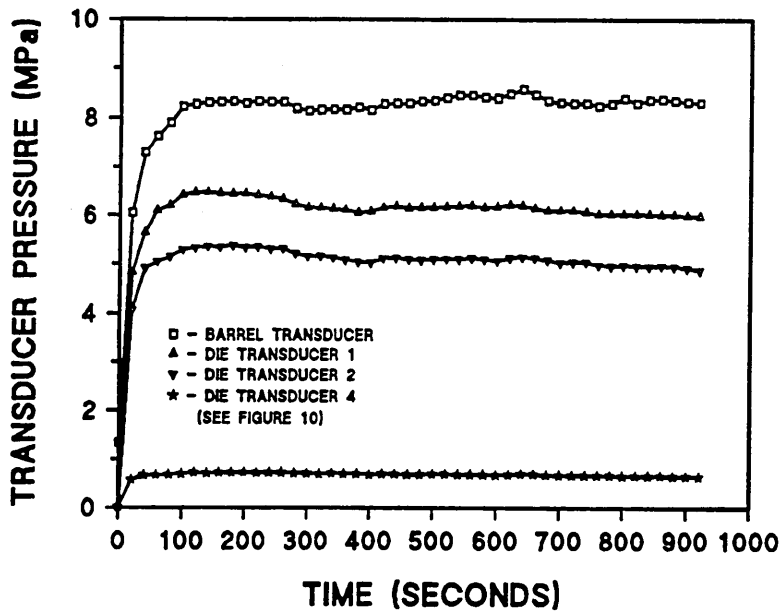


Figure 95. The variation in measured wall pressure down the length of the slit die during the extrusion of C-11 polyborosiloxane through the slit die at a temperature of 43°C and a ram velocity of 1.25 cm/min (section 4.7.2).

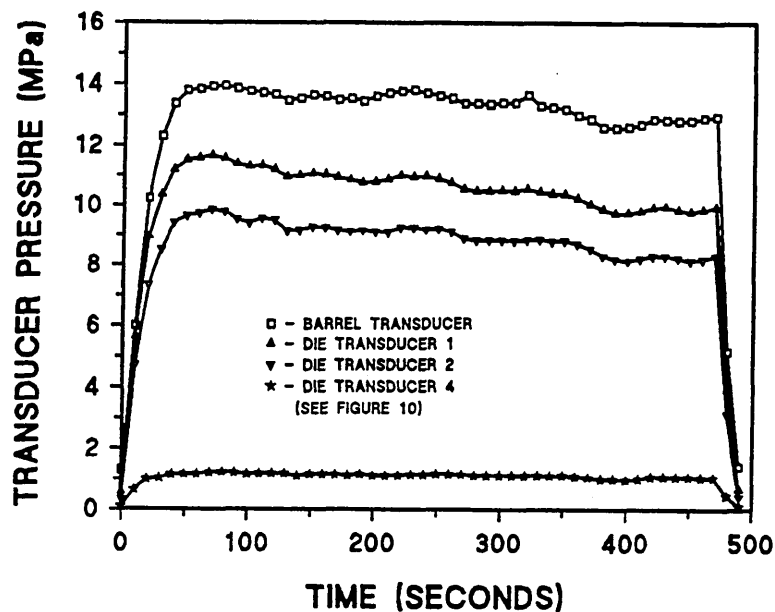


Figure 96. The variation in measured wall pressure down the length of the slit die during the extrusion of C-11 polyborosiloxane through the slit die at a temperature of 43°C and a ram velocity of 2.5 cm/min (section 4.7.2).

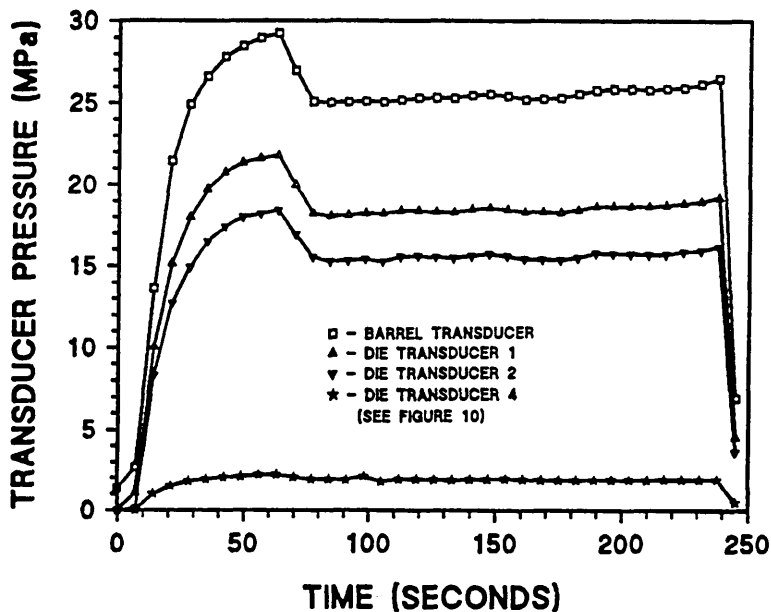


Figure 97. The variation in measured wall pressure down the length of the slit die during the extrusion of C-11 polyborosiloxane through the slit die at a temperature of 43°C and a ram velocity of 5 cm/min (section 4.7.2).

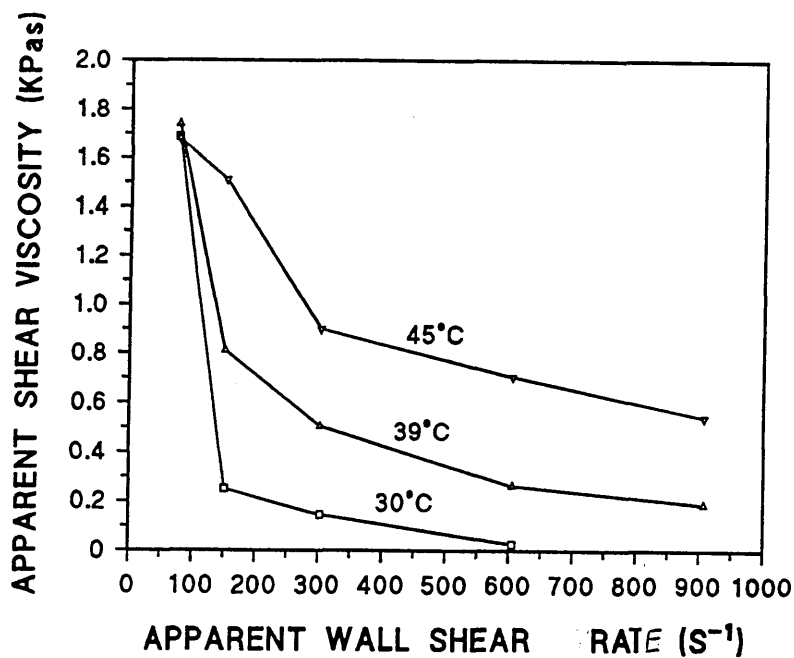


Figure 98. The variation in the apparent shear viscosity with apparent shear strain rate for C-11 polyborosiloxane at temperatures of 30°C, 39°C and 45°C as determined by capillary rheometer experiments.

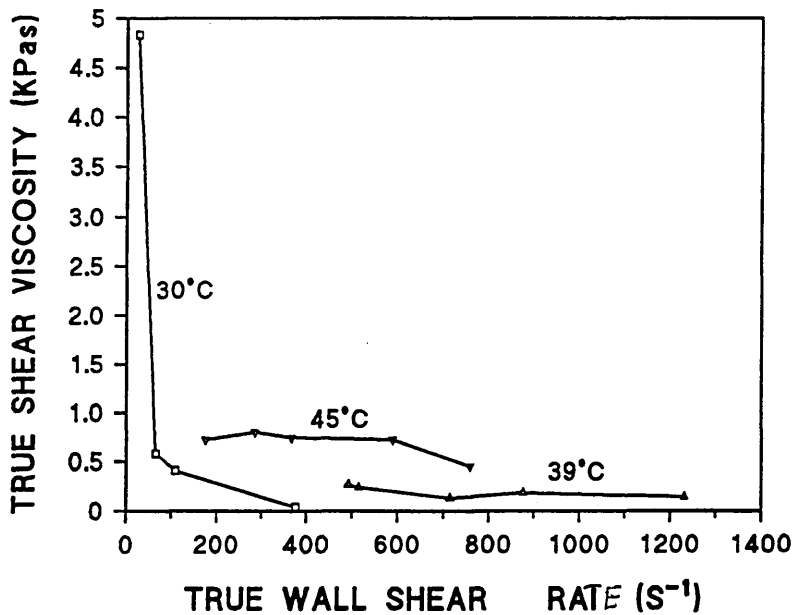


Figure 99. The variation in the shear viscosity with shear strain rate for C-11 polyborosiloxane at temperatures of 30°C, 39°C and 45°C as determined by capillary rheometer experiments (Rabinowitch [25] corrected data).

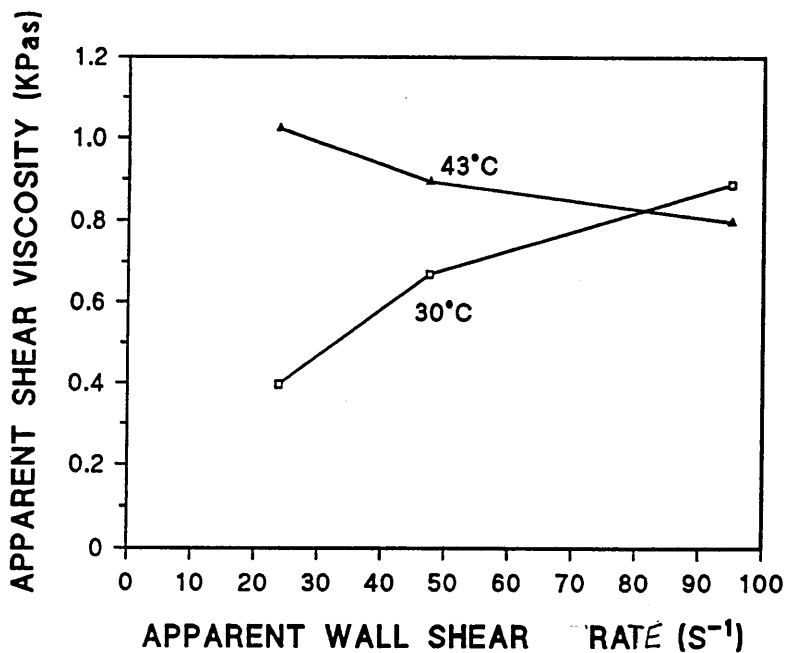


Figure 100. The variation in the apparent shear viscosity with apparent shear strain rate for C-11 polyborosiloxane at temperatures of 30°C and 43°C as determined by slit die rheometer experiments.

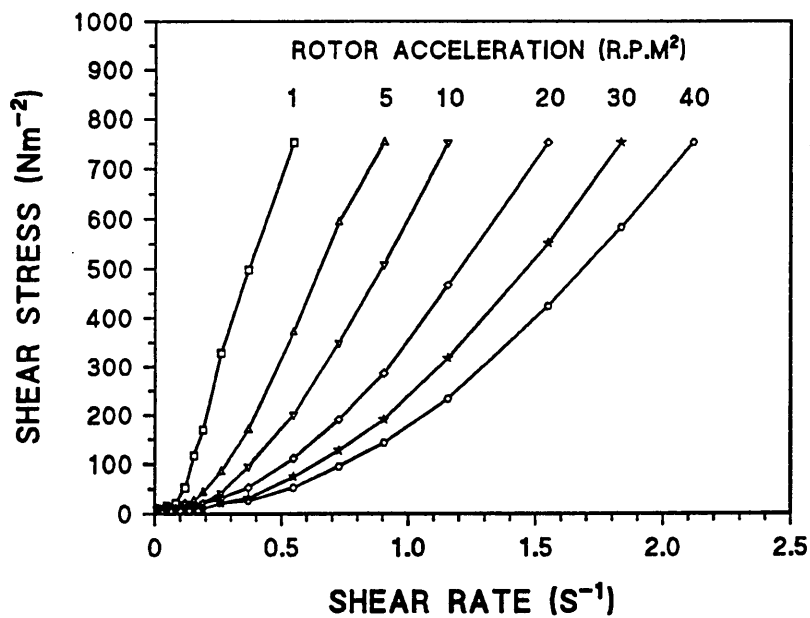


Figure 101. The variation in the shear stress with the shear rate for C-11 polyborosiloxane at 30°C as determined by the concentric cylinder rheometer for a range of rotor accelerations (section 4.8.3).

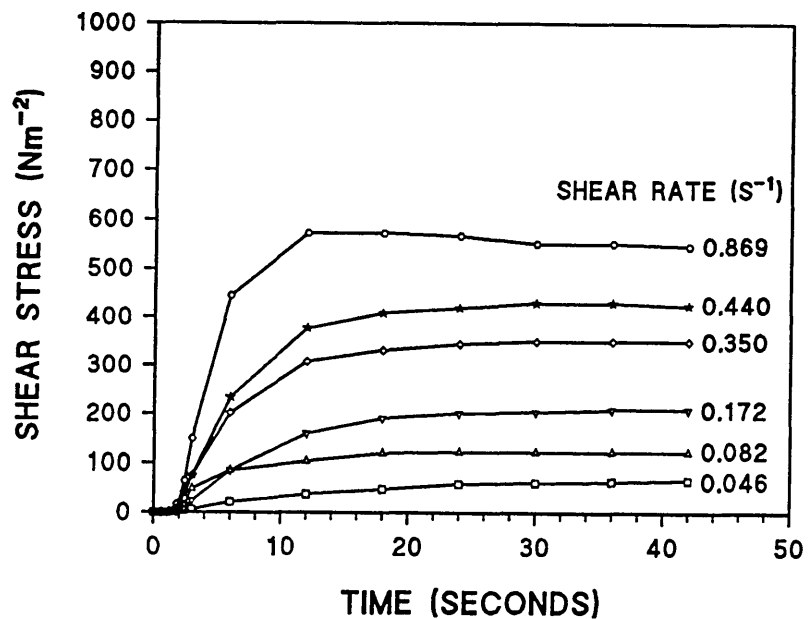


Figure 102. The variation in shear stress with duration of shear for C-11 polyborosiloxane at 30°C as determined by the concentric cylinder rheometer for a range of shear rates (section 4.8.3).

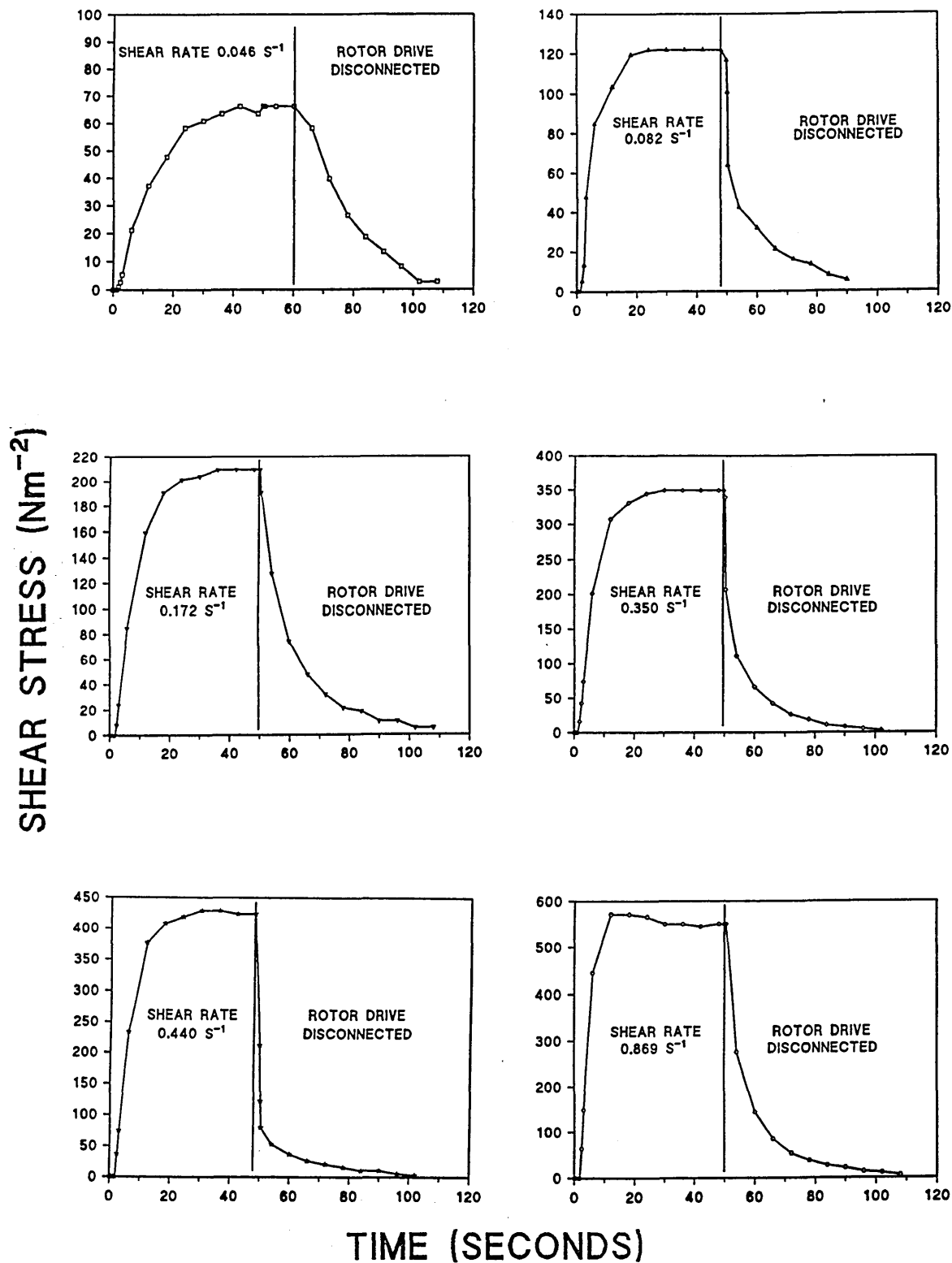


Figure 103. The variation in the measured shear stress during a period of shear followed by a period in which the rheometer drive was disconnected for C-11 polyborosiloxane at  $30^{\circ}\text{C}$  as determined by the concentric cylinder rheometer for a range of shear rates (section 4.8.3).

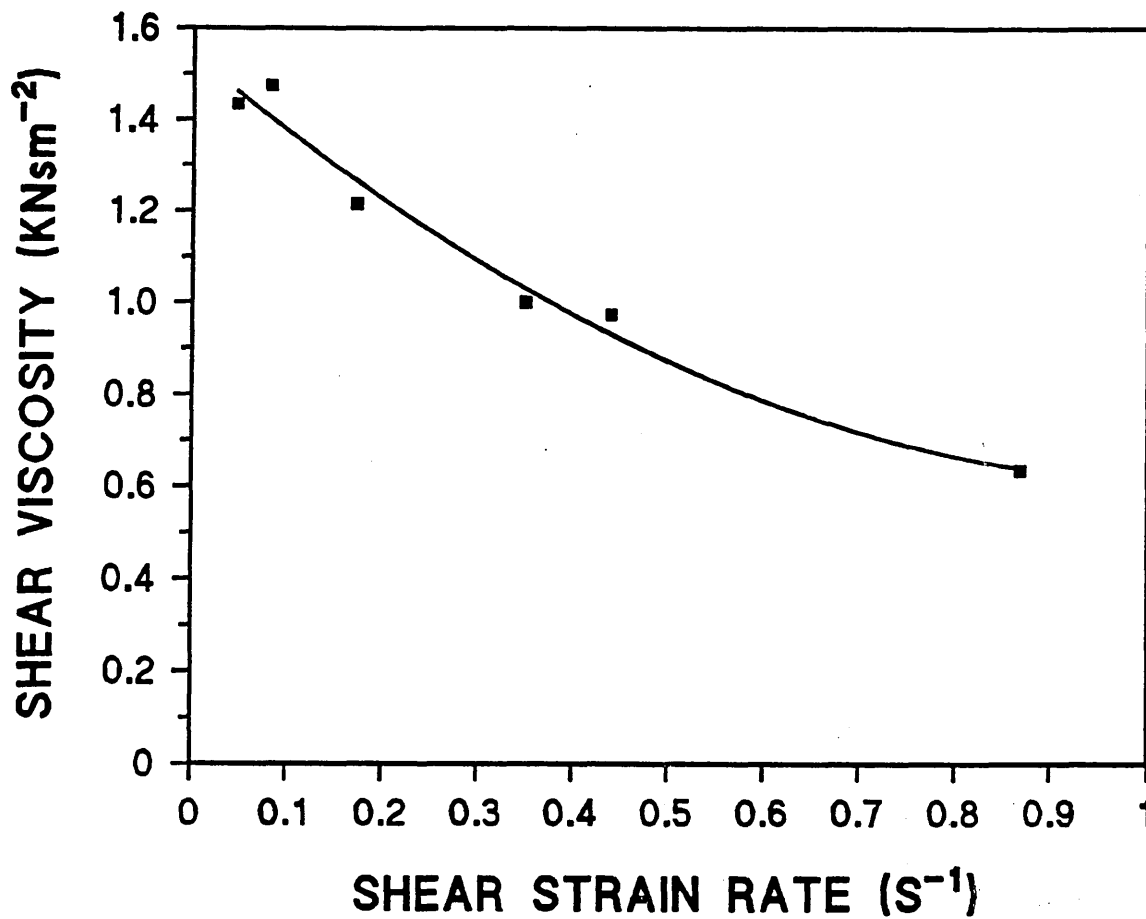


Figure 104. The variation in shear viscosity with shear strain rate for C-11 polyborosiloxane at 30°C as determined by the concentric cylinder rheometer (section 4.8.3).

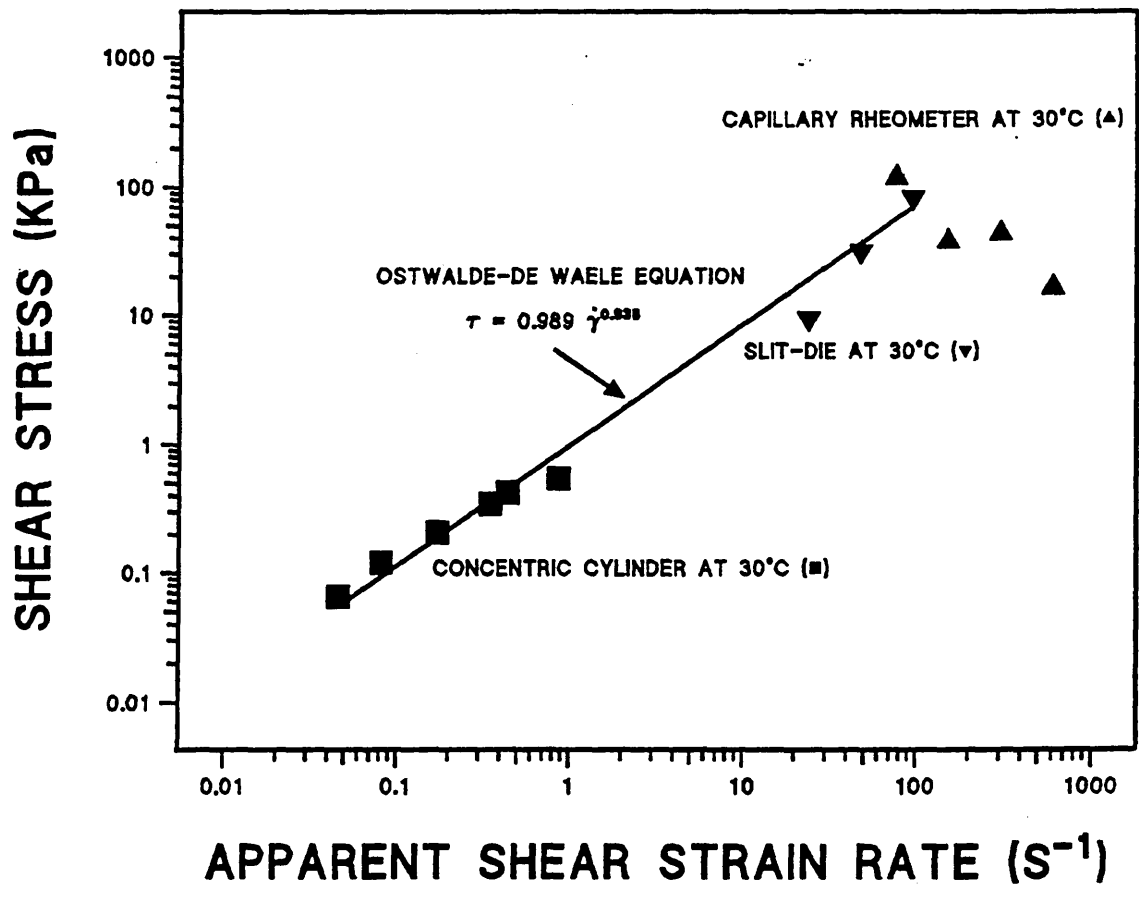


Figure 105. The relationship between the apparent shear stress (log) and the apparent shear strain rate (log) for C-11 polyborosiloxane at 30°C as determined by the concentric cylinder, the slit die, and the capillary die rheometers (section 4.9).

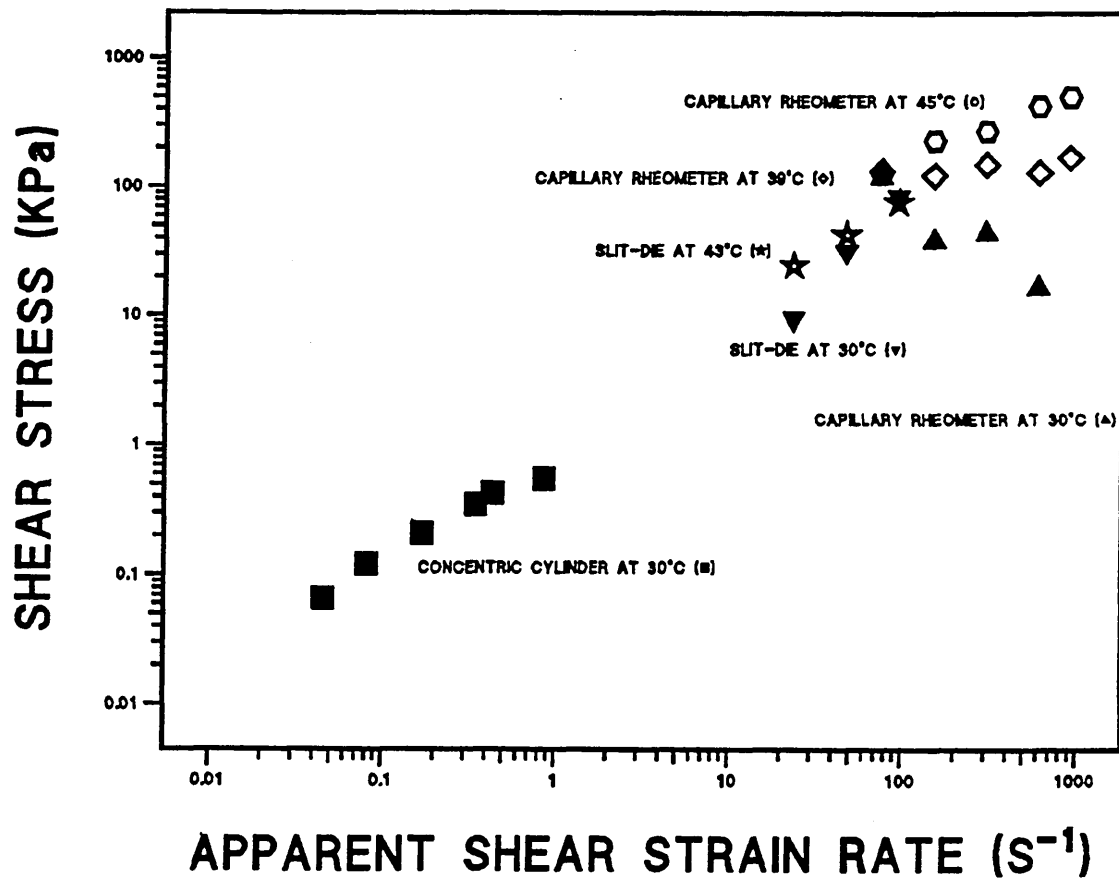


Figure 106. The relationship between the apparent shear stress (log) and the apparent shear strain rate (log) for C-11 polyborosiloxane at 30°C-45°C as determined by the concentric cylinder, the slit die, and the capillary die rheometers (section 4.9).

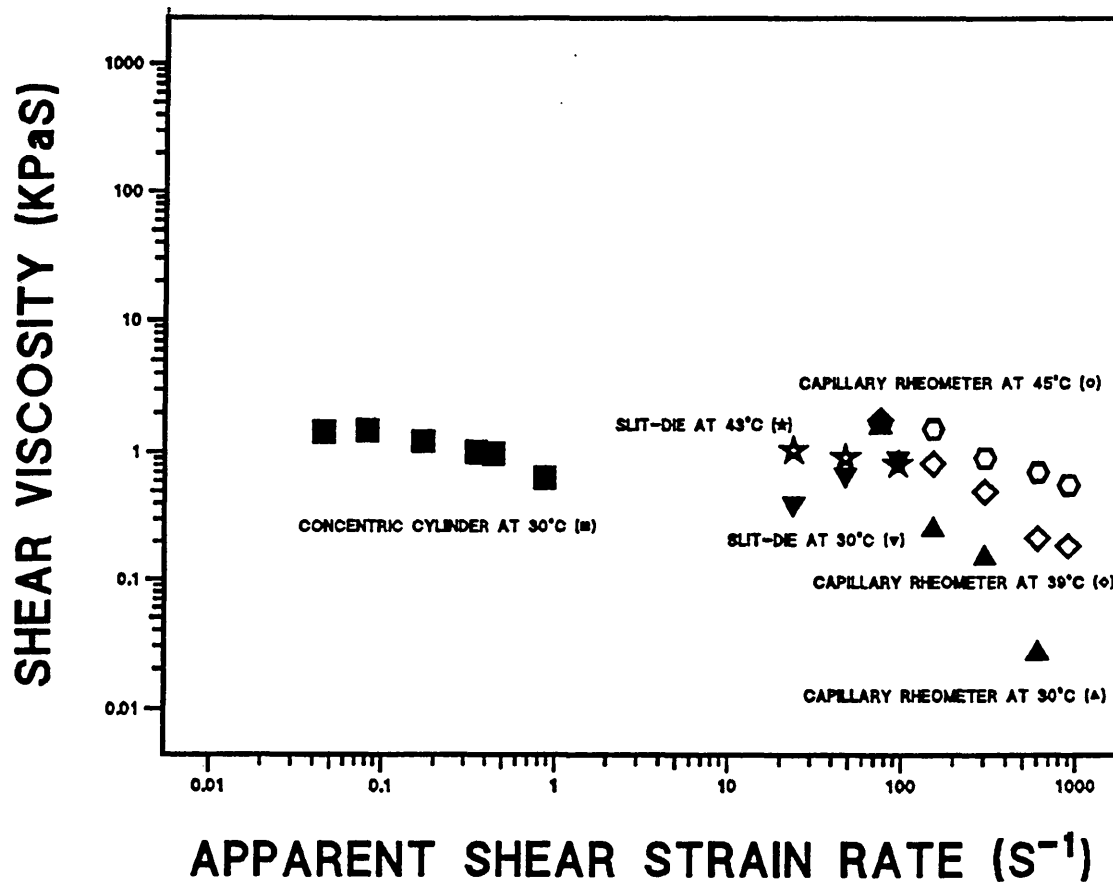


Figure 107. The relationship between the apparent shear viscosity (log) and the apparent shear strain rate (log) for C-11 polyborosiloxane at 30°C-45°C as determined by the concentric cylinder, the slit die, and the capillary die rheometers (section 4.9).

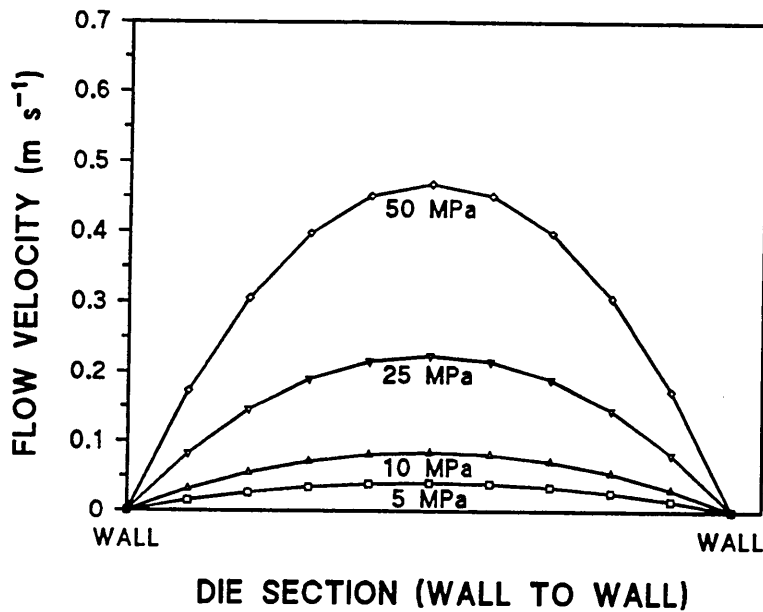


Figure 108. The velocity distribution across an extrusion die 40mm in length and of 2mm internal diameter as determined by the model described in section 3.3.4 for C-11 polyborosiloxane at 30°C at extrusion pressures of 5, 10, 25 and 50 MPa.

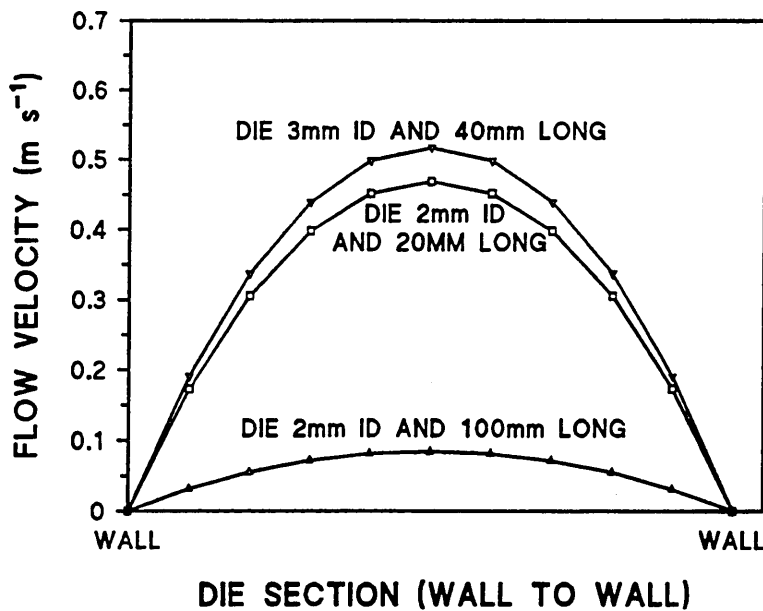


Figure 109. The velocity distribution across extrusion dies of dimensions 20mm long and 2mm internal diameter, 100 mm long and 2mm internal diameter, and 40mm long and 3mm internal diameter as determined by the model described in section 3.3.4 for C-11 polyborosiloxane at 30°C at an extrusion pressure of 25 MPa.

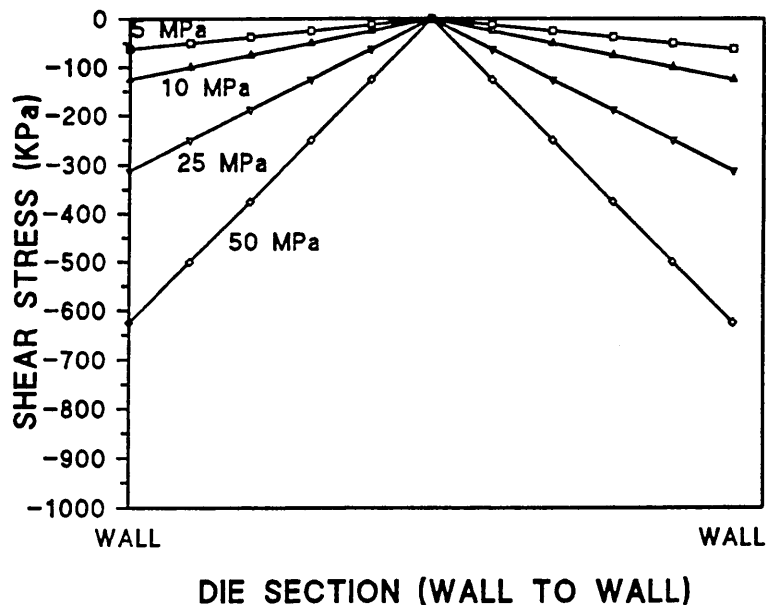


Figure 110. The shear stress distribution across an extrusion die 40mm in length and of 2mm internal diameter as determined by the model described in section 3.3.6 for C-11 polyborosiloxane at 30°C at extrusion pressures of 5, 10, 25 and 50 MPa.

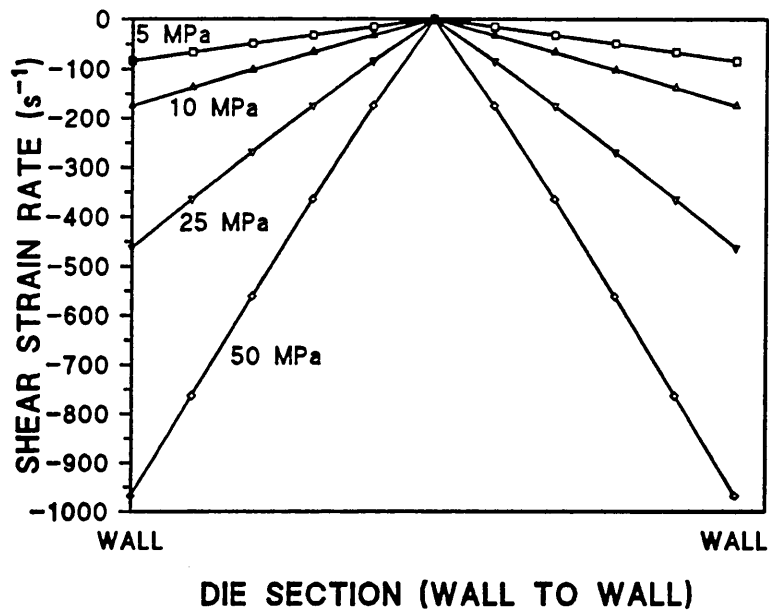


Figure 111. The shear strain rate distribution across an extrusion die 40mm in length and of 2mm internal diameter as determined by the model described in section 3.3.5 for C-11 polyborosiloxane at 30°C at extrusion pressures of 5, 10, 25 and 50 MPa.

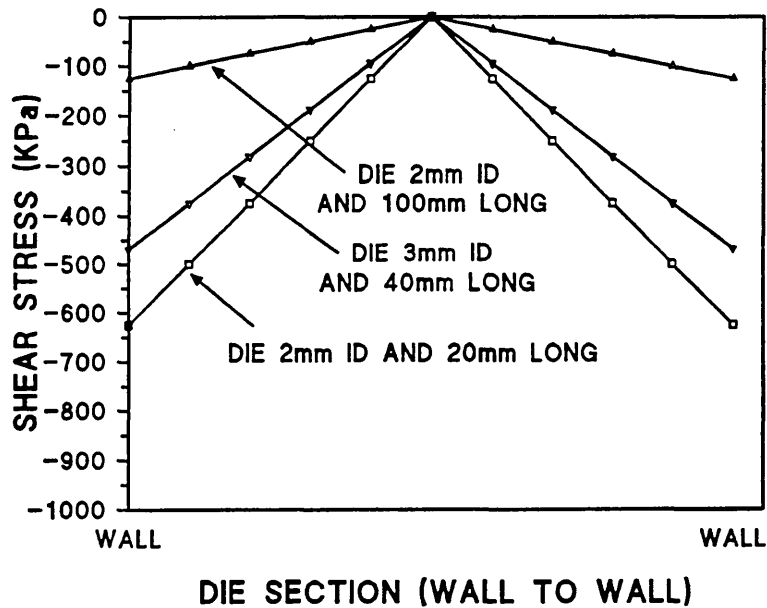


Figure 112. The shear stress distribution across extrusion dies of dimensions 20mm long and 2mm internal diameter, 100 mm long and 2mm internal diameter, and 40mm long and 3mm internal diameter as determined by the model described in section 3.3.6 for C-11 polyborosiloxane at 30°C at an extrusion pressure of 25 MPa.

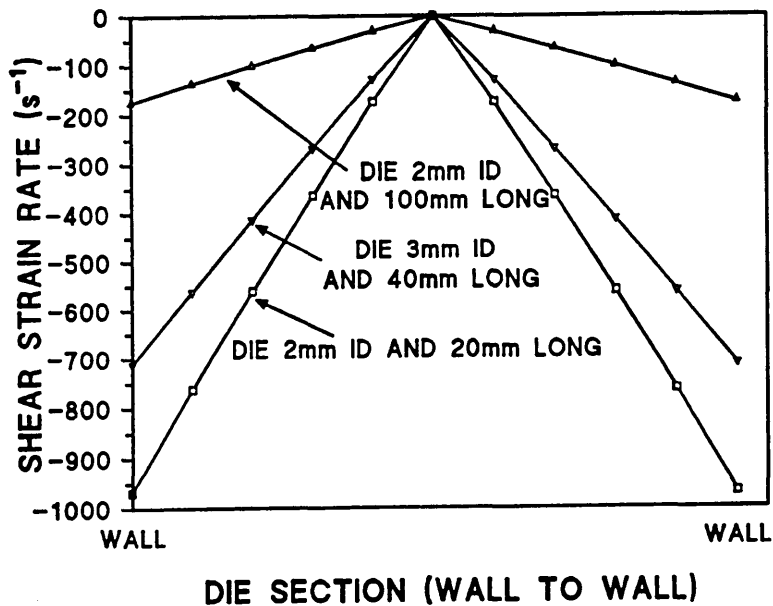


Figure 113. The shear strain rate distribution across extrusion dies of dimensions 20mm long and 2mm internal diameter, 100 mm long and 2mm internal diameter, and 40mm long and 3mm internal diameter as determined by the model described in section 3.3.5 for C-11 polyborosiloxane at 30°C at an extrusion pressure of 25 MPa.

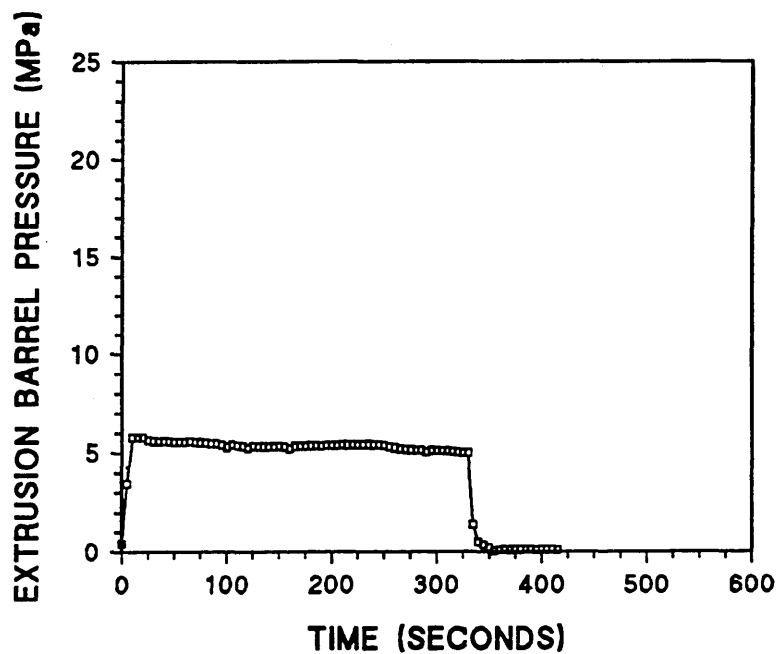


Figure 114 The variation in extrusion barrel pressure during extrusion of polystyrene on the capillary rheometer at a constant ram velocity of 2.5 cm/min at 230°C using a die of 2mm internal diameter and 40mm length (packing method A) (section 4.12).

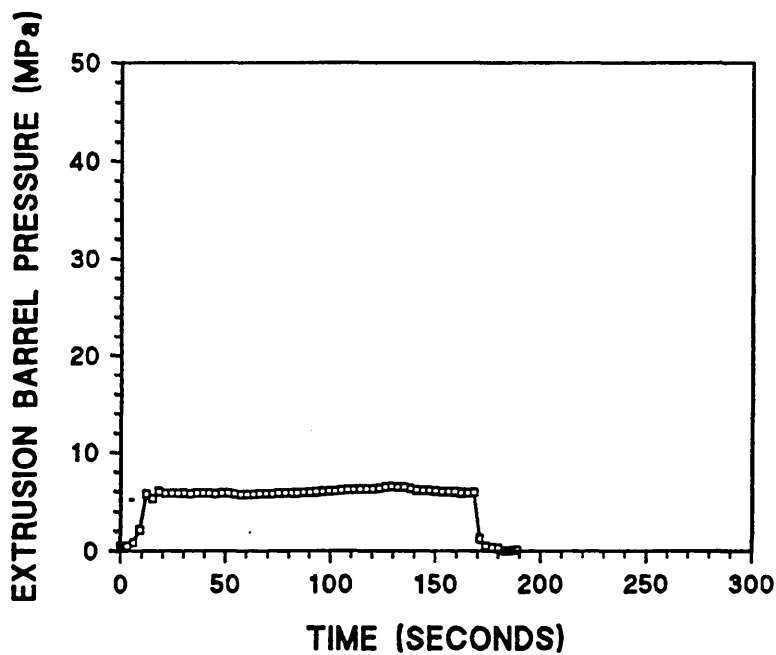


Figure 115. The variation in extrusion barrel pressure during extrusion of polystyrene on the capillary rheometer at a constant ram velocity of 5 cm/min at 230°C using a die of 2mm internal diameter and 40mm length (packing method A) (section 4.12).

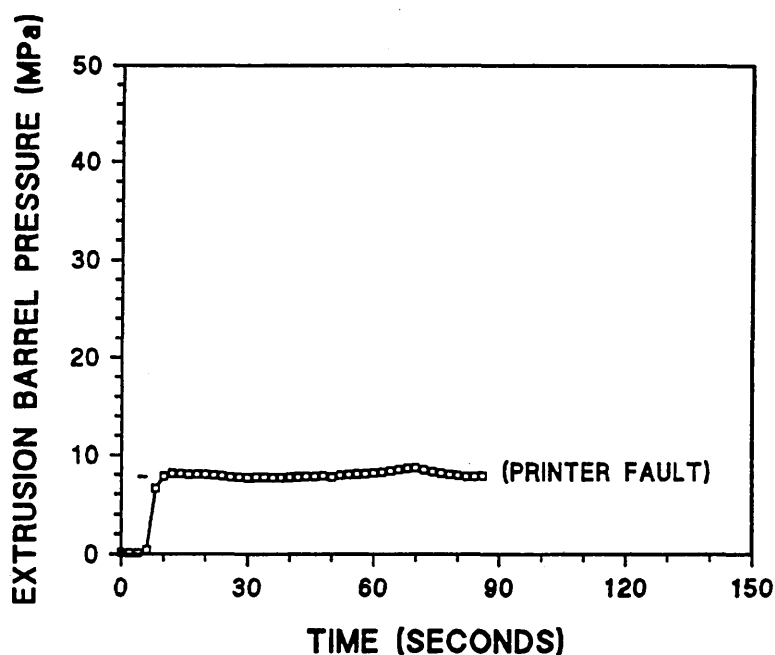


Figure 116. The variation in extrusion barrel pressure during extrusion of polystyrene on the capillary rheometer at a constant ram velocity of 10 cm/min at 230°C using a die of 2mm internal diameter and 40mm length (packing method A) (section 4.12).

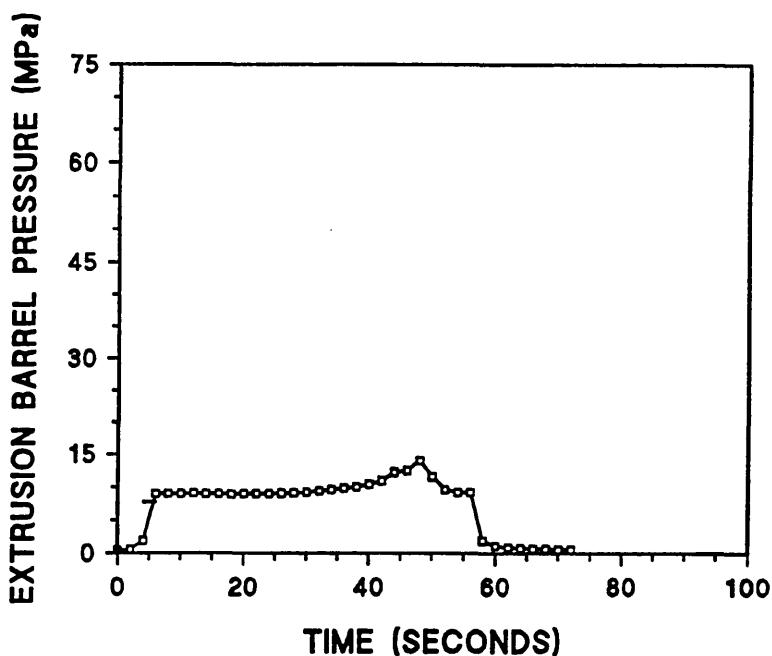


Figure 117. The variation in extrusion barrel pressure during extrusion of polystyrene on the capillary rheometer at a constant ram velocity of 15 cm/min at 230°C using a die of 2mm internal diameter and 40mm length (packing method A) (section 4.12).

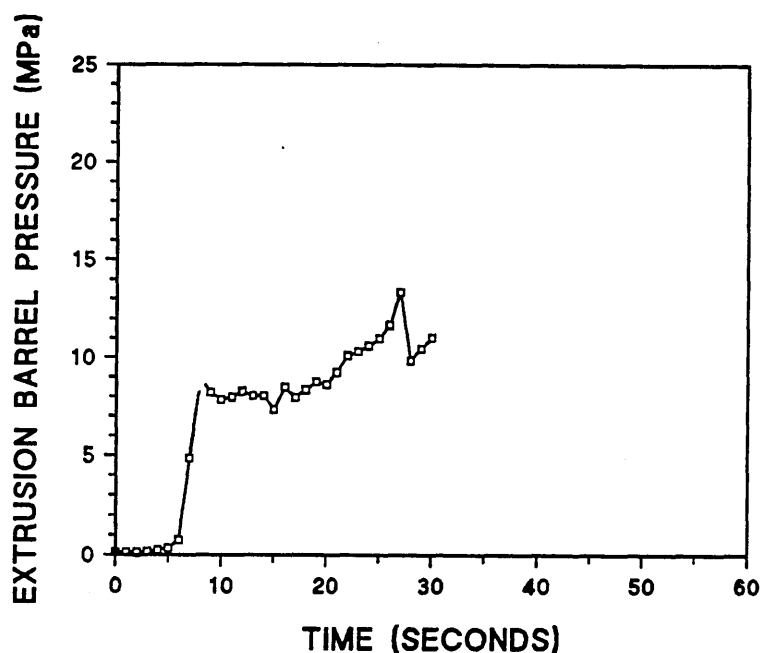


Figure 118. The variation in extrusion barrel pressure during extrusion of polystyrene on the capillary rheometer at a constant ram velocity of 20 cm/min at 230°C using a die of 2mm internal diameter and 40mm length (packing method A) (section 4.12).

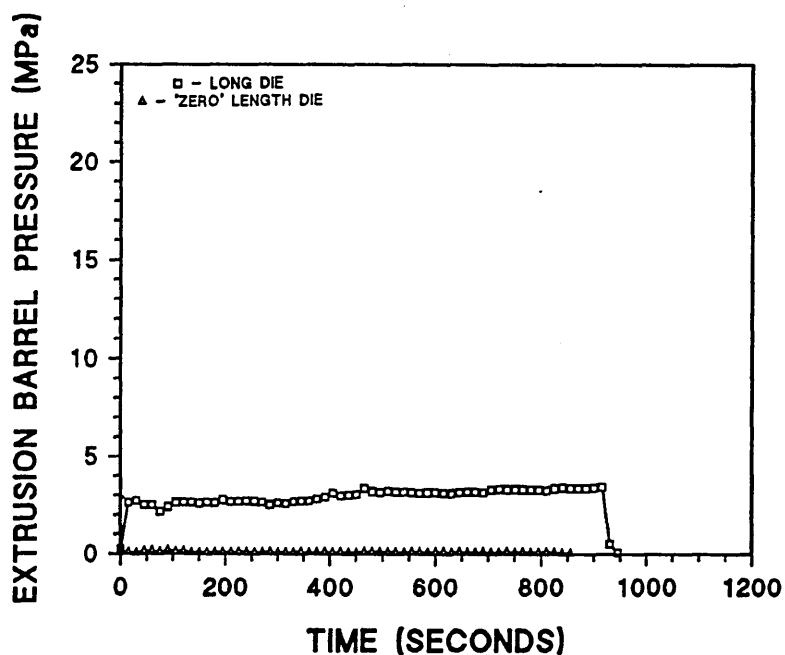


Figure 119. The variation in extrusion barrel pressure during extrusion of polystyrene on the capillary rheometer at a constant ram velocity of 1.25 cm/min at 230°C using dies of 2mm internal diameter and both nominally zero (orifice die) and 40 mm long (packing method C) (section 4.12).

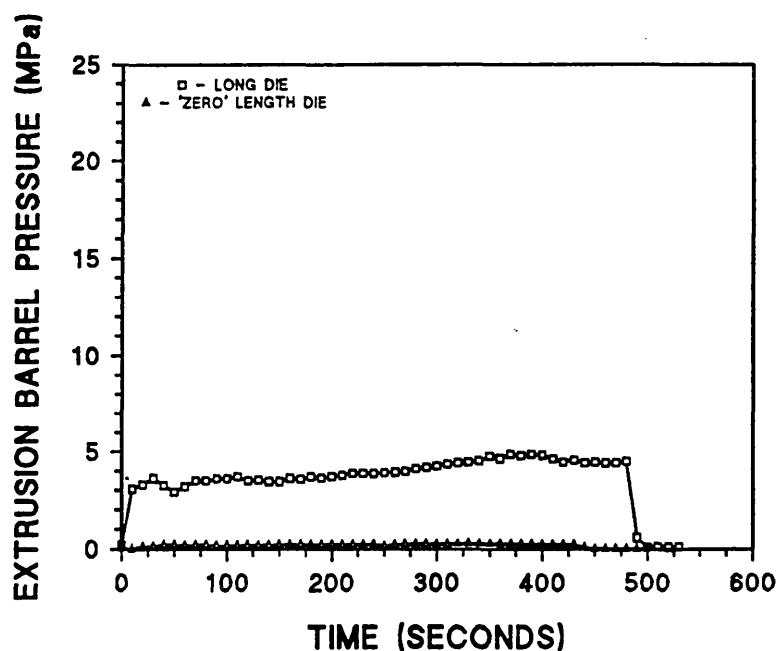


Figure 120. The variation in extrusion barrel pressure during extrusion of polystyrene on the capillary rheometer at a constant ram velocity of 2.5 cm/min at 230°C using dies of 2mm internal diameter and both nominally zero (orifice die) and 40 mm long (packing method C) (section 4.12).

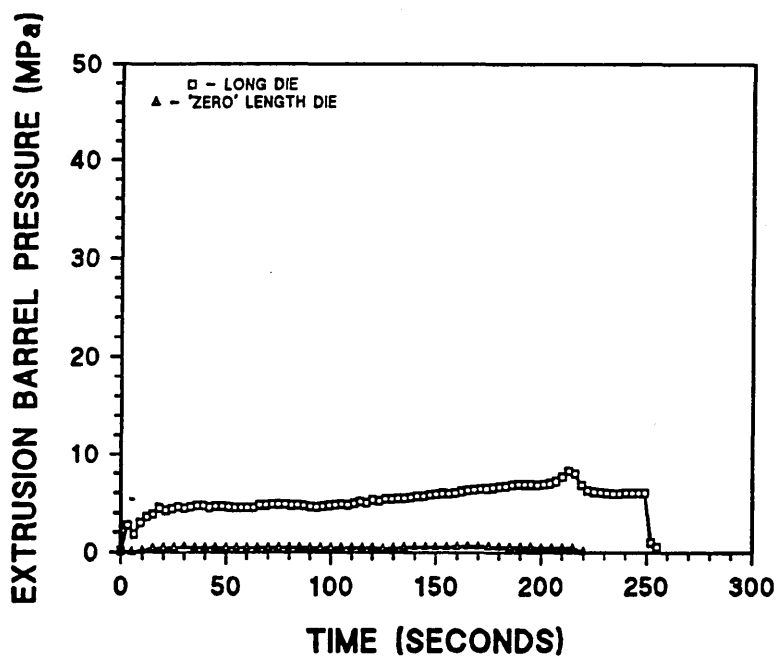


Figure 121. The variation in extrusion barrel pressure during extrusion of polystyrene on the capillary rheometer at a constant ram velocity of 5 cm/min at 230°C using dies of 2mm internal diameter and both nominally zero (orifice die) and 40 mm long (packing method C) (section 4.12).

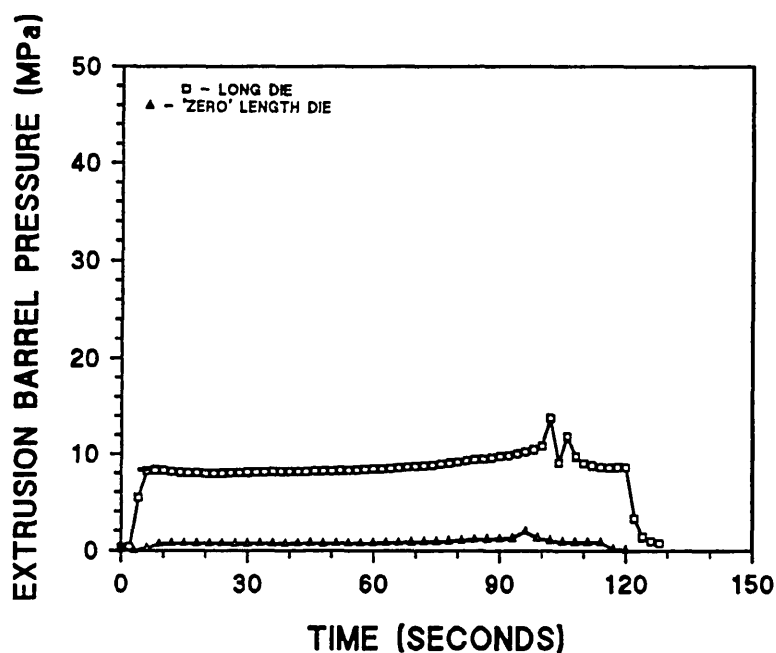


Figure 122. The variation in extrusion barrel pressure during extrusion of polystyrene on the capillary rheometer at a constant ram velocity of 10 cm/min at 230°C using dies of 2mm internal diameter and both nominally zero (orifice die) and 40 mm long (packing method B) (section 4.12).

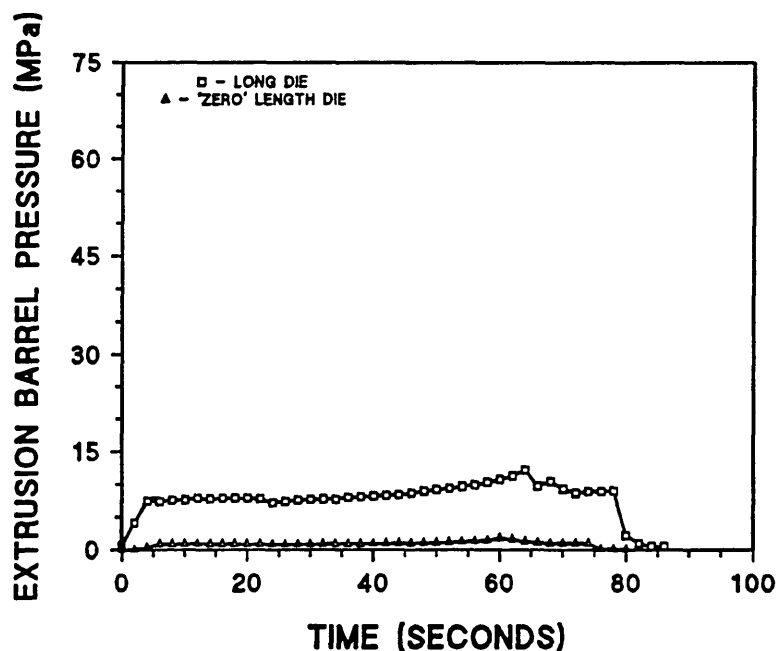


Figure 123. The variation in extrusion barrel pressure during extrusion of polystyrene on the capillary rheometer at a constant ram velocity of 15 cm/min at 230°C using dies of 2mm internal diameter and both nominally zero (orifice die) and 40 mm long (packing method B) (section 4.12).

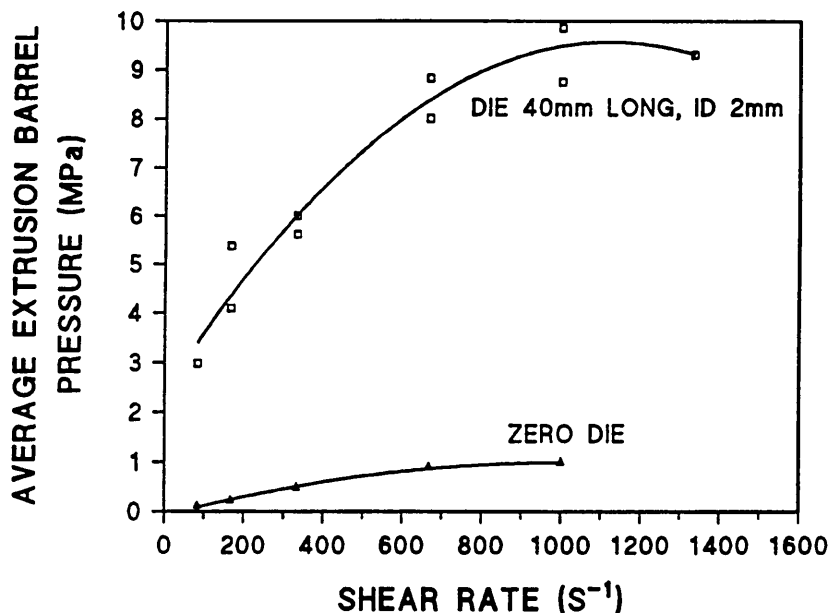


Figure 124. The variation in extrusion barrel pressure with apparent shear rate for polystyrene extruded through dies of 2mm internal diameter and 40mm in length, and nominally zero (orifice die) length at 230°C on the capillary rheometer.

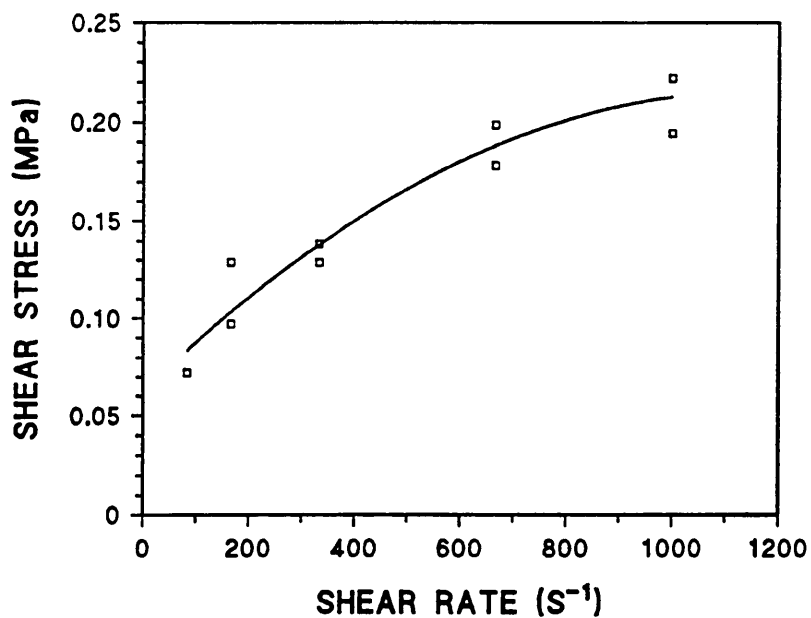


Figure 125. The variation in apparent shear stress with apparent shear rate for polystyrene extruded through a die of 2mm internal diameter and 40mm in length at 230°C on the capillary rheometer.

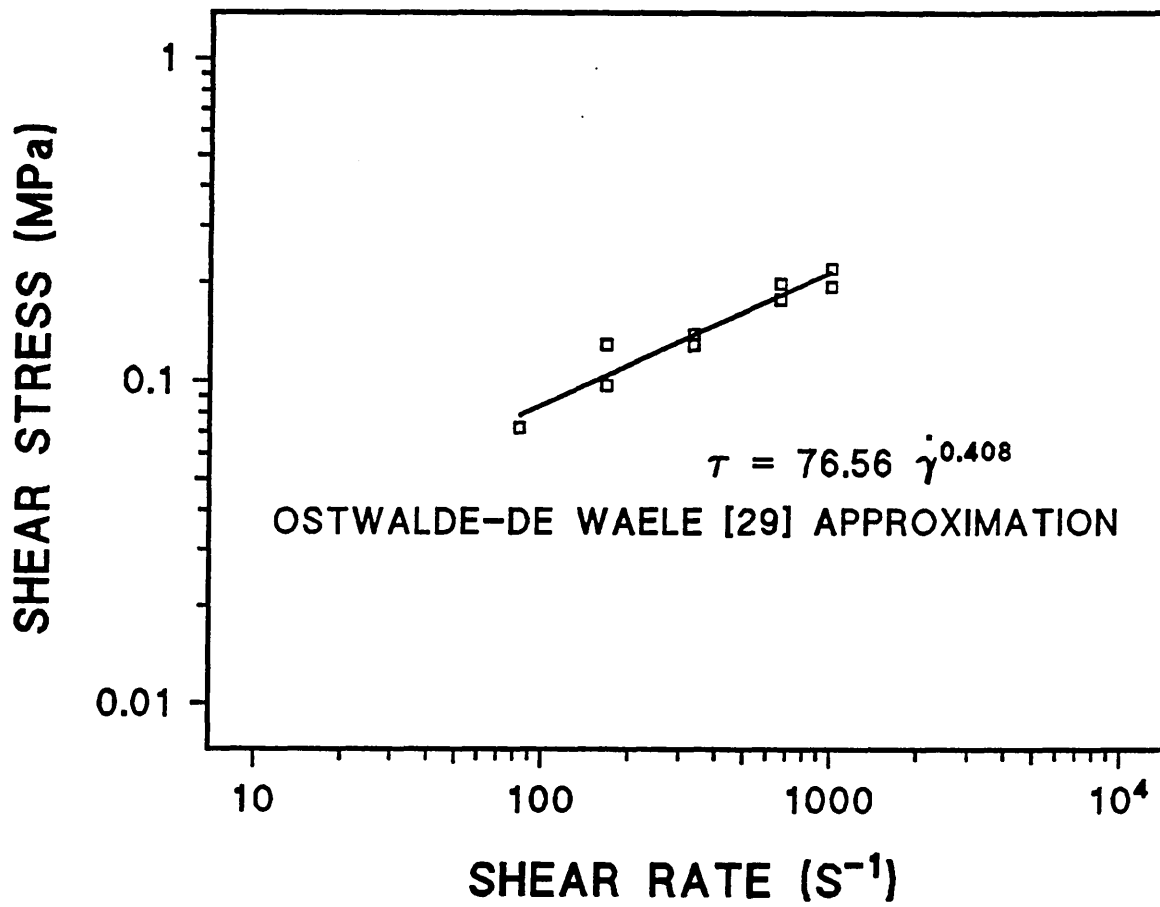


Figure 126. The variation in apparent shear stress (log) with apparent shear rate (log) for polystyrene extruded through a die of 2mm internal diameter and 40mm in length at 230°C on the capillary rheometer.

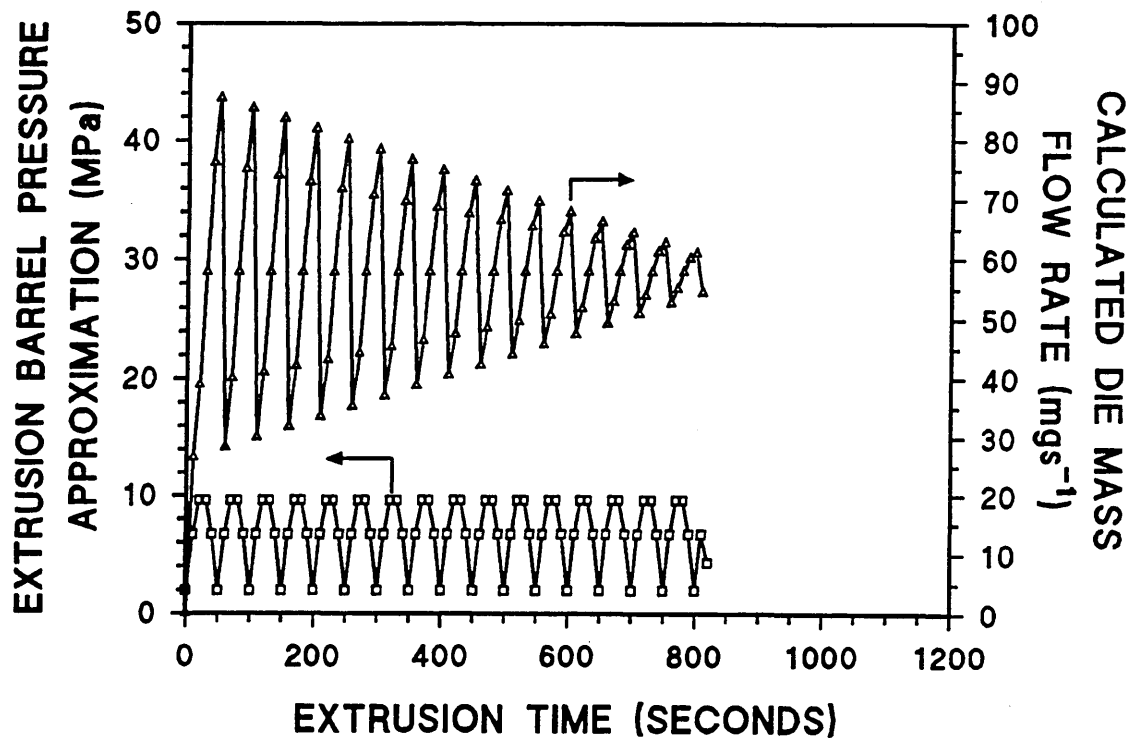


Figure 127. Capillary flow density and mass flow rate model. Extrusion barrel pressure during capillary flow approximated from the minimum, maximum and wavelength of the experimental pressure (Figure 86). The die mass flow rate is calculated as described in section 3.4.3. Calculation is for capillary flow of C-11 polyborosiloxane at 30°C at a ram velocity of 1.25 cm/min through a die 2mm internal diameter and 40 mm long. (section 4.1.3)

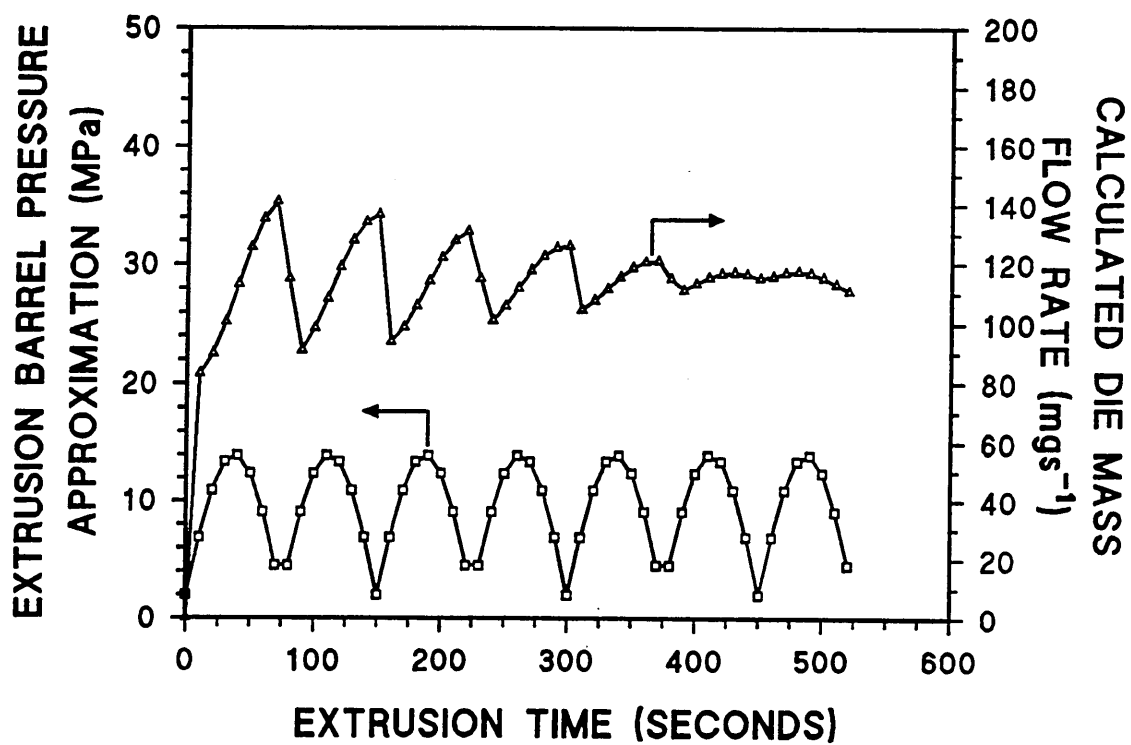


Figure 128. Capillary flow density and mass flow rate model. Extrusion barrel pressure during capillary flow approximated from the minimum, maximum and wavelength of the experimental pressure (Figure 87). The die mass flow rate is calculated as described in section 3.4.3. Calculation is for capillary flow of C-11 polyborosiloxane at 39°C at a ram velocity of 2.5 cm/min through a die 2mm internal diameter and 40 mm long. (section 4.1.3)

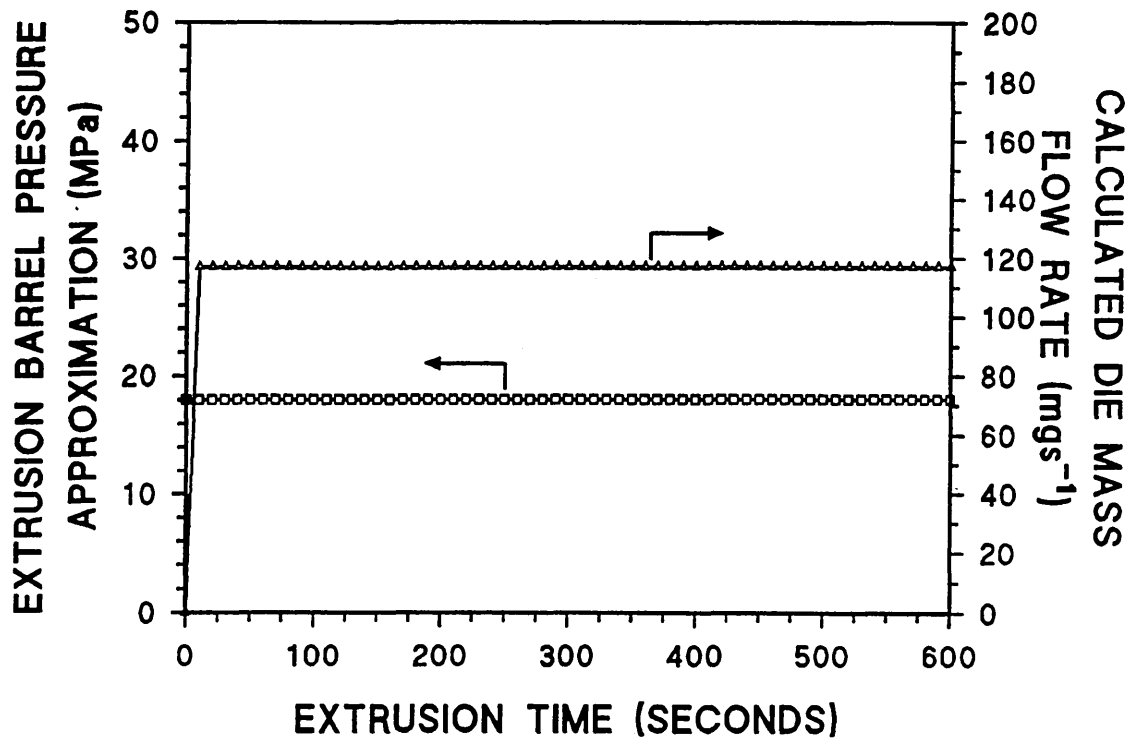


Figure 129. Capillary flow density and mass flow rate model. Extrusion barrel pressure during capillary flow approximated from the minimum, maximum and wavelength of the experimental pressure (Figure 88). The die mass flow rate is calculated as described in section 3.4.3. Calculation is for capillary flow of C-11 polyborosiloxane at 45°C at a ram velocity of 2.5 cm/min through a die 2mm internal diameter and 40 mm long. (section 4.1.3)

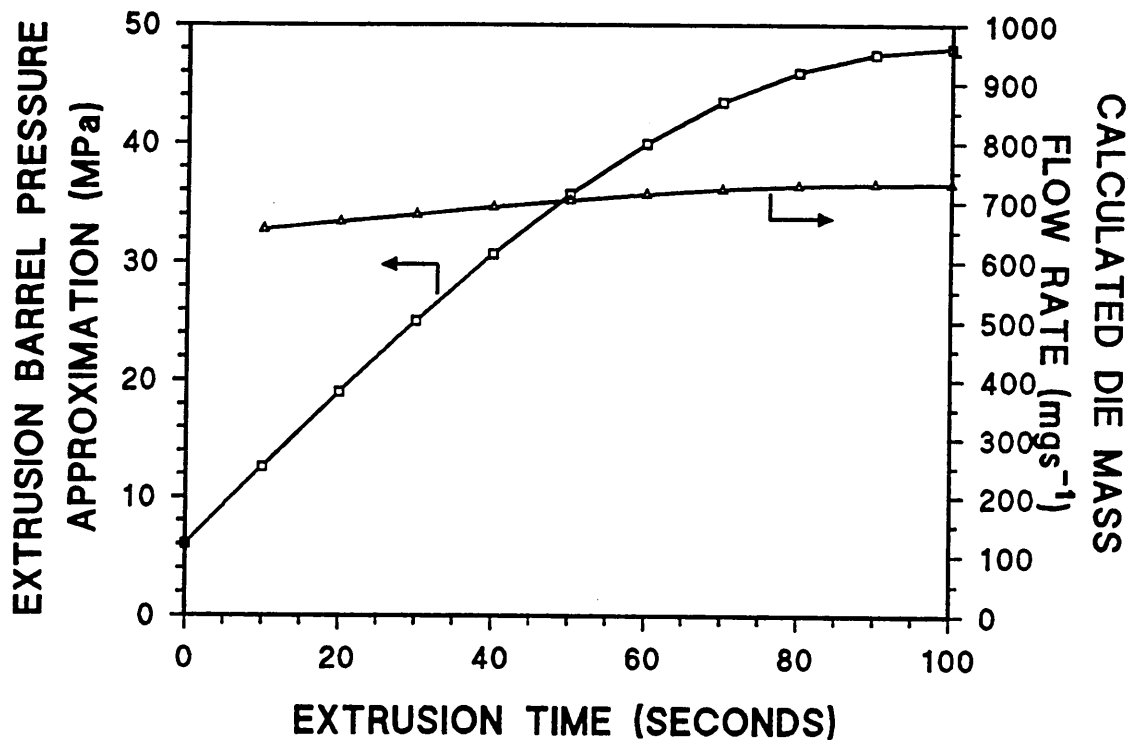


Figure 130. Capillary flow density and mass flow rate model. Extrusion barrel pressure during capillary flow approximated from the minimum, maximum and wavelength of the experimental pressure (Figure 89). The die mass flow rate is calculated as described in section 3.4.3. Calculation is for capillary flow of C-11 polyborosiloxane at 45°C at a ram velocity of 15 cm/min through a die 2mm internal diameter and 40 mm long. (section 4.1.3)

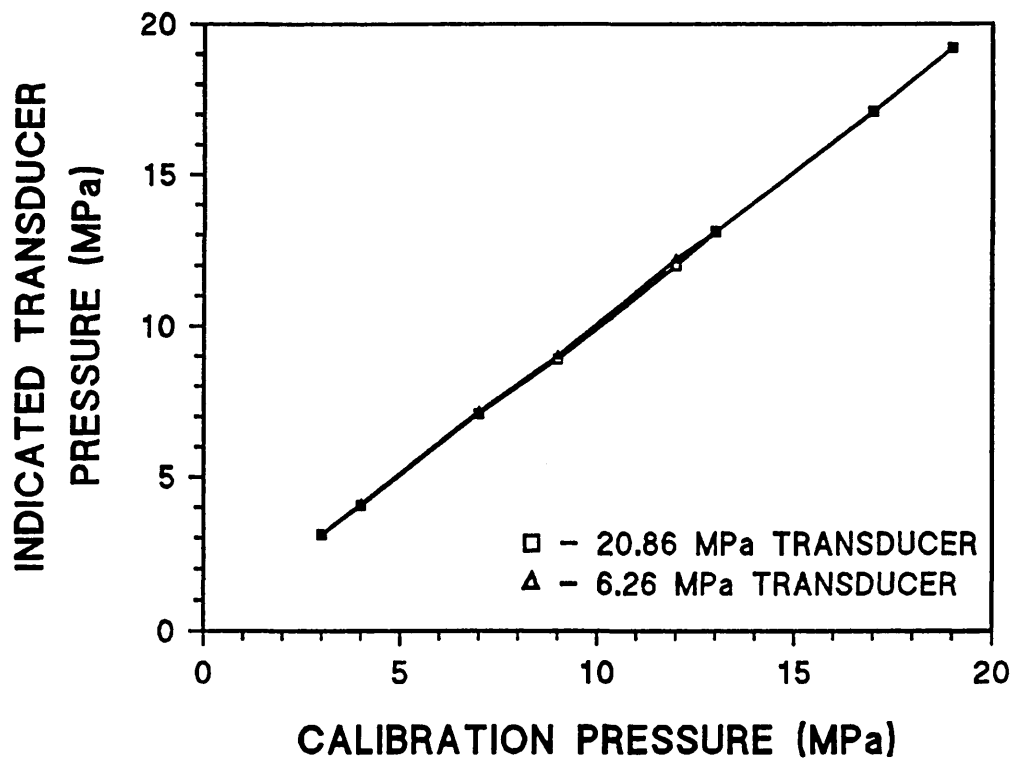


Figure 131. Capillary rheometer pressure transducer calibration.

# APPENDIX A

---

## **The measurement of extrusion honing media flow properties for quality assurance purposes - a technico-economic case study**

### **1. Introduction**

This case study assesses the requirements of both the quality system and the test equipment necessary to ensure the quality of the extrusion honing abrasive medium. This assessment considers the requirements with reference to international quality standard ISO 9000 [1]. The selection of a suitable type of rheometer for this particular application has been discussed, followed by consideration of the two options available, which are;

- a) The construction of 'in-house' test equipment specific to the requirements of Extrude Hone, or
- b) The purchase of rheological test equipment from established manufacturers.

The relative merits of these two options with respect to Extrude Hone's specific requirements, the requirements of ISO 9000 [1], and the technical requirements indicated by the results presented in this thesis are discussed.

The financial aspects of each of the two options are presented and discussed. In the concluding section a recommended course of action is proposed based on the data presented within the case study.

## **2. Quality System Requirements**

Quality systems and test equipment are necessary to ensure customer satisfaction that extrusion honing medium is manufactured to recognised quality standards, that each batch of medium is of consistent quality and that each batch can be traced back to detailed quality records.

Benefits of such a system may include improved customer satisfaction, a superior product to competitors and greater control of the extrusion honing process (by reducing one system variable).

Quality standard ISO 9000 [1] specifies quality system requirements for use where a contract between two parties requires demonstration of a supplier's capability to control the processes that determine the acceptability of a supplied product. The requirements specified in this international standard are aimed primarily at preventing and at detecting any non-conformity during production and installation, and implementing the means to prevent its recurrence.

In order to satisfy the requirements of the standard a quality parameter is required against which the quality of the extrusion honing medium can be specified and monitored. The selection of a suitable quality parameter is discussed in the following section together with consideration of appropriate test equipment to measure such a parameter.

## **3. The Selection of Suitable Test Equipment**

In the selection of suitable test equipment the first and most important question that must be asked is why the rheological data is required. This has previously been addressed to

some extent within section 2 in that a quality parameter is required in order to monitor quantitatively the quality of the extrusion honing medium in order to satisfy the requirements of ISO 9000 [1]. As the measurements are to be made for routine quality control, it is desirable that the testing procedure be simple and rapid. More elaborate measurements than those used for quality control are not necessary as it is not within the scope of this proposal to determine material constants of constitutive equations for use in detailed process modelling [2].

It is important to select a rheological property to be measured that is most appropriate for the particular application as it is often difficult to show direct quantitative links between test results and processing behaviour [2]. The property of melt flow index is therefore considered appropriate in this case as the procedure is simple and rapid and the deformation process is very similar to that experienced on an extrusion honing machine. Of all the family of capillary flow systems the Melt Flow indexer is the cheapest and most widely used. It is also capable of much more versatile use than the measurement of a single value. Flow rate may be determined as a function of applied load so that a qualitative indication of pseudoplasticity is readily obtained by comparing the ratios of flow rate at two different loads [3].

The main limitation of the use of a melt flow indexer for this application is the extrusion pressure range in which the machine can be operated. There are practical limitations on the pressures available due to the size of the extrusion weights that can be used. Whilst high pressure testing is desirable from the point of view of testing in the normal operating range of an extrusion honing machine, it is not considered essential for quality control purposes. It should be noted that higher pressures can only be achieved by the use of more elaborate and expensive extrusion ram driving mechanisms (such as gas pressure, electro-mechanical, hydraulic, positive displacement pumps or extruder mechanisms).

Specific requirements of the technical specification of a melt flow indexer for testing extrusion honing medium are as follows;

- (i) An operating temperature range of 20-80°C. (Which is typical of the operating range of extrusion honing machines).
- (ii) Accurate temperature control to ensure process repeatability.
- (iii) A variety of die sizes and driving weights to be available as many viscosities of extrusion honing medium are available.
- (iv) All components that come into contact with the medium must be relatively wear resistant and replaceable as necessary in order to allow the testing of abrasive laden (silicon carbide, boron carbide etc.) extrusion honing medium.
- (v) Due consideration must be given to the level of automation which can be incorporated into the design. A balance must be found between the additional complexity and cost of the apparatus associated with automation and the benefit of automation to reduced time and effort required to complete a test.
- (vi) It has been reported [2] that rheological data for polymers are not as reproducible as those for low molecular weight liquids. Variations between runs of 5% cannot be considered as significant, and for many purposes 10% accuracy may be acceptable. Variations from one batch to another of resin produced under the same nominal conditions can be somewhat greater than this and would thus be detectable even at this level of precision [2]. It is therefore suggested that the repeatability of the apparatus be 10% or better.

- (vii) The equipment must be suitable for use by personnel with limited training in the use of rheological test equipment.

Considering the technical requirements listed above, two options are available with regard to the acquisition of a melt flow indexer; either to purchase equipment from an established manufacturer or to manufacture equipment 'in-house'. These two options are considered in the sections below.

#### **4. Option 1 - 'In-House' Manufacture of Test Equipment**

The main advantage of manufacturing 'in-house' equipment is that it can be manufactured to the specific requirements of the application. An 'in-house' design for a melt flow indexer for quality testing extrusion honing medium is described below. The proposed design is shown schematically in Figure 1 .

The proposed design is based on a weight driven piston mechanism extruding extrusion honing medium through a restrictive die. A weight driven piston was chosen for low cost and simplicity of design, construction and operation. It is considered that a weight driven device is adequate for the quality testing required for this particular application. (If absolute viscosity calculation is required then gas pressure, electro-mechanical, hydraulic, positive displacement pumps or extruder mechanisms must be considered and the additional cost factor allowed for).

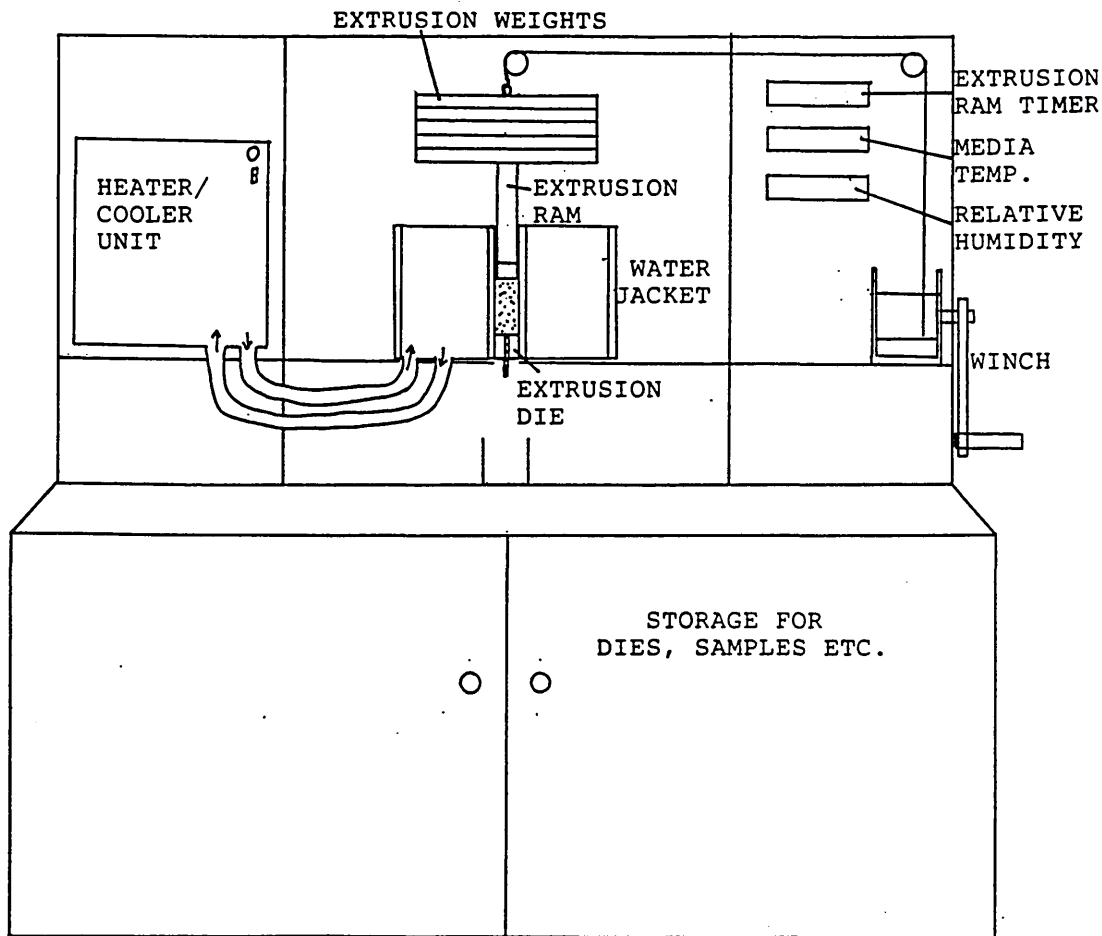


Figure 1. Proposed design of 'in-house' melt flow indexer.

It is proposed that five extrusion weights are manufactured (each weighing 5 Kg) such that a total weight between 0 and 25 Kg may be selected in 5 Kg intervals. The lifting of weights and extrusion ram prior to test may be by hand winch pulley system with auto-brake safety mechanism. The proposed design utilises a steel housing containing all the main components to provide a robust and aesthetically pleasing housing. The housing may also provide adequate storage for spare dies, samples, tools etc. In this case it is highly desirable that the equipment is manufactured with replaceable wear parts such that extrusion honing

medium containing abrasive particles (silicon carbide, boron carbide etc.) may be tested. The proposed design therefore incorporates replaceable barrel linings, extrusion dies and ram tips (Figure 1). A steel extrusion barrel would ensure wear resistance and good thermal diffusivity for media temperature control. The dies may be manufactured from drill bushes to ensure dimensional accuracy and wear resistance. The ram tip may be nylon to allow a close fit to the extrusion barrel, wear resistance and ease of replacement.

It is proposed that the extrusion barrel be enclosed by a water jacket manufactured from nylon for its thermal insulation properties. The temperature of the extrusion barrel may be controlled by a low temperature bath circulator operating in the range -20 to 100°C.

Both the facilities and the expertise are available within Extrude Hone to manufacture equipment 'in-house'. In addition the exercise of manufacturing equipment would serve as useful practical experience in understanding and performing rheological testing. Despite these advantages the manufacture of such specialist equipment in-house may be uneconomic compared to purchasing equipment. This aspect is briefly considered within section 5.

## **5. Option 2 - Purchased Equipment**

Dealy [2] has stated that if machine fabrication facilities or manhours are not available then the industrial rheologist may wish to purchase a commercially manufactured instrument.

The extrusion plastometer, or 'melt-indexer', as it is often called, is the most popular melt tester now in use [2]. Its design grew out of the need for a simple, reliable method for characterising molten thermoplastics.

A wide range of commercial extrusion plastometers or 'melt- indexers' are available. Whilst it is beyond the scope of this case study to review them all in detail, a number of the designs most appropriate to this application are briefly described below.

Melt plastometers designed in accordance with one or more of the various standard test methods are manufactured by a least 12 companies in 5 countries. A basic unit will have relatively simple temperature control and be suitable for operation at temperatures up to 200°C. Higher priced units generally have more sophisticated temperature control and higher maximum operating temperatures.

Additional features which may be available include plunger guides, either manual or pneumatic weight lift devices, built in manual or automatic extrudate cutting devices, piston travel versus time recorders, and microprocessors for automatic calculation and display of the melt flow. Several models are available with some degree of automation such as a microprocessor which receives a signal from a piston travel timer and calculates the melt flow. In the Kayeness Model D-9052, it is possible to preprogramme a sequence of five successive tests, all at one loading, each involving the travel of the piston through a distance of 1/4 inch with pre-selected delay time between tests. Thus, a single loading of the barrel yields five successive values of the time required for the piston to fall  $\frac{1}{4}$  inch, so that the time dependency of the flow can be observed.

The main advantage of purchasing a commercial melt flow indexer is the high precision of manufacture available (honed bores, alignment, dimensional tolerances etc.) which would be difficult and costly to incorporate into an 'in- house' design. However, this high level of precision may be problematic for testing abrasive filled extrusion honing media where high wear rates may occur. It would be important to ensure that barrel linings,

pistons and dies could be replaced at reasonable cost if the purchase of a commercial melt flow indexer were considered.

The majority of commercial melt flow indexers employ electrical heating for temperature control up to 400°C. Electrical heating may be unsuitable for testing extrusion honing medium as temperature control at near ambient temperature is usually poor using this method. The availability of a more suitable 'water jacket type' temperature control in the range 20-80°C would need to be ascertained.

A further consideration with regard to commercial melt flow indexers is delivery time. Delivery times vary depending on many factors. A standard model of a simple device may be available from stock. In other cases delays of six to ten months may be involved [2].

## **6. Cost Analysis**

### **6.1 'In-House' Manufacturing Costs**

A component list with approximate cost for the 'in-house' design described in section 4 is presented in Table 1.

<b>Component</b>	<b>Supplier</b>	<b>Cost</b>
Steel Housing	Scroll Fabrications	£1100
Steel for Fabrication	Northern Tube/Parkside	£80
Plastic for Fabrication	Advanced Plastic Tec.	£100
Heater/Cooler Unit	Grant Instruments	£1400
Humidity Meter	The Control House	£230
Temperature Display & misc. electronics	Farnell Electronics	£260
Dies	Boneham & Turner	£28
Misc. Components	Various	£163
	<b>TOTAL</b>	<b>£3170</b>

Table 1. 'In-House' manufacturing component listing showing supplier and approximate cost.

(N.B. All prices were obtained from suppliers in January 1993 and are approximate.)

Further costs associated with this project have been estimated as follows:

Installation and Training	£480
Workshop Labour	£1700
Design Labour	£3000

This would give a total 'In-House' manufacture cost of £8350. It should be noted that if further machines were manufactured than the cost would be £5350 as the design labour would not be necessary.

## **6.2 Purchased Equipment Costs**

As for the 'In-House' option installation and training costs of £480 would be incurred.

The cost estimates for purchased equipment as presented below are approximate and serve only as a rough guide for comparative purposes. Specific costs with respect to technical specifications should be obtained from suppliers if the proposals outlined in this case study are to be pursued.

Cogswell [3] has quoted a minimum cost for a basic melt flow indexer to be around £3450 (£1000 in 1980 discounted at 10% per annum). For a more complex rheometer Cogswell [3] quotes a figure of around £20700 (£6000 in 1980 discounted at 10% per annum).

Dealy [2] has also provided cost estimates for the purchase of melt flow index equipment. Dealy [2] has estimated the cost of a basic unit with simple temperature control up to 200°C to be around £5000. More sophisticated temperature control may increase the melt flow indexer cost to £10,000- £14,000.

## **6. Conclusions**

There is no doubt that in order to satisfy the requirements of ISO 9000 [1], the quality of the extrusion honing abrasive medium must be monitored by measuring an appropriate flow property of the material. The melt flow index is considered to be an appropriate quality control parameter as the deformation regime imposed on the material during the measurement is very similar to that in the extrusion honing machine. In addition the measurement of melt flow index does not necessitate the expense associated with high

pressure ram driving mechanisms. The measurement of melt flow index is quick and simple and is considered to be appropriate in this case.

From the technical specification presented in Section 3 and the preliminary cost analysis presented in Section 6 it is recommended that as a first step in installing a quality system a melt flow indexer is manufactured 'In-House'. This is because control at high temperature available on commercial machines is not necessary in this case, wear resistance to the abrasive particles can be designed into an 'In-House' design, and preliminary cost comparisons show the cost of 'In-House' or purchased equipment to be similar. However it is recommended that manufacturers be consulted for more detailed cost estimates, details of low temperature control available, details of wear resistance, and the availability and cost of components which may wear. The number of units to be acquired is also an important consideration as a large proportion of the cost of the 'In- House' design is design costs, such that the cost of the second and subsequent 'In-House' machines would be approximately £3000 less than the first.

## **References**

1. ISO 9000, International Quality Standard
2. Dealy, J. M., Rheometers for Moulten Plastics, Van Nostrand Reinhold.
3. Cogswell, F. N., Polymer Melt Rheology, A Guide for Industrial Practice, George Godwin Ltd.

## COMPUTER MODELLING OF THE ABRASIVE FLOW MACHINING PROCESS

A. J. Fletcher, J. B. Hull, J. Mackie\* and S. A. Trengove

Sheffield City Polytechnic  
Sheffield  
UK

\*Extrude Hone Ltd  
Milton Keynes  
UK

### Abstract

Abrasive flow machining (AFM) is a process for finish machining of edges and surfaces by the controlled extrusion of an abrasive laden viscoelastic polymer across these edges or surfaces.

Since the initial development of the process in the mid-1960's, to deburr hydraulic control blocks used in the radar-guided target acquisition systems for Phantom Jets, the process has gained widespread acceptance across the broad spectrum of modern manufacturing industry. Applications now range from high technology aerospace components to high volume automotive components [1].

The Authors are currently involved in an extensive research and development programme into the abrasive flow machining (AFM) process. The aim of the research programme is

to achieve a better understanding of the the thermal and fluid flow properties of polymers used in AFM, in order to establish a basis for the control and optimisation of the process.

The results reported here include the rheological characteristics of the Extrude Hone MV polyborosiloxane material, a description of the AFM process and consideration of the relationship between these rheological properties and the process.

## **INTRODUCTION**

Abrasive flow machining is a technique used for the final stages of the machining of engineering components. The process may be used to deburr or modify the intersections of machined surfaces, or polish machined areas, resulting in a significant improvement to the surface finish. Additional benefits of the process include surface texture modifications and the removal of surface layers which have been subject to mechanical or thermal damage.

The process utilises the viscoelastic polymer polyborosiloxane, which is mixed with fine abrasive particles and forced through or around the component using an abrasive flow machine, thus achieving the machining action.

The process has been developed over the last 20 years and is used extensively for a variety of engineering components from high volume operations such as fuel injection nozzles or sewing machine eyes as well as the machining of specialised components of very complex geometry such as turbine blades and hydraulic control blocks.

The aim of the research project is to achieve a better understanding of the thermal and fluid flow properties of polyborosiloxanes, in order to establish a basis for the control and

optimisation of abrasive flow machining, which is the main industrial use for these materials.

The research programme will include the determination of the rheological properties of the polyborosiloxane both on its own and when mixed with grit particles as well as consideration of heat generation and flow of the materials while passing through orifices of different diameters. This will be supported by the measurement of the relevant physical parameters. Subsequently, it is intended to use the information obtained to calculate velocity and stress profiles during abrasive flow machining.

This paper describes the abrasive flow machining process and considers the characteristics of Extrude Hone MV grade polyborosiloxane in relation to the machining process.

## **DESCRIPTION OF THE PROCESS**

### ***Process development***

The Extrude Hone abrasive flow machining process was initially developed in the mid 1960's in order to find a more effective method of deburring hydraulic control blocks , which at the time were being deburred by hand. The blocks were used at the centre of the hydraulic control system for the radar guided target acquisition systems of Phantom jets, and contained 83 intersecting holes in a block no bigger than 150 cm<sup>3</sup>. [1]

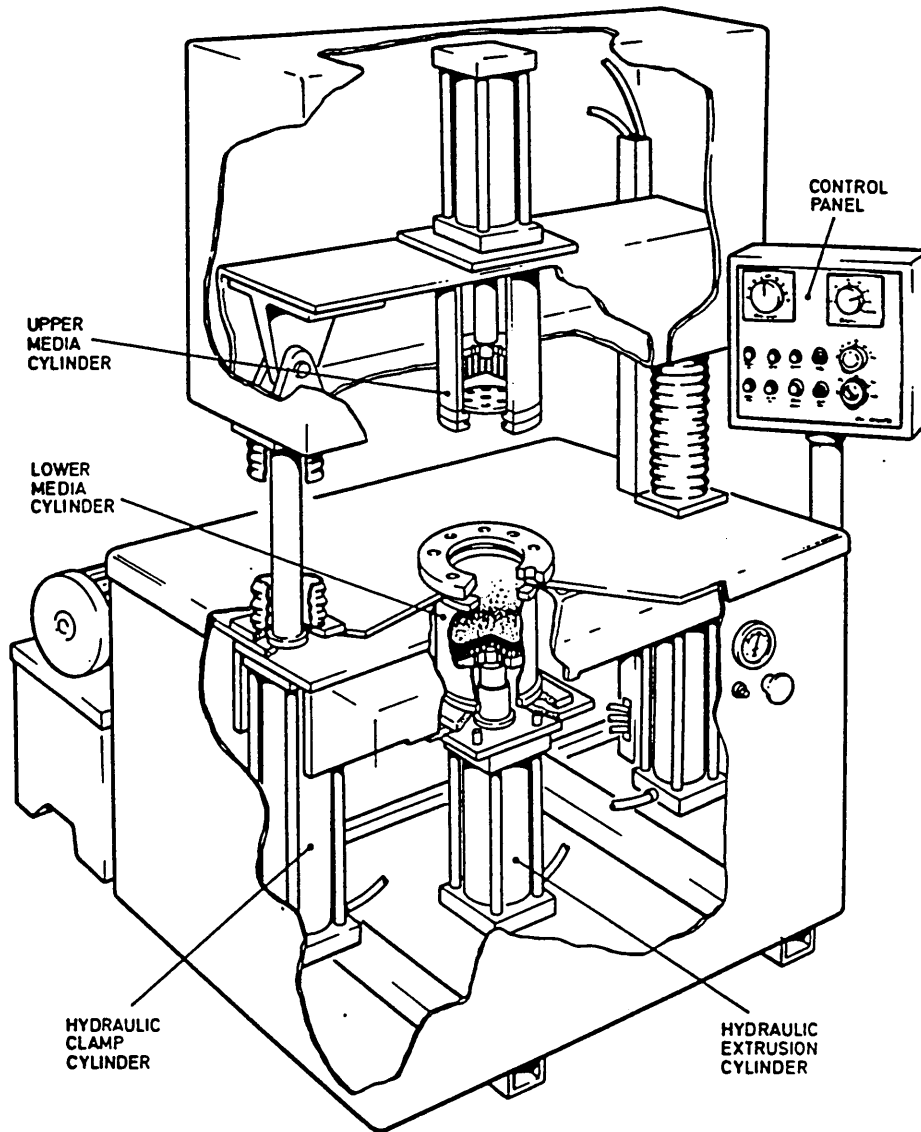


Figure 1. Schematic of a typical abrasive flow machine.

By 1968 the process had been successfully developed for application to the hydraulic control blocks by the Extrude Hone Corporation. The process was rapidly diversified into a number of additional applications such as aerospace components and die and mould polishing operations.

The Extrude Hone Corporation currently have over a thousand system applications throughout the world, and support an ambitious research and development effort aimed at meeting escalating requirements for precision machining in aerospace, automotive, die-making, and other major markets.

### ***The abrasive flow machine[2]***

All abrasive flow machines, such as the one shown in figure 1[3], are based on a common configuration. The equipment must clamp and seal the component in such a way that the polymer abrasive mixture is contained within the system. In addition it must pump a pre-selected quantity of abrasive media through the fixture at a specified pressure . To this end cylinders containing the abrasive mixture are mounted above and below the component.

The components, or fixture holding one or more components, are placed on top of the lower cylinder. A moveable rail is then lowered until it clamps the part or fixture between the two cylinders.

Abrasive media is forced hydraulically from the lower cylinder through, or across, the part and into the upper cylinder. Flow is then reversed to complete one cycle. When the appropriate number of cycles has been completed the moveable rail is raised to release the part or fixture.

Extrude Hone abrasive flow machines are available in a range of sizes depending on the specific application. These machines are available with adjustable controls for media flow pressure, media flow rate, and cycle times.

Machines may be operated manually or automatically from a control panel. Additional control systems may be added to measure parameters such as media temperature, viscosity, wear and flow speeds. Auxiliary systems for such operations as fixture handling, additional and refeed media supply to the process area, and media cooling systems are also available.

### ***The fixtures or tooling***

The function of the tooling is simply to hold the workpiece in position and to contain and direct the flow of media. In designing tooling, the areas where abrasion is desired are first identified. The tooling is constructed in such a way that the flow of media through or across these areas is restricted. For a workpiece with straight-through passages, such as a tube, an internal spline, a valve plate, or an extrusion die, the tooling merely holds the parts in place between the cylinders and allows the through-passages to restrict the flow. In many die polishing operations, no tooling is required.

To process external edges or surfaces, the part is contained within a flow passage, so that flow is restricted between the outside of the part and the interior of the flow passage.

Counterbores, recessed areas, or even blind cavities can be processed using a restrictor or mandrel to fit inside the components and restrict the flow at the desired areas.

Any number of parallel restrictions can be processed at once. In many cases, two (occasionally more than two) successive restrictions in the same flow stream can be

abraded, so long as the cross-sectional areas of the successive restricting passages are equal. However, if there are two successive restrictions in the same flow stream with significantly different cross-sectional areas, only the more restricted passages will be abraded.

Very complex parts, such as valve bodies, may require processing in two or more operations, processing some areas in one operation and others, with different flow paths in the next. Very large parts can be processed in sections [4].

### ***The abrasive media***

It is the abrasive laden polyborosiloxane material which transfers the machine extrusion force to the workpiece edges and surfaces to achieve the finishing action.

The polyborosiloxane material is available in a range of viscosities depending on the specific application.

The abrasive, which is dispersed evenly throughout the polyborosiloxane will also be selected depending on the application requirements. Typical abrasives used include silicon carbide, aluminium oxide and boron carbide. The machining characteristics of the polyborosiloxane/abrasive mixture can be modified further by alteration of the size range of abrasive used and the ratio in which it is mixed with the polymer.

## **Experimental procedure**

All results reported in this paper refer to Extrude Hone MV grade polyborosiloxane without abrasive addition.

The rheological evaluation of this material was completed on a Davenport capillary extrusion rheometer [5].

## **The rheological properties of the MV polyborosiloxane and their relationship to the afm process**

The polyborosiloxane material must flow sufficiently readily at room temperature for it to follow the contours of complex surfaces. At the same time, it must be sufficiently rigid to allow the transmission of the pressure from its point of application to the grit particles. Unless both these conditions are met the honing operation will not occur.

Furthermore, the applications of the process tend to involve selective machining at points of restriction. It is often undesirable that universal honing should occur.

The amount of metal removal achieved during abrasive flow machining has been investigated by consideration of the wall shear stress,  $\tau$ . The wall shear stress for a circular restriction may be calculated using equation 1, below [6].

$$\tau = \frac{pr}{2l}$$

Where  $p$  is the pressure drop along the restriction, and  $r$  and  $l$  refer to the radius and length of the restriction respectively.

Thus for a given restriction geometry the shear stress is a linear function of the pressure across the restriction. The significant relationship between extrusion pressure and metal removal has been shown previously [7].

As the shear rate of the polymer increases in the vicinity of restrictions the relationship between shear rate and shear stress is very important.

The shear rate in the vicinity of a restriction during abrasive flow machining is determined by the piston speed, the cross-sectional area of the piston and the cross-sectional area of the restriction.

This becomes clear when the shear rate equation is considered for a circular restriction [6].

$$\dot{\gamma} = \frac{4Q}{\pi r^3}$$

Where  $\dot{\gamma}$  is the shear rate,

Q is the volumetric flowrate of polymer/abrasive mixture, and hence is determined from the piston velocity and cross-sectional area, and, r represents the radius of the circular restriction.

Thus the shear rate increases if either the radius of the restriction decreases, the piston velocity increases, or a larger diameter piston (AFM) is used.

The relationship between wall shear stress and shear rate for MV polyborosiloxane has been determined by capillary rheometry and can be seen below, in figure 2.

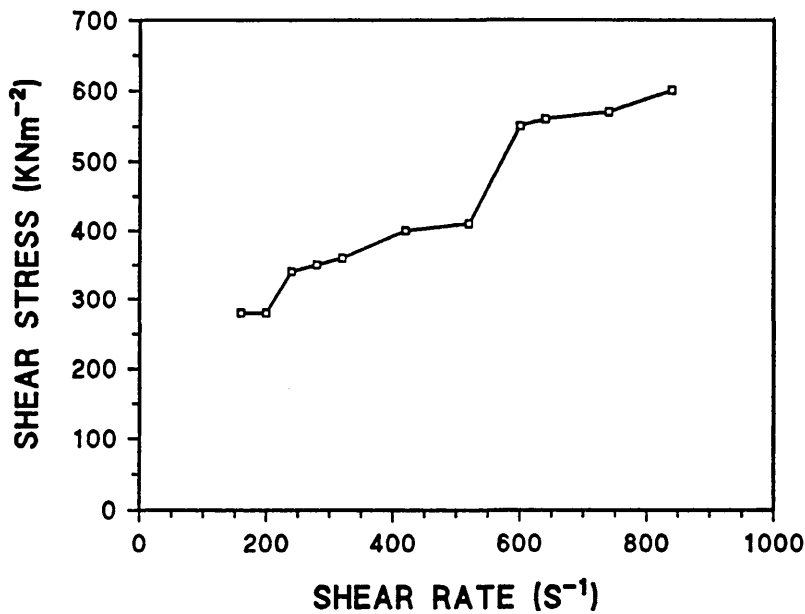


Figure 2. The variation in wall shear stress with shear rate for MVpolyborosiloxane without abrasive.

The slope of this curve, which is a measure of the coefficient of viscosity of the material, reduces as the shear rate increases i.e. the material is pseudoplastic. The shear viscosity shear rate relationship for the MV polyborosiloxane can be seen in figure 3.

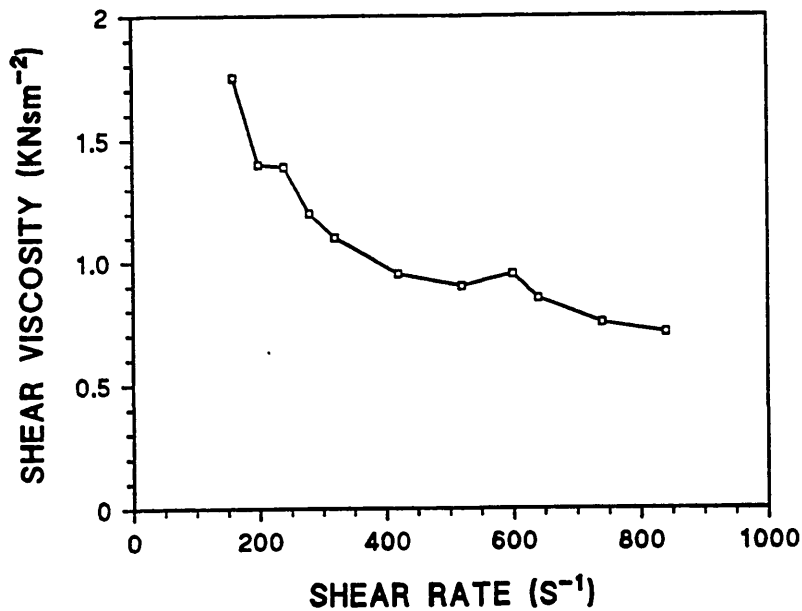


Figure 3. The variation in shear viscosity with shear rate for MVpolyborosiloxane without abrasive.

Thus, the material flows more readily in restrictions as the coefficient of viscosity will be lower on account of the increased shear rate. At the same time, the wall shear stress will be higher. The success of the Extrude Hone abrasive flow machining operation may be associated with these properties.

Another important variable to consider with respect to the abrasive media property requirements is the variation in wall shear stress with time.

The variation in wall shear stress with time for various shear rates has been investigated on the Davenport capillary rheometer.

The variation in wall shear stress with time at a high and low shear rate respectively can be seen in figures 4a and 4b.

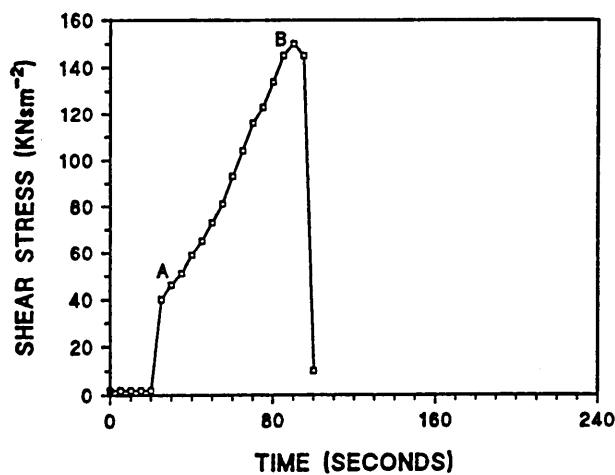


Figure 4a. Wall shear stress/time relationship for MV polyborosiloxane without abrasive at high shear rate.

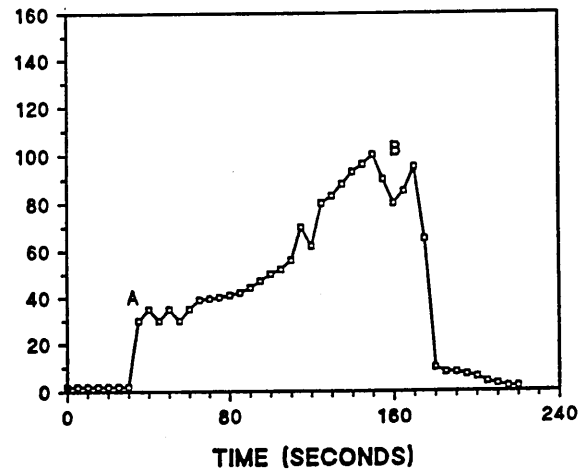


Figure 4b. Wall shear stress/time relationship for MV polyborosiloxane without abrasive at low shear rate.

The wall shear stress can be seen to vary considerably with time, despite the shear rate being maintained at a constant rate (piston speed, piston cross-section and die cross-section all constant).

Results from the capillary rheometer show a two stage increase in shear stress. The first, a very sharp increase may be associated with elastic compression of the polyborosiloxane in the barrel up to point A. The shear stress value of point A has been shown to increase as the shear rate increases. Some simple barrel compression tests for MV borosiloxane have been completed and confirm that the material has a degree of compressibility (see figure 5).

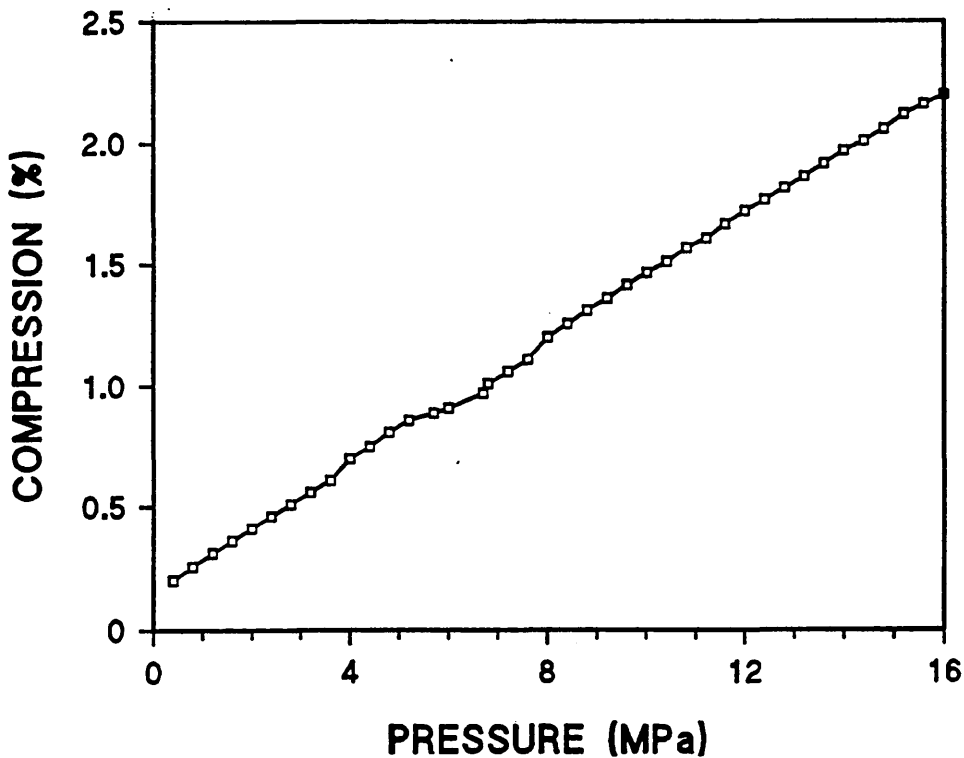


Figure 5. Compression test results for MV polyborosiloxane without abrasive.

The second section of the shear stress/time graphs from point A to point B is generally of a less inclined gradient than the section up to point A. The gradient of this part of the graph has been shown to increase as the shear rate is increased.

Reference to figures 4a and 4b indicates time dependent rheotropic behaviour for the MV polyborosiloxane. This indicates that material extruded through the die has a variable shear history with time. For this to be so, the assumption that the barrel on a capillary rheometer is purely a reservoir for providing 'fresh' polymer to be continuously extruded through the die cannot be true. The borosiloxane in the extrusion barrel must be subject to significant shear in order for extruded polyborosiloxane to have a variable shear history. Thus the wall shear stress variations with time in the die are significantly influenced by the previous shear history of the polyborosiloxane.

In order to investigate the time dependent properties of the polyborosiloxane material further, a rheological evaluation using a concentric cylinder rheometer is currently under investigation (results to be published). This type of rheometer enables close control of the polymer shear history.

This time-dependent wall shear stress at constant shear rate for MV polyborosiloxane may have considerable effect on the abrasive flow machining operation. The duration of the piston stroke (stroke capacity) will determine the maximum wall shear stress obtained in one stroke.

It would therefore be expected that greater machining action would be achieved as a result of longer piston stroke durations, due to the higher wall shear stresses generated.

## Conclusions

Abrasive flow machining is a highly successful finish machining process used in a wide range of engineering fields. However, as with all finish machining processes, further optimisation and control of the process may be achieved from greater understanding of the mechanisms of the machining action.

To date, research has shown that the rheology of the MV grade polyborosiloxane contributes significantly to the success of the process. The pseudoplastic nature of the polymer enables selective machining in areas of restriction. In addition, the rheotropic nature of the material indicates that the AFM piston stroke capacity may be significant in determining the machining action achieved.

## References

1. L. J. Rhoades, True grit: The Extrude Hone story, Pittsburgh high technology, November-December 1988.
2. L. J. Rhoades, Abrasive flow machining and its use, Non-traditional machining conference, December 2-3 1985.
3. Extrude Hone sales brochure.
4. Extrude Hone technical booklet.
5. Rheological properties of thermoplastics with a capillary rheometer, ASTM standard D3835-79.
6. F. N. Cogswell, Polymer melt rheology, George Godwin Limited, 1981, pp24-28.
7. Robert E. Williams, M. S. Thesis, University of Nebraska, 1989.

## Acknowledgements

The Authors wish to express their gratitude to The Extrude Hone Corporation for their continued financial, material and technical support of this project. One of the Authors (S.A.T.) also wishes to acknowledge the financial support of the Science and Engineering Research Council during the course of this research programme.